NEUROINFLAMMATION IN ACQUIRED EPILEPSY

EDITED BY: Jianxiong Jiang, Vijayalakshmi Santhakumar and Xinjian Zhu
PUBLISHED IN: Frontiers in Cell and Developmental Biology and
Frontiers in Neurology

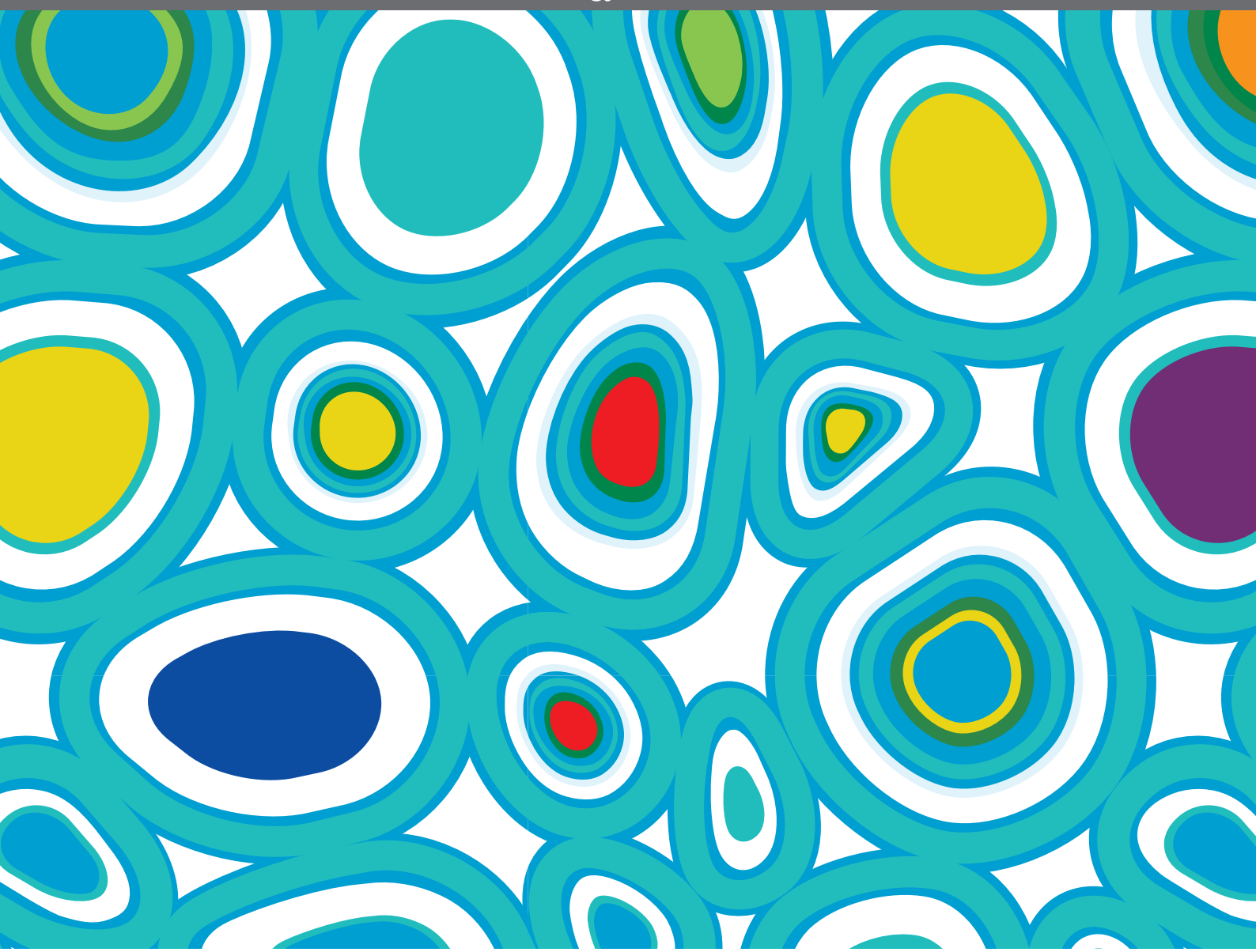

frontiers Research Topics

ISSN 1664-8714
ISBN 978-2-83250-825-1
DOI 10.3389/978-2-83250-825-1

About Frontiers

Frontiers is more than just an open-access publisher of scholarly articles: it is a pioneering approach to the world of academia, radically improving the way scholarly research is managed. The grand vision of Frontiers is a world where all people have an equal opportunity to seek, share and generate knowledge. Frontiers provides immediate and permanent online open access to all its publications, but this alone is not enough to realize our grand goals.

Frontiers Journal Series

The Frontiers Journal Series is a multi-tier and interdisciplinary set of open-access, online journals, promising a paradigm shift from the current review, selection and dissemination processes in academic publishing. All Frontiers journals are driven by researchers for researchers; therefore, they constitute a service to the scholarly community. At the same time, the Frontiers Journal Series operates on a revolutionary invention, the tiered publishing system, initially addressing specific communities of scholars, and gradually climbing up to broader public understanding, thus serving the interests of the lay society, too.

Dedication to Quality

Each Frontiers article is a landmark of the highest quality, thanks to genuinely collaborative interactions between authors and review editors, who include some of the world's best academicians. Research must be certified by peers before entering a stream of knowledge that may eventually reach the public - and shape society; therefore, Frontiers only applies the most rigorous and unbiased reviews.
Frontiers revolutionizes research publishing by freely delivering the most outstanding research, evaluated with no bias from both the academic and social point of view. By applying the most advanced information technologies, Frontiers is catapulting scholarly publishing into a new generation.

What are Frontiers Research Topics?

Frontiers Research Topics are very popular trademarks of the Frontiers Journals Series: they are collections of at least ten articles, all centered on a particular subject. With their unique mix of varied contributions from Original Research to Review Articles, Frontiers Research Topics unify the most influential researchers, the latest key findings and historical advances in a hot research area! Find out more on how to host your own Frontiers Research Topic or contribute to one as an author by contacting the Frontiers Editorial Office: frontiersin.org/about/contact

NEUROINFLAMMATION IN ACQUIRED EPILEPSY

Topic Editors:
Jianxiong Jiang, University of Tennessee Health Science Center (UTHSC), United States
Vijayalakshmi Santhakumar, University of California, Riverside, United States
Xinjian Zhu, Southeast University, China

Citation: Jiang, J., Santhakumar, V., Zhu, X., eds. (2022). Neuroinflammation in Acquired Epilepsy. Lausanne: Frontiers Media SA.
doi: 10.3389/978-2-83250-825-1

Table of Contents

04 ***Editorial: Neuroinflammation in Acquired Epilepsy***
Jianxiong Jiang, Vijayalakshmi Santhakumar and Xinjian Zhu

07 ***Characterization of Cortical Glial Scars in the Diisopropylfluorophosphate (DFP) Rat Model of Epilepsy***
Meghan Gage, Megan Gard and Thimmasettappa Thippeswamy

22 ***DFP-Induced Status Epilepticus Severity in Mixed-Sex Cohorts of Adult Rats Housed in the Same Room: Behavioral and EEG Comparisons***
Nikhil S. Rao, Christina Meyer, Suraj S. Vasanthi, Nyzil Massey, Manikandan Samidurai, Meghan Gage, Marson Putra, Aida N. Almanza, Logan Wachter and Thimmasettappa Thippeswamy

36 ***Distinct Cell-specific Roles of NOX2 and MyD88 in Epileptogenesis***
Cayo Almeida, Renan Paschoalino Pongilio, Marília Inês Móvio, Guilherme Shigueto Vilar Higa, Rodrigo Ribeiro Resende, Jianxiong Jiang, Erika Reime Kinjo and Alexandre Hiroaki Kihara

44 ***Brain-Derived Neurotrophic Factor Inhibits the Function of Cation-Chloride Cotransporter in a Mouse Model of Viral Infection-Induced Epilepsy***
Dipan C. Patel, Emily G. Thompson and Harald Sontheimer

58 ***Crosstalk Between Neuroinflammation and Oxidative Stress in Epilepsy***
Timothy Fabisiak and Manisha Patel

69 ***Time and Age Dependent Regulation of Neuroinflammation in a Rat Model of Mesial Temporal Lobe Epilepsy: Correlation With Human Data***
Sinem Erisken, George Nune, Hyokwon Chung, Joon Won Kang and Sookyong Koh

95 ***Diagnostic Value of an Algorithm for Autoimmune Epilepsy in a Retrospective Cohort***
Mitsuhiro Sakamoto, Riki Matsumoto, Akihiro Shimotake, Jumpei Togawa, Hirofumi Takeyama, Katsuya Kobayashi, Frank Leypoldt, Klaus-Peter Wandinger, Takayuki Kondo, Ryosuke Takahashi and Akio Ikeda

105 ***Low-intensity Exercise Combined With Sodium Valproate Attenuates Kainic Acid-induced Seizures and Associated Co-morbidities by Inhibiting NF-κB Signaling in Mice***
Yuxiang Jia, Lele Tang, Yu Yao, Limin Zhuo, Dongxiao Qu, Xingxing Chen, Yonghua Ji, Jie Tao and Yudan Zhu

121 ***Identification of mRNA Expression Biomarkers Associated With Epilepsy and Response to Valproate With Co-expression Analysis***
Jun Min, Qinglan Chen, Wenyue Wu, Jing Zhao and Xinming Luo

frontiers | Frontiers in Cell and Developmental Biology

TYPE Editorial
PUBLISHED 07 November 2022
DOI 10.3389/fcell.2022.1074537

OPEN ACCESS

EDITED AND REVIEWED BY
Ana Cuenda,
Spanish National Research Council (CSIC), Spain

*CORRESPONDENCE
Jianxiong Jiang,
jjiang18@uthsc.edu

SPECIALTY SECTION
This article was submitted to Signaling, a section of the journal Frontiers in Cell and Developmental Biology

RECEIVED 19 October 2022
ACCEPTED 25 October 2022
PUBLISHED 07 November 2022

CITATION
Jiang J, Santhakumar V and Zhu X (2022), Editorial: Neuroinflammation in acquired epilepsy.
Front. Cell Dev. Biol. 10:1074537.
doi: 10.3389/fcell.2022.1074537

Editorial: Neuroinflammation in acquired epilepsy

Jianxiong Jiang[1]*, Vijayalakshmi Santhakumar[2] and Xinjian Zhu[3]

[1]Department of Pharmaceutical Sciences, College of Pharmacy, The University of Tennessee Health Science Center, Memphis, TN, United States, [2]Department of Molecular, Cell and Systems Biology, University of California, Riverside, Riverside, CA, United States, [3]Department of Pharmacology, Medical School of Southeast University, Nanjing, China

KEYWORDS

epileptogenesis, BDNF, biomarker, brain infection, NADPH oxidase, oxidative stress, reactive oxygen species

Editorial on the Research Topic
Neuroinflammation in acquired epilepsy

In spite of astonishing advances in epilepsy research and treatment over the past few decades, epilepsy remains one of the most common and devastating brain diseases and still affects approximately 65 million people globally (Devinsky et al., 2018). In addition to their wide-ranging side effects, antiseizure drugs (ASDs) are not effective in controlling seizures in more than 30% of patients who have pharmacoresistant epilepsy (Janmohamed et al., 2020). It is rather unfortunate that current medications provide merely symptomatic relief and have not been demonstrated to prevent epilepsy in people at risk or modify the disease progression (Galanopoulou et al., 2021). Therefore, there remains an urgent need for alternative antiepileptic treatments, despite the rapid expansion of modern ASDs that emerged during the first 2 decades of this century (Varvel et al., 2015; Löscher and Klein, 2020; Yu et al., 2022).

Mounting lines of evidence support an essential role for proinflammatory mediators in the brain in acquired epileptogenesis, a pathogenic process that is proposed to transform a normal brain to one generating seizures following various brain insults, such as *de novo* status epilepticus (SE), brain infections, traumatic brain injuries, brain tumors, and strokes (Yu et al., 2019; Korgaonkar et al., 2020; Terrone et al., 2020). It has been widely proposed that modulating key proinflammatory mediators might disrupt the epileptogenic processes and lead to modification and/or even prevention of epilepsy. In the current Research Topic, we bring together a diverse collection of primary research and review articles that highlight the roles of brain inflammation in epilepsy of various etiologies and pathogeneses.

Both inflammation and oxidative stress are well known for their pathophysiological roles in the epileptic brain. However, they are often studied as separate entities despite the evidence that the redox-based signaling cascades and inflammatory reactions have extensive crosstalk (Fabisiak and Patel). Recent studies have uncovered a variety of mechanisms whereby oxidative stress and neuroinflammation greatly influence each other in the context of epilepsy. For instance, neuroinflammation can be regulated by

transcription factors such as NF-κB and nrf2 that are activated by reactive oxygen species (ROS). Neuroinflammation in turn can induce the expression and activity of NADPH oxidase (NOX), fostering a highly oxidative environment. Moreover, the oxidative and proinflammatory mediators can moulate distinct intracellular pathways expressed in different cell-types, exemplified by NOX-2 dependent increase in ROS in neurons and astrocytes triggered by SE, and myeloid differentiation primary response 88 (MyD88) dependent glial activation through Toll-like receptors (TLRs) (Almeida et al.). The reviews presented in this collection highlight how signaling crosstalk between neuroinflammation and oxidative stress and their cell type specific roles may be leveraged for novel therapeutic strategies for epilepsy.

Neuroinflammatory processes triggered by acute brain insults such as SE are highly regulated and show time- and age-dependency. Using a rat model of kainate-induced SE, Erisken et al. demonstrate prolonged induction of many key inflammatory genes, particularly those associated with stress-activated protein kinases, p38 and JNK signaling pathways, uniquely in adult brains. In contrast, many of the same genes show relatively transient expression in developing brains under similar experimental conditions, suggesting that the immature brains might be more resistant to SE-induced cell death and neuropathology. In line with findings in adult animals, hippocampal tissues from mesial temporal lobe epilepsy patients showed upregulation of inflammation-related genes. These results highlight the association between uncontrolled neuroinflammation and epileptogenesis and suggest that epileptic seizures might result from prolonged activation of neuroimmune processes beyond the homeostatic threshold.

Brain infection is a leading cause of epilepsy, but the underlying molecular mechanisms are poorly understood. Patel et al. use Theiler's murine encephalomyelitis virus (TMEV) infection to generate acute brain inflammation and the subsequent spontaneous seizures in mice. They show TMEV infection-induced seizures likely due to impaired GABAergic inhibition, secondary to alterations in neuronal intracellular chloride regulation. Their results further suggest that the brain-derived neurotrophic factor (BDNF) might contribute to the development of brain infection-triggered seizures by reducing the expression of K^+/Cl^- cotransporter 2 (KCC2). This has the potential to enhance accumulation of intracellular chloride and increases excitability by rendering GABA depolarizing instead of hyperpolarizing as observed in chemoconvulsant models of SE (Pathak et al., 2007; Yu et al., 2013). Notably, the upregulation of brain BDNF observed in TMEV-infected mice has also been found in chemoconvulsant models of SE (Zhu et al., 2012; Thomas et al., 20162016; Yu and Jiang 2020), and is believed to contribute to acquired epileptogenesis by acting on its high-affinity receptor, the tropomyosin related kinase B (TrkB) (Lin et al., 2020).

Exposure to diisopropylfluorophosphate (DFP), a structural analog of type G chemical warfare agents (e.g., sarin and soman), is well known to induce SE, gliosis, neuronal death, and eventually the development of spontaneous recurrent seizures in rodents. Gage et al. show that both male and female rats which experience DFP-induced SE develop unique regions of glial scarring in the piriform cortex and amygdala, but not in the hippocampus. DFP-induced cortical glial scars are characterized by a massive clustering of reactive microglia, with increase in Iba1-and CD68-positive cells, surrounded by hypertrophic astrocytes and a decrease in NeuN-positive neurons in the scar core. Although female rats have been shown to require a higher dose of DFP to induce SE when housed in a room with only females, Rao et al. demonstrate that when both sexes are housed in the same room and administered the same DFP solution, SE severity was not different between sexes. These results reinforce the importance of sex as a key biological variable in experimental design and suggest that housing animals of both sexes together and using the same batch of test reagents will reduce experimental variability.

The benefits of low-intensity physical exercise to the CNS have been shown in animal models and patients with neurological diseases, such as Alzheimer's disease, Parkinson's disease, stroke, epilepsy, multiple sclerosis, anxiety and depression (Allendorfer and Bamman, 2018). Jia et al. demonstrate that the conventional ASD, valproate, combined with low-intensity exercise can reduce seizures and associated co-morbidities in kainate-treated mice. The reduction in seizure burden appears to be correlated with the suppression of inflammatory cytokines (IL-1β, IL-6, and TNF-α) and the immune receptor TLR4 in the hippocampus. Given that TLR4 is involved in epileptogenesis of diverse etiologies (Maroso et al., 2010; Korgaonkar et al., 2020), these findings suggest that the non-pharmacological intervention like low-intensity exercise might reduce neuroinflammation and provide an adjunctive strategy to enhance efficacy of conventional ASDs to treat epilepsy.

Developing preventive treatment for epilepsy is challenging because it is currently impossible to identify individuals that will develop epilepsy after initial precipitating brain insults. Theoretically, biomarkers that identify "at risk" individuals would facilitate the development of potential antiepileptogenic treatment (Simonato et al., 2021). By reviewing data from 60 human patients with focal epilepsy of autoimmune etiology, Sakamoto et al. propose a diagnostic algorithm that might help to predict the underlying autoimmune etiology of epilepsy before antibody testing results become available. Over 30% of epilepsy patients suffer from pharmacoresistant seizures associated with cognitive and psychiatric co-morbidities. Analyzing a microarray dataset from the Gene Expression Omnibus database, Min et al. identify 25 genes differentially expressed in the peripheral blood of patients with valproate resistance in epilepsy and significantly enriched in T-cell

receptor recognition. While the potential confound posed by the differential seizure burden between valproate sensitive and resistant groups needs to be considered, these findings suggest that the peripheral blood T-cells and the differentially expressed genes could serve as biomarkers for refractory epilepsy. Identification of reliable biomarkers for diverse types of epilepsy and pharmacoresistance could facilitate both early diagnosis and development of new therapies, needed to achieve the ultimate goals of "no seizures, no side effects, and no co-morbidities" in epilepsy treatment.

The series of articles presented here address diverse ways in which neuroinflammation could shape acquired epilepsy and offers insights into how these processes may be leveraged to inform mechanisms of epileptogenesis, identify biomarkers, and to develop novel strategies for disease modification and treatment in epilepsy.

Author contributions

All authors listed have made a substantial, direct, and intellectual contribution to the work and approved it for publication.

Funding

JJ is supported by the NIH/NINDS grants (R01NS100947, R21NS109687, and R61NS124923). VS is supported by the NIH/NINDS grants (R01NS069861 and R01NS097750).

Conflict of Interest

The authors declare that the research was conducted in the absence of any commercial or financial relationships that could be construed as a potential conflict of interest.

Publisher's note

All claims expressed in this article are solely those of the authors and do not necessarily represent those of their affiliated organizations, or those of the publisher, the editors and the reviewers. Any product that may be evaluated in this article, or claim that may be made by its manufacturer, is not guaranteed or endorsed by the publisher.

References

Allendorfer, J. B., and Bamman, M. M. (2018). Getting the brain into shape: Exercise in neurological disorders. *Clin. Ther.* 40, 6–7. doi:10.1016/j.clinthera.2017.12.003

Devinsky, O., Vezzani, A., O'Brien, T. J., Jette, N., Scheffer, I. E., de Curtis, M., et al. (2018). *Epilepsy*. Nat. Rev. Dis. Prim. 4, 18024. doi:10.1038/nrdp.2018.24

Galanopoulou, A. S., Loscher, W., Lubbers, L., O'Brien, T. J., Staley, K., Vezzani, A., et al. (2021). Antiepileptogenesis and disease modification: Progress, challenges, and the path forward-Report of the Preclinical Working Group of the 2018 NINDS-sponsored antiepileptogenesis and disease modification workshop. *Epilepsia Open* 6, 276–296. doi:10.1002/epi4.12490

Janmohamed, M., Brodie, M. J., and Kwan, P. (2020). Pharmacoresistance - epidemiology, mechanisms, and impact on epilepsy treatment. *Neuropharmacology* 168, 107790. doi:10.1016/j.neuropharm.2019.107790

Korgaonkar, A. A., Li, Y., Sekhar, D., Subramanian, D., Guevarra, J., Swietek, B., et al. (2020). Toll-like receptor 4 signaling in neurons enhances calcium-permeable alpha-amino-3-hydroxy-5-methyl-4-isoxazolepropionic acid receptor currents and drives post-traumatic epileptogenesis. *Ann. Neurol.* 87, 497–515. doi:10.1002/ana.25698

Lin, T. W., Harward, S. C., Huang, Y. Z., and McNamara, J. O. (2020). Targeting BDNF/TrkB pathways for preventing or suppressing epilepsy. *Neuropharmacology* 167, 107734. doi:10.1016/j.neuropharm.2019.107734

Löscher, W., and Klein, P. (2020). The feast and famine: Epilepsy treatment and treatment gaps in early 21st century. *Neuropharmacology* 170, 108055. doi:10.1016/j.neuropharm.2020.108055

Maroso, M., Balosso, S., Ravizza, T., Liu, J., Aronica, E., Iyer, A. M., et al. (2010). Toll-like receptor 4 and high-mobility group box-1 are involved in ictogenesis and can be targeted to reduce seizures. *Nat. Med.* 16, 413–419. doi:10.1038/nm.2127

Pathak, H. R., Weissinger, F., Terunuma, M., Carlson, G. C., Hsu, F. C., Moss, S. J., et al. (2007). Disrupted dentate granule cell chloride regulation enhances synaptic excitability during development of temporal lobe epilepsy. *J. Neurosci.* 27, 14012–14022. doi:10.1523/JNEUROSCI.4390-07.2007

Simonato, M., Agoston, D. V., Brooks-Kayal, A., Dulla, C., Fureman, B., Henshall, D. C., et al. (2021). Identification of clinically relevant biomarkers of epileptogenesis - a strategic roadmap. *Nat. Rev. Neurol.* 17, 231–242. doi:10.1038/s41582-021-00461-4

Terrone, G., Balosso, S., Pauletti, A., Ravizza, T., and Vezzani, A. (2020). Inflammation and reactive oxygen species as disease modifiers in epilepsy. *Neuropharmacology* 167, 107742. doi:10.1016/j.neuropharm.2019.107742

Thomas, A. X., Cruz Del Angel, Y., Gonzalez, M. I., Carrel, A. J., Carlsen, J., Lam, P. M., et al. (2016). Rapid increases in proBDNF after pilocarpine-induced status epilepticus in mice are associated with reduced proBDNF cleavage machinery. *eNeuro* 3, ENEURO.0020. doi:10.1523/ENEURO.0020-15.2016

Varvel, N. H., Jiang, J., and Dingledine, R. (2015). Candidate drug targets for prevention or modification of epilepsy. *Annu. Rev. Pharmacol. Toxicol.* 55, 229–247. doi:10.1146/annurev-pharmtox-010814-124607

Yu, J., Proddutur, A., Elgammal, F. S., Ito, T., and Santhakumar, V. (2013). Status epilepticus enhances tonic GABA currents and depolarizes GABA reversal potential in dentate fast-spiking basket cells. *J. Neurophysiol.* 109, 1746–1763. doi:10.1152/jn.00891.2012

Yu, Y., and Jiang, J. (2020). COX-2/PGE2 axis regulates hippocampal BDNF/TrkB signaling via EP2 receptor after prolonged seizures. *Epilepsia Open* 5, 418–431. doi:10.1002/epi4.12409

Yu, Y., Li, W., and Jiang, J. (2022). TRPC channels as emerging targets for seizure disorders. *Trends Pharmacol. Sci.* 43, 787–798. doi:10.1016/j.tips.2022.06.007

Yu, Y., Nguyen, D. T., and Jiang, J. (2019). G protein-coupled receptors in acquired epilepsy: Druggability and translatability. *Prog. Neurobiol.* 183, 101682. doi:10.1016/j.pneurobio.2019.101682

Zhu, X., Han, X., Blendy, J. A., and Porter, B. E. (2012). Decreased CREB levels suppress epilepsy. *Neurobiol. Dis.* 45, 253–263. doi:10.1016/j.nbd.2011.08.009

frontiers in Cell and Developmental Biology

ORIGINAL RESEARCH
published: 16 March 2022
doi: 10.3389/fcell.2022.867949

Characterization of Cortical Glial Scars in the Diisopropylfluorophosphate (DFP) Rat Model of Epilepsy

Meghan Gage[1,2], *Megan Gard*[1] *and Thimmasettappa Thippeswamy*[1,2]*

[1]Department of Biomedical Sciences, College of Veterinary Medicine, Iowa State University, Ames, IA, United States, [2]Neuroscience Interdepartmental Program, Iowa State University, Ames, IA, United States

OPEN ACCESS

Edited by:
Jianxiong Jiang,
University of Tennessee Health Science Center (UTHSC), United States

Reviewed by:
Vijayalakshmi Santhakumar,
University of California, Riverside, United States
Melissa Barker-Haliski,
University of Washington, United States

***Correspondence:**
Thimmasettappa Thippeswamy
tswamy@iastate.edu

Specialty section:
This article was submitted to Signaling, a section of the journal Frontiers in Cell and Developmental Biology

Received: 01 February 2022
Accepted: 03 March 2022
Published: 16 March 2022

Citation:
Gage M, Gard M and Thippeswamy T (2022) Characterization of Cortical Glial Scars in the Diisopropylfluorophosphate (DFP) Rat Model of Epilepsy. Front. Cell Dev. Biol. 10:867949. doi: 10.3389/fcell.2022.867949

Glial scars have been observed following stab lesions in the spinal cord and brain but not observed and characterized in chemoconvulsant-induced epilepsy models. Epilepsy is a disorder characterized by spontaneous recurrent seizures and can be modeled in rodents. Diisopropylfluorophosphate (DFP) exposure, like other real-world organophosphate nerve agents (OPNAs) used in chemical warfare scenarios, can lead to the development of *status epilepticus* (SE). We have previously demonstrated that DFP-induced SE promotes epileptogenesis which is characterized by the development of spontaneous recurrent seizures (SRS), gliosis, and neurodegeneration. In this study, we report classical glial scars developed in the piriform cortex, but not in the hippocampus, by 8 days post-exposure. We challenged both male and female rats with 4–5 mg/kg DFP (s.c.) followed immediately by 2 mg/kg atropine sulfate (i.m.) and 25 mg/kg pralidoxime (i.m.) and one hour later by midazolam (i.m). Glial scars were present in the piriform cortex/amygdala region in 73% of the DFP treated animals. No scars were found in controls. Scars were characterized by a massive clustering of reactive microglia surrounded by hypertrophic reactive astrocytes. The core of the scars was filled with a significant increase of IBA1 and CD68 positive cells and a significant reduction in NeuN positive cells compared to the periphery of the scars. There was a significantly higher density of reactive GFAP, complement 3 (C3), and inducible nitric oxide synthase (iNOS) positive cells at the periphery of the scar compared to similar areas in controls. We found a significant increase in chondroitin sulfate proteoglycans (CS-56) in the periphery of the scars compared to a similar region in control brains. However, there was no change in TGF-β1 or TGF-β2 positive cells in or around the scars in DFP-exposed animals compared to controls. In contrast to stab-induced scars, we did not find fibroblasts (Thy1.1) in the scar core or periphery. There were sex differences with respect to the density of iNOS, CD68, NeuN, GFAP, C3 and CS-56 positive cells. This is the first report of cortical glial scars in rodents with systemic chemoconvulsant-induced SE. Further investigation could help to elucidate the mechanisms of scar development and mitigation strategies.

Keywords: astrocytes, microglia, glial scar, epilepsy, chrondrotin sulfate proteoglycans (CS-56), CD68

INTRODUCTION

Glial scars in the spinal cord, following traumatic injury, have been described for decades (DB., 1930; Wanner et al., 2013). Progress in research techniques has allowed for the characterization of these scars. Typically, the spinal cord scars consist of two major parts: the scar core, which contains macrophages and fibroblasts; and the scar periphery, which consists of surrounding reactive astrocytes (Silver and Miller, 2004; Wang et al., 2018). These scars have been primarily studied with respect to their inhibitory effect on axon regeneration at the site of injury (Sugar and Gerard, 1940; Fawcett and Asher, 1999). For many years, these scars were thought to be barriers to recovery after spinal cord injury, but some recent studies suggest that they may be protective (Anderson et al., 2016; Yang et al., 2020). Importantly, the most persuasive argument is that the scar periphery prevents the spread of neuroinflammation, thereby protecting the undamaged tissue (Voskuhl et al., 2009; Sofroniew, 2015). Although most glial scar studies focus on spinal cord injury, there has been some description of scar pathology in the brain following traumatic brain injury as well as stroke (Yutsudo and Kitagawa, 2015; Frik et al., 2018; Schiweck et al., 2021). Importantly, some studies do describe "glial scarring", usually referring to a massive infiltration and activation of both microglia and astrocytes, but such scarring pathology does not provide evidence to fit the classical definition of "glial scar", i.e., scar core and scar periphery.

The molecular markers found in glial scars are also known to play a role in epilepsy. For example, increased proliferation and activation of glial cells (astrocytes and microglia) and loss of neurons has been shown in both human and animal models of epilepsy (Farrell et al., 2017; Rana and Musto, 2018). Similarly, glial scars usually have an upregulated expression of transforming growth factor beta (TGFβ) and proteoglycans (Lagord et al., 2002; Hussein et al., 2020) which are also implicated in epileptogenesis (Bar-Klein et al., 2014; Yutsudo and Kitagawa, 2015). TGFβs are pleiotropic cytokines and some studies have shown that they may be responsible for the initiation of glial scar formation (Buss et al., 2007). Proteoglycans are thought to inhibit neurite growth post spinal cord injury by altering the extracellular matrix (McKeon et al., 1999). These commonalities imply that glial scars may be prevalent in epilepsy, though the classical glial scars as presented in this study have not yet been reported in most models.

In this study, we are the first to describe a characteristic glial scar observed 8 days after the induction of *status epilepticus* (SE) in a rat model of systemic chemoconvulsant-induced epilepsy. Epilepsy is the fourth most prevalent neurological disease and is characterized by spontaneous recurrent seizures, gliosis, and neurodegeneration (Fisher et al., 2005; Hirtz et al., 2007; Todorovic et al., 2012; Beghi and Hesdorffer, 2014; Pitkänen and Engel, 2014; Stafstrom and Carmant, 2015; Seinfeld et al., 2016). Despite many available therapeutic agents, approximately 30% of people with epilepsy develop pharmacoresistance; this underscores the importance of studying epilepsy and the discovery of new therapeutic drugs (French, 2007; Engel, 2014). This study aimed to characterize SE-induced glial scars using several molecular markers previously known to play a role in glial scarring after spinal cord injury (glial and neuronal markers, TGFβs, proteoglycans, fibroblasts). We also characterized astrocytic expression of complement 3 (C3), which has previously been used as a marker for astrocytic activation and inducible nitric oxide synthase (iNOS), which is indicative of oxidative stress and neurotoxicity (Garry et al., 2015; Liddelow et al., 2017). Importantly, we previously showed that pharmacological inhibition of iNOS by 1400 W led to reduced gliosis, neurodegeneration, and seizure frequency in a rodent model of diisopropylfluorophosphate (DFP)-induced epilepsy (Putra et al., 2020a).

In this study, we utilized the rat DFP model of epilepsy. We have previously demonstrated that DFP-induced SE, depending on the initial severity, promotes the development epilepsy (Gage et al., 2021a; Putra et al., 2020b). The features of DFP-induced epilepsy are similar to other chemoconvulsant models of epilepsy, such as kainate/pilocarpine model, with respect to the onset of neuroinflammation, neurodegeneration, and spontaneous recurrent seizures (SRS) (Curia et al., 2008; Putra et al., 2020a; Sharma et al., 2021). DFP is an irreversible inhibitor of acetylcholinesterase, leading to accumulation of acetylcholine and overstimulation of cholinergic receptors (McDonough and Shih, 1997; Millard et al., 1999; Todorovic et al., 2012; Puttachary et al., 2016; Gage et al., 2020). DFP is used to model the effects of other organophosphate nerve agents (OPNAs) such as Soman and Sarin, which have been previously used as chemical weapons (Morita et al., 1995; Suzuki et al., 1995; Okumura et al., 1996; Miyaki et al., 2005; Yanagisawa et al., 2006). OPNAs or DFP exposure leads to the development of cholinergic crisis, which includes symptoms such as bronchoconstriction, salivation, lacrimation, gastrointestinal distress, bradycardia, and convulsions or SE (McDonough and Shih, 1997; Jett, 2012). In this study, we challenged animals with DFP and observed glial scars in the amygdala/piriform cortex, which look like those observed post-stab injury to the brain or spinal cord. This study aimed to determine the prevalence of these scars as well as to characterize the cell types located at both the scar core and scar periphery.

METHODS

Animals, Care and Ethics

25 male and female Sprague Dawley rats were purchased from Charles River (Wilmington MA, United States). Fifteen (7 male, 8 female) animals were challenged with DFP, and 10 animals (5 male, 5 female) were left untreated as controls. All animals were sacrificed with 100 mg/kg pentobarbital sodium (i.p.) purchased from the Lloyd Veterinary Medical Center Hospital Pharmacy, Ames, Iowa. The procedures were approved by the Institutional Care and Use Committee (IACUC-21-109) at Iowa State University. Animals were single housed with 12-h light and dark cycles and given *ab libitum* access to food and water.

Chemicals

Diisopropylfluorophosphate (Sigma-Aldrich, purity >97%) was prepared fresh in cold phosphate-buffered saline (PBS) prior to

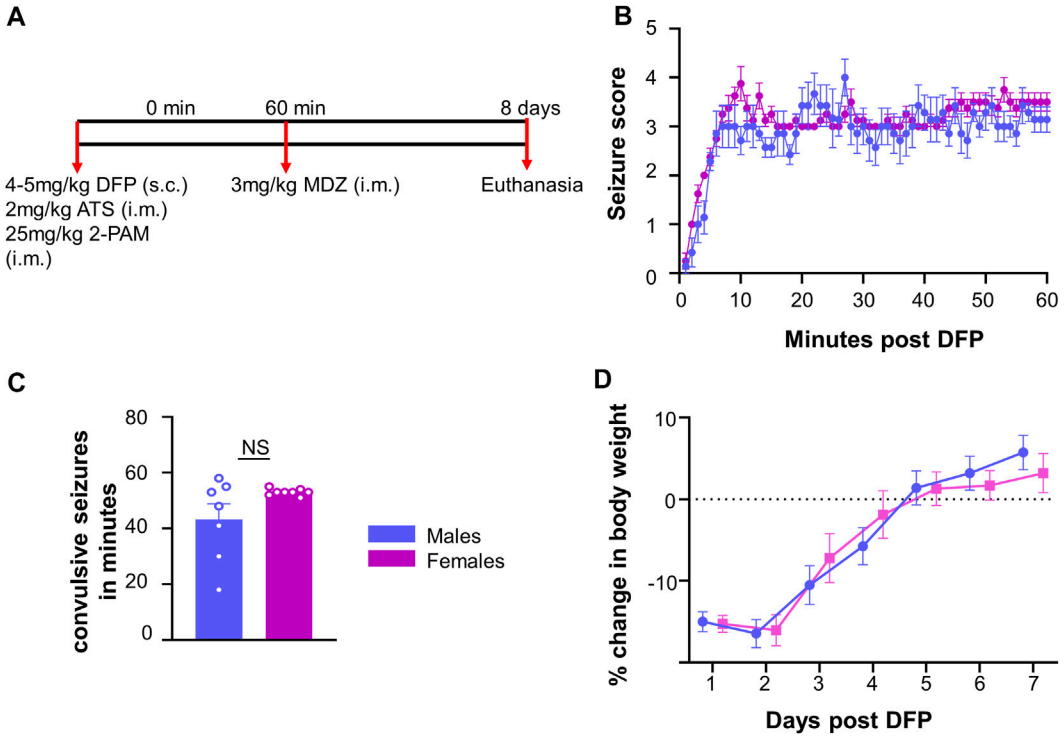

FIGURE 1 | Experimental outline for challenge with diisopropylfluorophosphate (DFP). **(A)** Male and female rats were injected with 4–5 mg/kg DFP (s.c.) followed immediately by 2 mg/kg atropine sulfate (ATS, i.m.) and 25 mg/kg 2-PAM (i.m.). One hour later, behavioral seizures were terminated with 3 mg/kg midazolam (MDZ, i.m.). **(B)** Average seizure stage each minute following DFP (mixed measures ANOVA, $n = 7–8$). **(C)** Number of minutes in a CS prior to MDZ administration; **(D)** Average change in body weight after DFP intoxication. *t*-test or mixed measures ANOVA ($n = 7–8$).

administration. Atropine sulfate (ATS, Thermo-Fisher Scientific) and 2-pralidoxime (2-PAM) were prepared fresh in saline. Midazolam (MDZ) was purchased from the Lloyd Veterinary Medical Center Hospital Pharmacy. Gelatin for tissue embedding consisted of 15% type A porcine gelatin, 7.5% sucrose, and 0.1% sodium azide. Citric acid buffer contained 10 mM citric acid and 0.05% tween-20 at a pH of 6. Blocking buffer consisted of 10% donkey serum and 0.05% tritonX-100 in PBS. Antibodies used for immunohistochemistry (IHC) are summarized in **Supplementary Table S1**. All antibodies were tested with a negative control simultaneously, and the optimal concentration was determined by serial dilution. Antibodies were diluted in PBS containing 2.5% donkey serum, 0.1% tritonX-100 and 0.25% sodium azide. Streptavidin conjugated antibodies were diluted in PBS.

Seizure Induction and Seizure Scoring

The experimental design is illustrated in **Figure 1A**. Fifteen rats (7 males and 8 females) were challenged with 4 mg/kg (males) or 5 mg/kg (females) DFP (s.c.) followed by 2 mg/kg ATS (i.m.) and 25 mg/kg 2-PAM (i.m.) to reduce mortality. In our previous studies, female rats required a higher dose of DFP than males when they were challenged independently (Gage et al., 2020). Animals developed seizures within 5–10 min after DFP, and one hour later, MDZ (3 mg/kg, i.m.) was administered.

Prior to MDZ, animals were scored on each minute for seizure stage based on a modified Racine scale (Racine, 1972) as described in our previous publications (Putra et al., 2020b; Gage et al., 2021b; Sharma et al., 2021). Stage one was characterized by salivation, lacrimation, urination, defecation, and mastication, while stage two was characterized by head nodding and tremors. Stage three was characterized by rearing, Straub tail, and forelimb extension. Stage four presented with the loss of the righting reflex and forelimb clonus, while stage five included repeated rearing, falling, and circling. To measure seizure duration and severity, we calculated the number of minutes in which each animal was in a convulsive seizure (CS) (stage 3–5); stages 1 and 2 were considered nonconvulsive seizures (NCS).

Immunohistochemistry

Animals were sacrificed 8 days after DFP exposure. Transcardiac perfusion with PBS followed by 4% paraformaldehyde was performed to preserve the morphology. Brains were dissected and incubated for 24 h in 4% paraformaldehyde followed by 25% sucrose (in PBS) for 72 h in a refrigerator. Brains were embedded in gelatin, rapidly frozen in liquid nitrogen cooled isopentane, and stored at −80°C. Coronal brains were then sectioned serially using a cryostat (ThermoFisher) into 16 µm sections beginning at the most rostral portion of the hippocampus. Each slide contained sections approximately 480 µm apart to cover

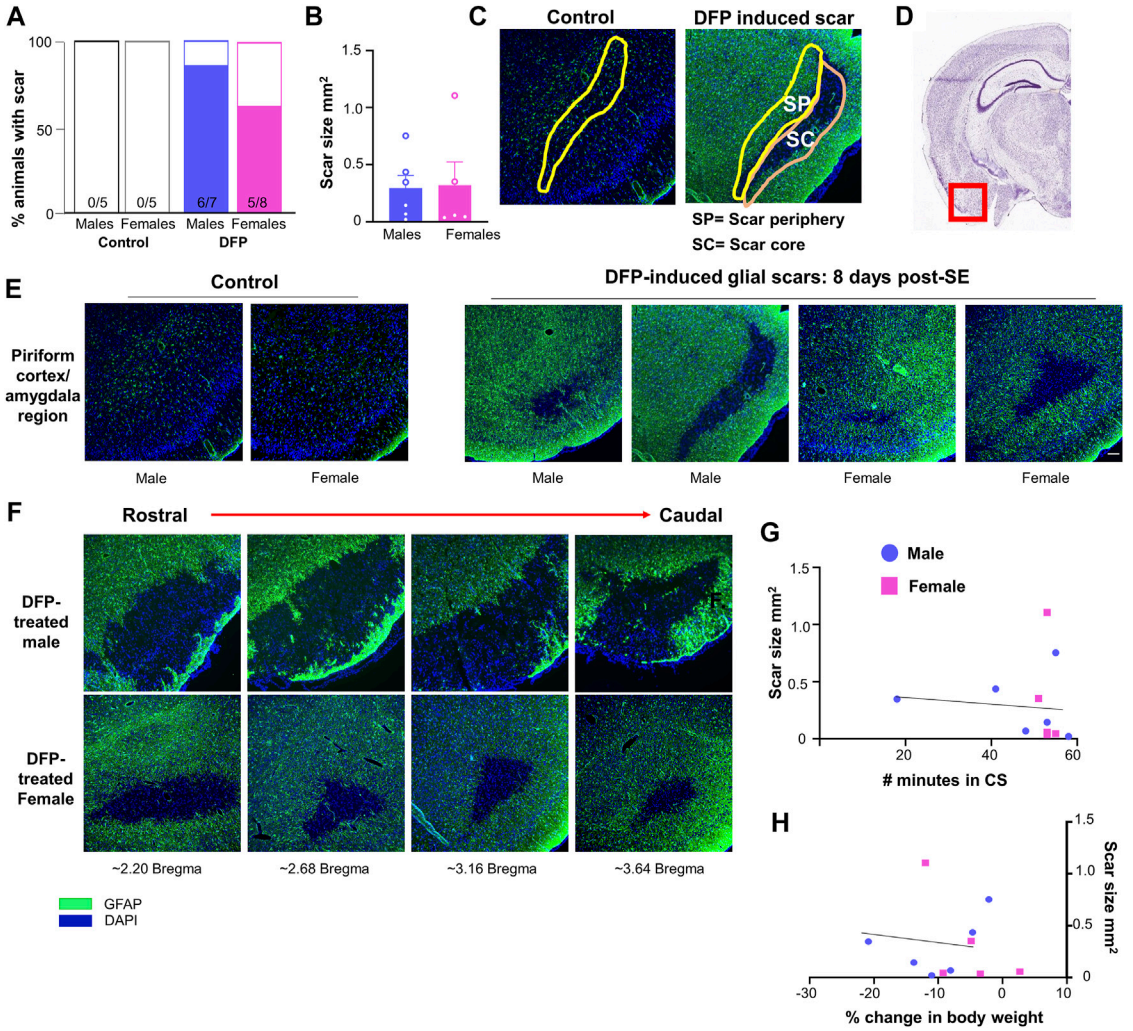

FIGURE 2 | Glial scar prevalence, shape, and size. **(A)** Percent of animals displaying a glial scar in male and female rats. **(B)** Average scar area comparison between male and females across sections. **(C)** Example of areas quantified in the scar core (SC) and scar periphery (SP). A similar region was analyzed in control animals. **(D)** Region imaged relative to the rest of brain (Image courtesy: Allen brain atlas, United States) **(E)** Representations of the variability in scar shape and size in the piriform cortex/amygdala region. **(F)** Scars often extended over multiple sections; images are from the same animal in the amygdala/piriform cortex region spreading from rostral to caudal. **(G, H)** Relationship between scar size and the number of minutes in a convulsive seizure (CS) during SE or the loss in body weight over the first three days post-DFP.

regions of the brain from rostral to caudal. Slides were stored at −20°C and once stained, stored at 4°C.

Slides were subjected to antigen retrieval in citric acid buffer at 95°C for 23 min. After transferring to Shandon racks, slides were washed with PBS for one hour and then incubated in blocking buffer for one hour. Slides were incubated with the desired primary antibodies overnight at 4°C. The next day, slides were again washed with PBS for one hour and incubated with the appropriate biotinylated, alexaflour, or FITC-conjugated secondary antibodies. Slides were again washed with PBS for one hour prior to incubation with streptavidin-conjugated antibodies. After another hour wash in PBS, slides were mounted with a medium containing DAPI (Vectashield).

Cell Quantification

The Lecia DMi8 inverted fluorescence microscope and Leica K5 passive cooled sCMOS camera were used to image the slides. Images were taken from at least four sections per animal for each marker. For animals with glial scars, images were taken only from sections containing the scar. For controls without glial scars, images were taken from a similar region to the scar location (amygdala/piriform cortex region). Values were averaged across the sections. ImageJ was used to isolate the desired regions of the brain (scar core and scar periphery) based upon the localization of GFAP staining. The scar core was defined as the GFAP negative region amidst intensely stained GFAP cells in the periphery. The scar periphery (200–350 μm) was defined as the inner region adjacent to the scar core (represented in **Figure 2C**) since the

outer region of the scar was close to the surface of the brain/the pyramidal cell layer. We chose this layer rather than the outer layer as some of the scars did not have an intact outer layer of GFAP positive cells (for example, **Figure 2E**). A similar area was isolated in controls without scars. ImageJ was also used to measure the area of the scars; area was averaged between sections. ImageJ and cell profiler software were used to quantify various molecular markers in the brain. The general parameters used for each marker are described in **Supplementary Table S2**.

Statistics and Rigor

GraphPad Prism (version 9.3.0) was used to graph the data and perform various statistical analyses. Where appropriate, experimenters were blind to treatment groups. Normality was assessed *via* the Shapiro-Wilk test, and Grubb's test was used to eliminate outliers. Linear models and regression analyses were used to analyze the data and included both treatment and sex as a variable. Sex was analyzed within treatment groups and treatment was analyzed within region. Specific statistical tests can be found in the corresponding figure legends.

RESULTS

Initial Seizure Response to DFP and Glial Scar Prevalence

Following DFP intoxication, both male and female animals developed CS in 5–10 min. The average seizure stage at each minute is represented in **Figure 1B**. There was no significant difference in the amount of time male and female animals spent in CS during SE although females received 1 mg/kg more DFP than males (**Figure 1C**). However, the females had a less variable response than males which could be due to the higher dose of DFP. We considered SE severity as a criterion, irrespective of the dose of DFP, to compare the prevalence of the glial scars between sexes (**Figure 1C**).

Glial scars were recognized by intense GFAP positive cells (astrocytes) concentrated around a GFAP negative brain region in the piriform cortex and amygdala regions in both males and females (**Figures 2D,E**). Located just deep to the pyramidal cell layer of the piriform cortex, astrocytes formed the borders around a "hole-like" structure, the periphery of glial scar as described for the spinal cord injury models. We did not observe the glial scars in other regions of the brain. No control animals (not treated with DFP) had any glial scars while 6/7 DFP treated males and 5/8 DFP treated females had a glial scar in at least one section 8 days after exposure to DFP (**Figure 2A**). There was variability in the size of the scar though they were typically "bean shaped" as shown in **Figure 2E**. There was no difference in the size of the scar between sexes (**Figure 2B**). Scars spanned from the rostral to caudal end of the brain in both sexes (**Figure 2F)**. DFP treated animals, irrespective of sex, lose bodyweight for the first three days (Gage et al., 2021a). In this study too, both sexes lost weight but recovered to their basal levels by day 5 (**Figure 1D**). There was no significant correlation between scar size and initial SE duration or change in body weight in the first three days (**Figures 2G,H**).

Microglia, CD68 Positive Phagocytic Microglia, and Neurons in and Around the Scar

For DFP treated animals with scars, we quantified the cell types in the region inside the scar (scar core) and a similar surface area of a region outside the scar (scar periphery), as shown in **Figure 2C**. Images are taken from the same animal. To verify that the changes in cellular density are not due to differences in cortical regions, we also analyzed two similar regions in control animals. For controls, the "scar core equivalent" was a region just adjacent to the pyramidal cell layer while the "scar periphery equivalent" was a region further deep to the "scar core equivalent". We used a linear model to compare treatment, location (scar core versus periphery), and sex. In the scar region of DFP-treated males and females, compared to the controls, there were significantly more IBA1-positive and CD68-positive microglia cells (**Figures 3A,B**). In DFP treated animals, in both sexes, there was a significant upregulation of IBA1 positive cells in the scar core compared to the periphery (**Figure 3A**). There was also an upregulation of CD68 positive cells in the scar core compared to the periphery in DFP treated animals, but the upregulation was statistically significant in females only (**Figure 3B**). In DFP treated females, there was also a statistically significant reduction in the number of NeuN positive cells in the scar core compared to the scar periphery, but in males, the differences were not significant (**Figure 3C**). Interestingly, when DFP-treated animals were compared with their respective sex-matched controls, there were no significant differences in NeuN positive cells in either the scar core or the scar periphery (**Figure 3C**). In controls, there was no change in either IBA1, CD68, or NeuN positive cells between scar core or peripheral equivalent regions. When sex was directly compared within each region (scar core or scar periphery in DFP treated groups and scar core equivalent or scar periphery equivalent in controls) there were no statistical differences (**Figures 3A–C**).

GFAP and C3 Positive Cells

The core of the glial scar had no GFAP positive astrocytes. Hypertrophic astrocytes surrounded the core of the glial scar (**Figure 4A**). There was an upregulation of astrocytes (GFAP positive cells) in the scar periphery compared to a similar area in untreated sex-matched control animals (**Figure 4B**). This was significant in males but only trending in females. We co-stained sections with GFAP and C3, a complement component marker, which is also a marker for astrocytic activation (Liddelow et al., 2017; Putra et al., 2020a). Both control animals and DFP treated animals had astrocytic C3 positive staining, but there was a significant increase in the number of GFAP and C3 positive cells in a male DFP treated animals with scars compared to male control animals (**Figures 4B,C**). Again, this was only trending in females. There were no statistically significant sex differences in GFAP or C3 positive cells (**Figures 4B,C**).

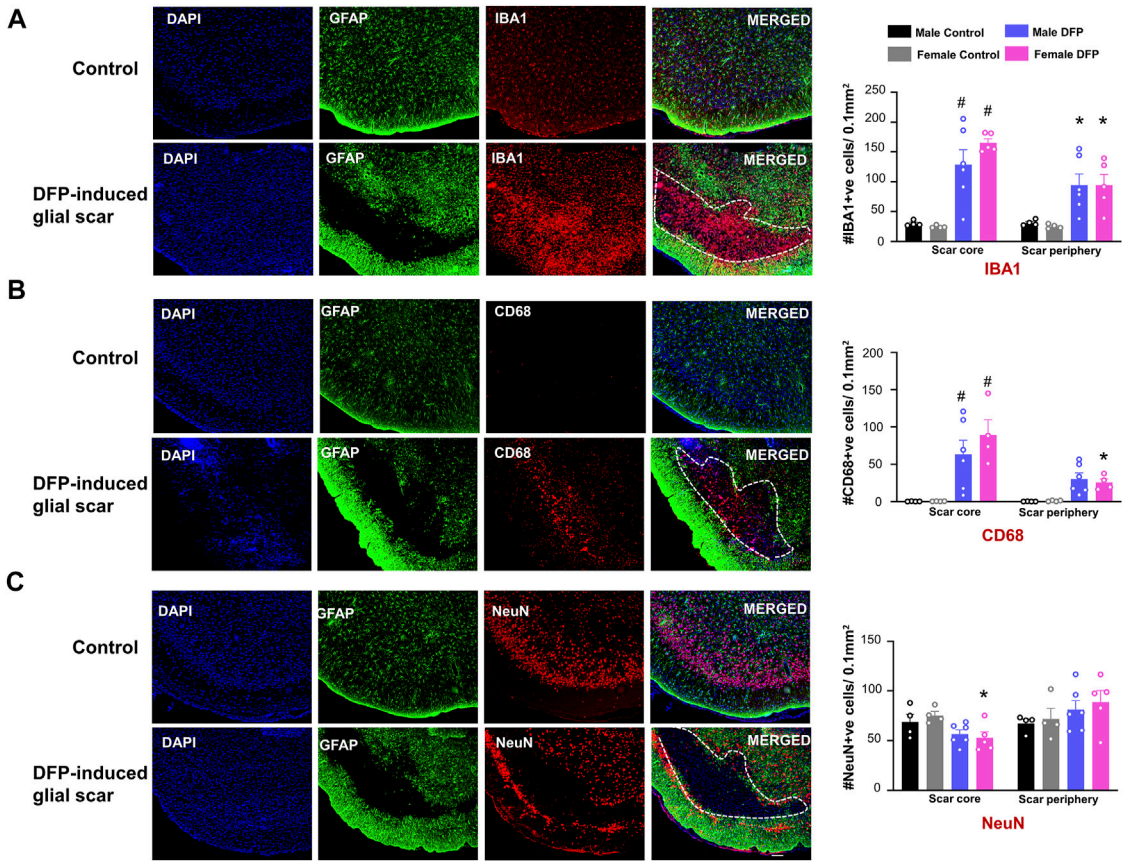

FIGURE 3 | Characterization of the glial scars. We compared the cell markers in the scar core with the scar periphery. **(A)** Number of IBA1 positive microglia and macrophages **(B)** Number of CD68 positive phagocytic cells **(C)** Number of NeuN positive cells. Mixed measures ANOVA with Tukey post-hoc, n = 4–6, $^{*}p < 0.05$ comparison of sex matched "scar core versus scar periphery", #<p< 0.05 compared to sex matched control in the same region. Scale = 100 μm.

TGF-β Positive Cells

TGF-β1 and TGF-β2 regulate both inflammation as well as the extension of neurites at the vicinity of glial scars (Shiying et al., 2017). We hypothesized that the density of TGF-β positive cells in the scar periphery might be different from the scar core or from control animals (**Figure 2C**). TGF-β1and TGF-β2 immunopositive cells did not colocalize with GFAP and were present in both controls, and DFP treated animals (**Figures 5A**, **6A**). There was no significant difference between the DFP treated animals (scar periphery) and control animals in the number of TGF-β1 or TGF-β2 positive cells (**Figure 5B**, **Figure 6B**). There was also no difference in the of TGF-β1 or TGF-β2 positive cells in the scar periphery compared to the scar core in DFP treated animals (**Figure 5C**, **Figure 6C**). There were no significant sex differences in the number of TGF-β1 or TGFβ-2 positive cells either (**Figure 5B,C**, **Figure 6B,C**).

iNOS Positive Cells

Since we found a significant neuronal loss in glial scar, we hypothesized that iNOS may be relevant to glial scars. Representative images of GFAP (to visualize the scars) and iNOS positive staining are shown in **Figure 7A**. There was a significant upregulation of iNOS positive cells in the scar periphery compared to a similar region in controls (**Figure 7B**). There were no significant differences between the density of iNOS positive cells in the scar periphery versus the scar core (**Figure 7C**). Within the scar core, females had significantly more iNOS positive cells compared to males (**Figure 7C**), which corroborates with a significant reduction in NeuN positive cells (**Figure 3C**).

Characteristic Glial Scar Markers: Chromatin Sulfate Proteoglycans (CS-56) and Fibroblasts (Thy 1.1)

Proteoglycans and fibroblasts are highly associated with glial scars in spinal cord injury (Silver and Miller, 2004; Properzi et al., 2005). In DFP treated males and females with glial scars, CS-56 was observed in both core and the periphery. In DFP treated males, compared to sex matched controls, there was a significant increase in positive staining for CS-56, which indicates the presence of chondroitin sulfate proteoglycans (CSPG) (**Figures 8A,B**). The same trend was observed in females, but it was not significant. CS-56 cells were primarily co-localized with astrocytes (GFAP positive cells) at the scar periphery**.** We did not detect Thy 1.1 fibroblasts either in the DFP treated animals or

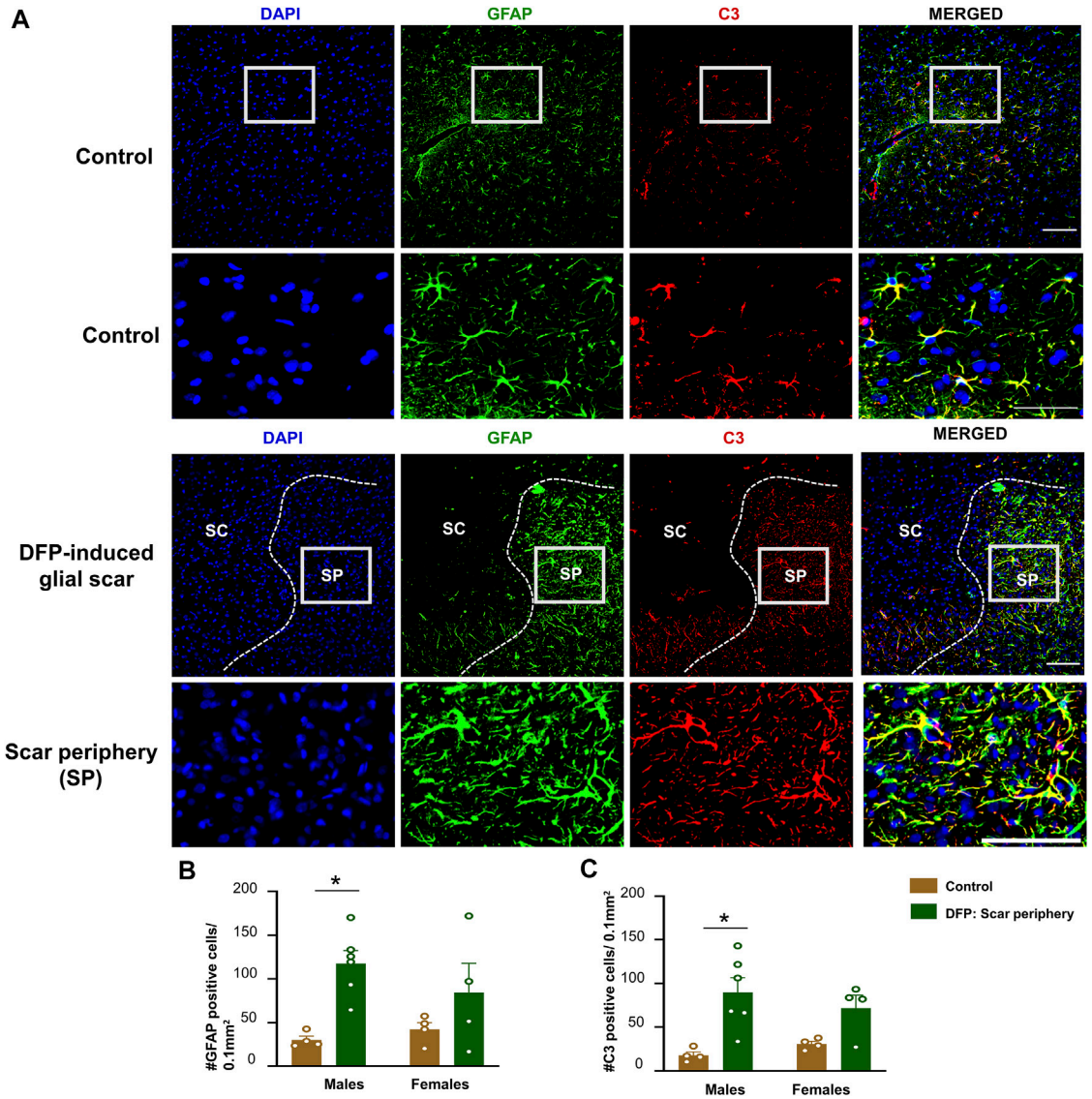

FIGURE 4 | Characterization of the glial scar cells outside the core. **(A)** Representative images for GFAP and C3 staining in control animals and DFP treated animals with glial scars. We compared the cell counts in the scar periphery to a similar region in controls. **(B)** Number of GFAP positive cells. **(C)** Number of C3 positive cells. Mixed measures ANOVA, $n = 4–6$, $^*p < 0.05$. Scale = 50 μm.

controls in the specified areas (**Figure 9A**). We used sections of spleen tissue (untreated rat) as a positive control for Thy1.1 staining (**Figure 9B**).

DISCUSSION

This is the first study to report the presence of glial scars in the brain following DFP-induced epilepsy. Glial scars have long since been reported in the spinal cord following traumatic injury (Silver and Miller, 2004; Leal-Filho, 2011; Yuan and He, 2013). For many years, these scars were thought to be barriers to axonal regeneration. However, current evidence suggests that glial scars can be protective by limiting the spread of injury (Rolls et al., 2009; Cregg et al., 2014; Yang et al., 2020). Though far more studied in spinal cord injury, these types of glial scars have also been described in traumatic brain injury, ischemia, and multiple sclerosis (Robel et al., 2015; Frik et al., 2018; Luo et al., 2018; Wang et al., 2018). Some studies have associated the glial scars with post-traumatic epilepsy (Robel, 2017; Xu et al., 2019). Another study reported a similar glial scar 15 days post kainate (KA) injection directly into the rat thalamus (Dusart et al., 1991). Although the latter KA model is an acquired epilepsy, our study is different in that the epileptic insult arose from a systemic chemical insult (DFP). In this study, we found a high prevalence of scars (73%) following DFP-induced SE. Also interesting, the glial scars were localized to the piriform cortex/amygdala region. Neuropathological changes in these regions,

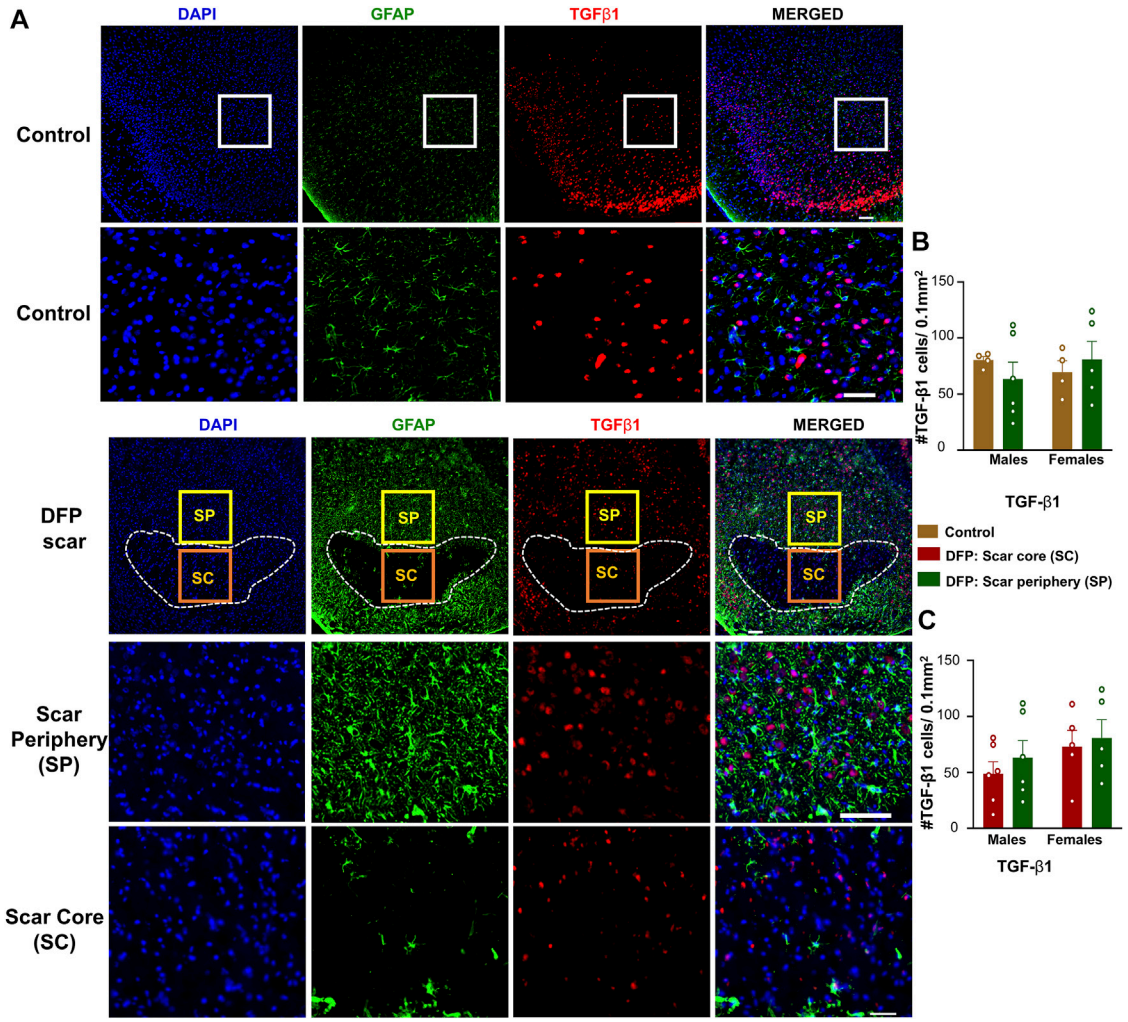

FIGURE 5 | TGF-β1 signaling in control animals and DFP treated animals with glial scarring. **(A)** Representative images for GFAP and TGF-β1. **(B)** The number of TGF-β1 positive cells in the scar periphery (SP) were compared to a similar region in controls. **(C)** Comparison of the number of TGF-β1 positive cells in the scar periphery and the scar core (SC). Mixed measures ANOVA, $n = 4–6$, $^*p < 0.05$. Scale = 50 μm.

such as neurodegeneration and gliosis, have been reported following OP exposure, but glial scars are not reported (Aroniadou-Anderjaska et al., 2009, 2016).

There was a significant increase in iNOS positive cells in the female glial scar cores compared to male glial scar cores. In DFP treated females, but not males, there was a significant increase in CD68 positive cells and significant reduction in NeuN positive cells in the scar core compared to the periphery. Compared to sex-matched controls, there was also a DFP-induced increase in GFAP, C3 and CS-56 positive cells that was only significant in males. Also of note, this study relies on behavioral evaluation of seizures rather than a more robust method such as electroencephalography (EEG). Electrode implantation could lead to changes in neuroinflammation and possibly influence the glial scarring, which can confound the real effects of systemic chemoconvulsant induced glial scars (Tse et al., 2021). We have previously demonstrated that these behaviors are strongly associated with EEG changes and thus, visual behavioral seizure scoring by an experienced experimenter is a reliable measure of initial SE severity (Putra et al., 2020a; Putra et al., 2020b).

It is well established that epilepsy is associated with abnormal regulation and excessive proliferation of glial cells (Vezzani et al., 2015). Our previous studies and others' studies have demonstrated that DFP-induced epilepsy is also characterized by neuroinflammation and neurodegeneration (Gage et al., 2021a; Gage et al., 2021b; Guignet et al., 2019; Putra et al., 2020a). Reactive astrogliosis exists on a spectrum ranging from hypertrophy of astrocytes and progressing into the formation of a glial scar (Sofroniew, 2005; Pekny and Pekna, 2016). The roles of astrocytes in both the normal and epileptic brains are becoming more diverse. Historically, astrocytes are associated with the formation of the blood-brain barrier, metabolic processes, neurodevelopment, and maintenance of cellular homeostasis (Abbott et al., 2006; Clarke and Barres, 2013; Benarroch, 2016). Reactive astrogliosis has become a hallmark of

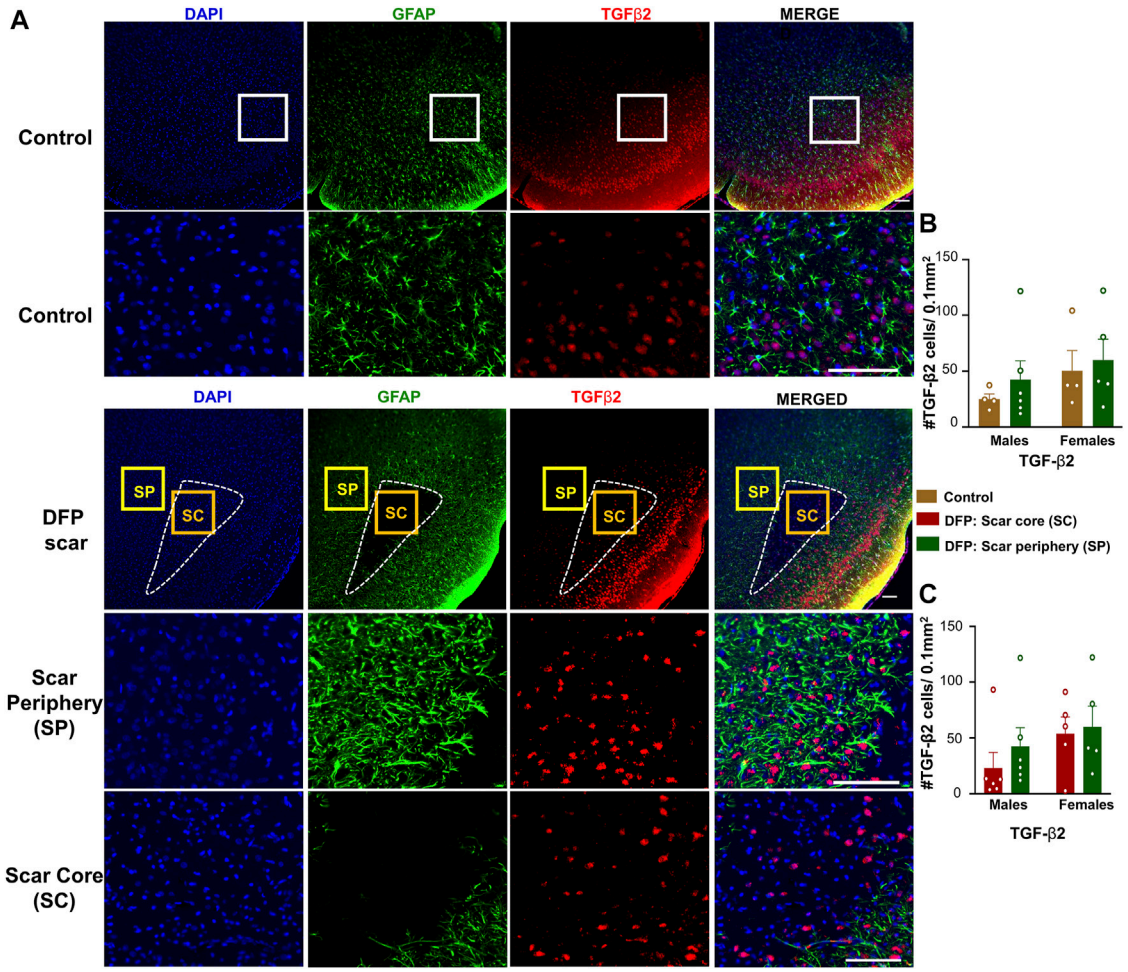

FIGURE 6 | TGF-β2 signaling in control animals and DFP treated animals with glial scarring. **(A)** Representative images for GFAP and TGF-β2. **(B)** The number of TGF-β2 positive cells in the scar periphery (SP) were compared to a similar region in controls. **(C)** Comparison of the number of TGF-β2 positive cells in the scar periphery and the scar core (SC). Mixed measures ANOVA, $n = 4–6$, $^*p < 0.05$. Scale = 50 μm.

epileptogenesis, though to our knowledge, no study has described reactive astrogliosis in which these cells form the periphery of a scar following systemic chemical epileptic insult (de Lanerolle et al., 2010; Robel et al., 2015; Verhoog et al., 2020).

Astrocytes surrounded the core of the scar. Compared to controls, these cells were more in number, hypertrophic, and expressed C3, which is considered a marker for reactive astrocytes (Liddelow et al., 2017; Hartmann et al., 2019; Putra et al., 2020b). C3 is part of the complement system, which is an important regulator of chemotaxis, phagocytosis, and cell adhesion (Frank and Fries, 1991). Though it was upregulated in DFP treated animals, there was still C3 positive staining in the control animals, which may suggest that basal levels play a role in normal brain function. One study showed that C3 knockout mice had increased axon regeneration following spinal cord injury implying its inhibitory role in neurite outgrowth (Peterson et al., 2017). In addition, C3 and other complement proteins are also known to play a role in astrocytes and microglia interaction. Following injury, C1q binds to the cell surface, leading to the cleavage of C3; the proteolytic products then bind to various receptors to initiate the activation of phagocytes (Van Beek et al., 2003; Wagner and Frank, 2009). However, it is unknown whether the C3 proteolytic products of the astrocytes surrounding the scar would influence the microglial function in the scar core.

Like the scars in the spinal cord injury, reactive astrocytes in glial scars of the piriform cortex surrounded a region containing large clusters of microglia. These microglia were reactive in their morphology and also expressed CD68, a marker for microglial activation (Di Gregorio et al., 2005). Notably, both microglia and macrophages express both IBA1 and CD68, so it is possible that macrophages were also present due to the disruption of the blood-brain-barrier post-SE (da Fonseca et al., 2014; Ramprasad et al., 1996). In this study, we found a reduction in neurons (NeuN positive cells) in the scar core (compared to the scar periphery in females), indicating neuronal death and clearance by microglia and macrophages (CD68 positive cells). Similarly, there was an increase in iNOS positive cells in the glial scar region implying increased release of NO that causes neurodegeneration

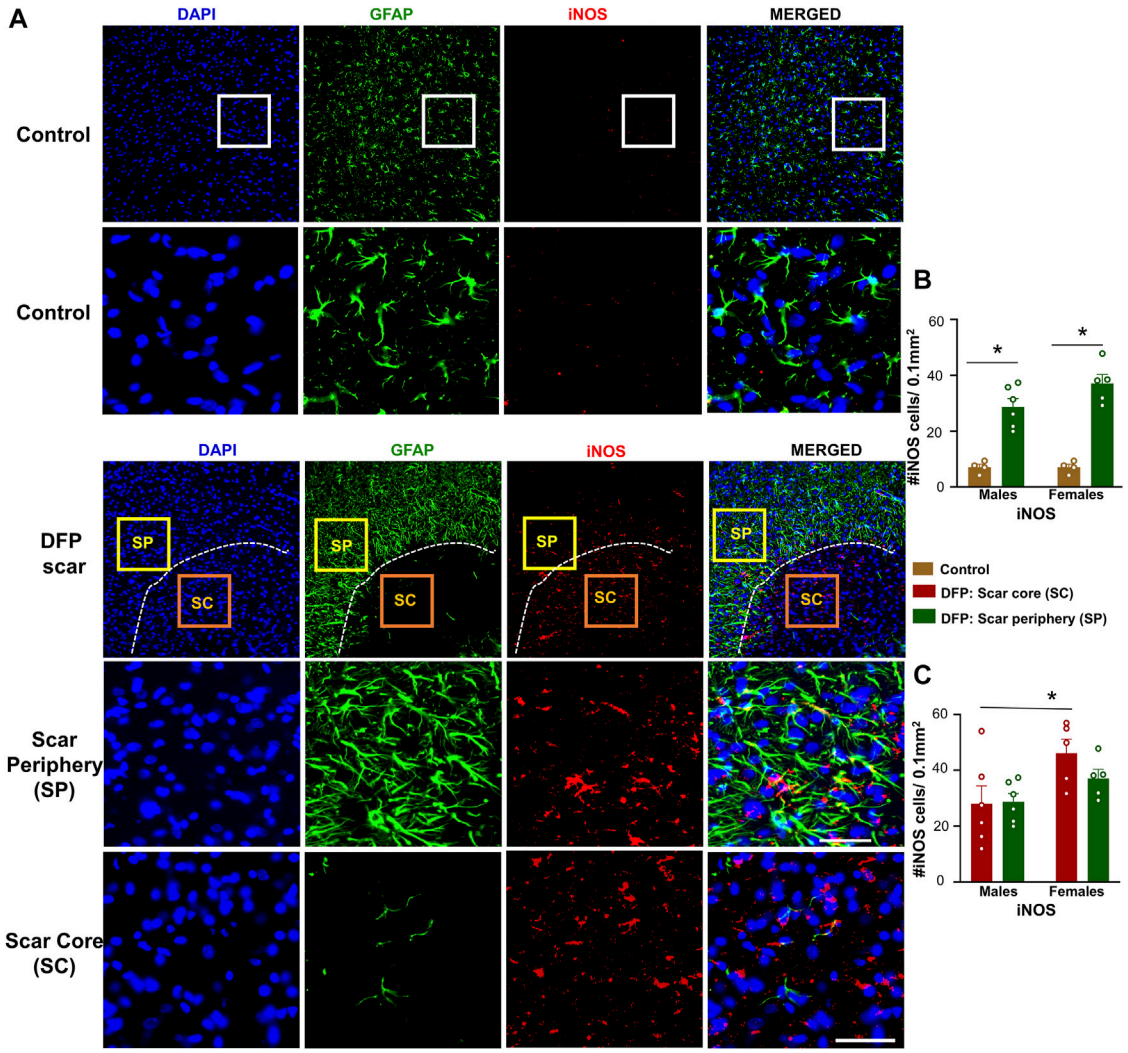

FIGURE 7 | Inducible nitric oxide synthase (iNOS) signaling in control animals and DFP treated animals with glial scarring. **(A)** Representative images for GFAP and iNOS. **(B)** The number of iNOS positive cells in the scar periphery (SP) were compared to a similar region in controls. **(C)** Comparison of the number of iNOS positive cells in the scar periphery and the scar core (SC). Mixed measures ANOVA, $n = 4–6$, $^*p < 0.05$. Scale = 50 μm.

(Thippeswamy et al., 2006; Doherty, 2011). It is important to note that there was no significant reduction in neurons in the DFP-treated groups compared to their respective controls (though there was a trend). This requires further investigation, perhaps with a large sample size and SE severity-matched DFP-treated animals. Likely, the astrocytes respond to microglia-induced neuronal injury to form the scar (Van Beek et al., 2003; Wagner and Frank, 2009). Further investigation will reveal the time-dependent progression of glial scar formation development.

TGF-βs are a pleiotropic cytokines that are involved in regulating the growth and differentiation of various cells, immune regulation, and extracellular matrix metabolism (Vivien and Ali, 2006; Dobolyi et al., 2012). TGF-βs elicit responses *via* interaction with TGF-β receptors and subsequent activation of Smad transcription factors (Hiew et al., 2021). In the context of neurological disease, TGF-βs are sometimes shown to be neuroprotective and are downregulated in many models of neurological disease (Tesseur et al., 2006; Vivien and Ali, 2006; Kashima and Hata, 2018). In contrast, some studies show that TGF-βs could be responsible for the initiation of the glial scar post spinal cord injury (Buss et al., 2007; Shiying et al., 2017; Song et al., 2019). TGF-β1 has been reported to be upregulated early in scar formation while TGF-β2 is upregulated at a later stage (Lagord et al., 2002; Silver and Miller, 2004). Interestingly, we did not find a significant upregulation of TGF-β1 or TGF-β2 in the scars of the DFP treated animals compared to controls which might suggest that these scars respond to injury independent of TGF-β signaling or that the signaling plays a role earlier or later into scar development as this study was limited to 8 days post-DFP intoxication.

Glial scars elsewhere are also associated with the upregulation of chondroitin sulfate proteoglycans (CPSGs). CSPGs are one of several proteoglycan families, which perform a wide variety of functions throughout the body related to development, tissue repair, and organization of cellular structure (Couchman and Pataki, 2012; Iozzo and Schaefer, 2015). In the brain, CSPGs are

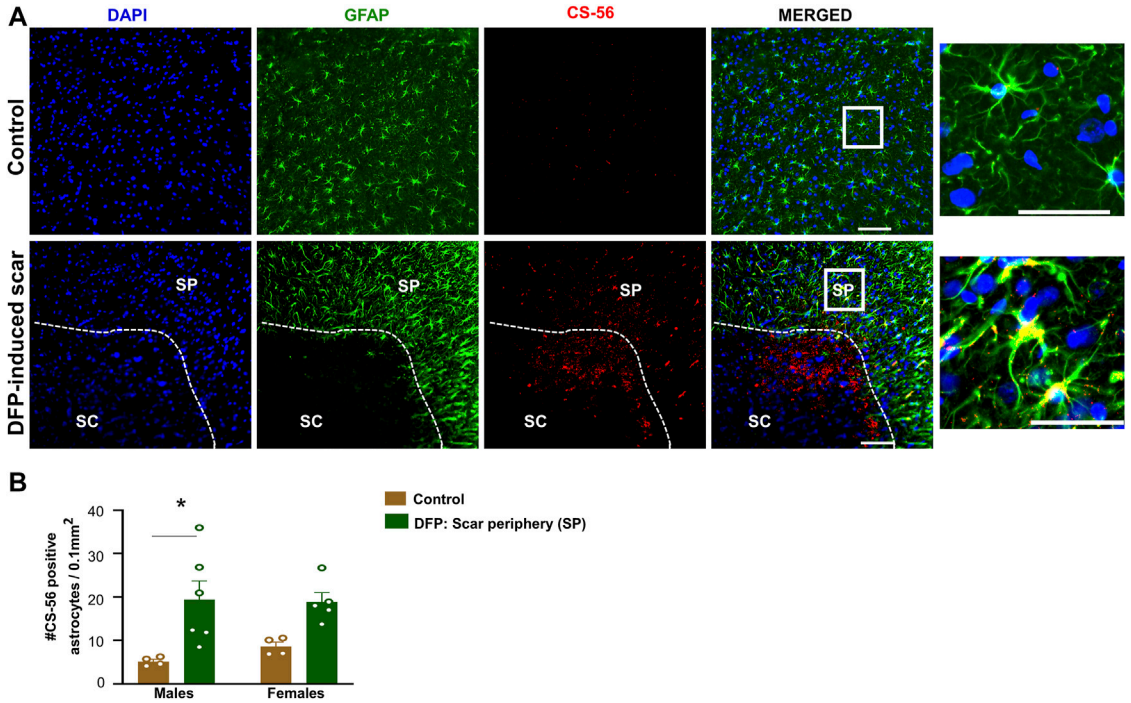

FIGURE 8 | Chromatin sulfate proteoglycan (CS-56) and GFAP staining. **(A)** Representative images for GFAP and CS-56. **(B)** CS-56 positive astrocytes in the scar periphery (SP) were compared to a similar region in controls. Mixed measures ANOVA, $n = 4–6$, $^*p < 0.05$. Scale = 50 μm.

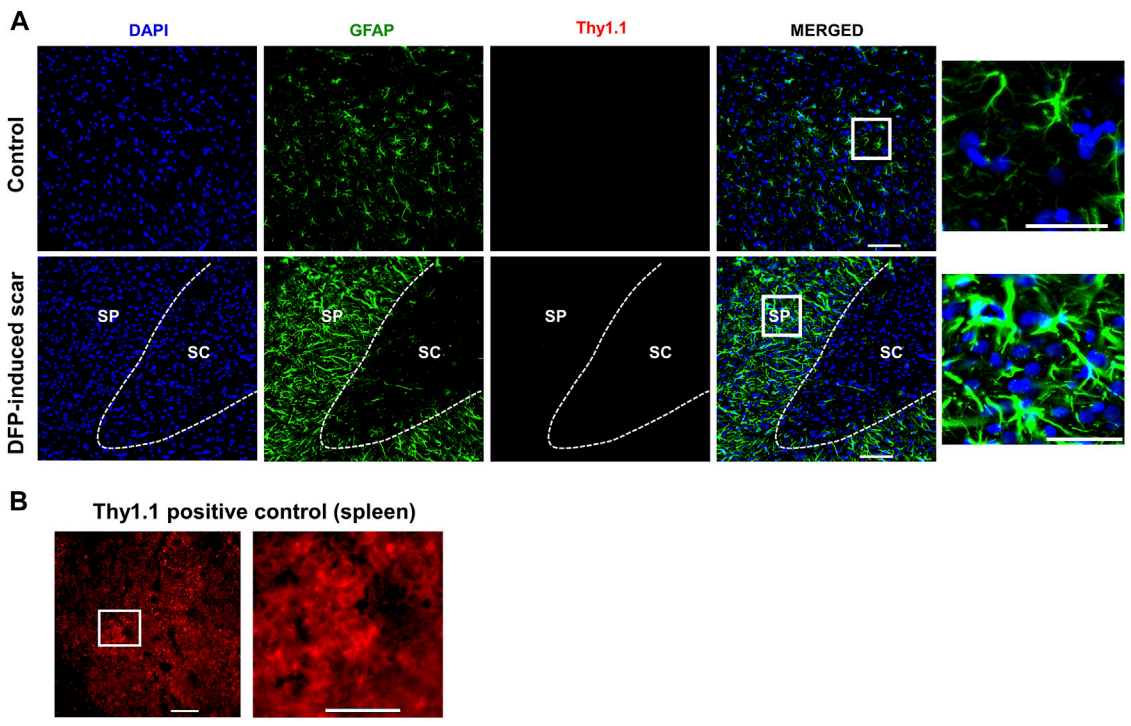

FIGURE 9 | No fibroblasts (Thy1.1) in the scar region. **(A)** There was no Thy 1.1 positive staining in the scar periphery (SP) or scar core (SC) DFP-induced glial scars or in controls. **(B)** Thy1.1 positive staining in the spleen. Scale = 50 μm.

known to be produced by neurons and astrocytes and are upregulated in a variety of neurological disorders, including spinal cord injury, multiple sclerosis, ischemia (Davies et al., 1999; Carmichael et al., 2005; Deguchi et al., 2005; Siebert et al., 2014). One study in an epilepsy model found increased CPSGs in the mouse cortex following kainate administration (i.p); they also showed increased seizure susceptibility in mice overexpressing chondroitin 6-sulfated chains (C6ST-1) (Yutsudo and Kitagawa, 2015). However, the mouse study did not report the occurrence of glial scars in the hippocampus or in the cortex in either C6ST-1 transgenic mice or wild-type C57BL/6 mice. In the rat DFP model, we found an increase of CS-56, a marker of CPSGs, in the astrocytes surrounding the scars. In the context of glial scars, proteoglycans are thought to be inhibitory for neuronal growth, but their function is unclear in DFP-induced neurotoxicity (McKeon et al., 1999). Importantly, the CSPGs consist of a wide family of molecules including, but not limited to, versican, neurocan, aggrecan and brevican, each of which may play different roles during scar development (Avram et al., 2014). Future work could determine the roles of each specific CSPGs as well as other families of proteoglycans.

Classical spinal cord glial scars also contain fibroblasts that originate from meninges, choroid plexus, and perivascular spaces (Dorrier et al., 2021; Silver and Miller, 2004; Xu and Yao, 2021). In the rat DFP study, no trauma was involved. However, we tested for fibroblasts marker, Thy 1.1, since the scar was close to the external surface of the cortex (Phipps et al., 1989). We did not detect Thy1.1 positive cells in the glial scars, likely due to the nature of injury caused by DFP. Traumatic brain injury compromises the blood-brain-barrier integrity; thus, reports suggest fibroblast infiltration into the injured site from the perivascular spaces (Kawano et al., 2012).

The cellular mechanisms of glial scars following spinal cord injury are temporal in nature (Silver and Miller, 2004; Duan et al., 2015). In our 8-days timepoint study, we characterized the cell types of the glial scar. However, it would be interesting to look at a longer timepoint, to see how long these scars persist and whether the molecular markers and cell-cell interactions change over time. Future work could use more advanced imaging techniques to track the presence and size of the scar over time and the impact of interventional drugs. It would also be interesting to characterize these scars in other models of chemoconvulsant-induced epilepsy such as the kainate, pilocarpine, or more potent OPNA models. This might reveal some interesting model differences in glial scar formation.

CONCLUSION

This is the first report of a cortical glial scar following systemic chemoconvulsant-induced SE, like those seen after mechanical injury to the brain or spinal cord (Silver and Miller, 2004; Wang et al., 2018). Scars were characterized by a core consisting of large clusters of phagocytic microglia and macrophages, characterized by a significant increase in iNOS and CD68. These phagocytic microglia and iNOS likely led to neurodegeneration which was evidenced by the reduction of NeuN in the scar core, though not statistically significant. The periphery of the scar consisted of hypertrophic, C3, and CSPG expressing astrocytes though there was no change in TGF-β1 or TGF-β2 expression. Future studies could use other glial and neuronal-specific signaling pathway markers to better understand the molecular mechanisms involved in scar formation. Importantly, it is unknown whether these scars are protective or harmful in the context of DFP-induced epilepsy. Future studies could correlate the prevalence or size of these scars with other epileptogenic parameters such as spontaneous seizures, electrographic spikes, or other changes in neurobehavior. With regard to spinal cord injury, these scars were first thought to be a barrier to recovery, but later studies revealed that these scars may be essential in preventing the spread of injury (Yang et al., 2020). Some studies have shown that scars can be modulated through a variety of pharmacological manipulation such as the inhibition of periostin (an extracellular matrix molecule) or inhibition of CSPGs to prevent the formation of scars (Yokota et al., 2017; Yang et al., 2020). Application of these inhibitors during early epileptogenesis combined with antiseizure drugs and/or disease-modifying agents could minimize undesired effects of these scars following DFP induced SE. In summary, this is the first study to characterize glial scars following chemoconvulsant induced SE in the rat DFP model.

DATA AVAILABILITY STATEMENT

The raw data supporting the conclusion of this article will be made available by the authors, without undue reservation.

ETHICS STATEMENT

The animal study was reviewed and approved by Iowa state Institutional Animal Care and Use Committee.

AUTHOR CONTRIBUTIONS

MEG (1st author) conducted DFP experiments, compiled and analysed data, drafted and edited the manuscript. MEG (2nd author) analysed data and edited the manuscript. TT secured funding for the project, offered intellectual input, and edited the manuscript.

FUNDING

Support to TT was provided by the National Institutes of Health/NINDS (NS110648 and NS120916) through the CounterACT program.

SUPPLEMENTARY MATERIAL

The Supplementary Material for this article can be found online at: https://www.frontiersin.org/articles/10.3389/fcell.2022.867949/full#supplementary-material

REFERENCES

Abbott, N. J., Rönnbäck, L., and Hansson, E. (2006). Astrocyte-endothelial Interactions at the Blood-Brain Barrier. *Nat. Rev. Neurosci.* 7 (Issue 1), 41–53. doi:10.1038/nrn1824

Anderson, M. A., Burda, J. E., Ren, Y., Ao, Y., O'Shea, T. M., Kawaguchi, R., et al. (2016). Astrocyte Scar Formation Aids central Nervous System Axon Regeneration. *Nature* 532 (7598), 195–200. doi:10.1038/NATURE17623

Aroniadou-Anderjaska, V., Figueiredo, T. H., Apland, J. P., Prager, E. M., Pidoplichko, V. I., Miller, S. L., et al. (2016). Long-term Neuropathological and Behavioral Impairments after Exposure to Nerve Agents. *Ann. N.Y. Acad. Sci.* 1374 (1), 17–28. doi:10.1111/NYAS.13028

Aroniadou-Anderjaska, V., Figueiredo, T. H., Apland, J. P., Qashu, F., and Braga, M. F. M. (2009). Primary Brain Targets of Nerve Agents: The Role of the Amygdala in Comparison to the hippocampus. *NeuroToxicology* 30 (5), 772–776. doi:10.1016/j.neuro.2009.06.011

Avram, S., Shaposhnikov, S., Buiu, C., and Mernea, M. (2014). Chondroitin Sulfate Proteoglycans: Structure-Function Relationship with Implication in Neural Development and Brain Disorders. *Biomed. Res. Int.* 2014, 1–11. doi:10.1155/2014/642798

Bar-Klein, G., Cacheaux, L. P., Kamintsky, L., Prager, O., Weissberg, I., Schoknecht, K., et al. (2014). Losartan Prevents Acquired Epilepsy *via* TGF-β Signaling Suppression. *Ann. Neurol.* 75 (6), 864–875. doi:10.1002/ana.24147

Beek, J., Elward, K., and Gasque, P. (2003). Activation of Complement in the Central Nervous System. *Ann. N Y Acad. Sci.* 992 (1), 56–71. doi:10.1111/J.1749-6632.2003.TB03138.X

Beghi, E., and Hesdorffer, D. (2014). Prevalence of Epilepsy-An Unknown Quantity. *Epilepsia* 55 (7), 963–967. doi:10.1111/epi.12579

Benarroch, E. E. (2016). Astrocyte Signaling and Synaptic Homeostasis. *Neurology* 87 (3), 324–330. doi:10.1212/WNL.0000000000002875

Buss, A., Pech, K., Kakulas, B. A., Martin, D., Schoenen, J., Noth, J., et al. (2007). TGF-β1 and TGF-B2 Expression after Traumatic Human Spinal Cord Injury. *Spinal Cord* 46 (55), 364–371. doi:10.1038/sj.sc.3102148

Carmichael, S. T., Archibeque, I., Luke, L., Nolan, T., Momiy, J., and Li, S. (2005). Growth-associated Gene Expression after Stroke: Evidence for a Growth-Promoting Region in Peri-Infarct Cortex. *Exp. Neurol.* 193 (2), 291–311. doi:10.1016/J.EXPNEUROL.2005.01.004

Clarke, L. E., and Barres, B. A. (2013). Emerging Roles of Astrocytes in Neural Circuit Development. *Nat. Rev. Neurosci.* 14 (5), 311–321. doi:10.1038/nrn3484

Couchman, J. R., and Pataki, C. A. (2012). An Introduction to Proteoglycans and Their Localization. *J. Histochem. Cytochem.* 60 (12), 885–897. doi:10.1369/0022155412464638

Cregg, J. M., DePaul, M. A., Filous, A. R., Lang, B. T., Tran, A., and Silver, J. (2014). Functional Regeneration beyond the Glial Scar. *Exp. Neurol.* 253, 197–207. doi:10.1016/J.EXPNEUROL.2013.12.024

Curia, G., Longo, D., Biagini, G., Jones, R. S. G., and Avoli, M. (2008). The Pilocarpine Model of Temporal Lobe Epilepsy. *J. Neurosci. Methods* 172 (Issue 2), 143–157. doi:10.1016/j.jneumeth.2008.04.019

da Fonseca, A. C. C., Matias, D., Garcia, C., Amaral, R., Geraldo, L. H., Freitas, C., et al. (2014). The Impact of Microglial Activation on Blood-Brain Barrier in Brain Diseases. *Front. Cel. Neurosci.* 8 (Issue November), 1–13. doi:10.3389/fncel.2014.00362

Davies, S. J. A., Goucher, D. R., Doller, C., and Silver, J. (1999). Robust Regeneration of Adult Sensory Axons in Degenerating White Matter of the Adult Rat Spinal Cord. *J. Neurosci.* 19 (14), 5810–5822. doi:10.1523/JNEUROSCI.19-14-05810.1999

Db, D. (1930). Degeneration and Regeneration of the Nervous System. *Nature* 125 (3146), 3146230–3146231. doi:10.1038/125230a0

Deguchi, K., Takaishi, M., Hayashi, T., Oohira, A., Nagotani, S., Li, F., et al. (2005). Expression of Neurocan after Transient Middle Cerebral Artery Occlusion in Adult Rat Brain. *Brain Res.* 1037 (1–2), 194–199. doi:10.1016/J.BRAINRES.2004.12.016

Di Gregorio, G. B., Yao-Borengasser, A., Rasouli, N., Varma, V., Lu, T., Miles, L. M., et al. (2005). Expression of CD68 and Macrophage Chemoattractant Protein-1 Genes in Human Adipose and Muscle Tissues. *Diabetes* 54 (8), 2305–2313. doi:10.2337/DIABETES.54.8.2305

Dobolyi, A., Vincze, C., Pál, G., and Lovas, G. (2012). The Neuroprotective Functions of Transforming Growth Factor Beta Proteins. *Ijms* 13 (7), 8219–8258. doi:10.3390/IJMS13078219

Doherty, G. H. (2011). Nitric Oxide in Neurodegeneration: Potential Benefits of Non-steroidal Anti-inflammatories. *Neurosci. Bull.* 27 (6), 366–382. doi:10.1007/S12264-011-1530-6

Dorrier, C. E., Jones, H. E., Pintarić, L., Siegenthaler, J. A., and Daneman, R. (2021). Emerging Roles for CNS Fibroblasts in Health, Injury and Disease. *Nat. Rev. Neurosci.* 2323 (11), 23–34. doi:10.1038/s41583-021-00525-w

Duan, H., Ge, W., Zhang, A., Xi, Y., Chen, Z., Luo, D., et al. (2015). Transcriptome Analyses Reveal Molecular Mechanisms Underlying Functional Recovery after Spinal Cord Injury. *Proc. Natl. Acad. Sci. U.S.A.* 112 (43), 13360–13365. doi:10.1073/PNAS.1510176112/-/DCSUPPLEMENTAL

Dusart, I., Marty, S., and Peschanski, M. (1991). Glial Changes Following an Excitotoxic Lesion in the CNS-II. Astrocytes. *Neuroscience* 45 (3), 541–549. doi:10.1016/0306-4522(91)90269-T

Engel, J. (2014). Approaches to Refractory Epilepsy. *Ann. Indian Acad. Neurol.* 17 (Suppl. 1), 12. doi:10.4103/0972-2327.128644

Farrell, J. S., Wolff, M. D., and Teskey, G. C. (2017). Neurodegeneration and Pathology in Epilepsy: Clinical and Basic Perspectives. *Adv. Neurobiol.* 15, 317–334. doi:10.1007/978-3-319-57193-5_12

Fawcett, J. W., and Asher, R. A. (1999). The Glial Scar and central Nervous System Repair. *Brain Res. Bull.* 49 (6), 377–391. doi:10.1016/S0361-9230(99)00072-6

Fisher, R. S., Boas, W. v. E., Blume, W., Elger, C., Genton, P., Lee, P., et al. (2005). Epileptic Seizures and Epilepsy: Definitions Proposed by the International League against Epilepsy (ILAE) and the International Bureau for Epilepsy (IBE). *Epilepsia* 46 (4), 470–472. doi:10.1111/j.0013-9580.2005.66104.x

Frank, M. M., and Fries, L. F. (1991). The Role of Complement in Inflammation and Phagocytosis. *Immunol. Today* 12 (9), 322–326. doi:10.1016/0167-5699(91)90009-I

French, J. A. (2007). Refractory Epilepsy: Clinical Overview. *Epilepsia* 48 (Suppl. 1), 3–7. doi:10.1111/j.1528-1167.2007.00992.x

Frik, J., Merl-Pham, J., Plesnila, N., Mattugini, N., Kjell, J., Kraska, J., et al. (2018). Cross-talk between Monocyte Invasion and Astrocyte Proliferation Regulates Scarring in Brain Injury. *EMBO Rep.* 19 (5), e45294. doi:10.15252/EMBR.201745294

Gage, M., Golden, M., Putra, M., Sharma, S., and Thippeswamy, T. (2020). Sex as a Biological Variable in the Rat Model of Diisopropylfluorophosphate-induced Long-term Neurotoxicity. *Ann. N.Y. Acad. Sci.* 1479, 44–64. doi:10.1111/nyas.14315

Gage, M., Putra, M., Gomez-Estrada, C., Golden, M., Wachter, L., Gard, M., et al. (2021a). Differential Impact of Severity and Duration of Status Epilepticus, Medical Countermeasures, and a Disease-Modifier, Saracatinib, on Brain Regions in the Rat Diisopropylfluorophosphate Model. *Front. Cel. Neurosci.* 15, 426. doi:10.3389/FNCEL.2021.772868

Gage, M., Putra, M., Wachter, L., Dishman, K., Gard, M., Gomez-Estrada, C., et al. (2021b). Saracatinib, a Src Tyrosine Kinase Inhibitor, as a Disease Modifier in the Rat DFP Model: Sex Differences, Neurobehavior, Gliosis, Neurodegeneration, and Nitro-Oxidative Stress. *Antioxidants* 11 (1), 61. doi:10.3390/ANTIOX11010061

Garry, P. S., Ezra, M., Rowland, M. J., Westbrook, J., and Pattinson, K. T. S. (2015). The Role of the Nitric Oxide Pathway in Brain Injury and its Treatment - from Bench to Bedside. *Exp. Neurol.* 263, 235–243. doi:10.1016/j.expneurol.2014.10.017

Guignet, M., Dhakal, K., Flannery, B. M., Hobson, B. A., Zolkowska, D., Dhir, A., et al. (2020). Persistent Behavior Deficits, Neuroinflammation, and Oxidative Stress in a Rat Model of Acute Organophosphate Intoxication. *Neurobiol. Dis.* 133, 104431. doi:10.1016/j.nbd.2019.03.019

Hartmann, K., Sepulveda-Falla, D., Rose, I. V. L., Madore, C., Muth, C., Matschke, J., et al. (2019). Complement 3+-astrocytes Are Highly Abundant in Prion Diseases, but Their Abolishment Led to an Accelerated Disease Course and Early Dysregulation of Microglia. *Acta Neuropathol. Commun.* 7 (1), 83. doi:10.1186/S40478-019-0735-1/FIGURES/7

Hiew, L.-F., Poon, C.-H., You, H.-Z., and Lim, L.-W. (2021). TGF-β/Smad Signalling in Neurogenesis: Implications for Neuropsychiatric Diseases. *Cells* 10 (6), 1382. doi:10.3390/CELLS10061382

Hirtz, D., Thurman, D. J., Gwinn-Hardy, K., Mohamed, M., Chaudhuri, A. R., and Zalutsky, R. (2007). How Common Are the "Common" Neurologic Disorders? *Neurology* 68 (5), 326–337. doi:10.1212/01.wnl.0000252807.38124.a3

Hussein, R. K., Mencio, C. P., Katagiri, Y., Brake, A. M., and Geller, H. M. (2020). Role of Chondroitin Sulfation Following Spinal Cord Injury. *Front. Cel. Neurosci.* 14, 208. doi:10.3389/FNCEL.2020.00208/BIBTEX

Iozzo, R. V., and Schaefer, L. (2015). Proteoglycan Form and Function: A Comprehensive Nomenclature of Proteoglycans. *Matrix Biol.* 42, 11–55. doi:10.1016/J.MATBIO.2015.02.003

Jett, D. A. (2012). Chemical Toxins that Cause Seizures. *NeuroToxicology* 33 (6), 1473–1475. doi:10.1016/J.NEURO.2012.10.005

Kashima, R., and Hata, A. (2018). The Role of TGF-β Superfamily Signaling in Neurological Disorders. *Acta Biochim. Biophys. Sinica* 50 (1), 106–120. doi:10.1093/ABBS/GMX124

Kawano, H., Kimura-Kuroda, J., Komuta, Y., Yoshioka, N., Li, H. P., Kawamura, K., et al. (2012). Role of the Lesion Scar in the Response to Damage and Repair of the central Nervous System. *Cell Tissue Res* 349 (1), 169–180. doi:10.1007/S00441-012-1336-5

Lagord, C., Berry, M., and Logan, A. (2002). Expression of TGFβ2 but Not TGFβ1 Correlates with the Deposition of Scar Tissue in the Lesioned Spinal Cord. *Mol. Cell Neurosci.* 20 (1), 69–92. doi:10.1006/MCNE.2002.1121

Lanerolle, N. C., Lee, T.-S., and Spencer, D. D. (2010). Astrocytes and Epilepsy. *Neurotherapeutics* 7 (4), 424–438. doi:10.1016/j.nurt.2010.08.002

Leal-Filho, M. (2011). Spinal Cord Injury: From Inflammation to Glial Scar. *Surg. Neurol. Int.* 2 (1), 112. doi:10.4103/2152-7806.83732

Li, S., Gu, X., and Yi, S. (2017). The Regulatory Effects of Transforming Growth Factor-β on Nerve Regeneration. *Cel Transpl.* 26 (3), 381–394. doi:10.3727/096368916X693824

Liddelow, S. A., Guttenplan, K. A., Clarke, L. E., Bennett, F. C., Bohlen, C. J., Schirmer, L., et al. (2017). Neurotoxic Reactive Astrocytes Are Induced by Activated Microglia. *Nature* 541 (7638), 481–487. doi:10.1038/nature21029

Luo, F., Tran, A. P., Xin, L., Sanapala, C., Lang, B. T., Silver, J., et al. (2018). Modulation of Proteoglycan Receptor PTPσ Enhances MMP-2 Activity to Promote Recovery from Multiple Sclerosis. *Nat. Commun.* 9 (11), 1–16. doi:10.1038/s41467-018-06505-6

McDonough, J. H., and Shih, T.-M. (1997). Neuropharmacological Mechanisms of Nerve Agent-Induced Seizure and Neuropathology 1 1The Animals Used in Studies Performed in, or Sponsored by, This Institute Were Handled in Accordance with the Principles Stated in the Guide for the Care and Use of Laboratory Animals, Proposed by the Committee on Care and Use of Laboratory Animals of the Institute of Laboratory Animal Resources, National Research Council, DHHA, National Institute of Health Publication #85-23, 1985, and the Animal Welfare Act of 1966, as Amended. The Opinions, or Assertions Contained Herein Are the Private Views of the Authors, and Are Not to Be Construed as Reflecting the Views of the Department of the Army or the Department of Defense. *Neurosci. Biobehavioral Rev.* 21 (5), 559–579. doi:10.1016/S0149-7634(96)00050-4

McKeon, R. J., Jurynec, M. J., and Buck, C. R. (1999). The Chondroitin Sulfate Proteoglycans Neurocan and Phosphacan Are Expressed by Reactive Astrocytes in the Chronic CNS Glial Scar. *J. Neurosci.* 19 (24), 10778–10788. doi:10.1523/JNEUROSCI.19-24-10778.1999

Millard, C. B., Kryger, G., Ordentlich, A., Greenblatt, H. M., Harel, M., Raves, M. L., et al. (1999). Crystal Structures of Aged Phosphonylated Acetylcholinesterase: Nerve Agent Reaction Products at the Atomic Level,. *Biochemistry* 38 (22), 7032–7039. doi:10.1021/bi982678l

Miyaki, K., Nishiwaki, Y., Maekawa, K., Ogawa, Y., Asukai, N., Yoshimura, K., et al. (2005). Effects of Sarin on the Nervous System of Subway Workers Seven Years after the Tokyo Subway Sarin Attack. *Jrnl Occup. Health* 47 (4), 299–304. doi:10.1539/joh.47.299

Morita, H., Yanagisawa, N., Nakajima, T., Shimizu, M., Hirabayashi, H., Okudera, H., et al. (1995). Sarin Poisoning in Matsumoto, Japan. *Lancet* 346 (8970), 290–293. doi:10.1016/s0140-6736(95)92170-2

Okumura, T., Takasu, N., Ishimatsu, S., Miyanoki, S., Mitsuhashi, A., Kumada, K., et al. (1996). Report on 640 Victims of the Tokyo Subway Sarin Attack. *Ann. Emerg. Med.* 28 (2), 129–135. doi:10.1016/s0196-0644(96)70052-5

Pekny, M., and Pekna, M. (2016). Reactive Gliosis in the Pathogenesis of CNS Diseases. *Biochim. Biophys. Acta (Bba) - Mol. Basis Dis.* 1862 (3), 483–491. doi:10.1016/J.BBADIS.2015.11.014

Peterson, S. L., Nguyen, H. X., Mendez, O. A., and Anderson, A. J. (2017). Complement Protein C3 Suppresses Axon Growth and Promotes Neuron Loss. *Sci. Rep.* 7 (1), 1–13. doi:10.1038/s41598-017-11410-x

Phipps, R. P., Penney, D. P., Keng, P., Quill, H., Paxhia, A., Derdak, S., et al. (1989). Characterization of Two Major Populations of Lung Fibroblasts: Distinguishing Morphology and Discordant Display of Thy 1 and Class II MHC. *Am. J. Respir. Cel Mol Biol* 1 (1), 65–74. doi:10.1165/AJRCMB/1.1.65

Pitkänen, A., and Engel, J. (2014). Past and Present Definitions of Epileptogenesis and its Biomarkers. *Neurotherapeutics* 11 (2), 231–241. doi:10.1007/S13311-014-0257-2

Properzi, F., Carulli, D., Asher, R. A., Muir, E., Camargo, L. M., Van Kuppevelt, T. H., et al. (2005). Chondroitin 6-sulphate Synthesis Is Up-Regulated in Injured CNS, Induced by Injury-Related Cytokines and Enhanced in Axon-Growth Inhibitory Glia. *Eur. J. Neurosci.* 21 (2), 378–390. doi:10.1111/J.1460-9568.2005.03876.X

Putra, M., Gage, M., Sharma, S., Gardner, C., Gasser, G., Anantharam, V., et al. (2020b). Diapocynin, an NADPH Oxidase Inhibitor, Counteracts Diisopropylfluorophosphate-induced Long-term Neurotoxicity in the Rat Model. *Ann. N.Y. Acad. Sci.* 1479, 75–93. doi:10.1111/nyas.14314

Putra, M., Sharma, S., Gage, M., Gasser, G., Hinojo-Perez, A., Olson, A., et al. (2020a). Inducible Nitric Oxide Synthase Inhibitor, 1400W, Mitigates DFP-Induced Long-Term Neurotoxicity in the Rat Model. *Neurobiol. Dis.* 133, 104443. doi:10.1016/j.nbd.2019.03.031

Puttachary, S., Sharma, S., Verma, S., Yang, Y., Putra, M., Thippeswamy, A., et al. (2016). 1400W, a Highly Selective Inducible Nitric Oxide Synthase Inhibitor Is a Potential Disease Modifier in the Rat Kainate Model of Temporal Lobe Epilepsy. *Neurobiol. Dis.* 93, 184–200. doi:10.1016/j.nbd.2016.05.013

Racine, R. J. (1972). Modification of Seizure Activity by Electrical Stimulation: II. Motor Seizure. *Electroencephalography Clin. Neurophysiol.* 32 (3), 281–294. doi:10.1016/0013-4694(72)90177-0

Ramprasad, M. P., Terpstra, V., Kondratenko, N., Quehenberger, O., and Steinberg, D. (1996). Cell Surface Expression of Mouse Macrosialin and Human CD68 and Their Role as Macrophage Receptors for Oxidized Low Density Lipoprotein. *Proc. Natl. Acad. Sci.* 93 (25), 14833–14838. doi:10.1073/PNAS.93.25.14833

Rana, A., and Musto, A. E. (2018). The Role of Inflammation in the Development of Epilepsy. *J. Neuroinflammation* 15 (Issue 1), 1–12. doi:10.1186/s12974-018-1192-7

Robel, S. (2017). Astroglial Scarring and Seizures. *Neuroscientist* 23 (2), 152–168. doi:10.1177/1073858416645498

Robel, S., Buckingham, S. C., Boni, J. L., Campbell, S. L., Danbolt, N. C., Riedemann, T., et al. (2015). Reactive Astrogliosis Causes the Development of Spontaneous Seizures. *J. Neurosci.* 35 (8), 3330–3345. doi:10.1523/JNEUROSCI.1574-14.2015

Rolls, A., Shechter, R., and Schwartz, M. (2009). The Bright Side of the Glial Scar in CNS Repair. *Nat. Rev. Neurosci.* 10 (3), 235–241. doi:10.1038/nrn2591

Schiweck, J., Murk, K., Ledderose, J., Münster-Wandowski, A., Ornaghi, M., Vida, I., et al. (2021). Drebrin Controls Scar Formation and Astrocyte Reactivity upon Traumatic Brain Injury by Regulating Membrane Trafficking. *Nat. Commun.* 12 (1), 1–16. doi:10.1038/s41467-021-21662-x

Seinfeld, S., Goodkin, H. P., and Shinnar, S. (2016). Status Epilepticus. *Cold Spring Harb Perspect. Med.* 6 (3), a022830. doi:10.1101/cshperspect.a022830

Sharma, S., Carlson, S., Gregory-Flores, A., Hinojo-Perez, A., Olson, A., and Thippeswamy, T. (2021). Mechanisms of Disease-Modifying Effect of Saracatinib (AZD0530), a Src/Fyn Tyrosine Kinase Inhibitor, in the Rat Kainate Model of Temporal Lobe Epilepsy. *Neurobiol. Dis.* 156, 105410. doi:10.1016/j.nbd.2021.105410

Siebert, J. R., Conta Steencken, A., and Osterhout, D. J. (2014). Chondroitin Sulfate Proteoglycans in the Nervous System: Inhibitors to Repair. *Biomed. Res. Int.* 2014, 1–15. doi:10.1155/2014/845323

Silver, J., and Miller, J. H. (2004). Regeneration beyond the Glial Scar. *Nat. Rev. Neurosci.* 5 (22), 146–156. doi:10.1038/nrn1326

Sofroniew, M. V. (2015). Astrocyte Barriers to Neurotoxic Inflammation. *Nat. Rev. Neurosci.* 16 (5), 249–263. doi:10.1038/NRN3898

Sofroniew, M. V. (2005). Reactive Astrocytes in Neural Repair and protection. *Neuroscientist* 11 (5), 400–407. doi:10.1177/1073858405278321

Song, G., Yang, R., Zhang, Q., Chen, L., Huang, D., Zeng, J., et al. (2019). TGF-β Secretion by M2 Macrophages Induces Glial Scar Formation by Activating

Astrocytes *In Vitro*. *J. Mol. Neurosci.* 69 (2), 324–332. doi:10.1007/S12031-019-01361-5

Stafstrom, C. E., and Carmant, L. (2015). Seizures and Epilepsy: An Overview for Neuroscientists. *Cold Spring Harbor Perspect. Med.* 5 (6), a022426. doi:10.1101/CSHPERSPECT.A022426

Sugar, O., and Gerard, R. W. (1940). SPINAL CORD REGENERATION IN THE RAT. *J. Neurophysiol.* 3 (1), 1–19. doi:10.1152/JN.1940.3.1.1

Suzuki, T., Morita, H., Ono, K., Maekawa, K., Nagai, R., Yazaki, Y., et al. (1995). Sarin Poisoning in Tokyo Subway. *The Lancet* 345 (8955), 980–981. doi:10.1016/s0140-6736(95)90726-2

Tesseur, I., Zou, K., Esposito, L., Bard, F., Berber, E., Can, J. V., et al. (2006). Deficiency in Neuronal TGF-β Signaling Promotes Neurodegeneration and Alzheimer's Pathology. *J. Clin. Invest.* 116 (11), 3060–3069. doi:10.1172/JCI27341

Thippeswamy, T., McKay, J. S., Quinn, J. P., and Morris, R. (2006). Nitric Oxide, a Biological Double-Faced Janus-Iis This Good or Bad? *Histol. Histopathol* 21, 445–458. doi:10.14670/HH-21.445

Todorovic, M. S., Cowan, M. L., Balint, C. A., Sun, C., and Kapur, J. (2012). Characterization of Status Epilepticus Induced by Two Organophosphates in Rats. *Epilepsy Res.* 101 (3), 268–276. doi:10.1016/j.eplepsyres.2012.04.014

Tse, K., Beamer, E., Simpson, D., Beynon, R. J., Sills, G. J., and Thippeswamy, T. (2021). The Impacts of Surgery and Intracerebral Electrodes in C57BL/6J Mouse Kainate Model of Epileptogenesis: Seizure Threshold, Proteomics, and Cytokine Profiles. *Front. Neurol.* 12, 625017. doi:10.3389/FNEUR.2021.625017

Verhoog, Q. P., Holtman, L., Aronica, E., and van Vliet, E. A. (2020). Astrocytes as Guardians of Neuronal Excitability: Mechanisms Underlying Epileptogenesis. *Front. Neurol.* 11, 1541. doi:10.3389/FNEUR.2020.591690/BIBTEX

Vezzani, A., Dingledine, R., and Rossetti, A. O. (2015). Immunity and Inflammation in Status Epilepticus and its Sequelae: Possibilities for Therapeutic Application. *Expert Rev. Neurotherapeutics* 15 (9), 1081–1092. doi:10.1586/14737175.2015.1079130

Vivien, D., and Ali, C. (2006). Transforming Growth Factor-β Signalling in Brain Disorders. *Cytokine Growth Factor. Rev.* 17 (1–2), 121–128. doi:10.1016/J.CYTOGFR.2005.09.011

Voskuhl, R. R., Peterson, R. S., Song, B., Ao, Y., Morales, L. B. J., Tiwari-Woodruff, S., et al. (2009). Reactive Astrocytes Form Scar-like Perivascular Barriers to Leukocytes during Adaptive Immune Inflammation of the CNS. *J. Neurosci.* 29 (37), 11511–11522. doi:10.1523/JNEUROSCI.1514-09.2009

Wagner, E., and Frank, M. M. (2009). Therapeutic Potential of Complement Modulation. *Nat. Rev. Drug Discov.* 9 (1), 43–56. doi:10.1038/nrd3011

Wang, H., Song, G., Chuang, H., Chiu, C., Abdelmaksoud, A., Ye, Y., et al. (2018). Portrait of Glial Scar in Neurological Diseases. *Int. J. Immunopathol Pharmacol.* 31, 205873841880140–205873841880146. doi:10.1177/2058738418801406

Wanner, I. B., Anderson, M. A., Song, B., Levine, J., Fernandez, A., Gray-Thompson, Z., et al. (2013). Glial Scar Borders Are Formed by Newly Proliferated, Elongated Astrocytes that Interact to Corral Inflammatory and Fibrotic Cells *via* STAT3-dependent Mechanisms after Spinal Cord Injury. *J. Neurosci.* 33 (31), 12870–12886. doi:10.1523/JNEUROSCI.2121-13.2013

Xu, L., and Yao, Y. (2021). Central Nervous System Fibroblast-like Cells in Stroke and Other Neurological Disorders. *Stroke* 52 (7), 2456–2464. doi:10.1161/STROKEAHA.120.033431

Xu, S., Sun, Q., Fan, J., Jiang, Y., Yang, W., Cui, Y., et al. (2019). Role of Astrocytes in Post-traumatic Epilepsy. *Front. Neurol.* 10, 1149. doi:10.3389/FNEUR.2019.01149/BIBTEX

Yanagisawa, N., Morita, H., and Nakajima, T. (2006). Sarin Experiences in Japan: Acute Toxicity and Long-Term Effects. *J. Neurol. Sci.* 249 (1), 76–85. doi:10.1016/j.jns.2006.06.007

Yang, T., Dai, Y., Chen, G., and CuiSen, S. (2020). Dissecting the Dual Role of the Glial Scar and Scar-Forming Astrocytes in Spinal Cord Injury. *Front. Cel. Neurosci.* 14, 78. doi:10.3389/FNCEL.2020.00078/BIBTEX

Yokota, K., Kobayakawa, K., Saito, T., Hara, M., Kijima, K., Ohkawa, Y., et al. (2017). Periostin Promotes Scar Formation through the Interaction between Pericytes and Infiltrating Monocytes/Macrophages after Spinal Cord Injury. *Am. J. Pathol.* 187 (3), 639–653. doi:10.1016/J.AJPATH.2016.11.010

Yuan, Y.-M., and He, C. (2013). The glial scar in Spinal Cord Injury and Repair. *Neurosci. Bull.* 29 (4), 421–435. doi:10.1007/S12264-013-1358-3

Yutsudo, N., and Kitagawa, H. (2015). Involvement of Chondroitin 6-sulfation in Temporal Lobe Epilepsy. *Exp. Neurol.* 274, 126–133. doi:10.1016/J.EXPNEUROL.2015.07.009

Conflict of Interest: The authors declare that the research was conducted in the absence of any commercial or financial relationships that could be construed as a potential conflict of interest.

Publisher's Note: All claims expressed in this article are solely those of the authors and do not necessarily represent those of their affiliated organizations, or those of the publisher, the editors and the reviewers. Any product that may be evaluated in this article, or claim that may be made by its manufacturer, is not guaranteed or endorsed by the publisher.

frontiers | Frontiers in Cell and Developmental Biology

ORIGINAL RESEARCH
published: 10 May 2022
doi: 10.3389/fcell.2022.895092

DFP-Induced Status Epilepticus Severity in Mixed-Sex Cohorts of Adult Rats Housed in the Same Room: Behavioral and EEG Comparisons

*Nikhil S. Rao†, Christina Meyer†, Suraj S. Vasanthi†, Nyzil Massey, Manikandan Samidurai, Meghan Gage, Marson Putra, Aida N. Almanza, Logan Wachter and Thimmasettappa Thippeswamy**

Department of Biomedical Sciences, College of Veterinary Medicine, Iowa State University, Ames, IA, United States

OPEN ACCESS

Edited by:
Jianxiong Jiang, University of Tennessee Health Science Center (UTHSC), United States

Reviewed by:
Xinjian Zhu, Southeast University, China
Maria Braga, Uniformed Services University, United States

****Correspondence:***
Thimmasettappa Thippeswamy
tswamy@iastate.edu

†These authors have contributed equally to this work

Specialty section:
This article was submitted to Signaling, a section of the journal Frontiers in Cell and Developmental Biology

Received: *24 March 2022*
Accepted: *19 April 2022*
Published: *10 May 2022*

Citation:
Rao NS, Meyer C, Vasanthi SS, Massey N, Samidurai M, Gage M, Putra M, Almanza AN, Wachter L and Thippeswamy T (2022) DFP-Induced Status Epilepticus Severity in Mixed-Sex Cohorts of Adult Rats Housed in the Same Room: Behavioral and EEG Comparisons. Front. Cell Dev. Biol. 10:895092. doi: 10.3389/fcell.2022.895092

Sex is a biological variable in experimental models. In our previous diisopropylfluorophosphate (DFP) studies, female rats required a higher dose of DFP to achieve a somewhat similar severity of status epilepticus (SE) as males. In those studies, male and female rats were bought separately from the same vendor, housed in different rooms, and the DFP used was from different batches. We had also shown that surgery for epidural electrodes implantation reduces the threshold for SE. Our recent study in the soman (GD) model using a mixed-sex cohort of rats housed individually but in the same room showed that females achieved significantly higher SE severity than males for the same dose of GD. In this study, we demonstrate that housing the mixed-sex cohorts in the same room and treating them with DFP (4 mg/kg, s.c.) from the same pool, though from different batches, yielded reproducible SE severity in both sexes and both telemetry (surgery) and non-telemetry (non-surgery) groups. We conducted experiments in four mixed-sex cohorts of adult Sprague-Dawley rats. In females, the surgery for implanting the telemetry devices reduced the latency to convulsive seizure (CS) and increased SE severity compared to non-telemetry females. However, there were no sex differences in latency or SE severity within telemetry or non-telemetry groups. Once animals reached CS stage ≥3, they remained in CS stage in both sexes until midazolam was administered. Midazolam (3 mg/kg, i.m.) treatment 1-one-hour post-DFP significantly reduced epileptiform spikes in both sexes. The mortality was only 2% in 24 h. Irrespective of sex or stage of estrous cycle or surgery, the animals had continuous convulsive SE for ~40 min. In telemetry rats, electrographic changes correlated with behavioral seizures. However, there was a significant difference in SE severity and the latency between directly-observed behavioral CS and EEG-based CS quantification in both sexes. Overall, these results suggest that housing both sexes in the same room and treating with DFP in a mixed-sex cohort from the same pool of reagents will minimize variability in SE severity. Such rigorous experiments will yield better outcomes while testing disease-modifying agents in epilepsy models.

Keywords: sex as a biological variable, midazolam, telemetry, organophoshate, status epilepticus

INTRODUCTION

Developing experimental models that closely mimic human diseases has been challenging. Until recently, most of the experiments were done on males (Beery and Zucker, 2011). This can be a problem in translational research if a drug becomes ineffective in females or causes undesirable side effects (Franconi et al., 2007; Holdcroft, 2007; Tingen et al., 2010). Given this, the National Institute of Health has mandated the inclusion of sex as a biological variable in animal models (Clayton and Collins, 2014). Although initially, researchers perceived it as a burden to include both males and females in experimental design, its practical relevance persuaded the research community to accept and implement it in all relevant experiments.

Inclusion of females in animal models of seizures or acquired epilepsy requires meticulous planning to minimize confounding variables. Several previous elegant studies have reported variable responses to chemoconvulsants-induced status epilepticus (SE) in female rodent models (Tan and Tan, 2001; Scharfman and MacLusky, 2014; Smith et al., 2015). This is primarily due to the impact of the estrous cycle stages at the time of exposure to chemoconvulsants. Furthermore, some strains of mice or rats are resistant, while others are susceptible to the same dose of chemoconvulsant (Kosobud and Crabbe, 1990; Schauwecker and Steward, 1997; McLin and Steward, 2006). Other studies have also reported the source of the animals, housing conditions (single or grouped), age, and handling stress can contribute to variability in seizure response (Kelly, 2010; Novakova et al., 2013; Manouze et al., 2019).

Initial SE severity is a critical variable in all translational experimental models that involve testing disease modifiers after the induction of SE (Gage et al., 2021a). Achieving consistency in SE severity reduces sample size, cost, and time. In a kainic acid (KA) model, we demonstrated that repeated low doses of KA in both rat and mouse models produce reliable consistency in SE severity (Tse et al., 2014; Puttachary et al., 2016a, 2016b; Sharma et al., 2018b, 2021). This dosing modification reduced the disadvantages of a single dose of KA, such as inconsistent SE response, high mortality, and wastage of animals (Tse et al., 2014). The choice of chemoconvulsant depends on the objectives of the experiments. For instance, in organophosphate nerve agent (OPNA) toxicity, victims are exposed to a single acute dose. Thus, a repeated low-dose model is not appropriate. In the diisopropylfluorophosphate (DFP, an OPNA) rat model, a single dose of DFP (4 mg/kg) in telemetry rats yielded varying SE severity and high mortality in males, which prompted testing a lower dose of DFP in subsequent experiments (Gage et al., 2020; Putra et al., 2020a, 2020b). Our initial studies suggested that females required a higher dose of DFP to achieve the same SE response as males when the experiments were done independently (Gage et al., 2020). In subsequent studies, we challenged females with 5 mg/kg DFP rather than 4 mg/kg. We found no significant difference in initial SE severity in females treated with 5 mg/kg compared to males treated with 4 mg/kg (Gage et al., 2021a; Gage et al., 2022a). Interestingly, females had less variable SE severity at 5 mg/kg than males at 4 mg/kg. It is important to note that, though the animals were bought from the source, our previous experiments in males and females were conducted at different times with different batches of DFP (all from Sigma) due to logistic issues. Furthermore, in our previous DFP experiments, the males and females were housed in separate rooms.

Recently, in a soman (GD, an OPNA) model, we surprisingly found that the female rats without telemetry device implantation had significantly higher SE-severity than the males at the same dose of soman (132 μg/kg, 1.2 LD_{50}) (Gage et al., 2022b). In that study, both males and females were housed in the same room, but in separate cages, for several days before soman exposure. We thought co-housing may have synchronized the estrous and yielded relatively consistent higher SE severity to soman challenge. However, the vaginal cytology did not provide evidence for estrous cycle synchronization at the time of soman exposure, and there was no correlation between the stages of the estrous cycle and SE severity (Gage et al., 2022b). We speculated that handling stress during the vaginal lavage might have reduced the seizure threshold in females in soman studies. In this DFP study, based on our recent soman results in the mixed-sex cohort, we exposed the mixed-sex cohort of rats housed in the same room to 4 mg/kg of DFP. In this study, we used both male and female rats implanted with or without telemetry devices. In females, we did not perform vaginal cytology to rule out the impact of handing stress on SE severity outcome in this study. The findings from these rigorous experiments are discussed here.

METHODS

Animals, Care, and Ethics

We used 96 adult Sprague Dawley rats (49 females and 47 males) in this study. The mixed-sex cohort of animals was purchased from Charles River (Wilmington, MA, United States). All animals were challenged with DFP. The procedures were approved by the Institutional Care and Use Committee (IACUC protocols: 21-109 and 21-110) at Iowa State University (ISU). Animals were single housed (male and females in the same room but in separate cages) with 12-hour light and dark cycles and given *ab libitum* access to food and water. At the end of each experiment, all animals were euthanized with pentobarbital sodium (100 mg/kg, i.p.) as per the American Veterinary Medical Associations Guidelines for the Euthanasia of Animals. The euthanasia solution was purchased from the Lloyd Veterinary Medical Center Hospital Pharmacy, Ames, Iowa.

Chemicals

We prepared DFP (Sigma-Aldrich, purity, 97.8% by GC-MS) fresh in cold phosphate-buffered saline (PBS) before administration. Atropine sulfate (ATS, 99.9% pure by LC-MS, Tokyo Chemical Industry (TCI), United States) and 2-pralidoxime (2-PAM, 99.4% pure by LC-MS, Sigma) were prepared fresh in saline. Midazolam (MDZ) was purchased from the ISU Lloyd Veterinary Medical Center Hospital Pharmacy. Before administering the drugs to animals, their

TABLE 1 | The sample size used in different cohorts of experiments. The animals that died during SE were excluded from the analysis.

Batch #	# Of females	# Of males	Non-telemetry or telemetry
I	12	12	Non-telemetry
II	12	12	Non-telemetry
III	7 (1*)	6	Non-telemetry
IV	18	17 (1*)	Telemetry
Total	49	47	*2.04% mortality during SE

identity and purity were authenticated by LC/GC-MS at the Metabolomics Laboratory, Iowa State University, Ames, IA, United States.

Surgical Procedure for Telemetry Devices Implantation

We implanted telemetry devices in 35 rats (18 females and 17 males) about 10–12 days prior to the DFP exposure. We used the CTA-F40 PhysioTel™ devices (Data Science International (DSI), Minneapolis, MN, United States) to acquire integrated video-EEG. The device consists of bipotential electrodes for single-channel recording. As described in our previous publications, we implanted the electrodes bilaterally, one on each side on the surface of the cortex over the dura mater, and the device was placed in a subcutaneous pouch (Puttachary et al., 2016a; Putra et al., 2020a, 2020b; Sharma et al., 2021; Gage et al., 2022b). Before surgery, the animals were administered an analgesic, buprenorphine (0.3 mg/kg, s.c.). Anesthesia was induced by 3.0% isoflurane (flow rate at 1 L/min O_2) and maintained at 1.0–1.5% during surgery. We used Somnoflo anesthetic equipment (Kent Scientific, CT, United States). An artificial tears ointment was applied to prevent the drying of the eyes. After implanting the electrodes and the device, the incision was closed with sterile surgical clips. The standard postoperative care was given. Vetropolycin, a triple antibiotic ointment applied to the surgical site, Baytril (5 mg/kg, s.c., Bayer Pharma, PA, United States), and 1 ml of normal dextrose saline were administered. After recovery, the animals were individually caged and placed on PhysioTel receivers (RPC-1) connected to the Data Exchange Matrix 2.0 (DSI) for acquiring video-encephalography (vEEG) using the Ponemah Acquisition software. The baseline EEG was recorded to cover both day and night cycles to evaluate the impact of surgery on brain electrical activity. The telemetry devices have sensors to record body temperature and locomotor activity.

Status Epilepticus Induction With DFP and Seizures Scoring

All animals were randomized irrespective of sex and coded before exposure to DFP. We exposed the rats to DFP in four batches. The first three batches included non-telemetry animals (i.e., the animals without surgery). The fourth batch had telemetry animals (i.e., the animals had surgery for telemetry devices implantation). Each cohort had an equal number of males and females (±1 animal in some batches). The number of animals in each batch is given in **Table 1**. Irrespective of the batches or sex or telemetry or non-telemetry, all animals were challenged with 4 mg/kg DFP (s.c.) followed immediately (<1 min) by 2 mg/kg ATS (i.m.) and 25 mg/kg 2-PAM (i.m.) to reduce the peripheral effects of AChE inhibition. Most of the animals developed behavioral seizures in <10 min after DFP injection, and 1 h later, midazolam (MDZ, 3 mg/kg, i.m.) was administered to limit mortality.

In this study, behavioral SE severity is defined as the duration (in minutes) of convulsive seizures (stage 3 and above) an animal spends between DFP and MDZ treatments. Animals were directly observed and scored, by two experimenters, on each minute for the seizure stage based on a modified Racine scale (Racine, 1972) as described in our previous publications (Putra et al., 2020a; Gage et al., 2020, 2022b). In telemetry rats, in addition to the integrated vEEG acquisition, the seizures were also scored by direct observation (independent of vEEG). Stage 1 was characterized by salivation, lacrimation, urination, defecation, and mastication; Stage 2 was characterized by head nodding and tremors; Stage 3 was characterized by rearing, Straub tail, and forelimb extension; Stage 4 presented with the loss of the righting reflex and forelimb clonus, and Stage 5 included repeated rearing, falling, and circling. To measure seizure duration and severity, we calculated the number of minutes in which each animal was in a convulsive seizure (CS) (stages 3–5); stages 1 and 2 were considered non-convulsive seizures (NCS).

Integrated Video-EEG Based Status Epilepticus, Epileptiform Spikes, and Power Spectra Quantification

The baseline EEG from a day and night cycle was used to normalize the post-DFP EEG to accurately detect stage-specific epileptiform spikes and seizures. We used the NeuroScore 3.4.0 software for offline data analysis. The default settings for artifacts such as electrical noise, exploratory behavior, and grooming were identified and excluded from epileptiform spike analysis as described previously (Tse et al., 2014; Puttachary et al., 2015, 2016a; Sharma et al., 2018a, 2018b). The baseline EEG characteristics for each animal were used to set the threshold for spike amplitude. The values were summed across groups at different time points for male and female rats. Seizures on EEG were identified using an automated seizure detection module in NeuroScore with predetermined criteria, i.e., high ampliture and high frequency spike trains lasting at least 20 s with minimum intervals of 0.05 s and maximum intervals of 1 s. NeuroScore calculated the average duration of each seizure episode and the total time spent in a seizure with these parameters. All seizure events on EEG were manually verified for behavioral CS from an integrated video and the power spectrum in NeuroScore. Electrographic seizures and spikes per minute for each animal were generated, and the data were processed for statistical analysis and graphing. We calculated the average power, each one-minute epoch, over the 1 hour between DFP and MDZ and one-hour post-MDZ. The powerbands included the delta

TABLE 2 | Statistical tests and the values with ± SEM.

Figure 1	Non-telemetry	Telemetry	*p* value	Statistical analysis
A	5.259 ± 0.2095	4.147 ± 0.2538	0.0006***	Mann-Whitney test
B	5.433 ± 0.2612	4.111 ± 0.3605	0.0027**	Mann-Whitney test
C	5.071 ± 0.3330	4.188 ± 0.3676	0.0740	Mann-Whitney test
	Males	Females		
D	5.071 ± 0.3330	5.433 ± 0.2612	0.1875	Mann-Whitney test
E	4.188 ± 0.3676	4.111 ± 0.3605	0.9366	Mann-Whitney test
Figure 2	Non-Telemetry	Telemetry	*p* value	Statistical analysis
B	43.73 ± 1.840	50.50 ± 1.126	0.0062**	Mann-Whitney test
D	41.58 ± 2.602	51.28 ± 1.060	0.0050**	Mann-Whitney test
F	46.11 ± 2.568	49.63 ± 2.029	0.2452	Mann-Whitney test
Figure 3B	Males	Females	*p* value	Statistical analysis
	46.11 ± 2.568	41.58 ± 2.602	0.0796	Mann-Whitney test
Figure 3D	49.56 ± 2.035	51.28 ± 1.060	0.9795	Mann-Whitney test
Figure 5	Non-Telemetry	Telemetry	*p* value	Statistical analysis
B	Pre: 398.3 ± 25.47	Pre: 334.9 ± 24.42	<0.0001****	2-way ANOVA (Sidak's multiple comparison)
	Post: 204.8 ± 43.25	Post: 121.8 ± 20.36	<0.0001****	
C	43.3 ± 1.734	35.48 ± 2.937	0.0596	Mann-Whitney test
Figure 6	Males	Females	*p* value	Statistical analysis
A	0–15 min: 3.42 ± 0.67	0–15 min: 2.43 ± 0.51	0.6841	Mixed-effects analysis (Sidak's multiple comparison)
	16–30 min: 12.14 ± 0.96	16–30 min: 10.55 ± 0.89	0.6644	
	31–45 min: 11.32 ± 0.96	31–45 min: 10.94 ± 1.06	0.9983	
	46–60 min: 12.82 ± 0.65	46–60 min: 10.88 ± 1.10	0.4665	
B	0–15 min: 11.23 ± 0.61	0–15 min: 11.07 ± 0.64	0.9996	Mixed-effects analysis (Sidak's multiple comparison)
	16–30 min: 13.92 ± 0.49	16–30 min: 14.29 ± 0.26	0.9510	
	31–45 min: 14.33 ± 0.25	31–45 min: 14.36 ± 0.19	>0.9999	
	46–60 min: 13.83 ± 0.11	46–60 min: 13.86 ± 0.09	0.9997	
C	Behavioral seizure	Electrographic seizure	*p* value	Statistical analysis
	Male: 12.33 ± 0.33	Male: 3.42 ± 0.67	<0.0001****	2-way ANOVA (Sidak's multiple comparison)
	Female: 12 ± 0.36	Female: 2.43 ± 0.51	<0.0001****	
D	Male: 13.92 ± 0.49	Male: 12.14 ± 0.96	0.1679	2-way ANOVA (Sidak's multiple comparison)
	Female: 14.29 ± 0.26	Female: 10.55 ± 0.89	0.0008***	
E	Male: 14.33 ± 0.25	Male: 12.16 ± 0.51	0.0515	2-way ANOVA (Sidak's multiple comparison)
	Female: 14.36 ± 0.19	Female: 10.94 ± 1.06	0.0006***	
F	Male: 13.83 ± 0.11	Male: 12.82 ± 0.65	0.5277	2-way ANOVA (Sidak's multiple comparison)
	Female: 13.86 ± 0.09	Female: 10.88 ± 1.10	0.0042**	
Figure 7	Males	Females	*p* value	Statistical analysis
F (α)	19.25 ± 3.70	18.09 ± 2.36	0.8771	Mann-Whitney test
F (β)	16.55 ± 3.60	14.38 ± 2.17	0.6048	Unpaired *t*-test
F (γ)	18.77 ± 3.29	19.04 ± 2.22	0.9465	Unpaired *t*-test
F (δ)	82.52 ± 25.47	136.6 ± 35.05	0.1546	Mann-Whitney test
F (θ)	32.53 ± 8.65	41.80 ± 8.02	0.1279	Mann-Whitney test
F (σ)	12.92 ± 2.53	11.04 ± 1.69	0.7838	Mann-Whitney test
G (α)	6.12 ± 1.10	5.07 ± 1.16	0.2972	Mann-Whitney test
G (β)	5.34 ± 1.04	3.92 ± 0.97	0.1932	Mann-Whitney test
G (γ)	8.05 ± 1.83	5.28 ± 1.06	0.2520	Mann-Whitney test
G (δ)	33.11 ± 8.33	81.06 ± 27.18	0.1598	Mann-Whitney test
G (θ)	13.01 ± 2.90	14.61 ± 4.06	0.9798	Mann-Whitney test
G (σ)	4.22 ± 0.80	3.05 ± 0.72	0.2116	Mann-Whitney test
Figure 8	Males	Females	*p* value	Statistical analysis
A	EEG: 10.54 ± 0.9649	EEG: 10.64 ± 0.7457	<0.0001****	2-way ANOVA (Sidak's multiple comparison)
	Behavior: 3.692 ± 0.3985	Behavior: 4 ± 0.3780	<0.0001****	
B	6.846 ± 0.8537	6.643 ± 0.5800	0.8364	Mann-Whitney test
C	EEG: 40.29 ± 3.412	EEG: 35.48 ± 2.937	0.0106*	2-way ANOVA (Sidak's multiple comparison)
	Behavior: 50.85 ± 2.142	Behavior: 52.5 ± 0.9478	<0.0001****	

(0.5–4 Hz), theta (4–8 Hz**),** Alpha (8–12 Hz), Sigma (12–16 Hz), Beta (16–24 Hz), and Gamma (24–80 Hz).

Experimental Design, Statistics, and Rigor

The animals were randomized, ignoring sex and the estrous cycle stages, and the experimental groups were blinded until the data were analyzed. The normality of the data was tested with the Shapiro-Wilk test. We used GraphPad 9.0 for the statistical analysis and graphing. The specific statistical tests are outlined in the corresponding figure legends and **Table 2**. We had taken measures to minimize variables as in our previous studies: 1) behavioral seizure severity during SE was quantified by both direct observation and offline video analysis by at least two independent observers; 2) authentication of the identity and

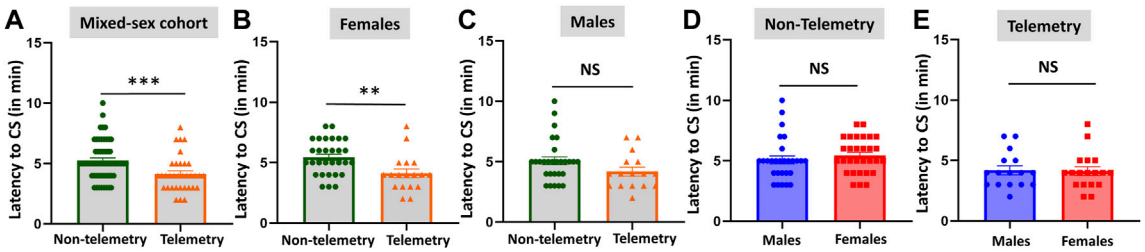

FIGURE 1 | Latency to the onset of convulsive seizures (CS) in non-telemetry and telemetry animals, and sex differences. Non-telemetry and telemetry mixed-sex cohorts **(A)**, females **(B)**, and males **(C)**. A significant reduction in latency was observed in the telemetry group **(A)** driven by females **(B)**. There were no significant sex differences within the non-telemetry **(D)** or telemetry **(E)** group. Mann-Whitney test [**(A)** n = 34–58; **(B)** n = 18–30; **(C)** n = 16–28; **(D)** n = 28–30; **(E)** n = 16–18]. $^{**}p$ = 0.0027, $^{***}p$ = 0.0006. NS, non-significant.

purity of key chemicals by LC/GC-MS; and 3) seizure events on EEG were manually verified with integrated video module for behavior and power spectrum in NeuroScore.

RESULTS

Latency to Behavioral CS Onset: Non-Telemetry Versus Telemetry and Sex Differences

The telemetry device implanted animals in the mixed-sex cohort had significantly lower latency to the onset of the first behavioral CS compared to the non-telemetry animals (p = 0.0006; **Figure 1A**). Further analysis of sex differences within telemetry and non-telemetry groups revealed that the difference in latency was only in females (p = 0.0027; **Figure 1B**). Though there was a reduction in latency in the telemetry males, the difference was not significant (**Figure 1C**). Based on direct observation by experimenters, both males and females had an average of 5 min latency in the non-telemetry group and 4 min in the telemetry group (**Figures 1D,E**). One out of 96 rats did not show CS, and it was excluded from the study. The exact values, statistical tests, and p-values are given in **Table 2**.

Behavioral Status Epilepticus Severity in Mixed-Sex Cohorts: Non-Telemetry Versus Telemetry and Sex Differences

Based on direct observation of behavioral CS in mixed-sex cohorts, telemetry animals had significantly more severe SE (duration of CS with stage ≥3) than non-telemetry animals (p = 0.0062; **Figures 2A,B**). The telemetry animals had 50.50 ± 1.126 min of CS, and non-telemetry animals seized for 43.73 ± 1.840 min (**Table 2**). Further analysis of sex differences in telemetry and non-telemetry groups revealed a significant difference in SE severity in females (p = 0.005) but not in males (**Figures 2C–F**). There were no significant differences when sex was compared within the non-telemetry and telemetry groups (**Figure 3**). The statistical tests and p-values for each comparison are included in **Table 2**.

EEG-Based Status Epilepticus Severity, Epileptiform Spikes, Power, Midazolam Effect, and Sex Differences

Representative EEG traces, the corresponding behavior and the power spectra from a male and female rat, and the CS stage-specific spike characteristics are shown in **Figure 4**. As expected, the epileptiform spiking on EEG increased over time in males and females after exposure to DFP (**Figure 5A**). The latency to CS-associated spiking pattern on EEG was about 10 min in both males and females (**Figures 5A**, **8A**). Once the animals reached a CS stage, the epileptiform spike rate and SE severity did not change significantly until they received MDZ (**Figures 5A–C**). In both sexes, MDZ significantly reduced the spike rate compared to the pre-MDZ period of the same duration (p < 0.0001; **Figure 5B**). There were no sex differences in their response to MDZ. There were also no significant differences in EEG-based SE severity between sexes before MDZ treatment (**Figure 5C**). We also further analyzed the average behavioral and electrographic seizure scores at different blocks of time (0–15 min; 16–30 min; 31–45 min, and 46–60 min) between DFP exposure and MDZ treatments (**Figure 6**). These analyses also confirmed no sex difference in SE severity in behavioral and EEG-based SE scores (**Figures 6A,B**). However, when behavioral SE scores were compared with EEG-based SE scores, there were significant differences in females at all time blocks, while in males, the differences were significant at 0–15 min only (**Figures 6C–F**). We further compared the power spectral differences between males and females over time. Interestingly, females appeared to have higher delta and theta powers than males. However, it was not statistically significant (**Figures 7D,E,G**). Overall, there were no significant sex differences for any power spectra (**Figures 7A–H**).

Discrepancies Between the Observed Behavioral CS Versus EEG Changes and the Latencies

Unlike the KA model of epilepsy, OP chemoconvulsants have both central and peripheral effects. Although the animals were treated with atropine sulfate and 2-PAM to counteract the peripheral effects of AChE inhibition, we wanted to verify whether the seizures originated in the brain. Therefore, the

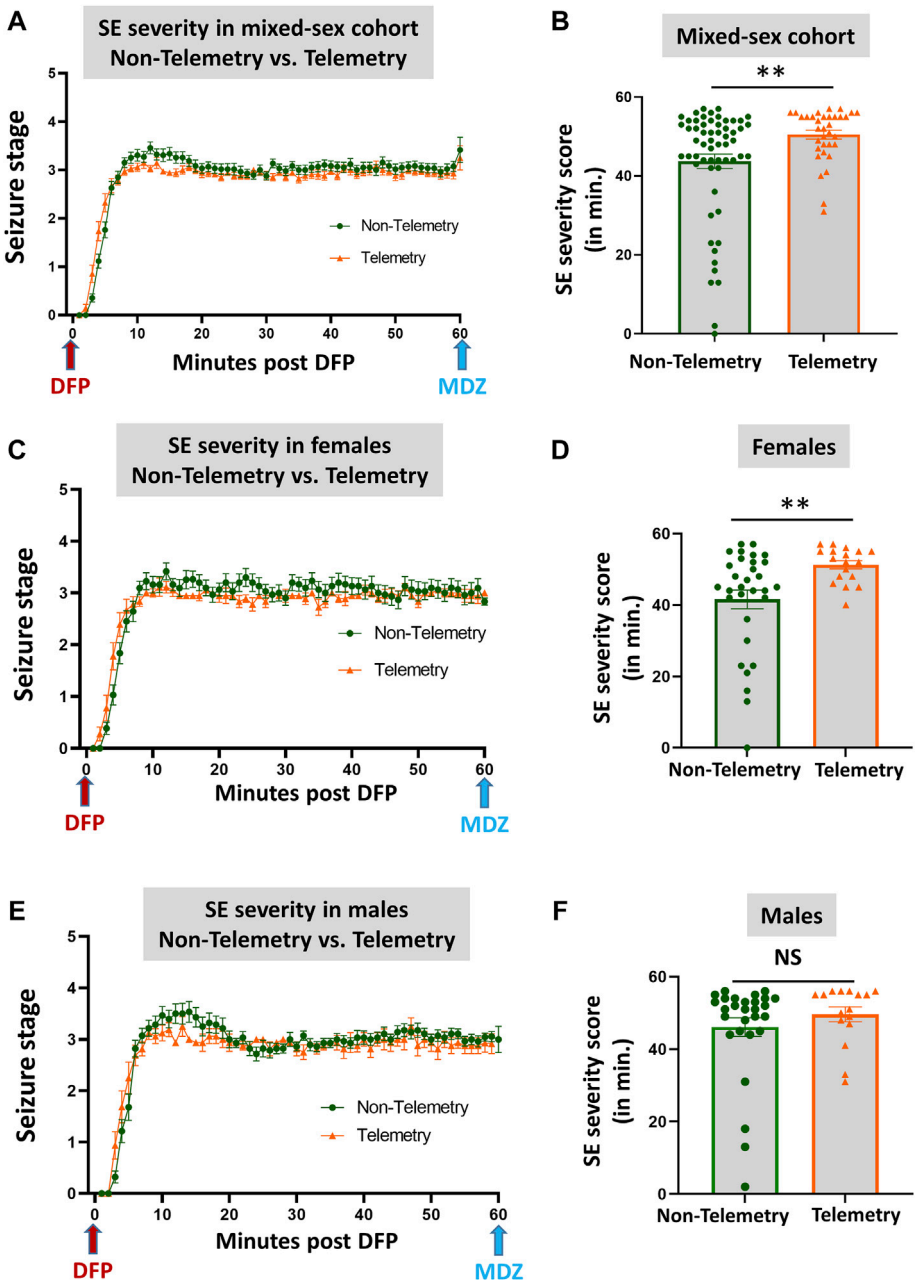

FIGURE 2 | SE severity comparison between non-telemetry and telemetry animals as a mixed-sex cohort **(A,B)**. SE severity was significantly increased in the telemetry group **(B)** and females **(D)** compared to the non-telemetry group. In males, no differences were observed between the telemetry and non-telemetry groups in the SE severity **(F)**. Mann-Whitney test [**(A,B)** n = 34–59; $^{**}p$ = 0.0062; **(C,D)** n = 18–31, $^{**}p$ = 0.005; **(E,F)** n = 16–28]. NS, non-significant.

initial SE severity in telemetry rats was scored by direct observation and EEG-based approaches. In both sexes, there was a significant difference between the observed behavioral latency and the EEG-based latency to the onset of the first CS ($p < 0.0001$; **Figure 8A**). The first 5 min of the observed behavioral CS did not correlate with EEG-based CS patterns in both sexes (**Figure 8B**). There was also an occasional mismatch between behavioral and EEG changes after the first CS. Therefore, there were also significant differences in the duration of CS between observed behavioral and EEG-based quantification in both sexes ($p = 0.01$, $p < 0.0001$; **Figure 8C**). Overall, we found that all EEG-based CS patterns correlated with behavioral CS (confirmed by the integrated video) but not all behavioral CS (directly observed by experimenters) correlated with EEG changes, especially in the first 15 min of post-DFP (**Figure 6C**). Interestingly, two animals with ~40 minof behavioral CS did not show any change on EEG post-DFP. Two other rats had about 3 min of EEG-based CS patterns

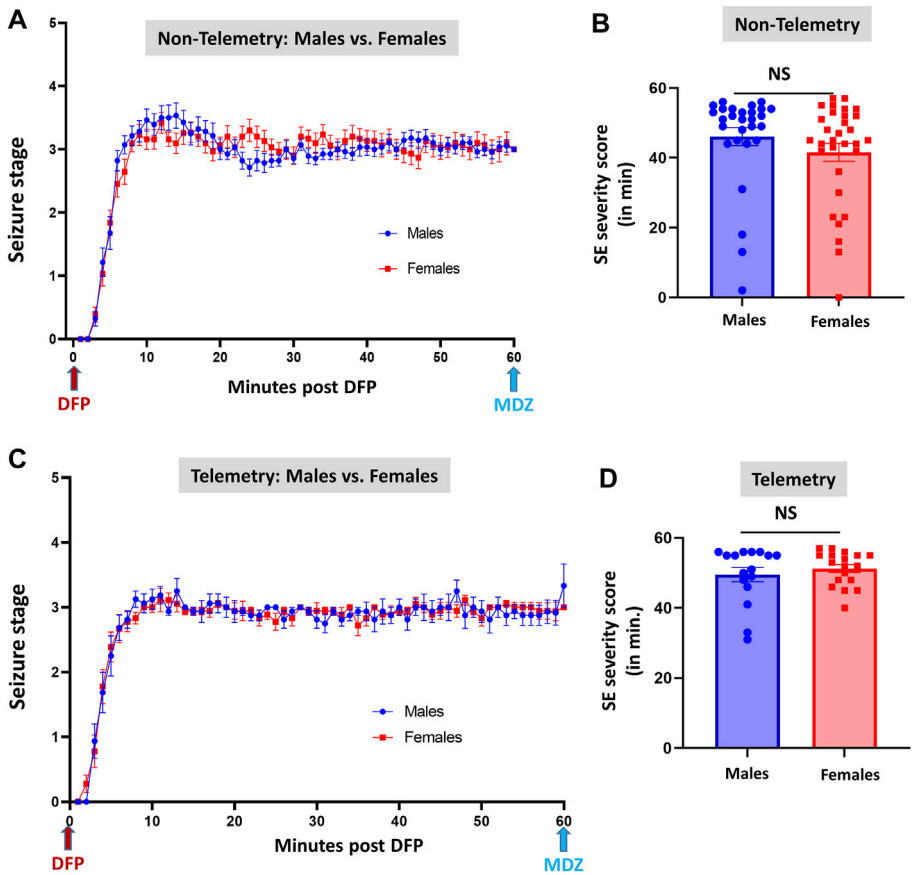

FIGURE 3 | Comparison of SE severity between male and female animals in non-telemetry **(A,B)** and telemetry **(C,D)** groups. No significant differences were observed between sexes. NS, non-significant.

before the MDZ injection. However, the baseline EEGs of all these rats were normal (**Figure 9**). Two more rats also had prolonged latency with occasional EEG seizures though they had severe behavioral SE as the other rats. A summary of the rats that were exceptional to the general trend, their behavioral SE severity, latency, and spike rate are compiled in **Table 3**. These animals were excluded from EEG analysis (**Figures 5**–**8**).

DISCUSSION

Our previous DFP studies were conducted in male and female rats at different time points, with or without telemetry devices (Gage et al., 2020, 2022b; Putra et al., 2020a, 2020b). The published literature on other chemoconvulsants such as KA and pilocarpine models (Tan and Tan, 2001; Scharfman and MacLusky, 2014; Smith et al., 2015), and our previous studies in the rat DFP model, led to the hypothesis that sex differences exist in SE severity in response to chemoconvulsant exposure. The animals were bought from the same vendor for all our experiments, including this study (Charles River, United States). The source of the DFP was from the same company (Sigma Aldrich, United States) for all our experiments, but the batches were different. In our previous studies, female rats always received higher doses than males to achieve a similar SE severity (Gage et al., 2020; 2021a; 2021b; 2022a). In this study, we also used the DFP from different batches but the same vendor as our previous studies. We administered the DFP as a single dose of 4 mg/kg to both males and females at the same time from the same pool of reconstituted drugs. In this study, the male and female animals were used as a mixed-sex cohort, initially ignoring sex as a variable. Furthermore, unlike in our recent soman study (Gage et al., 2022b), we did not conduct vaginal cytology to determine the estrous cycle stages before DFP exposure to rule out the handling stress-induced variability. However, as we did in the soman study, we conducted experiments in both non-telemetry and telemetry rats in a mixed-sex cohort (housed in the same room). We compared the latency and severity of SE between groups to determine the impact of surgery and sex. Therefore, this study is a well-controlled rigorous experiment that addresses the Rigor and Reproducibility concept of the NIH, which has been a concern in experimental models of epilepsy.

Initial SE severity is an important variable in translational experimental models of epilepsy, especially the studies investigating the efficacy of a test drug versus a vehicle (Puttachary et al., 2016a; Putra et al., 2020a; Sharma et al.,

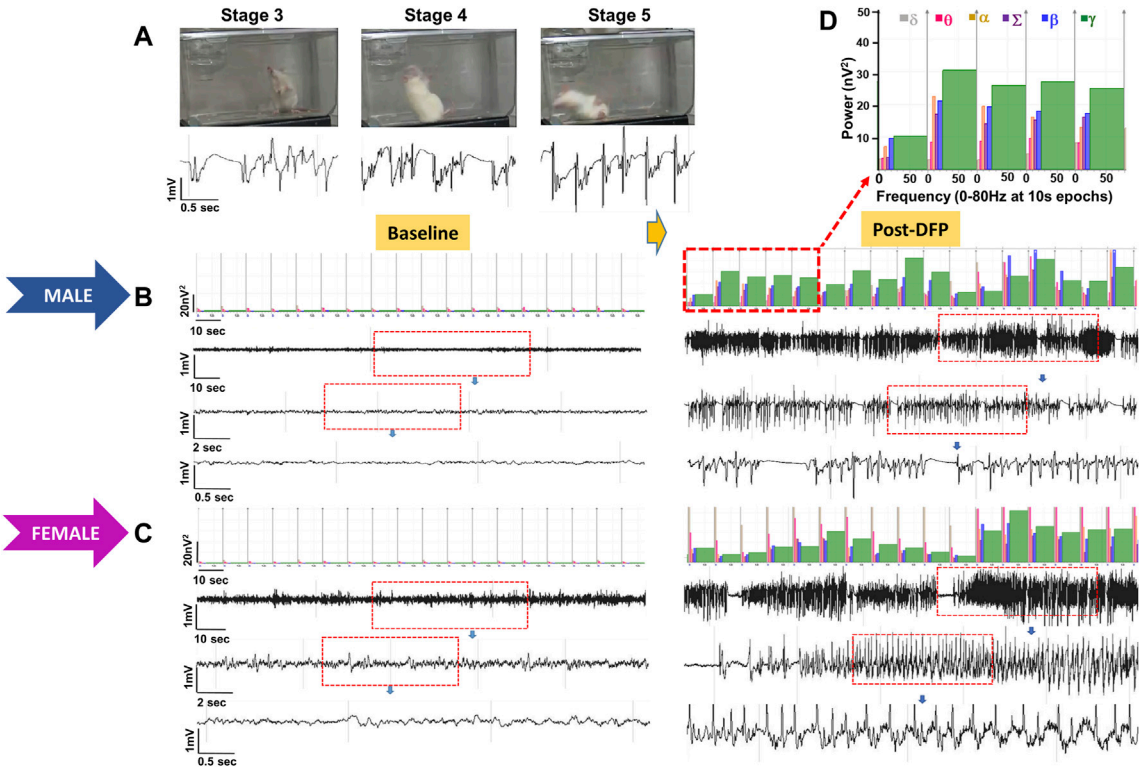

FIGURE 4 | Representative convulsive seizure stages 3–5 and the corresponding stage-specific spike characteristics are presented **(A)**. Representative baseline and post-DFP EEG traces and the corresponding power spectrum from the male **(B)** and female **(C)** are shown.

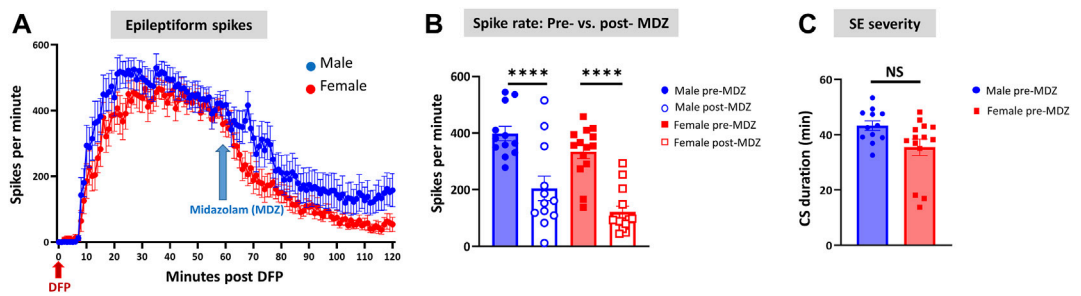

FIGURE 5 | Epileptiform spikes, latency, and SE severity quantification. Epileptiform spike rate and electrographic seizures were compared between post-DFP (i.e., pre-MDZ) and post-MDZ in males and females. The spike rate was significantly reduced in both sexes after MDZ **(A,B)**. There was no difference between males and females in the electrographic seizures duration between DFP and MDZ injections **(C)**. 2-way ANOVA [**(B)** n = 12–14], Mann-Whitney test [**(C)** n = 12–14]. NS, non-significant ****$p < 0.0001$.

2021). Achieving consistency in SE severity between batches and between sexes has been challenging. In our previous studies in the rat and mouse KA models, a modified approach, i.e., repeated low doses instead of a single high dose of KA, mitigated variability in initial SE severity (Tse et al., 2014; Puttachary et al., 2016a; Sharma et al., 2018a; Sharma et al., 2021). However, a repeated-low-dose approach is not suitable for DFP, soman, or other OPNA models as it does not mimic the real-world exposure of OPNAs to the general public. We and others have demonstrated that both DFP and soman models demonstrated the classical features of epilepsy, such as the onset of spontaneously recurring CS, gliosis, and neurodegeneration (Apland et al., 2014; Apland et al., 2018; Lumley et al., 2019; Putra et al., 2020a, 2020b; Rojas et al., 2020; Gage et al., 2021a, 2022a, 2022b; González et al., 2021; Reddy et al., 2021). Off note, some of these studies used pyridostigmine bromide (PB) or other medical countermeasures such as HI-6 or 2-PAM as a pretreatment to minimize mortality (Anderson et al., 1992;

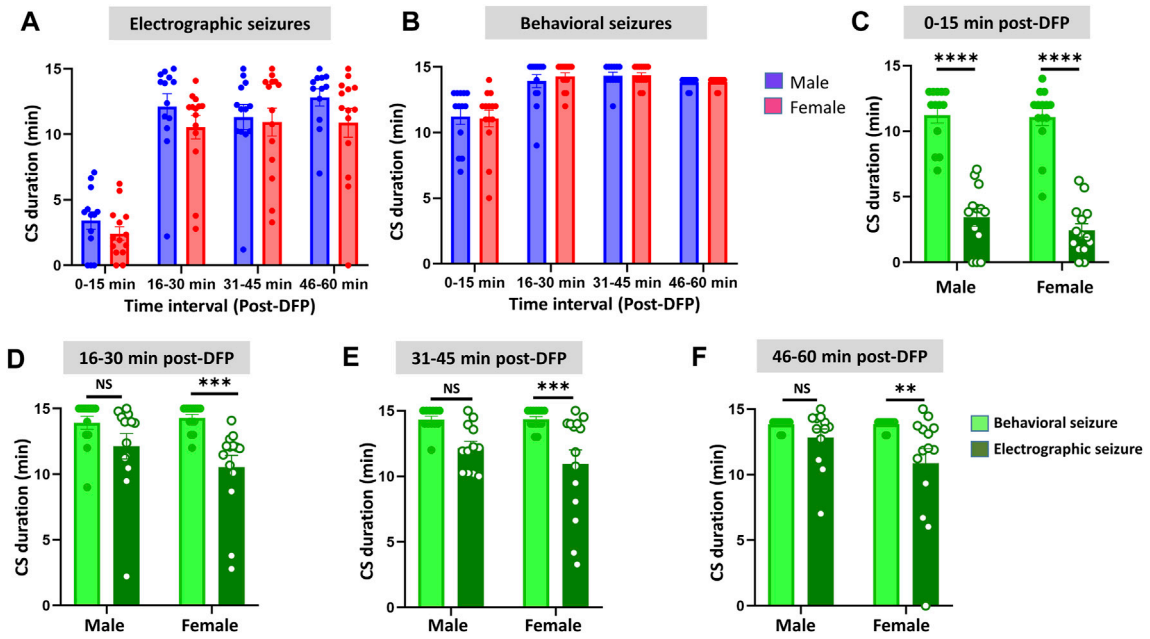

FIGURE 6 | Time-segment wise electrographic seizures **(A)** and behavioral seizures **(B)** severity during 60 min post-DFP exposure. There were no sex differences at any time segments **(A,B)**. There were significant reductions in both sexes during the first 15 min **(C)** and at all time segments in females but not in males **(D–F)** Mixed-effects analysis [**(A,B)** n = 13–14], 2-way ANOVA [**(C,D)** n = 13–14; **(E,F)**, n = 12–14]. $^{**}p$ = 0.0042, $^{***}p < 0.001$, $^{****}p < 0.0001$. NS, non-significant.

Apland et al., 2014; de Araujo Furtado et al., 2010; Reddy et al., 2020, 2021). Although some studies show that pretreatment has no impact on SE severity induced by DFP or soman, PB usage in a mixed-sex cohort can be a problem since females are less responsive to PB and confound SE severity and sex differences (Hernandez et al., 2020). The initial SE severity determines the onset of epileptogenesis in these models (Putra et al., 2020a; Gage et al., 2021a). The animals that had <20 min of SE in the rat DFP model did not develop epilepsy (Putra et al., 2020b). The initial SE severity also determines the extent of brain pathology in the rat DFP model. We defined SE severity as the duration of CS (stage ≥3) in minutes that an animal had between DFP and MDZ injections. Our previous study found that if animals had SE for ~20 min, the pathology would be limited to the amygdala and piriform cortex. In severe SE, i.e., >30 min, the hippocampus and the other brain regions are affected in addition to the amygdala and piriform cortex (Gage et al., 2021a). Therefore, achieving relative consistency in SE severity, whether mild or severe, between sexes, is vital for interpreting the efficacy of disease-modifying test drugs in OPNA models. In one of our past DFP studies, since the initial SE severity was compromised in a batch of rats, we could not draw meaningful conclusions about the drug efficacy in females (Gage et al., 2020).

Sex is a critical biological variable in all animal models of epilepsy. Unless we control other variables, such as initial SE severity and age, the impact of sex on anticipated outcomes can be problematic to interpret the efficacy of an investigational drug. In the past decades, the vast majority of the investigational new drugs were experimented on male animals (Beery and Zucker, 2011). The NIH Health Revitalization Act issued guidelines to include females in clinical trials in 1993 (The NIH policy and Guidelines). Subsequently, the NIH mandated that sex as a biological variable (SABV) be factored into research designs, analyses, and reporting in vertebrate animal and human studies (Clayton and Collins, 2014). Importantly some drugs in humans did not show efficacy in females or had adverse effects (Franconi et al., 2007; Holdcroft, 2007; Tingen et al., 2010; Zucker and Prendergast, 2020). The reluctance to use females in experiments has been likely due to the effects of the estrous cycle stages on experimental outcomes (Yoon et al., 2014; Beery, 2018). The hormone levels fluctuate with the estrous cycle stages, similar to humans though the rat estrous cycle is shorter, i.e., 4–5 days (Staley and Scharfman, 2005; Plant et al., 2015). As hormone levels influence the biological processes, the estrous staging is factored in experimental design in models of epilepsy or seizures.

The inclusion of females in epilepsy models is compelling since ~40% of females with epilepsy have catamenial epilepsy, likely due to a reduction in seizure threshold in response to hormonal changes (Penovich and Helmers, 2008; Herzog, 2015). Animal models of chemoconvulsants-induced epilepsy showed female resistance to the induction of seizures compared to males for the same dose of pilocarpine but not with KA (Scharfman and MacLusky, 2014). In the sarin model, female rats in proestrus required a higher concentration to induce SE than other females in estrus and males (Smith et al., 2015). There were sex-dependent differences in SE in a picrotoxin model due to hormones-induced changes (Tan and Tan, 2001). In our

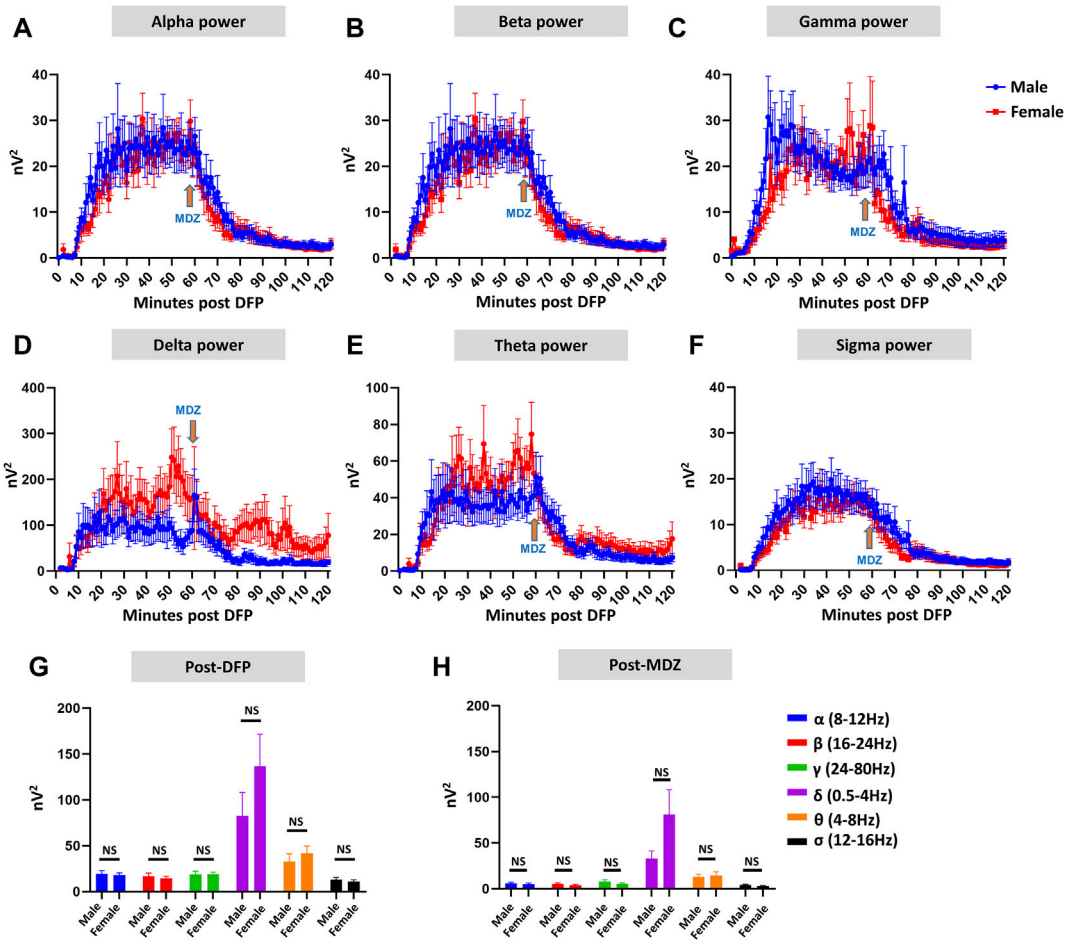

FIGURE 7 | EEG power analysis overtime during the 120 minutes of post-DFP exposure and comparison between males and females **(A–H)**. Power-wise comparison between males and females did not show significant sex differences **(G,H)**. The delta and theta powers were higher in females at certain time points than in males **(D,E)**. Mann-Whitney test [**(F)** (α, δ, θ, σ), **(G)** (α-σ)], Unpaired *t*-test [**(F)** (β, γ)]. NS, non-significant.

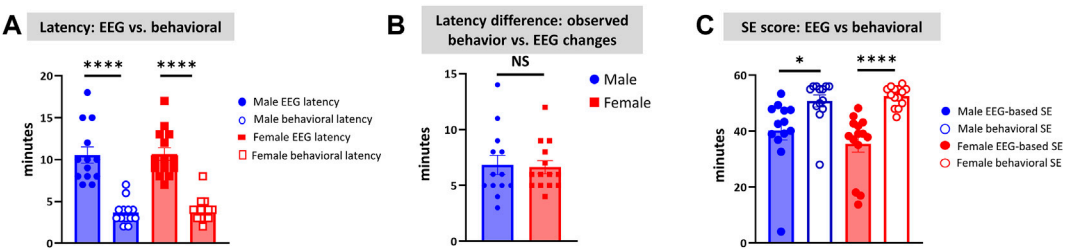

FIGURE 8 | Latency differences between the observed behavioral CS and EEG changes were significant in both sexes **(A)**. Both male and female rats had similar latency in behavioral and electrographic seizures **(B)**. There were also significant differences in the overall duration of CS in both sexes between direct observation of behavioral CS and EEG-based CS quantification **(C)**. Mann-Whitney test [**(B)** n = 13–14]. *p = 0.0106, ****p < 0.0001. NS, non-significant.

recent study in the soman model, female rats in non-telemetry, irrespective of the stage of the estrous cycle, had severe CS (stage ≥3) for 44 min, while males had an average of 32 min (Gage et al., 2022b). It is plausible that handling and procedural stress, induced during vaginal lavage for cytology, might have impacted females' response to soman. Interestingly, there were no sex differences in SE severity in response to soman in telemetry devices implanted animals. In our previous study, telemetry-implanted females exposed to DFP had significantly less severe SE and decreased

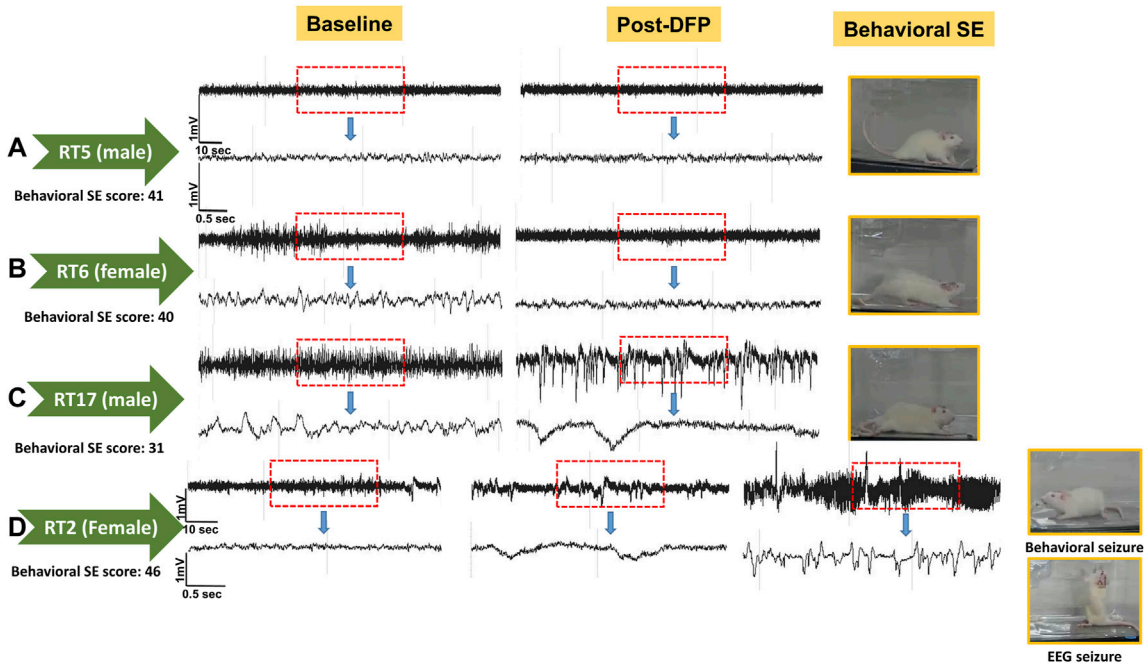

FIGURE 9 | EEG traces from the two rats that did not show EEG changes during post-DFP exposure **(A,B)**. Basal EEG (pre-DFP) and post-DFP EEG traces are shown side-by-side for each animal, suggesting no signal interference or issues with electrodes. C, D traces are from the rats that had seizures ~1 or 3 min before MDZ injection, i.e., about 57 or 59 min of latency.

TABLE 3 | The list of animals excluded from spike counts and electrographic seizure quantification. SE severity is the duration of convulsive seizures (CS, in minutes) ≥stage-3 between DFP and MDZ treatment.

Animal ID	Sex	Observed behavioral SE severity and latency (in min)	SPM post-DFP	EEG-based SE severity and latency (in min)	Comments
RT2	Female	46 (7)	5.30	3.1 (57)	Prolonged latency, occasional EEG seizures
RT3	Male	33 (4)	28.28	2.67 (19)	Prolonged latency, occasional EEG seizures
RT5	Male	41 (7)	0.12	0	No changes on EEG (but normal baseline)
RT6	Female	40 (5)	0	0	No changes on EEG (but normal baseline)
RT17	Male	31 (5)	16.21	0.78 (59)	Prolonged latency a single seizure
RT22	Female	57 (2)	136.08	6.15 (28)	Prolonged latency, occasional seizures

*The numbers in parenthesis indicate the latency to the onset of CS. Representative EEG traces are shown in **Figure 9**. SPM, spikes per minute.*

epileptiform spiking than males, although females received a higher dose (4 mg/kg) of DFP than males (3 mg/kg). The estrous stages had no impact on seizure susceptibility, but rats with severe SE had significantly prolonged diestrus (Gage et al., 2020). Interestingly, soman telemetry rats did not show any estrous-dependent differences. Based on these findings, in the present study, we did not determine the estrous cycle stages in both telemetry and non-telemetry experiments. As a mixed-sex cohort housed in the same room, we found that both males and females responded with similar SE severity to the same dose of DFP (4 mg/kg).

Continuous, integrated, video-EEG recording to detect seizures and epileptiform discharges have been a gold standard, unbiased technique in experimental models of epilepsy to determine the efficacy of disease modifiers. However, drilling holes through the skull to implant electrodes on the brain's surface reduces the seizure threshold in response to chemoconvulsants (Sharma et al., 2018b). We recently demonstrated the impact of depth electrodes on altered proteome levels in the hippocampus and cytokine levels in the brain and serum (Tse et al., 2021). In all our recent studies, the electrodes were placed epidurally rather than in the brain. We also verified any physical trauma to the brain after the animals were euthanized. None of the rats had depth electrodes in this study. In the rat soman model, the SE severity in the telemetry males was significantly higher than in non-telemetry males, which was similar to the KA model of epilepsy (Sharma et al., 2021; Gage et al., 2022b).

In females, there were no differences in SE severity in telemetry and non-telemetry rats in the soman model since it had reached the maximum in non-telemetry animals (Gage et al., 2022b).

This study did not reveal significant sex differences in SE severity in either telemetry or non-telemetry groups. There were no significant sex differences in latency to the electrographic seizures and EEG-based SE severity. There were also no significant sex differences in any power spectra. Both sexes responded to MDZ and significantly reduced epileptiform discharges, and there were no sex differences. Previous studies in the soman model demonstrated that midazolam was the most potent and rapidly acting drug (McDonough et al., 1999). We have recently shown in the rat DFP model that midazolam prevents mortality. In contrast, diazepam could not rescue animals from DFP-induced mortality (Gage et al., 2021a). Our previous studies did not test the sex difference in MDZ efficacy. The cytochrome P450 3A (CYP3A) enzyme metabolizes MDZ in the liver and gut to its active metabolites 1-hydroxy-midazolam and 4-hydroxymidazolam. Although women showed significantly greater hepatic CYP3A activity than men, there are no convincing and reproducible reports on whether these active metabolites were also higher in women than men. Most studies reported that no sex differences were reported in MDZ efficacy (for example, Chen et al., 2006; Hu and Zhao, 2010). In a healthy human volunteers' study, women exhibited 11% higher mean weight-corrected total body midazolam clearance and 28% higher oral clearance than men. However, they reported minor sex differences in area under curve (AUC) values (Chen et al., 2006). Therefore, it is not surprising that we observed no sex differences in the efficacy of MDZ in this study too.

The latency differences between the observed behavioral CS and the onset of electrographic changes, and the overall difference in SE severity in both sexes are intriguing observations in this study. These discrepancies could be due to the limited coverage of single-channel recording from epidurally implanted bipotential electrodes in this study. However, such discrepancy patterns were not observed in the kainate model when the same DSI transmitter devices were used in rats (Sharma et al., 2021). This suggests that the mismatch between the behavioral CS and the corresponding changes on EEG in <15 min of post-DFP exposure could be due to the effects of DFP in peripheral organs. The differences between 15–60 min post-exposure could be likely due to manually quantified seizures in one-minute epochs. The other interesting finding is that in four rats, there was significantly prolonged latency to the onset of the first electrographic CS pattern, although the behavioral CS latency was <8 min (**Table 3**). These observations suggest that the peripheral effects of atropine sulfate and 2-PAM may not be effective in some animals or may have a prolonged delayed effect. It would be interesting to investigate further; 1) the AChE levels in the peripheral tissues, 2) differences in brain pathology between the animals that had no EEG changes (despite behavioral CS) and the animals in which the behavioral seizures correlated with the electrographic changes. As reported in **Table 3**, the two rats (RT5 and RT6) with no EEG changes (despite 40 min of behavioral CS) had normal baseline EEG, and we did observe the expected day-night changes on the EEG baseline. These animals had occasional epileptiform spikes but no electrographic CS patterns. Therefore, it is unlikely due to epidurally placed electrodes or any technical issues. Furthermore, all other rats that showed CS changes on EEG (post-DFP) had similar baseline changes (day-night cycle). In these animals, AChE levels and their activation state in the brain and peripheral tissues may reveal the reason for behavioral vs. lack of EEG changes.

CONCLUSION

This study demonstrated that mixed-sex cohorts of males and females housed in the same room minimize variability in SE severity in response to DFP exposure. Injections from the same pool of reconstituted DFP in cold PBS minimize variability, although the DFP used in this study was from different batches but the same vendor. SE severity quantification (i.e., CS stages and duration) by direct observation, video, and EEG analyses yielded reproducible results when the experiments were conducted in mixed-sex cohorts. We found no sex differences in SE severity in either the telemetry or non-telemetry cohort. The female rats showed decreased latency and increased SE severity in the telemetry group compared to the non-telemetry group. Both sexes responded to MDZ and there was no sex difference. Out of 35 telemetry animals, 29 animals' EEG-based CS patterns correlated with the behavioral CS. The odd six animals had excellent EEG signals and normal baselines as the other animals, but surprisingly, there were no EEG changes in response to DFP despite severe behavioral CS (**Table 3**; **Figure 9**). Like the other animals, these six animals were also treated with atropine sulfate and 2-PAM to prevent peripheral effects of AChE inhibition by DFP. Our future studies will investigate whether brain pathology of these six animals correlates with the rest of the telemetry rats, which had similar behavioral SE severity. One of the limitations of this study is the lack of mechanistic or therapeutic aspects. The extension of this study will explore both a disease-modifying effect of an investigational new drug and its mechanism.

DATA AVAILABILITY STATEMENT

The raw data supporting the conclusion of this article will be made available by the authors, without undue reservation.

ETHICS STATEMENT

The animal study was reviewed and approved by the Iowa State University IACUC.

AUTHOR CONTRIBUTIONS

TT secured funding for the project, designed experiments, verified the data, offered intellectual input, and wrote the manuscript. All other authors conducted the experiments, compiled and cross-verified the data, proofread the manuscript with a significant contribution from the first three authors. The shared first three authors and MS participated in the design of the experiments and other logistics. NR cross-verified and analyzed the EEG data and graphed the data. NM pooled the other data, cross-verified, and graphed the data. AA and LW quantified the EEG data.

FUNDING

The Principal Investigator, TT, received the funding for this project from the National Institutes of Health/NINDS (U01 NS117284 and R21 NS120916) through the Counter ACT program.

REFERENCES

Anderson, D. R., Harris, L. W., Woodard, C. L., and Lennox, W. J. (1992). The Effect of Pyridostigmine Pretreatment on Oxime Efficacy against Intoxication by Soman or VX in Rats. *Drug Chem. Toxicol.*, 15(4), 285–294. doi:10.3109/01480549209014158

Apland, J. P., Aroniadou-Anderjaska, V., Figueiredo, T. H., De Araujo Furtado, M., and Braga, M. F. M. (2018). Full protection against Soman-Induced Seizures and Brain Damage by LY293558 and Caramiphen Combination Treatment in Adult Rats. *Neurotox Res.*, 34(3), 511–524. doi:10.1007/s12640-018-9907

Apland, J. P., Aroniadou-Anderjaska, V., Figueiredo, T. H., Rossetti, F., Miller, S. L., and Braga, M. F. (2014). The Limitations of Diazepam as a Treatment for Nerve Agent-Induced Seizures and Neuropathology in Rats: Comparison with UBP302. *J. Pharmacol. Exp. Ther.*, 351(2), 359–372. doi:10.1124/jpet.114.217299

Beery, A. K. (2018). Inclusion of Females Does Not Increase Variability in Rodent Research Studies. *Curr. Opin. Behav. Sci.*, 23, 143–149. doi:10.1016/J.COBEHA.2018.06.016

Beery, A. K., and Zucker, I. (2011). Sex Bias in Neuroscience and Biomedical Research. *Neurosci. Biobehavioral Rev.*, 35(3), 565–572. doi:10.1016/j.neubiorev.2010.07.002

Chen, M., Ma, L., Drusano, G., Bertinojr, J., Jr, and Nafziger, A. Sex Differences in CYP3A Activity Using Intravenous and Oral Midazolam. *Clin. Pharmacol. Ther.* 2006;80(5):531–538. doi:10.1016/j.clpt.2006.08.014

Clayton, J. A., and Collins, F. S. (2014). Policy: NIH to Balance Sex in Cell and Animal Studies. *Nature*, 509(7500), 282–283. doi:10.1038/509282A

De Araujo Furtado, M., Lumley, L. A., Robison, C., Tong, L. C., Lichtenstein, S., and Yourick, D. L. (2010). Spontaneous Recurrent Seizures after Status Epilepticus Induced by Soman in Sprague-Dawley Rats. *Epilepsia*, 51(8), 1503–1510. doi:10.1111/j.1528-1167.2009.02478.x

Franconi, F., Brunelleschi, S., Steardo, L., and Cuomo, V. (2007). Gender Differences in Drug Responses. *Pharmacol. Res.*, 55(2), 81–95. doi:10.1016/J.PHRS.2006.11.001

Gage, M., Gard, M., and Thippeswamy, T. (2022a). Characterization of Cortical Glial Scars in the Diisopropylfluorophosphate (DFP) Rat Model of Epilepsy. *Front. Cel Dev. Biol.*, 10. doi:10.3389/fcell.2022.867949

Gage, M., Golden, M., Putra, M., Sharma, S., and Thippeswamy, T. (2020, Sex as a Biological Variable in the Rat Model of Diisopropylfluorophosphate-induced Long-term Neurotoxicity, *Ann. N.Y. Acad. Sci.*, 1479). .44, 64. doi:10.1111/nyas.14315

Gage, M., Putra, M., Gomez-Estrada, C., Golden, M., Wachter, L., Gard, M., et al. (2021a). Differential Impact of Severity and Duration of Status Epilepticus, Medical Countermeasures, and a Disease-Modifier, Saracatinib, on Brain Regions in the Rat Diisopropylfluorophosphate Model. *Front. Cel. Neurosci.*, 15, 426. doi:10.3389/FNCEL.2021.772868

Gage, M., Putra, M., Wachter, L., Dishman, K., Gard, M., Gomez-Estrada, C., et al. (2021b). Saracatinib, a Src Tyrosine Kinase Inhibitor, as a Disease Modifier in the Rat DFP Model: Sex Differences, Neurobehavior, Gliosis, Neurodegeneration, and nitro-oxidative Stress. *Antioxidants* 2022, Vol. 11, (1), 61. doi:10.3390/ANTIOX11010061

Gage, M., Rao, N. S., Samidurai, M., Putra, M., Vasanthi, S. S., Meyer, C., et al. (2022b). Soman (GD) Rat Model to Mimic Civilian Exposure to Nerve Agent: Mortality, Video-EEG Based Status Epilepticus Severity, Sex Differences, Spontaneously Recurring Seizures, and Brain Pathology. *Front. Cel. Neurosci.*, 15, 573. doi:10.3389/fncel.2021.798247

González, E. A., Calsbeek, J. J., Tsai, Y.-H., Tang, M.-Y., Andrew, P., Vu, J., et al. (2021). Sex-specific Acute and Chronic Neurotoxicity of Acute Diisopropylfluorophosphate (DFP)-intoxication in Juvenile Sprague-Dawley Rats. *Curr. Res. Toxicol.*, 2, 341–356. doi:10.1016/j.crtox.2021.09.002

Hernandez, S., Morales-Soto, W., Grubišić, V., Fried, D., and Gulbransen, B. D. (2020). Pyridostigmine Bromide Exposure Creates Chronic, Underlying Neuroimmune Disruption in the Gastrointestinal Tract and Brain that Alters Responses to Palmitoylethanolamide in a Mouse Model of Gulf War Illness. *Neuropharmacology*, 179, 108264. doi:10.1016/J.NEUROPHARM.2020.108264

Herzog, A. G. (2015). Catamenial Epilepsy: Update on Prevalence, Pathophysiology and Treatment from the Findings of the NIH Progesterone Treatment Trial. *Seizure*, 28, 18–25. doi:10.1016/J.SEIZURE.2015.02.024

Holdcroft, A. (2007). Gender Bias in Research: How Does it Affect Evidence Based Medicine? *J. R. Soc. Med.*, 100(1), 2–3. doi:10.1177/014107680710000102doi:10.1258/jrsm.100.1.2

Hu, Z.-Y., and Zhao, Y.-S. (2010). Sex-dependent Differences in Cytochrome P450 3A Activity as Assessed by Midazolam Disposition in Humans: a Meta-Analysis. *Drug Metab. Dispos.*, 38(5):817–823. doi:10.1124/dmd.109.031328

Kelly, K. M. (2010). Aging Models of Acute Seizures and Epilepsy. *Epilepsy Curr.*, 10(1), 15, 20. doi:10.1111/J.1535-7511.2009.01341.X

Kosobud, A. E., and Crabbe, J. C. (1990). Genetic Correlations Among Inbred Strain Sensitivities to Convulsions Induced by 9 Convulsant Drugs. *Brain Res.*, 526(1), 8–16. doi:10.1016/0006-8993(90)90243-5

Lumley, L. A., Rossetti, F., de Araujo Furtado, M., Marrero-Rosado, B., Schultz, C. R., Schultz, M. K., et al. (2019). Dataset of EEG Power Integral, Spontaneous Recurrent Seizure and Behavioral Responses Following Combination Drug Therapy in Soman-Exposed Rats. *Data in Brief*, 27, 104629. doi:10.1016/J.DIB.2019.104629

Manouze, H., Ghestem, A., Poillerat, V., Bennis, M., Ba-M'hamed, S., Benoliel, J. J., et al. (2019). Effects of Single Cage Housing on Stress, Cognitive, and Seizure Parameters in the Rat and Mouse Pilocarpine Models of Epilepsy. *ENeuro*, 6(4, 0179, 18). doi:10.1523/ENEURO.0179-18.2019

McDonough, J. H., Jr, McMonagle, J., Copeland, T., Zoeffel, D., and Shih, T. M. (1999) Comparative Evaluation of Benzodiazepines for Control of Soman-Induced Seizures. *Arch. Toxicol.* 73(8-9):473–478. doi:10.1007/s002040050637

McLin, J. P., and Steward, O. (2006). Comparison of Seizure Phenotype and Neurodegeneration Induced by Systemic Kainic Acid in Inbred, Outbred, and Hybrid Mouse Strains. *Eur. J. Neurosci.*, 24(8), 2191–2202. doi:10.1111/J.1460-9568.2006.05111.X

Novakova, B., Harris, P. R., Ponnusamy, A., and Reuber, M. (2013). The Role of Stress as a Trigger for Epileptic Seizures: A Narrative Review of Evidence from Human and Animal Studies. *Epilepsia*, 54(11), 1866–1876. doi:10.1111/EPI.12377

Penovich, P. E., and Helmers, S. (2008). Chapter 4 Catamenial Epilepsy. In *Int. Rev. Neurobiol.* (Vol. 83, pp. 79–90). doi:10.1016/S0074-7742(08)00004-4

Plant, T. M., Zeleznik, A. J., and Albertini, D. F. (2015). Chapter 2 – the Mammalian Oocyte. *Knobil Neill's Physiol. Reprod.*, 59–97.

Putra, M., Gage, M., Sharma, S., Gardner, C., Gasser, G., Anantharam, V., et al. (2020b, Diapocynin, an NADPH Oxidase Inhibitor, Counteracts Diisopropylfluorophosphate-induced Long-term Neurotoxicity in the Rat Model, *Ann. N.Y. Acad. Sci.*, 1479). 75, 93. doi:10.1111/nyas.14314

Putra, M., Sharma, S., Gage, M., Gasser, G., Hinojo-Perez, A., Olson, A., et al. (2020a). Inducible Nitric Oxide Synthase Inhibitor, 1400W, Mitigates DFP-

Induced Long-Term Neurotoxicity in the Rat Model. *Neurobiol. Dis.*, 133, 104443. doi:10.1016/j.nbd.2019.03.031

Puttachary, S., Sharma, S., Thippeswamy, A., and Thippeswamy, T. (2016a). Immediate Epileptogenesis: Impact on Brain in C57BL/6J Mouse Kainate Model. *Front. Biosci. (Elite Ed.)*, 8, 390–411.doi:10.2741/e775

Puttachary, S., Sharma, S., Tse, K., Beamer, E., Sexton, A., Crutison, J., et al. (2015). Immediate Epileptogenesis after Kainate-Induced Status Epilepticus in C57BL/6J Mice: Evidence from Long Term Continuous Video-EEG Telemetry. *PLoS One*, 10(7), e0131705. doi:10.1371/journal.pone.0131705

Puttachary, S., Sharma, S., Verma, S., Yang, Y., Putra, M., Thippeswamy, A., et al. (2016b). 1400W, a Highly Selective Inducible Nitric Oxide Synthase Inhibitor Is a Potential Disease Modifier in the Rat Kainate Model of Temporal Lobe Epilepsy. *Neurobiol. Dis.*, 93, 184–200. doi:10.1016/j.nbd.2016.05.013

Racine, R. J. (1972). Modification of Seizure Activity by Electrical Stimulation: II. Motor Seizure. *Electroencephalography Clin. Neurophysiol.*, 32(3), 281–294.doi:10.1016/0013-4694(72)90177-0

Reddy, D. S., Zaayman, M., Kuruba, R., and Wu, X. (2021). Comparative Profile of Refractory Status Epilepticus Models Following Exposure of Cholinergic Agents Pilocarpine, DFP, and Soman. *Neuropharmacology* 191:108571. doi:10.1016/j.neuropharm.2021.108571

Reddy, S. D., Wu, X., Kuruba, R., Sridhar, V., and Reddy, D. S. (2020). Magnetic Resonance Imaging Analysis of Long-term Neuropathology after Exposure to the Nerve Agent Soman: Correlation with Histopathology and Neurological Dysfunction. *Ann. N.Y. Acad. Sci.*, 1480(1), 116–135. doi:10.1111/nyas.14431

Rojas, A., Ganesh, T., Wang, W., Wang, J., and Dingledine, R. (2020). A Rat Model of Organophosphate-Induced Status Epilepticus and the Beneficial Effects of EP2 Receptor Inhibition. *Neurobiol. Dis.*, 133, 104399. doi:10.1016/j.nbd.2019.02.010

Scharfman, H. E., and MacLusky, N. J. (2014). Sex Differences in the Neurobiology of Epilepsy: a Preclinical Perspective. *Neurobiol. Dis.*, 72 Pt B, 180–192. doi:10.1016/j.nbd.2014.07.004

Schauwecker, P. E., and Steward, O. (1997). Genetic Determinants of Susceptibility to Excitotoxic Cell Death: Implications for Gene Targeting Approaches. *Proc. Natl. Acad. Sci. U.S.A.*, 94(8), 4103–4108. doi:10.1073/PNAS.94.8.4103

Sharma, S., Carlson, S., Gregory-Flores, A., Hinojo-Perez, A., Olson, A., and Thippeswamy, T. (2021). Mechanisms of Disease-Modifying Effect of Saracatinib (AZD0530), a Src/Fyn Tyrosine Kinase Inhibitor, in the Rat Kainate Model of Temporal Lobe Epilepsy. *Neurobiol. Dis.*, 156, 105410. doi:10.1016/j.nbd.2021.105410

Sharma, S., Carlson, S., Puttachary, S., Sarkar, S., Showman, L., Putra, M., et al. (2018a). Role of the Fyn-Pkcδ Signaling in SE-Induced Neuroinflammation and Epileptogenesis in Experimental Models of Temporal Lobe Epilepsy. *Neurobiol. Dis.*, 110, 102–121. doi:10.1016/j.nbd.2017.11.008

Sharma, S., Puttachary, S., Thippeswamy, A., Kanthasamy, A. G., and Thippeswamy, T. (2018b). Status Epilepticus: Behavioral and Electroencephalography Seizure Correlates in Kainate Experimental Models. *Front. Neurol.*, 9, 7. doi:10.3389/fneur.2018.00007

Smith, C. D., Wright, L. K. M., Garcia, G. E., Lee, R. B., and Lumley, L. A. (2015). Hormone-dependence of Sarin Lethality in Rats: Sex Differences and Stage of the Estrous Cycle. *Toxicol. Appl. Pharmacol.*, 287(3), 253–257. doi:10.1016/j.taap.2015.06.010

Staley, K., and Scharfman, H. (2005). A Woman's Prerogative. *Nat. Neurosci.*, 8(6), 697–699. doi:10.1038/nn0605-697

Tan, M., and Tan, U. (2001). Sex Difference in Susceptibility to Epileptic Seizures in Rats: Importance of Estrous Cycle. *Int. J. Neurosci.*, 108(3–4), 175–191. doi:10.3109/00207450108986513

Tingen, C. M., Kim, A. M., Wu, P.-H., and Woodruff, T. K. (2010). Sex and Sensitivity: the Continued Need for Sex-Based Biomedical Research and Implementation. *Womens Health (Lond Engl.*, 6(4), 511–516. doi:10.2217/WHE.10.45

Tse, K., Beamer, E., Simpson, D., Beynon, R. J., Sills, G. J., and Thippeswamy, T. (2021). The Impacts of Surgery and Intracerebral Electrodes in C57BL/6J Mouse Kainate Model of Epileptogenesis: Seizure Threshold, Proteomics, and Cytokine Profiles. *Front. Neurol.*, 12:625017. doi:10.3389/FNEUR.2021.625017

Tse, K., Puttachary, S., Beamer, E., Sills, G. J., and Thippeswamy, T. (2014). Advantages of Repeated Low Dose against Single High Dose of Kainate in C57BL/6J Mouse Model of Status Epilepticus: Behavioral and Electroencephalographic Studies. *PLoS ONE*, 9(5), e96622. doi:10.1371/journal.pone.0096622

Yoon, D. Y., Mansukhani, N. A., Stubbs, V. C., Helenowski, I. B., Woodruff, T. K., and Kibbe, M. R. (2014). Sex Bias Exists in Basic Science and Translational Surgical Research. *Surgery*, 156(3), 508–516. doi:10.1016/J.SURG.2014.07.001

Zucker, I., and Prendergast, B. J. (2020). Sex Differences in Pharmacokinetics Predict Adverse Drug Reactions in Women. *Biol. Sex. Differ.*, 11(1), 32–14. doi:10.1186/S13293-020-00308-5/TABLES/3

Conflict of Interest: The authors declare that the research was conducted in the absence of any commercial or financial relationships that could be construed as a potential conflict of interest.

Publisher's Note: All claims expressed in this article are solely those of the authors and do not necessarily represent those of their affiliated organizations, or those of the publisher, the editors and the reviewers. Any product that may be evaluated in this article, or claim that may be made by its manufacturer, is not guaranteed or endorsed by the publisher.

frontiers | Frontiers in Cell and Developmental Biology

MINI REVIEW
published: 04 July 2022
doi: 10.3389/fcell.2022.926776

Distinct Cell-specific Roles of NOX2 and MyD88 in Epileptogenesis

*Cayo Almeida[1], Renan Paschoalino Pongilio[1], Marília Inês Móvio[1], Guilherme Shigueto Vilar Higa[1], Rodrigo Ribeiro Resende[2], Jianxiong Jiang[3], Erika Reime Kinjo[1] and Alexandre Hiroaki Kihara[1]**

[1]Laboratório de Neurogenética, Universidade Federal do ABC, São Bernardo do Campo, Brazil, [2]Laboratório de Sinalização Celular e Nanobiotecnologia, Departamento de Bioquímica e Imunologia, Universidade Federal de Minas Gerais, Belo Horizonte, Brazil, [3]Department of Pharmaceutical Sciences, College of Pharmacy, University of Tennessee Health Science Center, Memphis, TN, United States

It is well established that temporal lobe epilepsy (TLE) is often related to oxidative stress and neuroinflammation. Both processes subserve alterations observed in epileptogenesis and ultimately involve distinct classes of cells, including astrocytes, microglia, and specific neural subtypes. For this reason, molecules associated with oxidative stress response and neuroinflammation have been proposed as potential targets for therapeutic strategies. However, these molecules can participate in distinct intracellular pathways depending on the cell type. To illustrate this, we reviewed the potential role of nicotinamide adenine dinucleotide phosphate (NADPH) oxidase 2 (NOX2) and myeloid differentiation primary response 88 (MyD88) in astrocytes, microglia, and neurons in epileptogenesis. Furthermore, we presented approaches to study genes in different cells, employing single-cell RNA-sequencing (scRNAseq) transcriptomic analyses, transgenic technologies and viral serotypes carrying vectors with specific promoters. We discussed the importance of identifying particular roles of molecules depending on the cell type, endowing more effective therapeutic strategies to treat TLE.

Keywords: epilepsy, neuroinflammatory diseases, temporal lobe, single-cell analysis, cre recombinase, adeno-associated virus, toll-like receptors, transgenic mice

OPEN ACCESS

Edited by:
Xu Wang,
Affiliated Hospital of Jiangsu University, China

Reviewed by:
Shaunik Sharma,
The University of Iowa, United States
Xuefeng Wang,
Jiangsu University, China
Ha-Reum Lee,
Chungnam National University, South Korea

****Correspondence:***
Alexandre Hiroaki Kihara
alexandrekihara@gmail.com

Specialty section:
This article was submitted to Signaling, a section of the journal Frontiers in Cell and Developmental Biology

Received: *23 April 2022*
Accepted: *15 June 2022*
Published: *04 July 2022*

Citation:
Almeida C, Pongilio RP, Móvio MI, Higa GSV, Resende RR, Jiang J, Kinjo ER and Kihara AH (2022) Distinct Cell-specific Roles of NOX2 and MyD88 in Epileptogenesis. Front. Cell Dev. Biol. 10:926776. doi: 10.3389/fcell.2022.926776

INTRODUCTION

Temporal lobe epilepsy (TLE) is the most prevalent form of the disease, corresponding to ~40% of the cases, of which one-third are refractory to the current pharmacological treatments (Guedes et al., 2006; Organization, W. H, 2019; Falco-Walter, 2020). It is already established that epileptogenesis is an ongoing process even after the first unprovoked seizure, since rearrangements of the neural networks constantly occur (Kinjo et al., 2016; Kinjo et al., 2018; Royero et al., 2020). This is due to stress factors such as free radicals' production and neuroinflammation, and it contributes to the progression of epilepsy (Pitkänen et al., 2015; Jiang et al., 2019; Borowicz-Reutt and Czuczwar, 2020).

Free radicals, e.g., reactive oxygen species (ROS), play a physiological role in processes such as synaptic plasticity (Beckhauser et al., 2016). They also participate in the pathological aspects of TLE and several brain disorders, such as Alzheimer's and Parkinson's diseases, impairing neurotransmission and favoring lipid peroxidation of the neural membrane (Puttachary et al., 2015; Borowicz-Reutt and Czuczwar, 2020). Besides the contribution of ROS in epileptogenesis, damage-associated molecular patterns (DAMPs) interact with Toll-like receptors (TLRs) dependent on myeloid differentiation primary response 88 (MyD88) for glial cell activation, promoting the

release of interleukin 1β (IL-1β) and other proinflammatory molecules (Paschon et al., 2016). The following glial activation and the ongoing communication between astrocytes and microglia can be of most importance in deciding the neuroinflammation fate of the tissue in a pathology (Paschon et al., 2016; Kinoshita and Koyama, 2021).

Indeed, genes related to oxidative stress and neuroinflammation play different roles depending on the cell type in epileptogenesis. In this context, we approached the role of nicotinamide adenine dinucleotide phosphate (NADPH) oxidase 2 (NOX2), one of the main sources of ROS triggered by prolonged seizures (Shekh-Ahmad et al., 2019), and MyD88 in epileptogenesis. Furthermore, we discussed the employment of single-cell RNA-sequencing (scRNAseq) transcriptomic analyses, transgenic technologies, and viral serotypes carrying vectors with specific promoters to unravel the role of genes related to oxidative stress and neuroinflammation in epilepsy.

DISTINCT ROLES OF NOX2 IN MICROGLIA AND NEURONS

Microglial cells are known as the primary immune cells of the brain. As resident myeloid cells in the brain, they scour the environment removing cellular debris and releasing cytokines and free radicals such as ROS (Rettenbeck et al., 2015; Kinoshita and Koyama, 2021). Therefore, microglia plays a dual role in epileptogenesis, from distinct microglial phenotypes in sclerotic regions of the epileptic brain (Luo et al., 2016; Morin-Brureau et al., 2018) to promoting pro- and/or anti-epileptic activity (Kinoshita and Koyama, 2021).

Several studies demonstrated that *status epilepticus* (SE) elevates the level of ROS produced by microglia hours after its induction in animals (Dal-Pizzol et al., 2000; Sleven et al., 2006; Ryan et al., 2014). It has also been identified in the hippocampus of patients with refractory epilepsy (Shekh-Ahmad et al., 2019). The time course of ROS level alteration and the early microglial response may be associated with neural injury in the hippocampus following an insult that promotes epileptogenesis (Rettenbeck et al., 2015). Although other isoforms of the NOX family exist, NOX2 is of particular interest given its prominent expression by microglia. NOX2 is one of the main sources of ROS produced and released in epileptogenesis (Mcelroy et al., 2017; Shekh-Ahmad et al., 2019). In microglia, the GTPase Rab27 induces the movement of NOX2 complex to the plasma membrane (Ejlerskov et al., 2012). Nevertheless, in other cell types, Ras GTPase-activating-like protein (IQGAP1) is crucial for NOX2's movement towards the cell surface (Ikeda et al., 2005). The inhibition of NOX2 or its genetic ablation in mice reduces microglial activity and neuroinflammation (Guemez-Gamboa et al., 2011; Wang et al., 2013; Zhang et al., 2017; Chandran et al., 2018). This data suggests that ROS modulates the inflammatory response and microglial activation in epileptogenesis (Chhor et al., 2013; Shekh-Ahmad et al., 2019).

NOX2 catalyzes molecular oxygen into its oxidative form in microglia and neurons. Its activation is modulated by N-methyl-D-aspartate receptors (NMDAr) and metabotropic glutamatergic receptors of group II (mGluR3) and group III (mGluR4, 6, 7, 8), specifically (Haslund-Vinding et al., 2017). Besides that, DAMPs receptors coupled to G protein, i.e., N- formyl peptide receptors (FPRs) and P2Y receptors (P2YRs), which, upon stimulation, promote phosphorylation via RAC of cytosolic $p47^{phox}$, leading to its conformational change. Alongside $p67^{phox}$ and $p40^{phox}$, this protein migrates to the membrane. In their interaction with NOX2 and $p22^{phox}$, electrons are transferred from the substrate NADPH to molecular oxygen, resulting in superoxide production (Vermot et al., 2021). Additionally, hydrogen peroxide (H_2O_2) is suitable for triggering the phospholipase A2 (PLA2) pathway through signal-regulated kinase (ERK) and IL-1β production, which targets the IL-1β receptor and MyD88 pathway (**Figures 1Ai,ii,iii**) (Beckhauser et al., 2016).

The localization of NOX2 in the postsynaptic region is convenient for its role in synaptic plasticity (Bedard and Krause, 2007; Brennan et al., 2009). ROS physiologically acts as a second messenger in the nervous system, mostly supporting synaptic long-term potentiation (LTP) (Hidalgo and Arias-Cavieres, 2016) or long-term depression (LTD.) (Francis-Oliveira et al., 2018). In the hippocampus, for instance, ROS activates protein kinases that are essential for neural plasticity. Upon stimulation, NMDAr (containing the subunit GluN2B) promotes a calcium inflow into synapses, which leads to the production of ROS via Phosphoinositide 3-Kinase (PI3K)—Protein Kinase C (PKC), H_2O_2, and neural nitric oxide synthase (nNOS) (Beckhauser et al., 2016). Once produced, H_2O_2 can pass through the plasma membrane to interact with pre- and postsynaptic proteins, modulating the synaptic transmission (Quinn and Gauss, 2004). However, it can also induce damage on neuronal DNA, including chromosomal alterations, breakage of the DNA column and, in the absence of catalyst, oxidation of sulfhydryl compounds (–SH), leading to cell death in pathological conditions (**Figures 1Bi,ii,iii**) (Beckhauser et al., 2016).

DISTINCT ROLES OF MYD88 IN MICROGLIA AND ASTROCYTES

TLRs 2, 4, and 9 are expressed in astrocytes, while TLRs 1-9 are expressed in microglia. However, in neuroinflammation, the innate immune response mediated by microglia and astrocytes depends largely on TLR2 and TLR4, respectively, and IL-1R in both cell types. Most TLRs are coupled to the MyD88 adapter, the exception being TLR3, which is activated by double-strand DNA triggering the TRIF pathway. It is also important to mention that TLR4 can be activated by lipopolysaccharide to signal both pathways MyD88 and TRIF (Paschon et al., 2016; Fiebich et al., 2018).

These receptors can be activated by DAMPs, such as High Mobility Group Box 1 (HMGB-1), as observed in epilepsy, and beta-amyloid plaques and alpha-synuclein, in Alzheimer's and Parkinson's disease, respectively (Bernaus et al., 2020). These DAMPs can interact with TLR receptors located in astrocytes and microglia membranes. TLR activation leads both cells to secrete

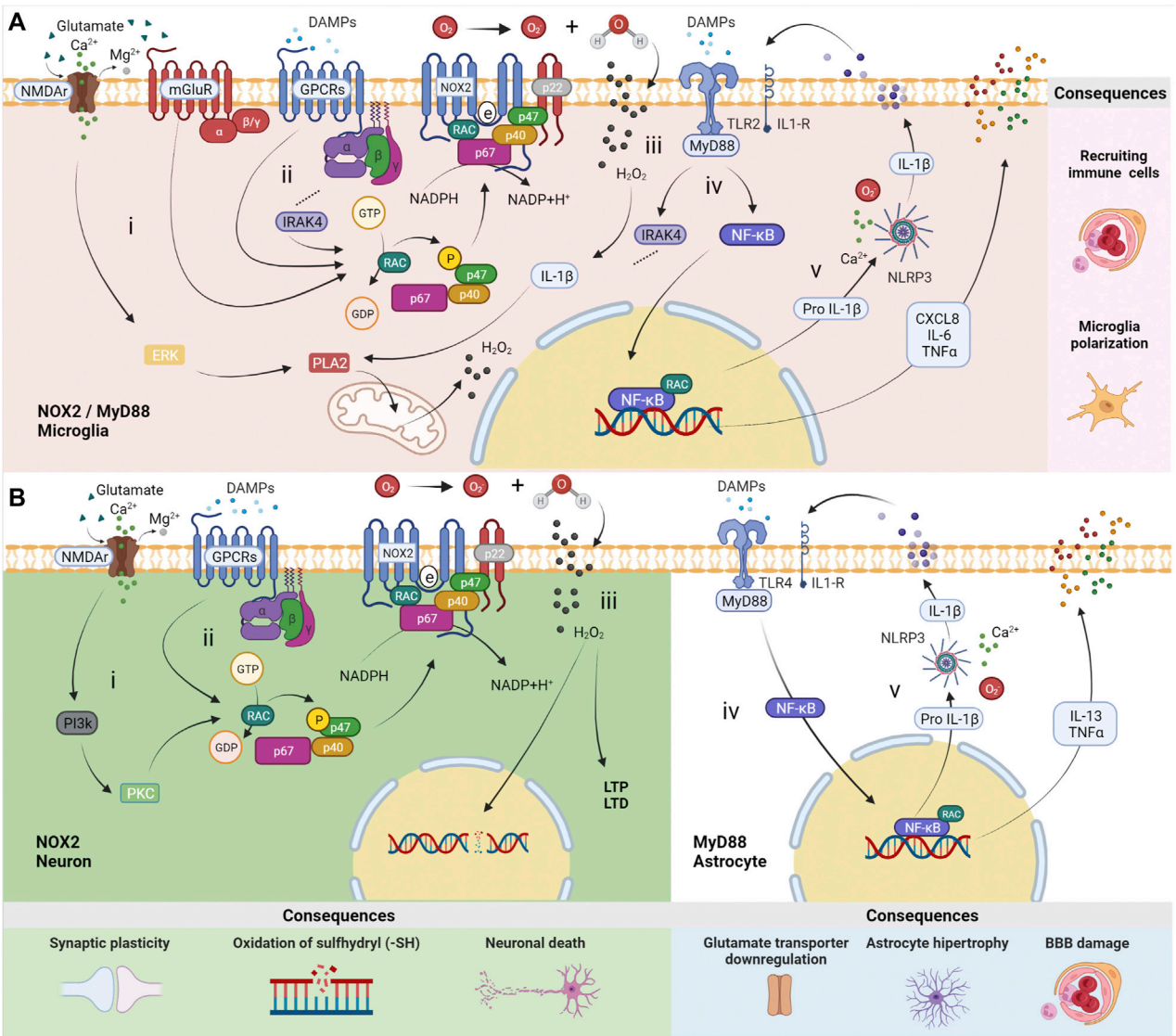

FIGURE 1 | Distinct roles of MyD88 and NOX2 in neurons, astrocytes and microglia. **(A)** In microglia, (i) N-methyl-D-aspartate receptors (NMDAr) promote a calcium inflow, which leads to the production of mitochondrial reactive oxygen species (ROS) *via* ERK-PLA2. The activation of metabotropic glutamatergic receptors from group II (mGluR3) and group III (mGluR4, 6, 7, 8) induces NOX2 activation throughout G_i/G_o alpha subunit. (ii) NOX2 can be activated by receptors of damage-associated molecular patterns (DAMPs) G-protein-dependent (GPCRs), i.e., N-formyl peptide receptors (FPRs) and P2Y receptors (P2YRs) *via* RAC, followed by phosphorylation of $p47^{phox}$ (p47) and migration to the membrane along with $p67^{phox}$ (p67) and $p40^{phox}$ (p40), resulting in ROS production. (iii) H_2O_2 produced from hydrogen and O_2 can cross membranes to participate in biochemistry reactions. (iv) Stimulation by DAMPs or cytokines throughout Toll-like Receptor 2 (TLR2) and interleukin-1 receptor (IL-1R), activates an intracellular signaling pathway involving the protein adaptor myeloid differentiation primary response 88 (MyD88). Specific consequences occur in microglia, such as NOX2 activation via IRAK4-RAC pathways. (v) NF-κB/RAC transcription factors promote the expression of chemokines CXCL8, IL-6, TNFα, and Pro IL-1β. The latter is transformed into mature IL-1β by the NLRP3 inflammasome dependent on calcium and ROS. The consequences are immune cell recruiting and microglia polarization. **(B)** Activation of NOX2 in neurons occurs (i) by NMDAr (containing subunit GluN2B) *via* PI3K-PKC and/or (ii) by DAMPs receptors (FPRs and P2YRs). (iii) H_2O_2 produced from hydrogen and O_2 induces long-term potentiation (LTP) and long-term depression (LTD.) in physiological situations. However, a high concentration of ROS, e.g., in *status epilepticus* (SE), results in neural DNA damage by oxidation of sulfhydryl compounds (–SH) and cell death due to influx of H_2O_2 to the nucleus. In astrocytes, (iv) MyD88 activation by TLR4 is followed by NF-κB/RAC transcription factors assembly, (v) promoting the expression of IL-6, TNFα, and Pro IL-1β. The latter is transformed into mature IL-1β by the NLRP3 inflammasome dependent on calcium and ROS. The consequences include ions and neurotransmitters unbalance, astrocytic hypertrophy, and blood-brain barrier (BBB) changes. The illustrations were obtained using BioRender software.

cytokines and inflammatory molecules that activate NADPH, which aids NOX2 and cyclooxygenase 2 (COX2) activation in microglia (Meng and Yao, 2020). The secretion of cytokines promotes autocrine and paracrine signaling, leading astrocytes and microglia activation into a vicious circle (Vezzani et al., 2013; Bernaus et al., 2020).

In the literature, it is regularly reported the expression of correspondent TLRs by astrocytes and microglia, however, the

release of specific cytokines by these cells depends on the stimulus or pathology. For instance, after seizure activity, the microglia of patients with TLE release IL-1β, CXCL8, IL-6 and TNFα (Morin-Brureau et al., 2018). On the other hand, in an LPS-induced Parkinson's model, the up-regulation of IFN-γ, IL-1β, IL-1R, IL-16, IL-17 levels in microglia have been reported. Therefore, it can be inferred that cytokines' release by microglia depends on many factors, although using the same intracellular signaling pathway, the NF-κB and NLRP3 inflammasome (Chien et al., 2016). When immunologically stimulated by TNFα or IL-1β, post-mortem or biopsy human astrocytes and cell-line NT2 astrocytes release cytokines IL-1β, TNFα, and IL-13. However, post-mortem or biopsy human astrocytes also produced IL-2, IL-7, TNFβ, and IF N-γ (**Figures 1iv,v**) (Burkert et al., 2012).

Microglia activation by TLRs and MyD88 modulate distinct epileptogenesis features. In this cell type, MyD88 signaling promotes cytokine secretion and induces apoptosis of neighboring cells. Microglia potentializes the immune response by recruiting peripheral immune system cells, increasing the inflammatory environment (Meng and Yao, 2020). TLR2 signalling activates IL-1 Receptor-Associated Kinase 4 (IRAK4) in the MyD88-dependent axis. Once activated, IRAK4 phosphorylates p47phox on several residues to activate NOX2 (Pacquelet et al., 2007). Besides that, microglia disrupts gamma-aminobutyric acid (GABA) signaling and regulates the neural expression of NR1 and NR2b subunits of NMDA receptor. These processes result in high excitability of neurons which, in turn, contributes to epileptogenesis (Vezzani et al., 2013; Liu et al., 2018; Xueying Li et al., 2021).

On the other hand, MyD88 signaling modulates the astroglial tissue-maintenance functions, such as ions and neurotransmitters homeostasis (Li et al., 2020; Vezzani et al., 2013). In neuroinflammation, astroglial activation through the MyD88 pathway creates a harmful environment to the neural tissue, characterized by an astrocytic hypertrophic state, which impairs the blood-brain barrier and neural communication maintenance. (Vezzani et al., 2013; Liu et al., 2018; Xueying Li et al., 2021). Astrocytic activation can occur by MyD88-dependent TLR4 via the extracellular signal-related kinase (ERK) pathway, and promotes excitatory synapse development, resulting in increased seizure susceptibility (Henneberger and Steinhauser, 2016; Shen et al., 2016). In this context, the increased expression of TLR4 in astrocytes, but not in microglia, suggests TLR4's role in seizure frequency in human epilepsy (Pernhorst et al., 2013).

The crosstalk involving the MyD88 pathway in microglia and astrocytes seems crucial in triggering inflammation in the central nervous system (CNS), given that the absence of microglia *in vitro* and *in vivo* leads to a failure of TLR4 activation in astrocytes, consequently reducing the inflammatory response (Barbierato et al., 2013; Liddelow et al., 2017). In epileptogenesis, neuroinflammation contributes to the pathological synaptic plasticity and dendrite growth by activating IL-1R/TLR receptors, transcription factor NF-κB, and cytokines effects (Vezzani et al., 2013; Meng and Yao, 2020).

Therefore, anti-inflammatory therapies and pharmacological drugs that influence the signaling pathway involving TLR4/MyD88/NF-κB/NLRP3/IL-1β, such as baicalin (TLR4 inhibitor) and agmatine (TLR4 down regulator), also reduce the frequency, duration and intensity of seizures (Lun Li et al., 2021; Yang et al., 2021). Furthermore, MyD88 inhibition reduces phosphorylation and expression of NMDAr, modulates proinflammatory microglia, and increases the expression of glutamate receptors in astrocytes (Wang et al., 2017; Liu et al., 2018). These mechanisms support the important role of MyD88 in neuroinflammation associated with epilepsy; in this sense, approaches that directly target MyD88 inhibition demonstrate positive effects in epilepsy. In summary, MyD88 and NOX2 are essential players in epileptogenesis, regulating the neuroinflammatory response in a cell-specific manner, promoting distinct outcomes.

DISCUSSION

Considering that specific cell types have distinct impacts on epilepsy, technologies that allow screening, such as scRNAseq, genetically modified animals, and cell-targeted gene control provide valuable approaches to study epilepsy. New therapeutic strategies are necessary since around one-third of patients with TLE are refractory to clinically available drug treatments.

scRNAseq allows the assessment of the transcriptomic profile of cell-type-specific (**Figure 2A**). This technique offers insights into the mechanisms involved in epileptogenesis and characterizes the specific contribution of microglia, astrocytes, and neurons in epilepsy (Olsen and Baryawno, 2018; Cid et al., 2021). This approach investigates NOX2 and MyD88 transcriptomic pathways in distinct time points in epileptogenesis in animal models and surgically-extracted nervous tissues. Specific cell types are separately analyzed, and a complete RNA profile is obtained. For instance, RNAseq data of epileptic hippocampus demonstrated the possibility of investigating oxidative stress regulation and inflammatory responses, such as cytokines, cell migration, proliferation, and cell death, which involve TLR2, TLR3, TLR4, TLR7, and C1qa, inflammasome genes, and pyroptosis (Cid et al., 2021).

Besides mapping changes in the transcriptome in cell-type-specific, transgenic animals allow the control of gene expression in a cell-specific manner, such as in the Cre/flox system (**Figure 2B**). Cre-mice breed with LoxP (floxed) mice results in Cre-LoxP animals. In this condition, Cre enzyme promotes the inversion or deletion of the genes flanked by LoxP sequences, which can be replaced by a reporter gene such as eGFP (Kim et al., 2018). Bringing this approach into the context of specific targets in epilepsy, it is possible to track the downstream effects of MyD88 and NOX2 loss-of-function in cell-type-specific. Indeed, the cell-type-specific gene ablation combined with pharmacological approaches has been demonstrated particularly useful in the determination of the roles of COX2 (Serrano et al., 2011) and prostaglandin receptor EP2 (Nagib et al., 2020; Sluter et al., 2021; Varvel et al., 2021) in animal models of SE.

For example, to test the downstream effects of MyD88 loss in microglia, a transgenic mice model was established to target

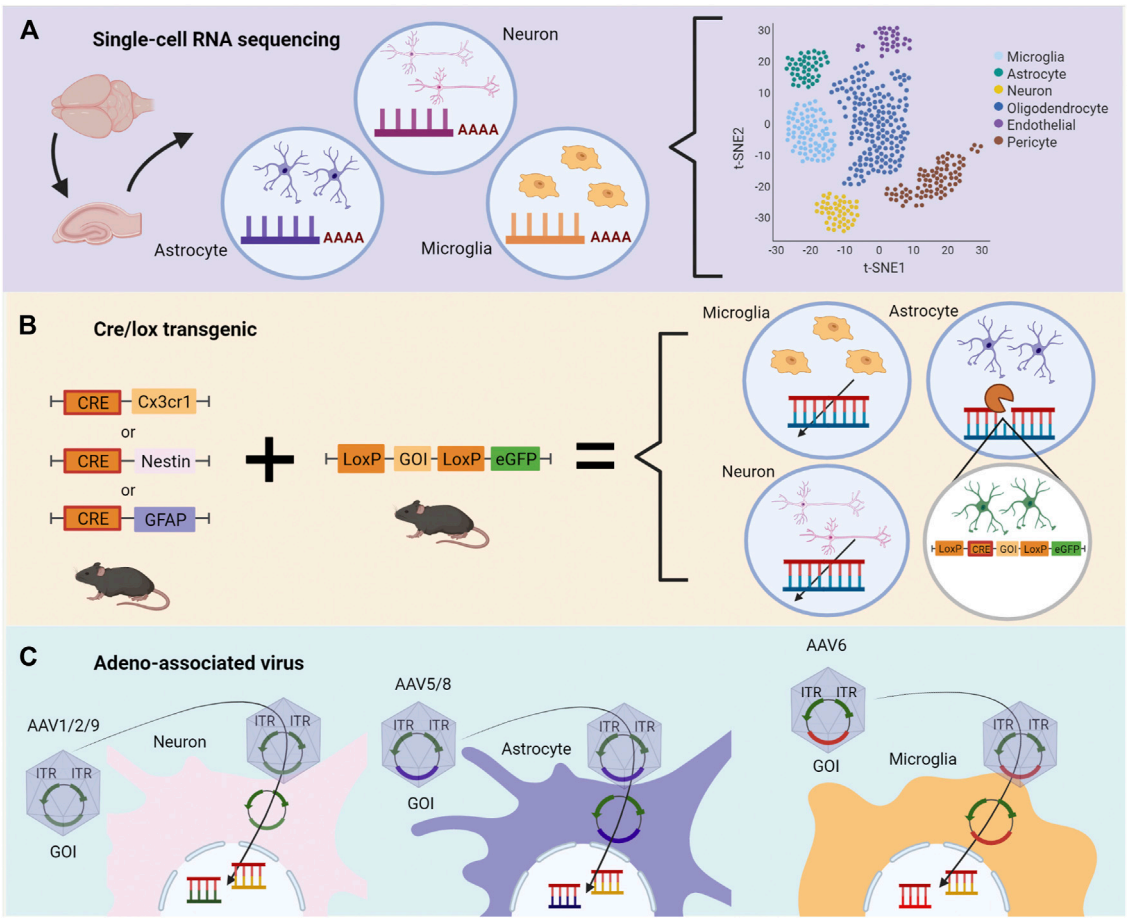

FIGURE 2 | Methodological strategies to assess specific roles of genes during epileptogenesis depending on the cell type. **(A)** Single-cell RNA sequencing (scRNA-seq) of the temporal lobe or hippocampus permits the evaluation of changes in transcriptomics triggered by epileptogenesis. Distinct cell types are separately analyzed, and a complete RNA profile is obtained. Changes in transcriptomics are described according to correlation, heatmaps, and quantitative analysis. **(B)** Cre/lox transgenic technologies can be used to evaluate the role of genes in cell-type-specific during epileptogenesis *in vivo*. In the first generation, two distinct animals are bred, one containing the Cre enzyme, the other containing two LoxP sequences between the gene of interest (GOI) and a gene reporter, as eGFP. Littermates receive genetic material necessary for the Cre/flox system to modify, delete or change the GOI. **(C)** Adeno-associated virus (AAV) contains the GOI with inverted terminal repeats (ITR) and viral capsid necessary for cell-specific targeting. The genetic modification occurs by the transported plasmid carrying the GOI. The illustrations were obtained using BioRender software.

microglia chemokine receptors (Cx3cr1) to knockout the MyD88 gene. The authors showed a relationship between neuron maturation and loss of MyD88 in microglia cells, which disrupts the reward-related-memory formation in morphine addiction (Rivera et al., 2019). On the other hand, the Nestin-Cre model directly induces gene modification into neurons and microglia, which showed that the presence of MyD88 in both cell types is not necessary to respond to a nocive stimulus (Braun et al., 2012). Specific neuron modifications are usually achieved with the Synapsin I Cre model (Mcnair et al., 2020), which is capable of modifying differentiated neurons. Regarding astrocytes, although the most used model is the GFAP-Cre, it also promotes changes in non-specific targets; S100b and GLAST are alternatives pointed out to decrease the off-target effects (Guttenplan and Liddelow, 2019; Mcnair et al., 2020). Also, the generation of brain-specific Mn-SOD-deficient mice (brain-Sod22/) to study ROS in the hypoxia model (Sasaki et al., 2011) and neurodegenerative diseases (Marecki et al., 2014; Park et al., 2022) demonstrates the application of this technology.

In addition to transgenic animal models, genetic modifications through viral vectors have also opened opportunities for studying TLE (**Figure 2C**). Amongst these, adeno-associated virus (AAV) stands out given that its variations have distinct tropism for cell-type-specific. Also, AAV vectors have been used for gene therapy applications due to their safety and the ability to infect dividing and non-dividing cells, performing a long-term transgene expression profile (Daya and Berns, 2008). For instance, AAV can be applied to increase CCL2, aiming to rescue the expression of cytokine levels (CCL2, IL-1β), since these cytokines were described as reduced by other therapies (Wu et al., 2019).

AAV allows control of the gene expression by inserting the gene of interest (GOI), or a sequence that generates a short hairpin RNA (shRNA) to target the GOI, in the host DNA. This

modification promotes overexpression or knockdown of the GOI in the host cell (Daya and Berns, 2008). Several serotypes have been identified in AAV, increasing the probability of transfection of cell-type-specific. For CNS, serotype 2 (AAV2) is the most adopted virus despite the variability of transfection efficiency regarding the cell type, which is overcome by using pseudotyping AAVs by recombining new capsids from different serotypes (Fakhiri and Grimm, 2021). Neurons and astrocytes are efficiently transfected by AAV, both *in vivo* and *in vitro*. Also, vectors have been tested for transfection efficiency and transgene expression, demonstrating that AAV5 (Griffin et al., 2019) and AAV8 (Aschauer et al., 2013) are potent viral vectors to transfect astrocytes, while AAV2/1 (Hammond et al., 2017) and AAV9 (Aschauer et al., 2013) are best suitable for neurons. Microglia are the most refractile cells in the nervous system to AAV transfection, but several improvements have been made. For instance, a modified rAAV6 combined with specific microglial promoters succeeded in transfecting these cells *in vitro* and *in vivo* (Rosario et al., 2016; Su et al., 2016). Therefore, by employing specific serotypes, it is possible to overexpress or knockdown the expression of genes implied in the epileptogenesis process, such as NOX2 and MyD88, in cell-type-specific.

Cell-type-specific approaches grant benefits in research and scientific study development. However, the lack of reproducibility and technical difficulties might be the reasons for possibly delivering biased results, such as in the RNA-seq case (Whitley et al., 2016). In the Cre/lox system, specific tissue promoters can be expressed in undesired tissues and at uncommon times (Sauer, 1998). At last, their use for in-human treatment may not be indicated, such as in the case of AAV therapies, which hold genotoxicity potential (Colella et al., 2018). Epilepsy has already demonstrated to be multifactorial, therefore a single treatment based on monotherapy will probably not be efficient, especially in refractory TLE (Vezzani et al., 2013; Organization, W. H, 2019; Falco-Walter, 2020).

In summary, cell-type-specific approaches should be applied to investigate mechanisms related to brain disorders. This strategy promotes a better understanding of genes involved in epileptogenesis, bringing new insights into treatments and therapies for TLE (Couvillion et al., 2009).

AUTHOR CONTRIBUTIONS

Wrote the first draft of the manuscript: CA, RP, MM, GH. Revised the manuscript: RR, JJ, EK, AK. Conceived the study: AK.

FUNDING

AK is grateful for grants from FAPESP (#2019/17892-8, #2020/11667-0), CNPq (#431000/2016-6 and #312047/2017-7), and CAPES (financial code 001). JJ is grateful for NIH/NINDS grants: R01NS100947, and R61NS124923. The funders had no role in study design, data collection and analysis, decision to publish, or manuscript preparation.

REFERENCES

Aschauer, D. F., Kreuz, S., and Rumpel, S. (2013). Analysis of Transduction Efficiency, Tropism and Axonal Transport of AAV Serotypes 1, 2, 5, 6, 8 and 9 in the Mouse Brain. *PLoS One* 8, e76310. doi:10.1371/journal.pone.0076310

Barbierato, M., Facci, L., Argentini, C., Marinelli, C., Skaper, S., and Giusti, P. (2013). Astrocyte-microglia Cooperation in the Expression of a Pro-inflammatory Phenotype. *Cnsnddt* 12, 608–618. doi:10.2174/18715273113129990064

Beckhauser, T. F., Francis-Oliveira, J., and De Pasquale, R. (2016). Reactive Oxygen Species: Physiological and Physiopathological Effects on Synaptic Plasticity. *J. Exp. Neurosci.* 10, 23–48. doi:10.4137/JEN.S39887

Bedard, K., and Krause, K.-H. (2007). The NOX Family of ROS-Generating NADPH Oxidases: Physiology and Pathophysiology. *Physiol. Rev.* 87, 245–313. doi:10.1152/physrev.00044.2005

Bernaus, A., Blanco, S., and Sevilla, A. (2020). Glia Crosstalk in Neuroinflammatory Diseases. *Front. Cell. Neurosci.* 14, 209. doi:10.3389/fncel.2020.00209

Borowicz-Reutt, K. K., and Czuczwar, S. J. (2020). Role of Oxidative Stress in Epileptogenesis and Potential Implications for Therapy. *Pharmacol. Rep.* 72, 1218–1226. doi:10.1007/s43440-020-00143-w

Braun, T. P., Grossberg, A. J., Veleva-Rotse, B. O., Maxson, J. E., Szumowski, M., Barnes, A. P., et al. (2012). Expression of Myeloid Differentiation Factor 88 in Neurons Is Not Requisite for the Induction of Sickness Behavior by Interleukin-1β. *J. Neuroinflammation* 9, 229. doi:10.1186/1742-2094-9-229

Brennan, A. M., Won Suh, S., Joon Won, S., Narasimhan, P., Kauppinen, T. M., Lee, H., et al. (2009). NADPH Oxidase Is the Primary Source of Superoxide Induced by NMDA Receptor Activation. *Nat. Neurosci.* 12, 857–863. doi:10.1038/nn.2334

Burkert, K., Moodley, K., Angel, C. E., Brooks, A., and Graham, E. S. (2012). Detailed Analysis of Inflammatory and Neuromodulatory Cytokine Secretion from Human NT2 Astrocytes Using Multiplex Bead Array. *Neurochem. Int.* 60, 573–580. doi:10.1016/j.neuint.2011.09.002

Chandran, R., Kim, T., Mehta, S. L., Udho, E., Chanana, V., Cengiz, P., et al. (2018). A Combination Antioxidant Therapy to Inhibit NOX2 and Activate Nrf2 Decreases Secondary Brain Damage and Improves Functional Recovery after Traumatic Brain Injury. *J. Cereb. Blood Flow. Metab.* 38, 1818–1827. doi:10.1177/0271678x17738701

Chhor, V., Le Charpentier, T., Lebon, S., Oré, M.-V., Celador, I. L., Josserand, J., et al. (2013). Characterization of Phenotype Markers and Neuronotoxic Potential of Polarised Primary Microglia *In Vitro*. *Brain, Behav. Immun.* 32, 70–85. doi:10.1016/j.bbi.2013.02.005

Chien, C.-H., Lee, M.-J., Liou, H.-C., Liou, H.-H., and Fu, W.-M. (2016). Microglia-Derived Cytokines/Chemokines Are Involved in the Enhancement of LPS-Induced Loss of Nigrostriatal Dopaminergic Neurons in DJ-1 Knockout Mice. *PLoS One* 11, e0151569. doi:10.1371/journal.pone.0151569

Cid, E., Marquez-Galera, A., Valero, M., Gal, B., Medeiros, D. C., Navarron, C. M., et al. (2021). Sublayer- and Cell-type-specific Neurodegenerative Transcriptional Trajectories in Hippocampal Sclerosis. *Cell Rep.* 35, 109229. doi:10.1016/j.celrep.2021.109229

Colella, P., Ronzitti, G., and Mingozzi, F. (2018). Emerging Issues in AAV-Mediated *In Vivo* Gene Therapy. *Mol. Ther. - Methods & Clin. Dev.* 8, 87–104. doi:10.1016/j.omtm.2017.11.007

Couvillion, M. T., Lee, S. R., Hogstad, B., Malone, C. D., Tonkin, L. A., Sachidanandam, R., et al. (2009). Sequence, Biogenesis, and Function of Diverse Small RNA Classes Bound to the Piwi Family Proteins of Tetrahymena Thermophila. *Genes. Dev.* 23, 2016–2032. doi:10.1101/gad.1821209

Dal-Pizzol, F., Klamt, F., Vianna, M. M. R., Schröder, N., Quevedo, J., Benfato, M. S., et al. (2000). Lipid Peroxidation in hippocampus Early and Late after Status

Epilepticus Induced by Pilocarpine or Kainic Acid in Wistar Rats. *Neurosci. Lett.* 291, 179–182. doi:10.1016/s0304-3940(00)01409-9

Daya, S., and Berns, K. I. (2008). Gene Therapy Using Adeno-Associated Virus Vectors. *Clin. Microbiol. Rev.* 21, 583–593. doi:10.1128/cmr.00008-08

Ejlerskov, P., Christensen, D. P., Beyaie, D., Burritt, J. B., Paclet, M.-H., Gorlach, A., et al. (2012). NADPH Oxidase Is Internalized by Clathrin-Coated Pits and Localizes to a Rab27A/B GTPase-Regulated Secretory Compartment in Activated Macrophages. *J. Biol. Chem.* 287, 4835–4852. doi:10.1074/jbc.m111.293696

Fakhiri, J., and Grimm, D. (2021). Best of Most Possible Worlds: Hybrid Gene Therapy Vectors Based on Parvoviruses and Heterologous Viruses. *Mol. Ther.* 29, 3359–3382. doi:10.1016/j.ymthe.2021.04.005

Falco-Walter, J. (2020). Epilepsy-Definition, Classification, Pathophysiology, and Epidemiology. *Semin. Neurol.* 40, 617–623. doi:10.1055/s-0040-1718719

Fiebich, B. L., Batista, C. R. A., Saliba, S. W., Yousif, N. M., and De Oliveira, A. C. P. (2018). Role of Microglia TLRs in Neurodegeneration. *Front. Cell. Neurosci.* 12, 329. doi:10.3389/fncel.2018.00329

Francis-Oliveira, J., Vilar Higa, G. S., Mendonça Munhoz Dati, L., Carvalho Shieh, I., and De Pasquale, R. (2018). Metaplasticity in the Visual Cortex: Crosstalk between Visual Experience and Reactive Oxygen Species. *J. Neurosci.* 38, 5649–5665. doi:10.1523/jneurosci.2617-17.2018

Griffin, J. M., Fackelmeier, B., Fong, D. M., Mouravlev, A., Young, D., and O'carroll, S. J. (2019). Astrocyte-selective AAV Gene Therapy through the Endogenous GFAP Promoter Results in Robust Transduction in the Rat Spinal Cord Following Injury. *Gene Ther.* 26, 198–210. doi:10.1038/s41434-019-0075-6

Guedes, F. A., Galvis-Alonso, O. Y., and Leite, J. P. (2006). Plasticidade neuronal associada à epilepsia Do lobo temporal mesial: insights a partir de estudos em humanos e em modelos animais. *J. epilepsy Clin. Neurophysiol.* 12, 10–17. doi:10.1590/s1676-26492006000200003

Guemez-Gamboa, A., Estrada-Sánchez, A. M., Montiel, T., Páramo, B., Massieu, L., and Morán, J. (2011). Activation of NOX2 by the Stimulation of Ionotropic and Metabotropic Glutamate Receptors Contributes to Glutamate Neurotoxicity *In Vivo* through the Production of Reactive Oxygen Species and Calpain Activation. *J. Neuropathol. Exp. Neurol.* 70, 1020–1035. doi:10.1097/nen.0b013e3182358e4e

Guttenplan, K. A., and Liddelow, S. A. (2019). Astrocytes and Microglia: Models and Tools. *J. Exp. Med.* 216, 71–83. doi:10.1084/jem.20180200

Hammond, S. L., Leek, A. N., Richman, E. H., and Tjalkens, R. B. (2017). Cellular Selectivity of AAV Serotypes for Gene Delivery in Neurons and Astrocytes by Neonatal Intracerebroventricular Injection. *PLoS One* 12, e0188830. doi:10.1371/journal.pone.0188830

Haslund-Vinding, J., Mcbean, G., Jaquet, V., and Vilhardt, F. (2017). NADPH Oxidases in Oxidant Production by Microglia: Activating Receptors, Pharmacology and Association with Disease. *Br. J. Pharmacol.* 174, 1733–1749. doi:10.1111/bph.13425

Henneberger, C., and Steinhäuser, C. (2016). Astrocytic TLR4 at the Crossroads of Inflammation and Seizure Susceptibility. *J. Cell Biol.* 215, 607–609. doi:10.1083/jcb.201611078

Hidalgo, C., and Arias-Cavieres, A. (2016). Calcium, Reactive Oxygen Species, and Synaptic Plasticity. *Physiology* 31, 201–215. doi:10.1152/physiol.00038.2015

Ikeda, S., Yamaoka-Tojo, M., Hilenski, L., Patrushev, N. A., Anwar, G. M., Quinn, M. T., et al. (2005). IQGAP1 Regulates Reactive Oxygen Species-dependent Endothelial Cell Migration through Interacting with Nox2. *Arterioscler Thromb Vasc Biol* 25, 2295–2300. doi:10.1161/01.atv.0000187472.55437.af

Jiang, J., Yu, Y., Kinjo, E. R., Du, Y., Nguyen, H. P., and Dingledine, R. (2019). Suppressing Pro-inflammatory Prostaglandin Signaling Attenuates Excitotoxicity-Associated Neuronal Inflammation and Injury. *Neuropharmacology* 149, 149–160. doi:10.1016/j.neuropharm.2019.02.011

Kim, H., Kim, M., Im, S.-K., and Fang, S. (2018). Mouse Cre-LoxP System: General Principles to Determine Tissue-specific Roles of Target Genes. *Lab. Anim. Res.* 34, 147–159. doi:10.5625/lar.2018.34.4.147

Kinjo, E. R., Higa, G. S. V., Santos, B. A., De Sousa, E., Damico, M. V., Walter, L. T., et al. (2016). Pilocarpine-induced Seizures Trigger Differential Regulation of microRNA-Stability Related Genes in Rat Hippocampal Neurons. *Sci. Rep.* 6, 20969. doi:10.1038/srep20969

Kinjo, E, Rodríguez, P, Dos Santos, B, Higa, G, Ferraz, M, Schmeltzer, C., et al. (2018). New Insights on Temporal Lobe Epilepsy Based on Plasticity-Related Network Changes and High-Order Statistics. *Mol. Neurobiol.* 55, 3990–3998. doi:10.1007/s12035-017-0623-2

Kinoshita, S., and Koyama, R. (2021). Pro- and Anti-epileptic Roles of Microglia. *Neural Regen. Res.* 16, 1369–1371. doi:10.4103/1673-5374.300976

Liddelow, S. A., Guttenplan, K. A., Clarke, L. E., Bennett, F. C., Bohlen, C. J., Schirmer, L., et al. (2017). Neurotoxic Reactive Astrocytes Are Induced by Activated Microglia. *Nature* 541, 481–487. doi:10.1038/nature21029

Liu, J.-T., Wu, S.-X., Zhang, H., and Kuang, F. (2018). Inhibition of MyD88 Signaling Skews Microglia/Macrophage Polarization and Attenuates Neuronal Apoptosis in the Hippocampus after Status Epilepticus in Mice. *Neurotherapeutics* 15, 1093–1111. doi:10.1007/s13311-018-0653-0

Lun Li, L., Acioglu, C., Heary, R. F., and Elkabes, S. (2021). Role of Astroglial Toll-like Receptors (TLRs) in Central Nervous System Infections, Injury and Neurodegenerative Diseases. *Brain, Behav. Immun.* 91, 740–755. doi:10.1016/j.bbi.2020.10.007

Luo, C., Koyama, R., and Ikegaya, Y. (2016). Microglia Engulf Viable Newborn Cells in the Epileptic Dentate Gyrus. *Glia* 64, 1508–1517. doi:10.1002/glia.23018

Marecki, J. C., Parajuli, N., Crow, J. P., and Macmillan-Crow, L. A. (2014). The Use of the Cre/loxPSystem to Study Oxidative Stress in Tissue-Specific Manganese Superoxide Dismutase Knockout Models. *Antioxidants Redox Signal.* 20, 1655–1670. doi:10.1089/ars.2013.5293

Mcelroy, P. B., Liang, L.-P., Day, B. J., and Patel, M. (2017). Scavenging Reactive Oxygen Species Inhibits Status Epilepticus-Induced Neuroinflammation. *Exp. Neurol.* 298, 13–22. doi:10.1016/j.expneurol.2017.08.009

Mcnair, L. F., Andersen, J. V., Nissen, J. D., Sun, Y., Fischer, K. D., Hodgson, N. W., et al. (2020). Conditional Knockout of GLT-1 in Neurons Leads to Alterations in Aspartate Homeostasis and Synaptic Mitochondrial Metabolism in Striatum and Hippocampus. *Neurochem. Res.* 45, 1420–1437. doi:10.1007/s11064-020-03000-7

Meng, F., and Yao, L. (2020). The Role of Inflammation in Epileptogenesis. *Acta Epileptol.* 2, 1–19. doi:10.1186/s42494-020-00024-y

Morin-Brureau, M., Milior, G., Royer, J., Chali, F., Le Duigou, C., Savary, E., et al. (2018). Microglial Phenotypes in the Human Epileptic Temporal Lobe. *Brain* 141, 3343–3360. doi:10.1093/brain/awy276

Nagib, M. M., Yu, Y., and Jiang, J. (2020). Targeting Prostaglandin Receptor EP2 for Adjunctive Treatment of Status Epilepticus. *Pharmacol. Ther.* 209, 107504. doi:10.1016/j.pharmthera.2020.107504

Olsen, T, and Baryawno, N. (2018). Introduction to Single-Cell RNA Sequencing. *Curr. Protoc. Mol. Biol.* 122, e57. doi:10.1002/cpmb.57

Organization, W. H (2019). *Epilepsy: A Public Health Imperative*. Geneva, Switzerland: WHO.

Pacquelet, S., Johnson, J. L., Ellis, B. A., Brzezinska, A. A., Lane, W. S., Munafo, D. B., et al. (2007). Cross-talk between IRAK-4 and the NADPH Oxidase. *Biochem. J.* 403, 451–461. doi:10.1042/bj20061184

Park, J. S., Saeed, K., Jo, M. H., Kim, M. W., Lee, H. J., Park, C. B., et al. (2022). LDHB Deficiency Promotes Mitochondrial Dysfunction Mediated Oxidative Stress and Neurodegeneration in Adult Mouse Brain. *Antioxidants (Basel)* 11 (2), 261. doi:10.3390/antiox11020261

Paschon, V., Takada, S, Ikebara, J, Sousa, E., Raeisossadati, R., Ulrich, H., et al. (2016). Interplay between Exosomes, microRNAs and Toll-like Receptors in Brain Disorders. *Mol. Neurobiol.* 53, 2016–2028. doi:10.1007/s12035-015-9142-1

Pernhorst, K., Herms, S., Hoffmann, P., Cichon, S., Schulz, H., Sander, T., et al. (2013). TLR4, ATF-3 and IL8 Inflammation Mediator Expression Correlates with Seizure Frequency in Human Epileptic Brain Tissue. *Seizure* 22, 675–678. doi:10.1016/j.seizure.2013.04.023

Pitkänen, A., Lukasiuk, K., Edward Dudek, F., and Staley, K. (2015). Epileptogenesis. *Cold Spring Harb. Perspect. Med.* 5 (10), a022822. doi:10.1101/cshperspect.a022822

Puttachary, S., Sharma, S., Stark, S., and Thippeswamy, T. (2015). Seizure-induced Oxidative Stress in Temporal Lobe Epilepsy. *Biomed. Res. Int.* 2015, 745613. doi:10.1155/2015/745613

Quinn, M. T., and Gauss, K. A. (2004). Structure and Regulation of the Neutrophil Respiratory Burst Oxidase: Comparison with Nonphagocyte Oxidases. *J. Leukoc. Biol.* 76, 760–781. doi:10.1189/jlb.0404216

Rettenbeck, M. L., Rüden, E.-L. V., Bienas, S., Carlson, R., Stein, V. M., Tipold, A., et al. (2015). Microglial ROS Production in an Electrical Rat Post-status

Epilepticus Model of Epileptogenesis. *Neurosci. Lett.* 599, 146–151. doi:10.1016/j.neulet.2015.05.041

Rivera, P. D., Hanamsagar, R., Kan, M. J., Tran, P. K., Stewart, D., Jo, Y. C., et al. (2019). Removal of Microglial-specific MyD88 Signaling Alters Dentate Gyrus Doublecortin and Enhances Opioid Addiction-like Behaviors. *Brain, Behav. Immun.* 76, 104–115. doi:10.1016/j.bbi.2018.11.010

Rosario, A. M., Cruz, P. E., Ceballos-Diaz, C., Strickland, M. R., Siemienski, Z., Pardo, M., et al. (2016). Microglia-specific Targeting by Novel Capsid-Modified AAV6 Vectors. *Mol. Ther. - Methods & Clin. Dev.* 3, 16026. doi:10.1038/mtm.2016.26

Royero, P. X., Higa, G. S. V., Kostecki, D. S., Dos Santos, B. A., Almeida, C., Andrade, K. A., et al. (2020). Ryanodine Receptors Drive Neuronal Loss and Regulate Synaptic Proteins during Epileptogenesis. *Exp. Neurol.* 327, 113213. doi:10.1016/j.expneurol.2020.113213

Ryan, K., Liang, L.-P., Rivard, C., and Patel, M. (2014). Temporal and Spatial Increase of Reactive Nitrogen Species in the Kainate Model of Temporal Lobe Epilepsy. *Neurobiol. Dis.* 64, 8–15. doi:10.1016/j.nbd.2013.12.006

Sasaki, T., Shimizu, T., Koyama, T., Sakai, M., Uchiyama, S., Kawakami, S., et al. (2011). Superoxide Dismutase Deficiency Enhances Superoxide Levels in Brain Tissues during Oxygenation and Hypoxia-Reoxygenation. *J. Neurosci. Res.* 89, 601–610. doi:10.1002/jnr.22581

Sauer, B. (1998). Inducible Gene Targeting in Mice Using the Cre/loxSystem. *Methods* 14, 381–392. doi:10.1006/meth.1998.0593

Serrano, G. E., Lelutiu, N., Rojas, A., Cochi, S., Shaw, R., Makinson, C. D., et al. (2011). Ablation of Cyclooxygenase-2 in Forebrain Neurons Is Neuroprotective and Dampens Brain Inflammation after Status Epilepticus. *J. Neurosci.* 31, 14850–14860. doi:10.1523/jneurosci.3922-11.2011

Shekh-Ahmad, T., Kovac, S., Abramov, A. Y., and Walker, M. C. (2019). Reactive Oxygen Species in Status Epilepticus. *Epilepsy & Behav.* 101, 106410. doi:10.1016/j.yebeh.2019.07.011

Shen, Y., Qin, H., Chen, J., Mou, L., He, Y., Yan, Y., et al. (2016). Postnatal Activation of TLR4 in Astrocytes Promotes Excitatory Synaptogenesis in Hippocampal Neurons. *J. Cell Biol.* 215, 719–734. doi:10.1083/jcb.201605046

Sleven, H., Gibbs, J. E., Heales, S., Thom, M., and Cock, H. R. (2006). Depletion of Reduced Glutathione Precedes Inactivation of Mitochondrial Enzymes Following Limbic Status Epilepticus in the Rat hippocampus. *Neurochem. Int.* 48, 75–82. doi:10.1016/j.neuint.2005.10.002

Sluter, M. N., Hou, R., Li, L., Yasmen, N., Yu, Y., Liu, J., et al. (2021). EP2 Antagonists (2011-2021): A Decade's Journey from Discovery to Therapeutics. *J. Med. Chem.* 64, 11816–11836. doi:10.1021/acs.jmedchem.1c00816

Su, W., Kang, J., Sopher, B., Gillespie, J., Aloi, M. S., Odom, G. L., et al. (2016). Recombinant Adeno-Associated Viral (rAAV) Vectors Mediate Efficient Gene Transduction in Cultured Neonatal and Adult Microglia. *J. Neurochem.* 136 (Suppl. 1), 49–62. doi:10.1111/jnc.13081

Varvel, N. H., Espinosa-Garcia, C., Hunter-Chang, S., Chen, D., Biegel, A., Hsieh, A., et al. (2021). Peripheral Myeloid Cell EP2 Activation Contributes to the Deleterious Consequences of Status Epilepticus. *J. Neurosci.* 41, 1105–1117. doi:10.1523/jneurosci.2040-20.2020

Vermot, A., Petit-Hartlein, I., Smith, S. M. E., and Fieschi, F. (2021). NADPH Oxidases (NOX): An Overview from Discovery,Molecular Mechanisms to Physiology and Pathology. *Antioxidants (Basel)* 10, 890. doi:10.3390/antiox10060890

Vezzani, A., Friedman, A., and Dingledine, R. J. (2013). The Role of Inflammation in Epileptogenesis. *Neuropharmacology* 69, 16–24. doi:10.1016/j.neuropharm.2012.04.004

Wang, Z., Wei, X., Liu, K., Zhang, X., Yang, F., Zhang, H., et al. (2013). NOX2 Deficiency Ameliorates Cerebral Injury through Reduction of Complexin II-Mediated Glutamate Excitotoxicity in Experimental Stroke. *Free Radic. Biol. Med.* 65, 942–951. doi:10.1016/j.freeradbiomed.2013.08.166

Wang, N., Han, X., Liu, H., Zhao, T., Li, J., Feng, Y., et al. (2017). Myeloid Differentiation Factor 88 Is Up-Regulated in Epileptic Brain and Contributes to Experimental Seizures in Rats. *Exp. Neurol.* 295, 23–35. doi:10.1016/j.expneurol.2017.05.008

Whitley, S. K., Horne, W. T., and Kolls, J. K. (2016). Research Techniques Made Simple: Methodology and Clinical Applications of RNA Sequencing. *J. Investigative Dermatology* 136, e77–e82. doi:10.1016/j.jid.2016.06.003

Wu, Z., Liu, Y., Huang, J., Huang, Y., and Fan, L. (2019). MiR-206 Inhibits Epilepsy and Seizure-Induced Brain Injury by Targeting CCL2. *Cytotechnology* 71, 809–818. doi:10.1007/s10616-019-00324-3

Xueying Li, X., Lin, J., Hua, Y., Gong, J., Ding, S., Du, Y., et al. (2021). Agmatine Alleviates Epileptic Seizures and Hippocampal Neuronal Damage by Inhibiting Gasdermin D-Mediated Pyroptosis. *Front. Pharmacol.* 12, 627557. doi:10.3389/fphar.2021.627557

Yang, J., Jia, Z., Xiao, Z., Zhao, J., Lu, Y., Chu, L., et al. (2021). Baicalin Rescues Cognitive Dysfunction, Mitigates Neurodegeneration, and Exerts Anti-epileptic Effects through Activating TLR4/MYD88/Caspase-3 Pathway in Rats. *Drug Des Devel Ther* 15, 3163–3180. doi:10.2147/dddt.s314076

Zhang, L., Li, Z., Feng, D., Shen, H., Tian, X., Li, H., et al. (2017). Involvement of Nox2 and Nox4 NADPH Oxidases in Early Brain Injury after Subarachnoid Hemorrhage. *Free Radic. Res.* 51, 316–328. doi:10.1080/10715762.2017.1311015

Conflict of Interest: The authors declare that the research was conducted in the absence of any commercial or financial relationships that could be construed as a potential conflict of interest.

Publisher's Note: All claims expressed in this article are solely those of the authors and do not necessarily represent those of their affiliated organizations, or those of the publisher, the editors and the reviewers. Any product that may be evaluated in this article, or claim that may be made by its manufacturer, is not guaranteed or endorsed by the publisher.

frontiers | Frontiers in Cell and Developmental Biology

ORIGINAL RESEARCH
published: 08 July 2022
doi: 10.3389/fcell.2022.961292

Brain-Derived Neurotrophic Factor Inhibits the Function of Cation-Chloride Cotransporter in a Mouse Model of Viral Infection-Induced Epilepsy

Dipan C. Patel[1], *Emily G. Thompson*[1,2] *and Harald Sontheimer*[1,3]*

[1]Glial Biology in Health, Disease, and Cancer Center, Fralin Biomedical Research Institute at Virginia Tech-Carilion, Roanoke, VA, United States, [2]Department of Neurobiology, University of Alabama at Birmingham, Birmingham, AL, United States, [3]School of Neuroscience, Virginia Tech, Blacksburg, VA, United States

OPEN ACCESS

Edited by:
Jianxiong Jiang,
University of Tennessee Health Science Center (UTHSC), United States

Reviewed by:
Xinjian Zhu,
Southeast University, China
Sonja Christina Bröer,
Freie Universität Berlin, Germany

***Correspondence:**
Harald Sontheimer
sontheimer@virginia.edu

Specialty section:
This article was submitted to Signaling, a section of the journal Frontiers in Cell and Developmental Biology

Received: *04 June 2022*
Accepted: *20 June 2022*
Published: *08 July 2022*

Citation:
Patel DC, Thompson EG and Sontheimer H (2022) Brain-Derived Neurotrophic Factor Inhibits the Function of Cation-Chloride Cotransporter in a Mouse Model of Viral Infection-Induced Epilepsy. Front. Cell Dev. Biol. 10:961292. doi: 10.3389/fcell.2022.961292

Well over 100 different viruses can infect the brain and cause brain inflammation. In the developing world, brain inflammation is a leading cause for epilepsy and often refractory to established anti-seizure drugs. Epilepsy generally results from an imbalance in excitatory glutamatergic and inhibitory GABAergic neurotransmission. GABAergic inhibition is determined by the intracellular Cl^- concentration which is established through the opposing action of two cation chloride cotransporters namely NKCC1 and KCC2. Brain-derived neurotrophic factor (BDNF) signaling is known to regulate expression of KCC2. Hence we hypothesized that viral induced epilepsy may result from aberrant BDNF signaling. We tested this hypothesis using a mouse model of Theiler's murine encephalomyelitis virus (TMEV) infection-induced epilepsy. We found that BDNF levels in the hippocampus from TMEV-infected mice with seizures was increased at the onset of acute seizures and continued to increase during the peak of acute seizure as well as in latent and chronic phases of epilepsy. During the acute phase of epilepsy, we found significant reduction in the expression of KCC2 in hippocampus, whereas the level of NKCC1 was unaltered. Importantly, inhibiting BDNF using scavenging bodies of BDNF in live brain slices from TMEV-infected mice with seizures normalized the level of KCC2 in hippocampus. Our results suggest that BDNF can directly decrease the relative expression of NKCC1 and KCC2 such as to favor accumulation of chloride intracellularly which in turn causes hyperexcitability by reversing GABA-mediated inhibition. Although our attempt to inhibit the BDNF signaling mediated through tyrosine kinase B–phospholipase Cγ1 (TrkB-PLCγ1) using a small peptide did not change the course of seizure development following TMEV infection, alternative strategies for controlling the BDNF signaling could be useful in preventing seizure generation and development of epilepsy in this model.

Keywords: brain-derived neurotrophic factor (BDNF), potassium chloride co-transporter-2 (KCC2), Theiler's murine encephalomyelitis virus (TMEV), infection, inflammation

INTRODUCTION

Epilepsy is a devastating neurological disorder affecting around 50 million people worldwide showing a higher prevalence in low/middle-income countries (LMIC) (Beghi, 2020). In these countries in particular, viral infection of the central nervous system (CNS) is a common cause of acquired temporal lobe epilepsy (TLE) for which there is currently no effective antiepileptic treatment for patients at risk (Patel and Wilcox, 2017; Löscher and Howe, 2022). Over two dozen antiseizure drugs are clinically approved that target primarily excitatory and inhibitory neurotransmission. However, almost one-third of the epilepsy patients remain pharmacoresistant. Several molecular mechanisms of epileptogenesis involving alternative molecular pathways regulating the excitation-inhibition balance have been proposed. One of these mechanisms involves brain-derived neurotrophic factor (BDNF) signaling through its major cognate receptor tyrosine kinase B (TrkB).

BDNF is a growth factor belonging to the neurotrophin family and mediates diverse functions through TrkB. Given its robust effects on neuronal development and differentiation, and synaptic plasticity, perturbations in the BDNF signaling has been reported in many neurological conditions including epilepsy (Park and Poo, 2013; Sasi et al., 2017). Earlier studies found that electric kindling-induced seizures caused an increase in gene expression of BDNF in cortical and hippocampal neurons (Ernfors et al., 1991). Similar increase in the induction of BDNF mRNA was also correlated with seizures induced by a systemic administration of kainic acid in rats (Dugich-Djordjevic et al., 1992). Increasing the BDNF signaling either by direct infusion of BDNF in hippocampus or by genetically overexpressing BDNF or TrkB in mice increased seizure severity or susceptibility, or induced spontaneous limbic seizures (Croll et al., 1999; Scharfman et al., 2002; Lahteinen et al., 2003; Xu et al., 2004). In contrast, kindling-induced epileptogenesis was markedly suppressed in mice with a heterozygous deletion of BDNF gene (Kokaia et al., 1995) and in mice infused intraventricularly with the recombinant TrkB receptor bodies that neutralize BDNF (Binder et al., 1999). Collectively these studies suggested that increased activation of TrkB through BNDF underlies network hyperexcitability and epileptogenesis. Further studies supported this conclusion by demonstrating reduction in seizures and epileptogenesis in mice using genetic and pharmacological tools designed to inhibit the BDNF-TrkB signaling (He et al., 2004; Liu et al., 2013; Gu et al., 2015).

BDNF-mediated hyperexcitability is partly caused by its inhibitory effects on fast GABAergic inhibition, which in turn, is maintained by low intracellular chloride concentration ($[Cl^-]_i$) (Doyon et al., 2016; Porcher et al., 2018). Two cation-chloride cotransporters, the K^+-Cl^- cotransporter 2 (KCC2) and the Na^+-K^+-Cl^- cotransporter (NKCC1), are responsible for shuttling Cl^- in and out of the cell, respectively (Doyon et al., 2016). An increase in the ratio of NKCC1/KCC2 can increase $[Cl^-]_i$ and cause depolarizing excitatory shift in GABAergic activity. Furthermore, loss-of-function mutations in KCC2 are causally linked with human infantile epilepsy and KCC2 impairment have been found in patients with idiopathic and acquired epilepsy (Moore et al., 2017). Importantly, BNDF has been shown to impair fast GABAergic inhibition by reducing the cell surface expression of KCC2 and raising the intracellular Cl^- level (Rivera et al., 2002; Ferrini et al., 2013).

The present study was performed to question whether BDNF-TrkB signaling contributes to hyperexcitability by altering the activity of cation-chloride cotransporters in a model of Theiler's murine encephalomyelitis virus (TMEV) infection-associated acquired limbic epilepsy. We found a significant increase in the protein levels of BDNF in hippocampus after TMEV infection that was coincident with seizure activity. Further, a decrease in the level of hippocampal KCC2 was correlated with peak acute seizures. Importantly, neutralizing endogenously released BDNF largely restored the level of KCC2 in hippocampal slices from the mice with acute seizures. However, treatment with pY816, an inhibitor of the BDNF-TrkB-PLCγ1 signaling cascade, had no effect on acute as well as chronic seizures. In conclusion, these results suggest that increased release of BDNF may contribute to TMEV infection-induced seizures by impairing KCC2-mediated maintenance of fast GABAergic inhibition.

MATERIALS AND METHODS

Animals

C57BL/6J (strain # 000664) and $BDNF^{+/-}$ mice (strain # 002266) were purchased from the Jackson laboratories, United States. Both male and female mice aged 7–9 weeks were included in all the experiments conducted. $BDNF^{+/-}$ mice are on a C57BL/6J genetic background, and they were genotyped to confirm the deletion of the gene. Upon arrival, mice were allowed to acclimatize for at least 3 days at our facility before conducting the experiments. Mice were housed in groups with maximum five mice per cage in an environmentally controlled vivarium room providing 12 h of light and dark cycles starting at 6:00 a.m. Food and water were freely accessible and provided ad libitum. Total 104 wild-type (WT) C57BL/6J and 10 $BDNF^{+/-}$ mice were used in the present study. A variation of block randomization method was used to assign a block of two mice randomly to either treatment or control group. All the procedures performed were in accordance with the guidelines provided and approved by the Institutional Animal Care and Use Committee of Virginia Tech.

Procedure of TMEV Infection and Handling-Induced Seizure Monitoring

A Daniel's strain of Theiler's murine encephalomyelitis virus (TMEV) was used to induce seizures in mice. TMEV was kindly provided by the laboratories of Drs. Karen S. Wilcox and Robert S. Fujinami from the University of Utah. The titer of the stock used was 2×10^7 plaque forming units (PFU) per ml.

Mice were briefly anesthetized with 3% isoflurane and injected with 20 µl of either phosphate-buffered saline (PBS) or TMEV solution (2×10^5 PFU (biochemical studies) or 3.5×10^5 PFU (electrocorticography)) intracortically (i.c.) in the right

hemisphere by inserting a 28-gauge needle perpendicular to the skull surface. The head surface was disinfected with 70% isopropyl alcohol swab and the injection site was approximated slightly medial to the equidistant point on the imaginary line connecting the right eye and the right ear. A sterilized syringe containing a plastic sleeve on the needle to expose only 2.5 mm of needle from the tip was used to restrict the injection in a cortical region about 2–3 mm lateral and 1–2 mm posterior to bregma without damaging the hippocampus. The needle was kept in place undisturbed for about 1 min after injection and retracted slowly to minimize leakage. The injury site was disinfected post-injection. Mice resumed their normal behavior within 5–10 min of the procedure.

TMEV-infected mice experience handling-induced acute behavioral seizures typically between 2–8 days post-infection (dpi) (Patel et al., 2017). Mice were briefly agitated by shaking their cage and observed for behavioral seizures for about 5 min in two observation sessions daily separately by at least 2 h. Most of the acute seizures occurred within a minute of handling the mice. Seizure severity was graded using a modified Racine scale as follows: stage 1, mouth and facial movements; stage 2, head nodding; stage 3, forelimb clonus; stage 4, forelimb clonus, rearing; stage 5, forelimb clonus, rearing, and falling; and stage 6, intense running, jumping, repeated falling, and severe clonus (Patel et al., 2019b).

Tissue Collection for Protein Analysis

Since most of the TMEV-infected mice developed handling-induced behavioral seizures, all the biochemical studies were conducted in TMEV-infected mice that showed acute seizures. TMEV- and sham-treated mice were sacrificed at 1, 3, 5, 14 and 60 dpi depending on the experiment. The ipsilateral and contralateral hippocampi were rapidly dissected out and collected separately. All the tissue samples were flash-frozen using 2-methylbutane chilled on dry ice and stored at −80°C until further processing.

Enzyme-Linked Immunoassay

Mature BDNF was measured in the hippocampal lysate using a rapid ELISA kit (BEK-2211, Biosensis) according to the manufacturer's instructions. Briefly, ipsilateral and contralateral hippocampi were homogenized in an acid extraction buffer (50 mM sodium acetate, 1 M sodium chloride, 0.1% Triton X-100, pH 4.0 using glacial acetic acid) in a 1:10 weight-by-volume ratio (10 µl buffer/mg of tissue) using a rotor-stator homogenizer. The homogenate was centrifuged (13,000 g, 30 min, 4°C), and the supernatant was collected. Since BDNF is bound to its receptors and chaperons within tissues, it is difficult to detect it by ELISA. However, extraction under acidic condition releases bound BDNF and precipitates its receptors, so that it can be immunodetected (Kolbeck et al., 1999). Protein concentration in supernatant was determined using bicinchoninic acid (BCA) assay (Pierce™ BCA Protein Assay Kit, Catalog #23225, ThermoFisher Scientific), and appropriate amount of supernatant was neutralized (100 mM phosphate buffer, pH 7.60) before using for ELISA. The concentration of mBDNF was determined by measuring the absorbance of final reaction product at 450 nm using a microplate reader (Epoch2, BioTek).

Gel Electrophoresis and Western Blot

Protein levels of KCC2 and NKCC1 were quantified by Western blot analysis. The hippocampi samples were homogenized using a rotor-stator homogenizer in a lysis buffer (50 mM Tris-HCl pH 8.00, 150 mM NaCl, 1% Triton X-100, 0.5% sodium deoxycholate, 0.1% sodium dodecyl sulfate, protease inhibitors (P8340, Sigma) and phosphatase inhibitors (P0044, Sigma); 10 µl lysis buffer per mg of tissue), and the supernatant was collected after centrifugation (15,000 g, 20 min, 4°C). Total protein concentration was measured by BCA protein assay. 10–25 µg total protein sample was denatured at 50°C for 15 min and then electrophoresed using polyacrylamide gel (4–15% or 4–20% tris-glycine extended polyacrylamide gel; 567–1,085 and 567–1,095, Bio-Rad) under denaturing conditions. The proteins were transferred to a PVDF membrane, and immunodetected by measuring either chemiluminescence or fluorescence. Densitometric analysis of protein levels was performed using ImageJ (NIH) or Image Studio (LI-COR) software.

Primary antibodies used were rabbit polyclonal anti-KCC2 IgG (1–2 µg/ml; 07–432, Millipore Sigma), mouse monoclonal anti-NKCC1 IgG1 (0.5 µg/ml; T4, Developmental Studies Hybridoma Bank), and mouse monoclonal anti-α-tubulin IgG1 (0.1–0.5 µg/ml; A11126, Invitrogen). Secondary antibodies used were goat anti-mouse IgG HRP (0.3 µg/ml, 62–6520, Invitrogen), goat anti-rabbit IgG HRP (0.2 µg/ml; 65–6120, Invitrogen), IRDyer® 680RD donkey anti-mouse IgG (0.05 µg/ml; 925–68072, LI-COR), and IRDyer® 800CW donkey anti-rabbit IgG (0.05 µg/ml; 925–32213, LI-COR).

BDNF-TrkB Inhibitors

Recombinant human TrkB Fc chimera protein (rhTrkB-Fc) (688-TK, R&D) (BDNF scavenging bodies) was used to inhibit BDNF-mediated signaling in acute brain slices. Recombinant human IgG1 Fc protein (rhIgG1-Fc) (110-HG, R&D) was used as a control recombinant protein for rhTrkB-Fc. To test the effect of these recombinant proteins on the protein level of KCC2, acute coronal brain slices (300 µm thick) from TMEV-infected mice with seizures and the control mice were prepared using vibratome (VT1200S, Leica) at 5 dpi in a cold N-methyl-D-glucamine (NMDG)-based slicing buffer (concentrations in mM: 130 NMDG, 1.5 KCl, 1.5 KH_2PO_4, 23 choline bicarbonate, 12.5 D-glucose, 0.4 L-ascorbic acid, 0.5 $CaCl_2$, and 3.5 $MgCl_2$; pH 7.3–7.4, osmolality 300–320 mOsm/kg). The slices were collected in artificial cerebrospinal fluid (ACSF) recovery buffer (concentrations in mM: 125 NaCl, 3 KCl, 1.25 NaH_2PO_4, 25 $NaHCO_3$, 12.5 D-glucose, 2 $CaCl_2$, and 2 $MgCl_2$; pH 7.3–7.4; osmolality, 310–320 mOsm/kg) and allowed to recover from the slicing-induced surface damage in ACSF at 32°C for 30 min. The slices were then washed with ACSF to remove dead surface cells and debris and incubated in 250 ng/ml solution of rhTrkB-Fc or rhIgG1-Fc in ACSF at 32°C. All the solutions used for processing brains and brain slices were continuously oxygenated with a mixture of 95% oxygen and 5% carbon dioxide. After 4.5 h, drug solution was discarded,

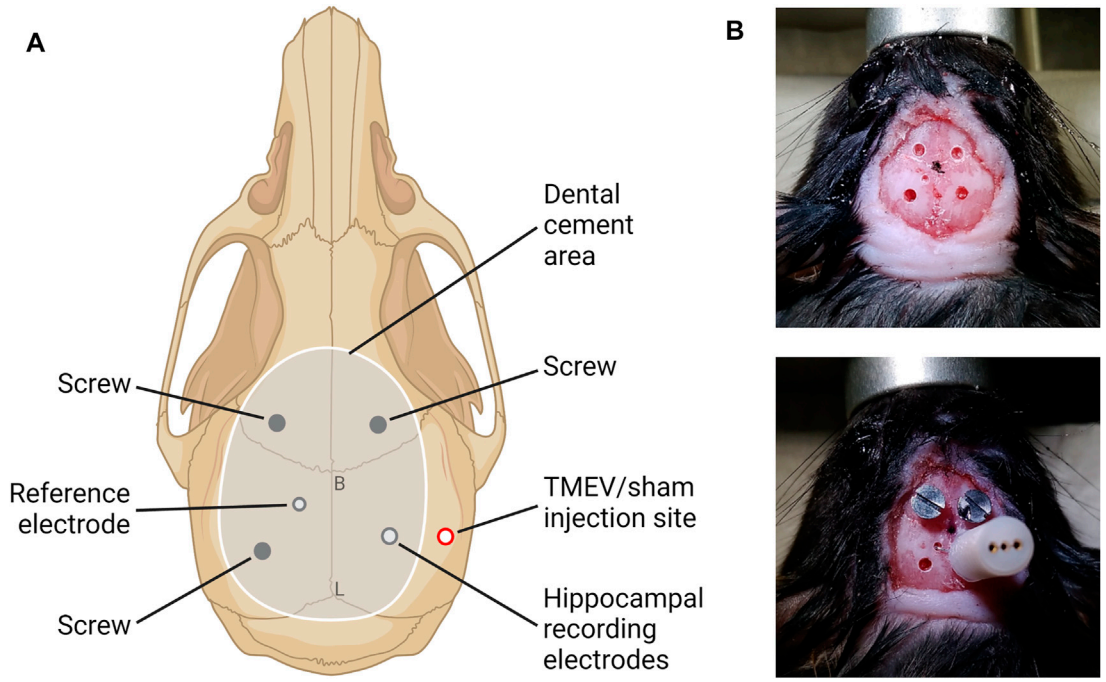

FIGURE 1 | Depiction of the placement of electrodes and the electrodes-anchoring assembly in mice for ECoG. **(A)** Schematic of the mouse skull showing the location for electrodes and anchoring screws over the dorsal surface of skull (B–bregma, L–lambda). This schematic was created with BioRender.com. **(B)** Photographs of the mouse head captured during surgical procedure showing the holes drilled in skull (upper panel) and the implant of electrodes and anterior screws (lower panel).

and the slices were washed with ACSF. The hippocampal and cortical regions were quickly dissected out and collected in vials containing lysis buffer (150 and 250 µl, respectively; recipe same as described in Western blot procedure). The samples were homogenized using a rotor-stator homogenizer and the supernatant was collected after centrifugation (15,000 g, 20 min, 4°C). Protein assay and western blot were then conducted as described above to measure the level of KCC2.

To inhibit BDNF signaling *in vivo*, a small peptide, pY816, was used. pY816 (YGRKKRRQRRR-LQNLAKASPVpYLDI) and its negative control scrambled (Scr) peptide sequence (YGRKKRRQRRR-LVApYQLKIAPNDLS) were synthesized by Tufts University peptide synthesis core facility. Mice were treated with a solution of pY816 or Scr prepared in PBS (10 mg/kg at 5 ml/kg body weight) by retroorbital intravenous (i.v.) injections once daily between 0–14 dpi starting immediately after TMEV-infection. Topical anesthetic bupivacaine was applied to the eyeballs of mice before performing retroorbital injections.

Surgical Procedure for Video-Electrocorticography (vECoG)

Mice were anesthetized using 3% isoflurane in oxygen, provided analgesia (0.1 mg/kg buprenorphine intraperitoneal (i.p). and 5 mg/kg carprofen (i.p.), and the head was affixed into a stereotaxic instrument (David Kopf Instruments). The hair over the skull area was removed using a hair-removal cream, the surgical area was cleaned and disinfected using iodine and 70% alcohol, and the skull was exposed. The pitch of head was adjusted to flatten the skull surface by setting the dorsoventral levels of bregma and lambda the same. Mice were continuously anesthetized using nasal tubing supplying 1–2% isoflurane throughout the surgical procedure. Total five holes (three for screws and two for electrodes) were drilled in the skull carefully without causing bleeding (**Figure 1**). Two electrodes of a three-channel electrode set up (MS333/8-A, P1 Technologies) were twisted and implanted in the CA3 region of hippocampus using stereotaxic coordinates of 1.8 mm lateral (ipsilateral to the infection site) and 2.00 mm posterior from bregma, and about 2.5 mm ventral from the skull surface to reach the target area at 1.8 mm ventral from the brain surface. The reference electrode was implanted in the contralateral cortical surface (1.0 mm lateral and 1.0 mm posterior from bregma). Two anchor screws were placed in the skull bilaterally anterior to the bregma, and the third screw was anchored over the left parietal cortex posterior to the reference electrode. The screws were carefully inserted into the skull without damaging the brain surface. The electrodes and all the screws were secured in position using a dental cement and the skin incision was closed using a tissue glue such that it provided a clear unobstructed space on the right hemisphere for TMEV/sham i. c. injection later (**Figure 1**). All surgically operated mice were treated humanely and provided post-operative care as per the NIH guidelines and the institutional animal care protocol.

vECoG and Seizure Analysis

After 10 days of recovery from the surgical procedure, mice were then enrolled for vECoG recording by connecting to an EEG100C differential amplifier (BIOPAC Systems) using a

lightweight three-channel cable with a three-channel rotating commutator (P1 Technologies). The MP160 data acquisition system and AcqKnowledge 5.0 software from BIOPAC Systems, Inc. were used to record ECoG. M1065-L network camera (Axis communications) and media Recorder 4.0 software (Noldus Information Technology) were used to record the behavior of each mouse. All the cables and electrical components were sufficiently shielded to minimize electrical noise. Video and EEG recordings were automatically synchronized using the Observer XT 14.1 software (Noldus Information Technology). ECoG signals were bandpass filtered between 0.5 and 100 Hz, amplified, and digited at a sampling frequency of 500 Hz. Mice had access to food and water conveniently during the entire vECoG recording. Mice were injected with 20 µl of TMEV (3.5×10^5 PFU) or PBS in the right somatosensory cortex as described above 1 day after the beginning of recording to get a 24-h baseline recording, and then the recording was continuously acquired for 100 days post-infection. The ECoG and video recordings were reviewed manually by an experimenter blinded to the treatment groups. Electrographic seizures were defined as rhythmic spikes or sharp-wave discharges with amplitudes at least two times the average amplitude of baseline, frequency at least 2 Hz, and duration at least 5 s. Seizures were also identified by verifying postictal suppression of the baseline ECoG activity which typically occurs after seizure but not accompanied by electrographic artifacts associated with mouse behavior other than seizures. At the end of the experiment, mice were transcardially perfused with ice-cold PBS followed by 4% paraformaldehyde, and the brains were collected, and the placement of the electrode was verified.

Statistics

Datasets with continuous variables are summarized by plotting mean and the standard error of mean as a scatter plot with bar showing individual datapoints, and the datasets with ordinal variables are represented by frequency distribution unless otherwise stated. Parametric statistical tests were used if the data were sufficiently normal distributed and variance within groups was sufficiently similar. Experimental designs with two comparison groups were analyzed by a two-tailed unpaired *t*-test and designs with more than two comparison groups were analyzed using either one-way or two-way analysis of variance (ANOVA). Multiple pairwise comparisons were performed by Tukey's or Šídák's posttest. Average cumulative seizure burden was calculated from a ranked dataset and analyzed by Scheirer–Ray–Hare test, which is an extension of the Kruskal–Wallis test for two randomized factorial designs (Scheirer et al., 1976). Two groups with binomial outcome were analyzed by Fisher's exact test. Survival (percent seizure free) curves were analyzed by log-rank test. The difference between the two groups was considered statistically significant with a *p*-value less than 0.05. GraphPad Prism 8 and Microsoft Excel software were used for statistical analysis.

RESULTS

Positive Correlation Between TMEV-Induced Seizures and mBDNF Level in Hippocampus

Transcription of the Bdnf gene can yield three distinct *BDNF*-derived bioactive proteins, namely proBDNF, mature BDNF (mBDNF), and the prodomain of BDNF (Sasi et al., 2017). Opposing effects of proBDNF and mBDNF on neuronal excitability and synaptic strength have been demonstrated through their preferential binding to p75 neurotrophin receptor (p75NTR) and TrkB receptor, respectively. Overall, the mBDNF-TrkB signaling contributes to neuronal hyperexcitability, whereas the proBDNF-p75NTR signaling dampens it (Sasi et al., 2017). To investigate any correlation between the level of mBDNF during the development of TMEV-induced seizures, we measured the level of mBDNF in the hippocampus of TMEV-infected mice by ELISA at various stages post-infection. The timepoints chosen were 1 dpi (before appearance of acute seizures), 3 dpi (beginning of acute seizures), 5 dpi (peak level of acute seizures), 14 dpi (latent period with no behavioral seizure) and 60 dpi (chronic epilepsy period with the occurrence of spontaneous seizures). Since previous studies had found differences in inflammatory and redox markers between ipsilateral and contralateral hippocampus after TMEV infection (Bhuyan et al., 2015), the level of mBDNF was measured in ipsilateral and contralateral hippocampus distinctly.

Figure 2 shows the absolute level of mBDNF in ipsilateral (panel A), contralateral (panel B), and in whole hippocampus (panel C). All the mice in the TMEV-infected group had seizures, whereas none of the sham-treated mice experienced any seizure. The level of mBDNF was not different between both the treatment groups at 1 dpi in both hippocampi. mBDNF started to increase with the appearance of seizures at 3 dpi and was significantly increased compared to the control mice at 5 dpi. The absolute level of mBDNF remained significantly elevated at 14 and 60 dpi in ipsilateral and in whole hippocampus. The changes in the mBDNF level in the infected mice can be conveniently viewed as a percentage of the corresponding control levels in panels D–F. These results show a positive correlation between the occurrence of TMEV-induced seizures and an increase in the levels of mBDNF in hippocampus. The level of mBDNF in the hippocampus of sham-injected control mice did not change significantly over 60 dpi. Since mice in this experiment were not monitored continuously for the seizures by vECoG, it was not possible to determine which mice had chronic seizures at 60 dpi. Although TMEV-infected mice generally do not show behavioral seizures between 2 weeks and 2 months post-infection, focal electrographic seizures have been recorded in the hippocampus during this period (Patel et al., 2017). It is likely that increased level of mBDNF in hippocampus at 60 dpi could be due to underlying network hyperexcitability. However, further work is needed to

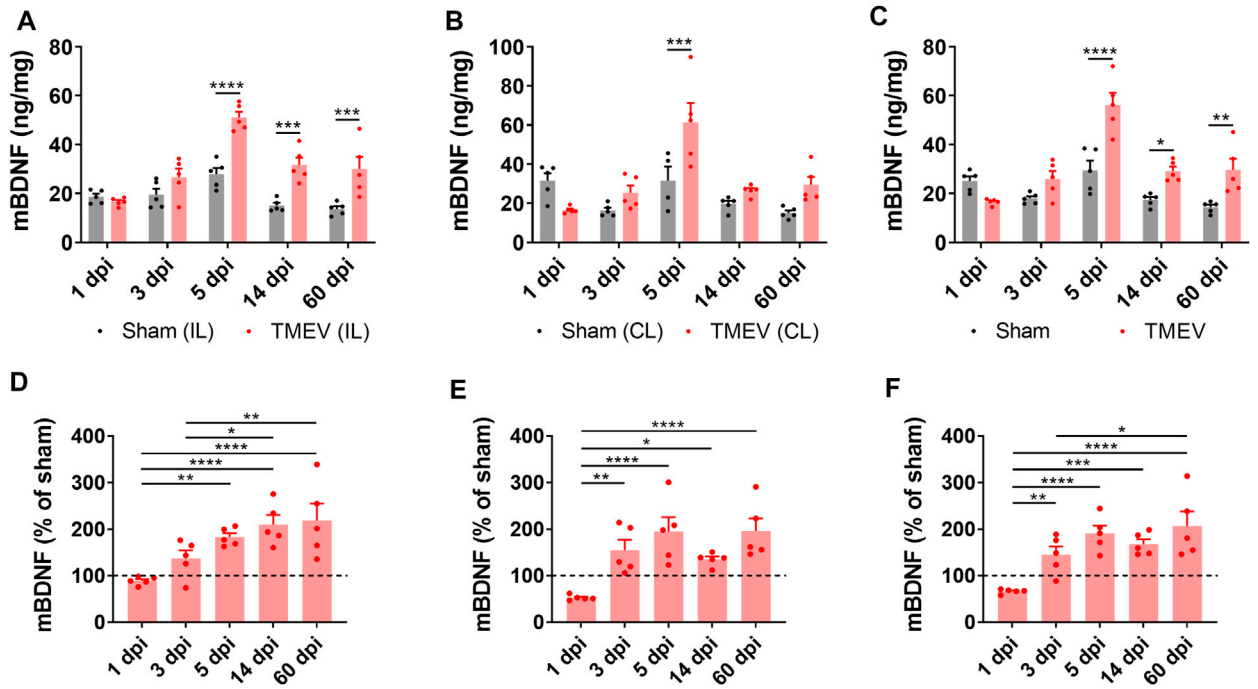

FIGURE 2 | Increase in the protein level of mature BDNF in the hippocampus of TMEV-infected mice during acute and chronic seizure period. **(A-C)** Absolute protein levels of mBDNF in the ipsilateral **(A)**, contralateral **(B)**, and whole hippocampus **(C)** are plotted at various days post-infection (dpi). **(D-F)** The protein level of mBDNF in the ipsilateral **(D)**, contralateral **(E)**, and whole hippocampus **(F)** at various timepoints after infection are normalized to their corresponding levels in the sham-treated control samples. Dashed line at 100% on *y*-axis indicates mean level of mBDNF in the sham-treated control samples. Statistics: Two-way ANOVA, Šídák's multiple comparison tests (comparison between the treatment groups at each timepoint, panels **A–C**) and Tukey's multiple comparisons tests (comparison between various timepoints within each treatment group, panels D–F); $n = 5$ mice per group at each timepoint; $^{*}p < 0.05$, $^{**}p < 0.01$, $^{***}p < 0.001$, $^{****}p < 0.0001$.

determine whether increase in mBDNF found in hippocampus at 60 dpi is mainly due to occurrence of chronic seizures or due to other pathological factors.

Increase in the Ratio of NKCC1/KCC2 in Hippocampus During Acute TMEV Infection

Whether increased levels of mBDNF are associated with the changes in the expression of cation-chloride cotransporters, we measured the level of NKCC1 and KCC2 in ipsilateral and contralateral hippocampus by western blot at 5 dpi. We found no change in NKCC1 in both hippocampi (**Figures 3A,C**), whereas KCC2 was found significanlty reduced in ipsilaeral hippampus and unchanged in contralateral hippocampus (**Figures 3B,D**). Overall the level of KCC2 in whole hippocampus was significanlty reduced (**Figure 3D**). Accordingly, the ratio of NKCC1/KCC2 was significantly elevated in the ipsilateral hippocampus (**Figure 3E**).

Neutralization of BDNF Rescues Reduction in Hippocampal KCC2 in Mice with TMEV-Induced Seizures

We next investigated any causality between an increase in mBDNF and a concurrent decrease in KCC2 in the hippocampus during peak TMEV-induced acute seizures using a recombinant human TrkB-Fc (rhTrkB-Fc), a biological inhibitor of BDNF signaling, in acute brain slices using western blot. rhTrkB-Fc is a decoy scavenging body that binds and sequesters BDNF, and thus inhibits the downstream effects of BDNF. Intracerebroventricular administration of rhTrkB-Fc inhibited the development of seizures in the rat model of electrical kindling-induced epilepsy (Binder et al., 1999). However, a major disadvantage of *in vivo* delivery of rhTrkB-Fc is a poor parenchymal penetration, and therefore, limited bioavailability of rhTrkB-Fc at the target site (Binder et al., 1999). To overcome this limitation, we incubated acute brain slices prepared at 5 days post-TMEV/sham treatment with rhTrkB-Fc or rhIgG1-Fc at 37°C in a custom-built six well incubation plate designed to provide continuous supply of 95% oxygen and 5% carbon dioxide (**Figure 4A**). The slices remained viable and healthy throughout the process using this system. The concentration of rhTrkB-Fc or rhIgG1-Fc (250 ng/ml) and incubation duration (4.5 h) were based on previously published studies and our pilot experiments (Rivera et al., 2002).

The results showed that scavenging endogenous BDNF significantly increased KCC2 level in the infected hippocampal slices (**Figures 4B,D**). However, it did not completely reverse the reduction in KCC2 as there was a small but significant difference between the sham and TMEV groups. We also measured the effect of rhTrkB-Fc on KCC2 in cortical slices, where we do not find a reduction in KCC2 during TMEV-induced seizures. There

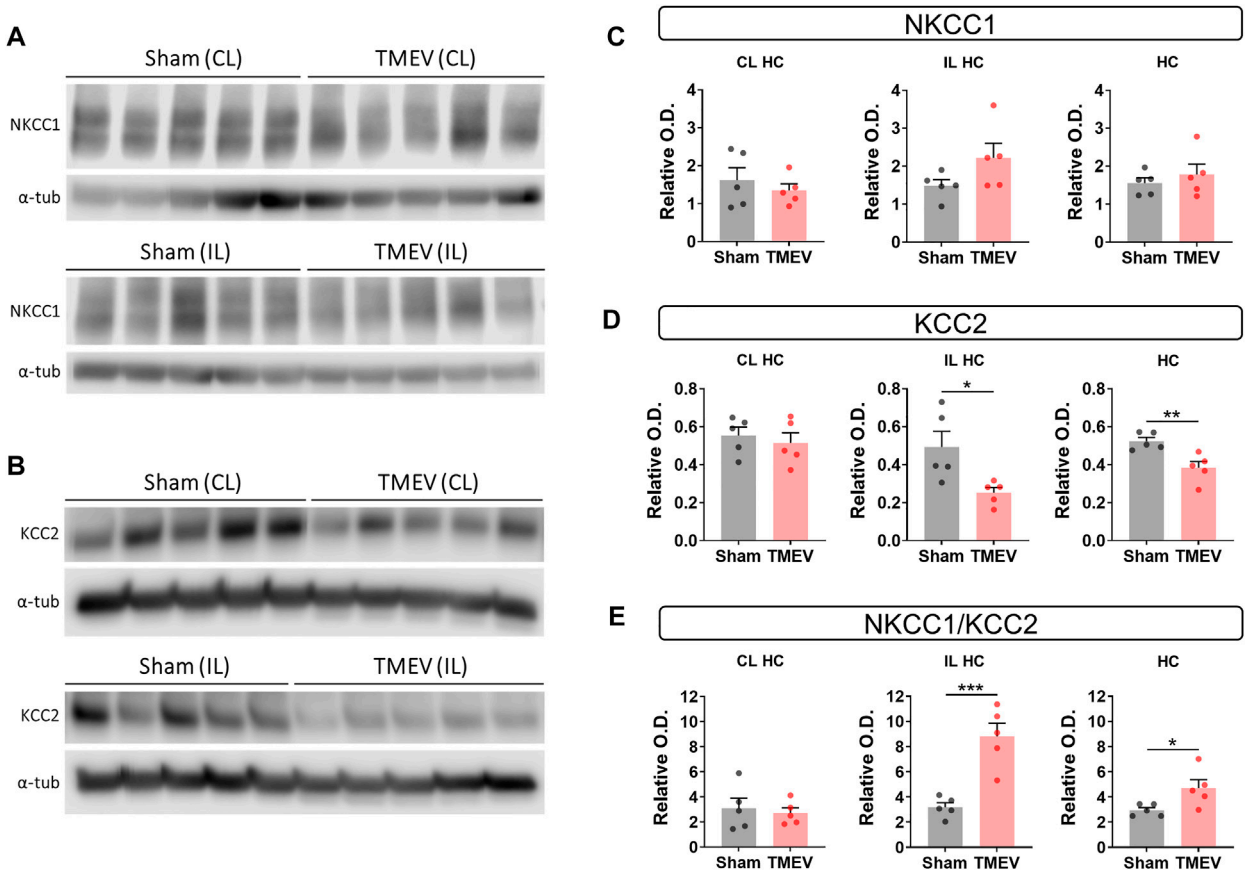

FIGURE 3 | Decrease in the protein level of KCC2 and increase in the ratio of NKCC1/KCC2 in the hippocampus of TMEV-infected mice with acute seizures at 5 dpi. **(A–B)** Immunoblots show the detection of NKCC1 **(A)**, KCC2 **(B)** and α-tubulin in the contralateral (CL) and ipsilateral (IL) hippocampi (HC) from the sham- and TMEV-infected mice. **(C–E)** Optical density (O.D.) of NKCC1 **(C)** and KCC2 **(D)** blots were normalized to the O.D. of α-tubulin blots from the same samples to compare the relative O.D. between the sham- and TMEV-infected mice. The relative O.D. ratios of NKCC1/KCC2 are plotted in panel **(E)**. Statistics: Unpaired two-tailed *t* test; $n = 5$ mice per group; $^{*}p < 0.05$, $^{**}p < 0.01$, $^{***}p < 0.001$.

was no change in the level of KCC2 between any of the treatment groups–cortical slices from sham or TMEV-infected mice treated with rhTrkB-Fc or rhIgG1-Fc (**Figures 4C,E**). These results suggest that increased release of endogenous BDNF during TMEV-induced acute seizures directly decrease the expression of KCC2, which in turn, may contribute to hyperexcitability by impairing GABAergic inhibition.

BDNF Heterozygous Knockout and Wild-type C57BL/6J Mice Are Equally Susceptible to TMEV-Induced Seizures

To test whether enhanced level of BDNF directly contributes to seizures, we compared the seizure susceptibility of $BDNF^{+/-}$ mice to TMEV-induced seizures with the WT C57BL/6J mice. It was desirable to utilize mice lacking both alleles of the *Bdnf* gene; however, $BDNF^{-/-}$ mice are growth-impaired and most die within 2 weeks of birth, whereas $BDNF^{+/-}$ mice are phenotypically comparable with the WT mice (Ernfors et al., 1994). Both $BDNF^{+/-}$ and WT mice ($n = 10$ per group; 5 male, 5 female) were infected with TMEV and monitored for behavioral seizures up to 2 weeks post-infection by an experimenter blinded to the genotype of mice. All the seizures observed are shown in the heatmap in **Figure 5A**. Average weight of $BDNF^{+/-}$ mice was about 2–3 g more than the WT mice (**Figure 5B**). Although 40% (4/10) of $BDNF^{+/-}$ mice developed acute seizures compared to 60% (6/10) of WT mice, this difference was not statistically significant (**Figure 5C**). Mean seizure frequency was measured as an average number of seizures during the entire acute seizure period (3-8 dpi) and found similar between both the groups (**Figure 5D**). Cumulative seizure burden, as a marker for seizure severity, at each dpi for each mouse was calculated by summing all its seizure scores up to corresponding dpi. Seizure severity was also found similar between both the groups (**Figure 5E**). Comparisons based on seizure score found no difference between both the groups (**Figures 5F,G**).

The level of mBDNF was measured by ELISA in ipsilateral (**Figure 6A**), contralateral (**Figure 6B**), and whole (**Figure 6C**) hippocampus collected from $BDNF^{+/-}$ and WT mice at 14 dpi. $BDNF^{+/-}$ mice had about half the level of mBDNF compared to the WT mice irrespective of seizures. Mice that exhibited TMEV-induced acute seizures had significantly higher level

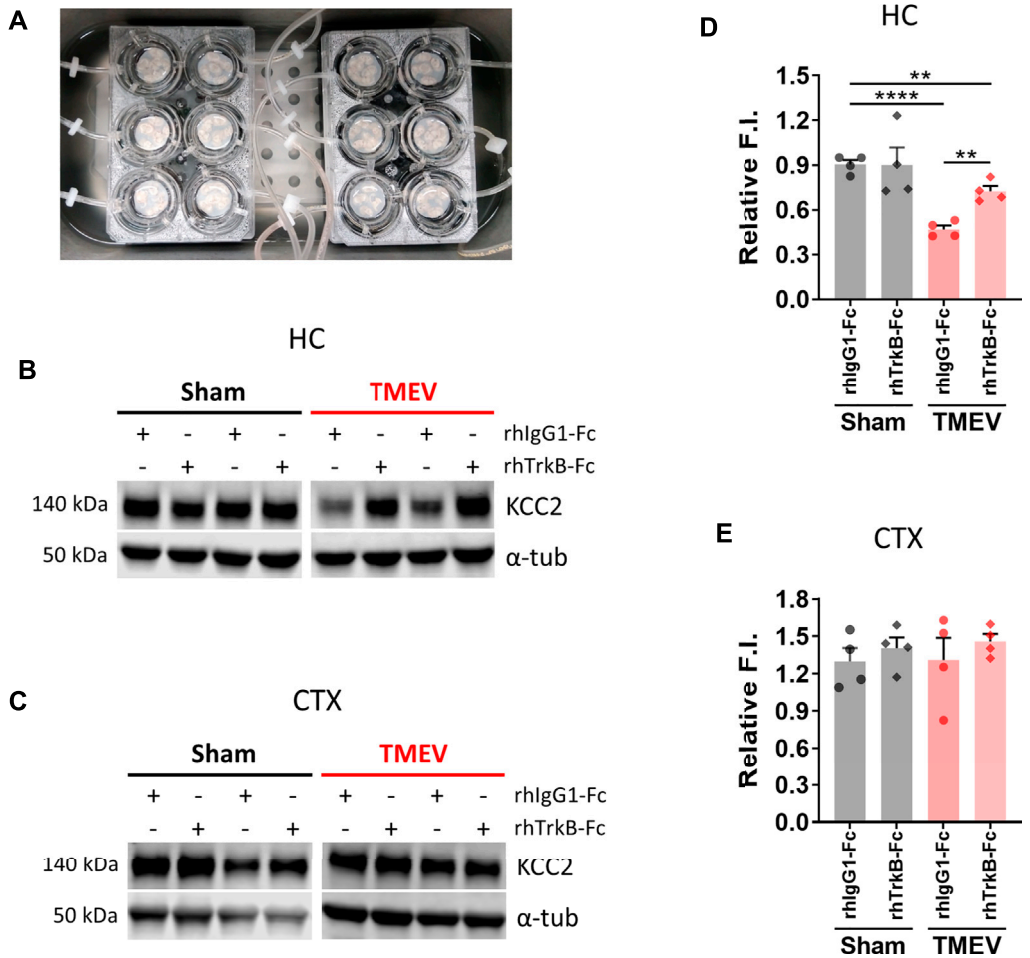

FIGURE 4 | Inhibition of BDNF increases the expression of KCC2 in hippocampal slices from mice during TMEV-induced acute seizure period. **(A)** Acute brain slices (300 μm thickness) from sham- or TMEV-infected mice were treated with rhTrkB-Fc or rhIgG1-Fc (250 ng/ml in ACSF) for 4.5 h at 37 C under continuous carbogenation (95% oxygen, 5% carbon dioxide) condition before dissecting out hippocampus (HC) and cortex (CTX). **(B–C)** Representative immunoblots show the detection of KCC2 and α-tubulin in hippocampi **(B)** and cortex **(C)** isolated from acute brain slices under different treatment conditions for both groups of mice. **(D–E)** Fluor intensity (F.I.) of KCC2 blots were normalized to the F.I. of α-tubulin blots from the same samples to compare the relative F.I. between the sham- and TMEV-infected slices treated either with rhIgG1-Fc or rhTrkB-Fc. Statistics: One-way ANOVA, Tukey's multiple comparisons test; $n = 4$ mice per group; $^{**}p < 0.01$, $^{****}p < 0.0001$.

of BDNF irrespective of their genotype compared to mice protected from acute seizures. These results suggest that upregulation of endogenous BDNF in hippocampus occurs as a consequence of acute seizures rather than TMEV infection itself.

No Effect of pY816-Mediated Inhibition of the BDNF-TrkB-PLCγ1 Signaling on TMEV Infection-Associated Seizures

To overcome the limitations of inhibiting endogenous release of BDNF, we employed a pharmacological approach using a peptide, pY816, to inhibit the downstream effects of BDNF mediated through TrkB receptor. Among the many downstream effector molecules that mediate the effects of BDNF through TrkB receptors, activation of PLCγ1 has been implicated in driving seizures (Gu et al., 2015). pY816 is a selective inhibitor of the PLCγ1-mediated effects of the BDNF-TrkB signaling. It is a membrane-permeable peptide containing a sequence of TrkB motif that directly binds with PLCγ1 and uncouples the interaction of PLCγ1 with activated TrkB, and thus, inhibits the downstream effects of BDNF (Gu et al., 2015). pY816 has been found to reduce seizures and epileptogenesis in the rodent models of seizures induced by kainic acid (Gu et al., 2015) or electrical kindling (Krishnamurthy et al., 2019). Since the BDNF-TrkB-PLCγ1 signaling cascade, along with the Shc/FRS-2 (src homology 2 domain containing transforming protein/FGF receptor substrate 2) pathway, was also implicated in downregulating KCC2 expression in hippocampal slices under hyperexcitable condition (Rivera et al., 2004), we asked whether treatment of TMEV-infected mice with pY816 might reduce acute and/or chronic seizure parameters.

We treated TMEV-infected mice with pY816 or Scr ($n = 13$ per group) once daily during the first 2 weeks of infection and

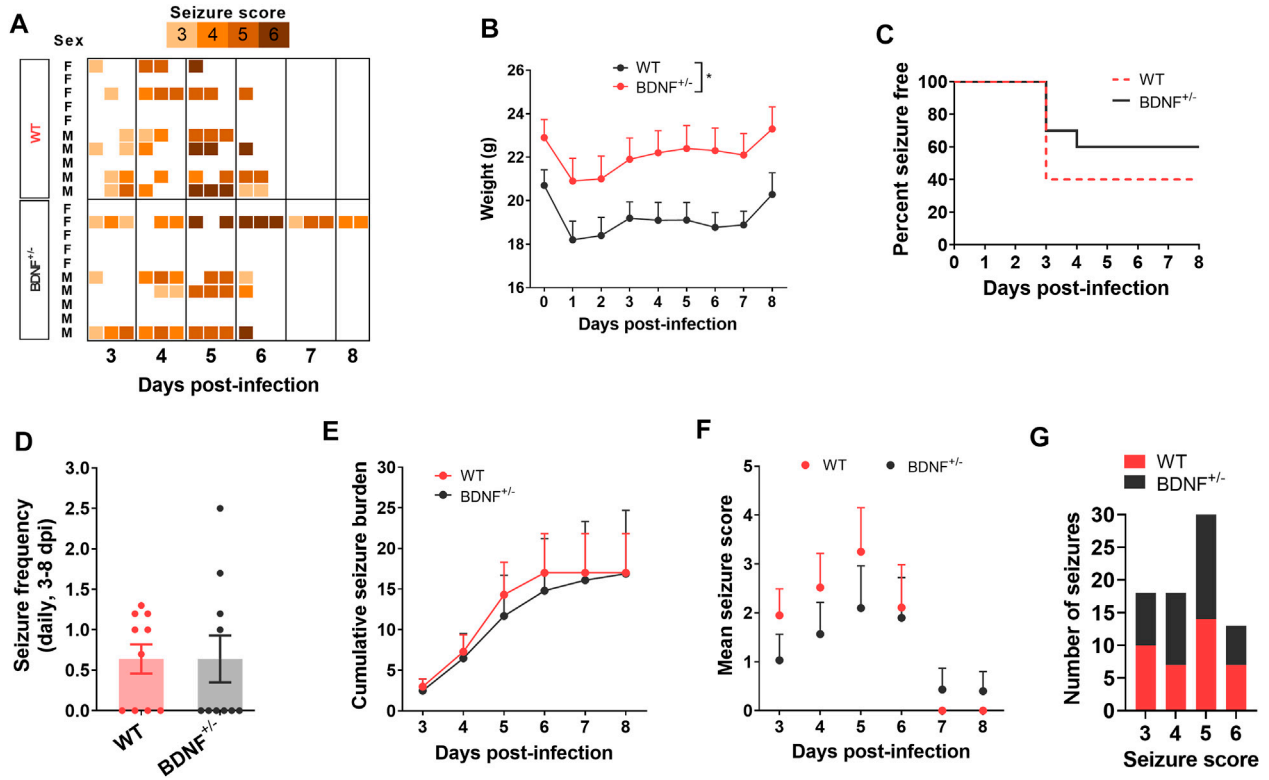

FIGURE 5 | No difference in TMEV-induced acute seizures between wild type (WT) and BDNF$^{+/-}$ C57BL/6J mice. **(A)** Heatmap shows all acute seizures observed based on their severity score for each mouse between 3–8 days post-infection (dpi). Seizures were induced by handing and the severity was scored three times a day with at least 2 h of undisturbed period between two observation sessions. **(B)** Average weight of mice in each group during acute infection period. **(C)** This panel shows the percentage of total infected mice in each group that remained seizure free at each day until 8 dpi. None of the mice developed seizures before 3 dpi. **(D)** Average number of seizures daily between 3-8 dpi is plotted for each mouse. **(E)** Average cumulative seizure burden, which is calculated as a mean of the summation of all seizure scores for each mouse over time, compares seizure severity between WT and BDNF$^{+/-}$ mice during acute infection period. **(F)** Mean seizure score at each day is compared. **(G)** It shows the total number of seizures based on their severity score.

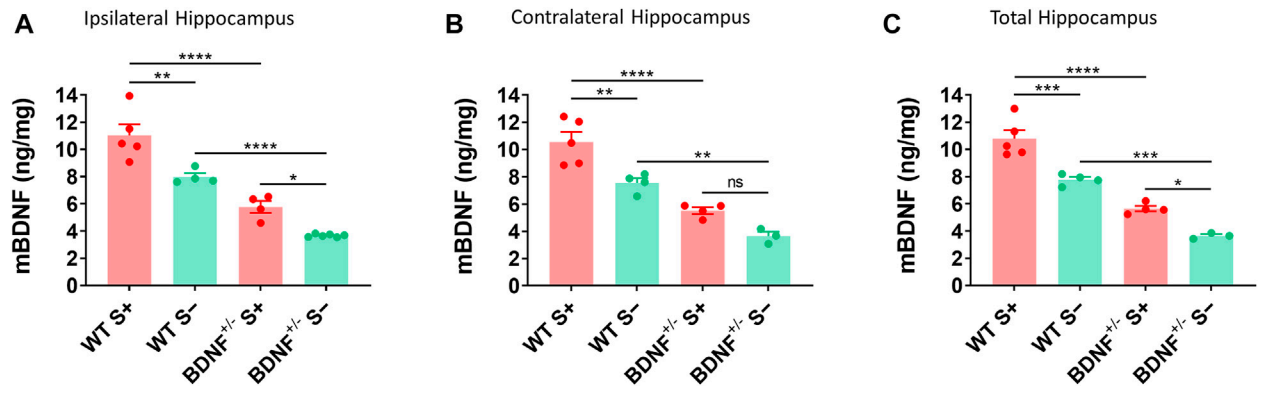

FIGURE 6 | Increase in mBDNF in hippocampus of WT compared to BDNF$^{+/-}$ mice with TMEV-infected acute seizures. **(A-C)** Absolute protein levels of mBDNF in the ipsilateral **(A)**, contralateral **(B)**, and total hippocampus **(C)** from WT and BDNF$^{+/-}$ mice at 14 days post-TMEV infection are compared. S+ indicates mice that developed acute TMEV-induced seizures and S- indicates mice that did not get seizures. Statistics: One-way ANOVA, Šídák's multiple comparisons test; n = 3-6 mice per group at each timepoint; *p < 0.05, **p < 0.01, ***p < 0.001, ****p < 0.0001.

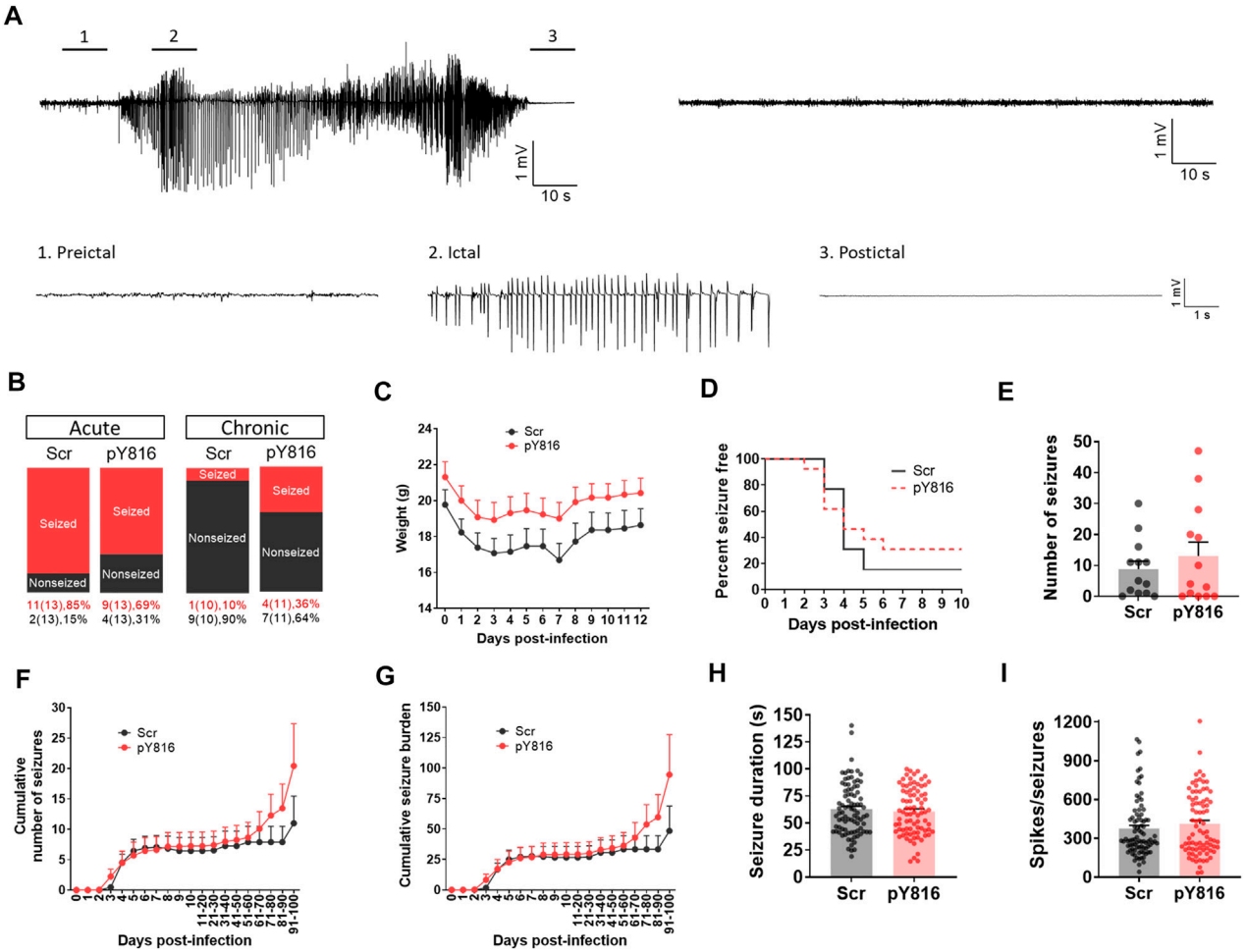

FIGURE 7 | No change in frequency, severity, and duration of TMEV-induced acute and chronic seizures between pY816- and sham-treated mice. **(A)** Representative EEG recordings from TMEV-infected mice treated with a scrambled control peptide (Scr). The recording on the upper left is from a mouse that developed seizures and the recording on the upper right is from a mouse that did not have any seizure. Expanded traces corresponding to preictal baseline, ictal spiking, and postictal suppression period from a tracing on upper left are shown below. **(B)** Percentage of all TMEV-infected mice treated with either pY816 or a scrambled control peptide (Scr) that presented with acute and chronic seizures are shown. **(C)** Average weight of mice in each group during acute infection period. **(D)** This panel shows the percentage of total infected mice in each group that remained seizure free at each day until 10 dpi. None of the mice developed seizures before 2 dpi. **(E)** Total number of seizures throughout the vECoG monitoring period post-TMEV infection is plotted for each mouse. **(F)** Average cumulative number of seizures for each treatment group over 100 days of vECoG monitoring post-TMEV infection. **(G)** Average cumulative seizure burden, which is calculated as a mean of the summation of all seizure scores for each mouse over time, compares seizure severity between Scr-treated and pY816-treated mice up to 100 dpi. **(H)** A graph plotting the duration of all seizures show no difference in mean seizure duration between both the treatment groups. **(I)** Total number of spikes plotted for each electrographic seizure shows no mean difference between both the treatment groups.

monitored them for seizures by continuous vECoG until 100 dpi. The recoding from three mice in the Scr group and from two in the pY816 group had to be stopped before 100 dpi due to loss of electrode or poor health. The representative recording traces from the Scr-treated mice with and without seizures are shown in **Figure 7A**. The recording from the pY816-treated mice also showed similar electrographic activity. Numbers of mice that had at least one acute seizure were similar for both the groups (Scr–11/13, 85%; pY816–9/13, 69%) (**Figure 7B**). Numbers of mice with chronic spontaneous seizures during 60–100 dpi were higher in the pY816 group (Scr–1/10, 10%; pY816–4/11, 36%); however, this difference was not statistically significant (**Figure 7B**). There was no difference in weight, occurrence of first seizure, and average number of seizures between both the groups (**Figures 7C–E**). Seizure frequency and severity, reported as cumulative number of seizures and cumulative seizure burden, respectively, were also not different between both the groups (**Figures 7F,G**). Seizure duration and number of spikes per ictal activity were calculated from the vECoG recording and found similar for both the treatment groups (**Figures 7H,I**).

DISCUSSION

We have investigated the role of the BDNF-TrkB signaling in the development of seizures in a model of TMEV infection-associated

limbic epilepsy. We found an inverse correlation between the protein levels of BDNF and KCC2 in mice hippocampus during the peak seizure activity period following viral infection. Increased expression of BDNF was found coincident with the occurrence of both acute and chronic seizures. We also found a causal connection between the level of BDNF and KCC2 as neutralizing endogenous BDNF by rhTrkB-Fc significantly increased the level of KCC2 in hippocampal slices from the mice with acute seizures. However, genetic and pharmacological approaches to inhibit excessive effects of BDNF did not show any difference in behavioral and electrographic seizures induced by TMEV. Overall, our results suggest that increased release of BDNF may contribute to TMEV infection-induced seizures by impairing KCC2-mediated regulation of $[Cl^-]_i$ important for maintaining fast GABAergic inhibition.

The role of BDNF in seizure development has been reported in some animal models of seizures and epilepsy, mostly electrical kindling, and post-status epilepticus (SE) models of TLE using kainic acid and pilocarpine (McNamara and Scharfman, 2012). These are useful and reliable methods to induce seizures, however, they are limited by the fact that normal healthy rodents are used in these models to induce seizures and that *de novo* SE is rather rare in humans and thus not a major cause of acquired epilepsy (Loscher, 2017). Animal models of acquired epilepsy caused by stroke, CNS infections, or traumatic brain injury, which are the major etiological factors for human acquired epilepsy, are more clinically relevant. Viral infection is a major cause of TLE especially in LMIC (Misra et al., 2008; Vezzani et al., 2016). However, animal models of TLE caused by infection are limited. Furthermore, high mortality rate and low rate of epilepsy development in majority of these models curtail their utility (Patel and Wilcox, 2017; Löscher and Howe, 2022). In contrast, TMEV-infected C57BL/6J mice exhibit acute seizures during active infection, survive the initial infection, exhibit hippocampal neuropathology and gliotic scar, develop behavioral comorbidities such as anxiety and cognitive impairment, and develop epilepsy after about 2–3 months post-infection (Libbey et al., 2008; Stewart et al., 2010a; b; Umpierre et al., 2014; Broer et al., 2016; Patel et al., 2017; Lawley et al., 2021). This model recapitulates many pathological and behavioral sequelae of human TLE patients, and therefore, offers a unique opportunity to study the molecular mechanism(s) underlying seizure generation and epileptogenesis.

The factors that upregulate BDNF expression during TMEV-induced seizures are speculative. Inflammation is a key driver of seizures in the TMEV model (Cusick et al., 2013; Patel et al., 2017; Waltl et al., 2018; Zhan et al., 2018; Juda et al., 2019; Howe et al., 2022). Similar to BDNF, increase in the levels of proinflammatory cytokines and chemokines correlates with the appearance and persistence of TMEV-induced seizures. Persistent inflammatory condition has been shown to upregulate BDNF level (Tao et al., 2014). Reactive microgliosis, which occurs during acute TMEV infection and known to release proinflammatory factors, can induce BDNF synthesis and release through the ATP-P2X4R signaling cascade (Ferrini and De Koninck, 2013). However, the interaction between BDNF and neuroinflammation in CNS disorders is not clearly understood as evident by many contrasting findings (Lima Giacobbo et al., 2019). Ca^{2+}-dependent synaptic release of BDNF has been demonstrated in response to spontaneous activity (Kuczewski et al., 2008), therefore, it is also likely that the network hyperexcitability ensued following TMEV infection could itself have contributed to the increased levels of BDNF. Since BDNF can cause hyperexcitability through intracellular Ca^{2+}-dependent mechanisms (Sasi et al., 2017), it is possible that there may be a positive feedback loop between the release of BDNF and seizures.

Accumulating evidence suggest that BDNF decreases KCC2 expression and function in several adult brain regions (Moore et al., 2017), under different neuropathological conditions including epilepsy (Rivera et al., 2002), traumatic brain injury (Shulga et al., 2008), and nociception (Ferrini et al., 2013). In a mature brain, cell surface expression of KCC2 is crucial for keeping $[Cl^-]_i$ low, which is essential for establishing and maintaining fast hyperpolarizing $GABA_A$ receptor currents. A decrease in the Cl^- extrusion function of KCC2 causes depolarizing excitatory shift in the GABAergic action which may underlie neuronal network hyperexcitability. Impairment in the function of KCC2 has been reported in many experimental studies from the animal models of epilepsy as well as in some cases of human epilepsy (Moore et al., 2017). Although the consequence of reduced KCC2 level on the fast $GABA_A$ receptor inhibition following TMEV infection is not studied in this present study, an impaired synaptic inhibition during both acute and chronic phases of TMEV-induced epilepsy has been reported in the CA3 region of hippocampus (Smeal et al., 2015) and in the dentate granule cells (our unpublished data). It is likely that BDNF-mediated reduction in KCC2 function may have contributed to this impaired inhibition.

In addition to BDNF, high extracellular glutamate has been shown to reduce KCC2 level through NMDA receptor and subsequently calcium-activated protease (Lee et al., 2011). Increased extracellular glutamate is commonly associated with neuronal network hyperexcitability (Coulter and Steinhauser, 2015; Patel et al., 2019a). Glutamate-mediated hyperexcitability occurs in CA3 pyramidal neurons during acute and chronic seizure periods in the TMEV model of epilepsy (Smeal et al., 2012). Given these findings, it is possible that excessive glutamate may have reduced KCC2 in hippocampus during acute TMEV-induced seizures. However, we have demonstrated a significant increase in KCC2 in TMEV-infected hippocampal slices after treatment with BDNF scavenging bodies. Although the level of KCC2 was still lower compared to control hippocampal slices, the reduction was much less compared to TMEV-infected hippocampal slices without any alternation of endogenous BDNF. Collectively, these results suggest that BDNF directly contributes in the reduction of KCC2 during TMEV-induced seizures, however, it may not be the only factor.

Our attempts to inhibit the consequences of increased release of BDNF either through genetic or pharmacological approaches did not affect acute as well as chronic seizures caused by TMEV infection. In contrast to the TMEV model, deletion of single allele of BDNF gene was sufficient to inhibit the development of

kindling in mice (Kokaia et al., 1995). As expected, the level of BDNF in the hippocampus of $BDNF^{+/-}$ mice was at half the level found in the WT mice. TMEV-infected $BDNF^{+/-}$ mice that did not have seizures had much less amount of BDNF in hippocampus compared to $BDNF^{+/-}$ mice that had seizures affirming a positive correlation between seizures and BDNF level. Alternatively, pharmacological inhibition of TrkB receptor has been attempted in other epilepsy models (Lin et al., 2020). Since TrkB also mediates neuroprotective effects of BDNF and the PLCγ1-mediated effects of the BDNF-TrkB signaling was primarily identified to impart antiseizure effects, pY816 was rationally designed to uncouple PLCγ1 from activated TrkB (Gu et al., 2015). Treatment of mice with pY816 (10 mg/kg, i. v.) once daily for 3 days following kainic acid-induced SE not only inhibited seizures within first 2 weeks post-SE but also prevented the development to epilepsy 5–6 weeks post-SE (Gu et al., 2015). Our pilot studies informed that this dosing regimen of pY816 may not be enough to control TMEV-induced seizures. Therefore, we treated TMEV-infected mice with pY816 (10 mg/kg, i. v.) once daily for the first 2 weeks starting immediately after infection as TMEV is cleared from the brain after 2 weeks of infection (Libbey et al., 2010). We chose retroorbital route for i. v. dosing because it is effective and less stressful method for chronic i. v. treatment (Steel et al., 2008). However, increasing the duration of pY816 treatment did not affect TMEV-induced seizures. In contrast to kindling and SE models of epilepsy, lack of effects on TMEV-induced seizures observed in pY816-treated and in $BDNF^{+/-}$ mice likely reflects model-specific differences in the mechanisms of ictogenesis. It is possible that the absence of anticonvulsant effects of pY816 observed in TMEV-infected mice could be due to lack of its effects on KCC2. However, further studies are needed to measure the level of KCC2 during the chronic TMEV infection and at various timepoints following pY816 treatment. Furthermore, BDNF-mediated downregulation of KCC2 required activation of both PLCγ1-CREB (phospholipase Cγ1–cAMP response element-binding protein) and Shc/FRC-2 (src homology 2 domain containing transforming protein/FGF receptor substrate 2)-mediated signaling cascade (Rivera et al., 2004). In fact, BDNF either had no effect on or increased the level of KCC2 respectively in mice with mutation in TrkB receptor that permitted the downstream signaling specifically through the PLCγ1-CREB or ShC/FRC-2 pathway (Rivera et al., 2004). It is likely based on this finding that uncoupling PLCγ1 from the activated TrkB alone using pY816 could be insufficient to ameliorate the reduction of KCC2 and suppress TMEV-induced seizures. Lastly, since excessive inflammatory reaction post-TMEV infection is a major driver for the development of seizures in this model (Löscher and Howe, 2022), it is likely that inhibiting BDNF signaling mediated through PLCγ1 alone may not have significant anticonvulsant effects.

In conclusion, the present work suggests that increased release of BDNF could contribute to the development seizures and epilepsy induced by TMEV infection. BDNF could cause neuronal network hyperexcitability by reducing the expression of KCC2, thereby impairing KCC2-mediated chloride homeostasis critical for maintaining inhibitory control over neural network. Further studies are warranted to test the strategies for modulating the BDNF-TrkB signaling and their impact on chloride homeostasis and occurrence of infection-associated seizures.

DATA AVAILABILITY STATEMENT

The original contributions presented in the study are included in the article/supplementary material, further inquiries can be directed to the corresponding author.

ETHICS STATEMENT

The animal study was reviewed and approved by Institutional Animal Care and Use Committee, Virginia Tech.

AUTHOR CONTRIBUTIONS

DP–designed, performed, and analyzed data from most of the experiments, wrote the manuscript. ET–performed and analyzed data from western blot experiments (**Figure 3**). HS–secured funding for the project, edited the manuscript, supervised the project.

FUNDING

This work was supported by the grants from the National Institutes of Health/National Institute of Neurological Disorders and Stroke (7R01NS036692-16 and 7R01NS082851-04), United States.

REFERENCES

Beghi, E. (2020). The Epidemiology of Epilepsy. *Neuroepidemiology* 54, 185–191. doi:10.1159/000503831

Bhuyan, P., Patel, D. C., Wilcox, K. S., and Patel, M. (2015). Oxidative Stress in Murine Theiler's Virus-Induced Temporal Lobe Epilepsy. *Exp. Neurol.* 271, 329–334. doi:10.1016/j.expneurol.2015.06.012

Binder, D. K., Routbort, M. J., Ryan, T. E., Yancopoulos, G. D., and Mcnamara, J. O. (1999). Selective Inhibition of Kindling Development by Intraventricular Administration of TrkB Receptor Body. *J. Neurosci.* 19, 1424–1436. doi:10.1523/jneurosci.19-04-01424.1999

Bröer, S., Käufer, C., Haist, V., Li, L., Gerhauser, I., Anjum, M., et al. (2016). Brain Inflammation, Neurodegeneration and Seizure Development Following Picornavirus Infection Markedly Differ Among Virus and Mouse Strains and Substrains. *Exp. Neurol.* 279, 57–74. doi:10.1016/j.expneurol.2016.02.011

Coulter, D. A., and Steinhauser, C. (2015). Role of Astrocytes in Epilepsy. *Cold Spring Harb. Perspect. Med.* 5, a022434. doi:10.1101/cshperspect.a022434

Croll, S. D., Suri, C., Compton, D. L., Simmons, M. V., Yancopoulos, G. D., Lindsay, R. M., et al. (1999). Brain-derived Neurotrophic Factor Transgenic Mice Exhibit Passive Avoidance Deficits, Increased Seizure Severity and *In Vitro* Hyperexcitability in the hippocampus and Entorhinal Cortex. *Neuroscience* 93, 1491–1506. doi:10.1016/s0306-4522(99)00296-1

Cusick, M. F., Libbey, J. E., Patel, D. C., Doty, D. J., and Fujinami, R. S. (2013). Infiltrating Macrophages Are Key to the Development of Seizures Following Virus Infection. *J. Virol.* 87, 1849–1860. doi:10.1128/jvi.02747-12

Doyon, N., Vinay, L., Prescott, S. A., and De Koninck, Y. (2016). Chloride Regulation: A Dynamic Equilibrium Crucial for Synaptic Inhibition. *Neuron* 89, 1157–1172. doi:10.1016/j.neuron.2016.02.030

Dugich-Djordjevic, M. M., Tocco, G., Lapchak, P. A., Pasinetti, G. M., Najm, I., Baudry, M., et al. (1992). Regionally Specific and Rapid Increases in Brain-Derived Neurotrophic Factor Messenger RNA in the Adult Rat Brain Following Seizures Induced by Systemic Administration of Kainic Acid. *Neuroscience* 47, 303–315. doi:10.1016/0306-4522(92)90246-x

Ernfors, P., Bengzon, J., Kokaia, Z., Persson, H., and Lindvall, O. (1991). Increased Levels of Messenger RNAs for Neurotrophic Factors in the Brain during Kindling Epileptogenesis. *Neuron* 7, 165–176. doi:10.1016/0896-6273(91)90084-d

Ernfors, P., Lee, K.-F., and Jaenisch, R. (1994). Mice Lacking Brain-Derived Neurotrophic Factor Develop with Sensory Deficits. *Nature* 368, 147–150. doi:10.1038/368147a0

Ferrini, F., and De Koninck, Y. (2013). Microglia Control Neuronal Network Excitability via BDNF Signalling. *Neural Plast.* 2013, 429815. doi:10.1155/2013/429815

Ferrini, F., Trang, T., Mattioli, T.-A. M., Laffray, S., Del'guidice, T., Lorenzo, L.-E., et al. (2013). Morphine Hyperalgesia Gated through Microglia-Mediated Disruption of Neuronal Cl− Homeostasis. *Nat. Neurosci.* 16, 183–192. doi:10.1038/nn.3295

Gu, B., Huang, Y. Z., He, X.-P., Joshi, R. B., Jang, W., and Mcnamara, J. O. (2015). A Peptide Uncoupling BDNF Receptor TrkB from Phospholipase Cγ1 Prevents Epilepsy Induced by Status Epilepticus. *Neuron* 88, 484–491. doi:10.1016/j.neuron.2015.09.032

He, X.-P., Kotloski, R., Nef, S., Luikart, B. W., Parada, L. F., and Mcnamara, J. O. (2004). Conditional Deletion of TrkB but Not BDNF Prevents Epileptogenesis in the Kindling Model. *Neuron* 43, 31–42. doi:10.1016/j.neuron.2004.06.019

Howe, C. L., Lafrance-Corey, R. G., Overlee, B. L., Johnson, R. K., Clarkson, B. D. S., and Goddery, E. N. (2022). Inflammatory Monocytes and Microglia Play Independent Roles in Inflammatory Ictogenesis. *J. Neuroinflammation* 19, 22. doi:10.1186/s12974-022-02394-1

Juda, M. B., Brooks, A. K., Towers, A. E., Freund, G. G., Mccusker, R. H., and Steelman, A. J. (2019). Indoleamine 2,3-dioxygenase 1 Deletion Promotes Theiler's Virus-Induced Seizures in C57 BL/6J Mice. *Epilepsia* 60, 626–635. doi:10.1111/epi.14675

Kokaia, M., Ernfors, P., Kokaia, Z., Elmér, E., Jaenisch, R., and Lindvall, O. (1995). Suppressed Epileptogenesis in BDNF Mutant Mice. *Exp. Neurol.* 133, 215–224. doi:10.1006/exnr.1995.1024

Kolbeck, R., Bartke, I., Eberle, W., and Barde, Y. A. (1999). Brain-derived Neurotrophic Factor Levels in the Nervous System of Wild-type and Neurotrophin Gene Mutant Mice. *J. Neurochem.* 72, 1930–1938. doi:10.1046/j.1471-4159.1999.0721930.x

Krishnamurthy, K., Huang, Y. Z., Harward, S. C., Sharma, K. K., Tamayo, D. L., and Mcnamara, J. O. (2019). Regression of Epileptogenesis by Inhibiting Tropomyosin Kinase B Signaling Following a Seizure. *Ann. Neurol.* 86, 939–950. doi:10.1002/ana.25602

Kuczewski, N., Porcher, C., Ferrand, N., Fiorentino, H., Pellegrino, C., Kolarow, R., et al. (2008). Backpropagating Action Potentials Trigger Dendritic Release of BDNF during Spontaneous Network Activity. *J. Neurosci.* 28, 7013–7023. doi:10.1523/jneurosci.1673-08.2008

Lähteinen, S., Pitkänen, A., Koponen, E., Saarelainen, T., and Castrén, E. (2003). Exacerbated Status Epilepticus and Acute Cell Loss, but No Changes in Epileptogenesis, in Mice with Increased Brain-Derived Neurotrophic Factor Signaling. *Neuroscience* 122, 1081–1092. doi:10.1016/j.neuroscience.2003.08.037

Lawley, K. S., Rech, R. R., Elenwa, F., Han, G., Perez Gomez, A. A., Amstalden, K., et al. (2021). Host Genetic Diversity Drives Variable Central Nervous System Lesion Distribution in Chronic Phase of Theiler's Murine Encephalomyelitis Virus (TMEV) Infection. *PLoS One* 16, e0256370. doi:10.1371/journal.pone.0256370

Lee, H. H. C., Deeb, T. Z., Walker, J. A., Davies, P. A., and Moss, S. J. (2011). NMDA Receptor Activity Downregulates KCC2 Resulting in Depolarizing GABAA Receptor-Mediated Currents. *Nat. Neurosci.* 14, 736–743. doi:10.1038/nn.2806

Libbey, J. E., Kirkman, N. J., Smith, M. C. P., Tanaka, T., Wilcox, K. S., White, H. S., et al. (2008). Seizures Following Picornavirus Infection. *Epilepsia* 49, 1066–1074. doi:10.1111/j.1528-1167.2008.01535.x

Libbey, J. E., Kirkman, N. J., Wilcox, K. S., White, H. S., and Fujinami, R. S. (2010). Role for Complement in the Development of Seizures Following Acute Viral Infection. *J. Virol.* 84, 6452–6460. doi:10.1128/jvi.00422-10

Lima Giacobbo, B., Doorduin, J., Klein, H. C., Dierckx, R. A. J. O., Bromberg, E., and De Vries, E. F. J. (2019). Brain-Derived Neurotrophic Factor in Brain Disorders: Focus on Neuroinflammation. *Mol. Neurobiol.* 56, 3295–3312. doi:10.1007/s12035-018-1283-6

Lin, T. W., Harward, S. C., Huang, Y. Z., and Mcnamara, J. O. (2020). Targeting BDNF/TrkB Pathways for Preventing or Suppressing Epilepsy. *Neuropharmacology* 167, 107734. doi:10.1016/j.neuropharm.2019.107734

Liu, G., Gu, B., He, X.-P., Joshi, R. B., Wackerle, H. D., Rodriguiz, R. M., et al. (2013). Transient Inhibition of TrkB Kinase after Status Epilepticus Prevents Development of Temporal Lobe Epilepsy. *Neuron* 79, 31–38. doi:10.1016/j.neuron.2013.04.027

Löscher, W. (2017). Animal Models of Seizures and Epilepsy: Past, Present, and Future Role for the Discovery of Antiseizure Drugs. *Neurochem. Res.* 42, 1873–1888. doi:10.1007/s11064-017-2222-z

Löscher, W., and Howe, C. L. (2022). Molecular Mechanisms in the Genesis of Seizures and Epilepsy Associated with Viral Infection. *Front. Mol. Neurosci.* 15, 870868. doi:10.3389/fnmol.2022.870868

Mcnamara, J. O., and Scharfman, H. E. (2012). "Temporal Lobe Epilepsy and the BDNF Receptor, TrkB," in *Jasper's Basic Mechanisms of the Epilepsies*. Editors Th, J. L. Noebels, M. Avoli, M. A. Rogawski, R. W. Olsen, and A. V. Delgado-Escueta (Bethesda (MD): National Center for Biotechnology Information). doi:10.1093/med/9780199746545.003.0039

Misra, U. K., Tan, C. T., and Kalita, J. (2008). Viral Encephalitis and Epilepsy. *Epilepsia* 49 (Suppl. 6), 13–18. doi:10.1111/j.1528-1167.2008.01751.x

Moore, Y. E., Kelley, M. R., Brandon, N. J., Deeb, T. Z., and Moss, S. J. (2017). Seizing Control of KCC2: A New Therapeutic Target for Epilepsy. *Trends Neurosci.* 40, 555–571. doi:10.1016/j.tins.2017.06.008

Park, H., and Poo, M.-m. (2013). Neurotrophin Regulation of Neural Circuit Development and Function. *Nat. Rev. Neurosci.* 14, 7–23. doi:10.1038/nrn3379

Patel, D. C., Wallis, G., Dahle, E. J., Mcelroy, P. B., Thomson, K. E., Tesi, R. J., et al. (2017). Hippocampal TNFα Signaling Contributes to Seizure Generation in an Infection-Induced Mouse Model of Limbic Epilepsy. *eNeuro* 4, ENEURO.0105-0117.2017. doi:10.1523/ENEURO.0105-17.2017

Patel, D. C., Tewari, B. P., Chaunsali, L., and Sontheimer, H. (2019a). Neuron-glia Interactions in the Pathophysiology of Epilepsy. *Nat. Rev. Neurosci.* 20, 282–297. doi:10.1038/s41583-019-0126-4

Patel, D. C., Wallis, G., Fujinami, R. S., Wilcox, K. S., and Smith, M. D. (2019b). Cannabidiol Reduces Seizures Following CNS Infection with Theiler's Murine Encephalomyelitis Virus. *Epilepsia Open* 4, 431–442. doi:10.1002/epi4.12351

Patel, D. C., and Wilcox, K. S. (2017). "Postinfectious Epilepsy," in *Models of Seizures and Epilepsy*. Editors A. Pitkänen, P. S. Buckmaster, A. S. Galanopoulou, and S. L. Moshé. Second Edition (Massachusetts: Academic Press), 683–696. doi:10.1016/b978-0-12-804066-9.00047-x

Porcher, C., Medina, I., and Gaiarsa, J.-L. (2018). Mechanism of BDNF Modulation in GABAergic Synaptic Transmission in Healthy and Disease Brains. *Front. Cell. Neurosci.* 12, 273. doi:10.3389/fncel.2018.00273

Rivera, C., Li, H., Thomas-Crusells, J., Lahtinen, H., Viitanen, T., Nanobashvili, A., et al. (2002). BDNF-Induced TrkB Activation Down-Regulates the K+-Cl− Cotransporter KCC2 and Impairs Neuronal Cl− Extrusion. *J. Cell. Biol.* 159, 747–752. doi:10.1083/jcb.200209011

Rivera, C., Voipio, J., Thomas-Crusells, J., Li, H., Emri, Z., Sipila, S., et al. (2004). Mechanism of Activity-dependent Downregulation of the Neuron-specific K-Cl Cotransporter KCC2. *J. Neurosci.* 24, 4683–4691. doi:10.1523/jneurosci.5265-03.2004

Sasi, M., Vignoli, B., Canossa, M., and Blum, R. (2017). Neurobiology of Local and Intercellular BDNF Signaling. *Pflugers Arch. - Eur. J. Physiol.* 469, 593–610. doi:10.1007/s00424-017-1964-4

Scharfman, H. E., Goodman, J. H., Sollas, A. L., and Croll, S. D. (2002). Spontaneous Limbic Seizures after Intrahippocampal Infusion of Brain-

Derived Neurotrophic Factor. *Exp. Neurol.* 174, 201–214. doi:10.1006/exnr.2002.7869

Scheirer, C. J., Ray, W. S., and Hare, N. (1976). The Analysis of Ranked Data Derived from Completely Randomized Factorial Designs. *Biometrics* 32, 429–434. doi:10.2307/2529511

Shulga, A., Thomas-Crusells, J., Sigl, T., Blaesse, A., Mestres, P., Meyer, M., et al. (2008). Posttraumatic GABAA-Mediated [Ca2+]i Increase Is Essential for the Induction of Brain-Derived Neurotrophic Factor-dependent Survival of Mature Central Neurons. *J. Neurosci.* 28, 6996–7005. doi:10.1523/jneurosci.5268-07.2008

Smeal, R. M., Fujinami, R., White, H. S., and Wilcox, K. S. (2015). Decrease in CA3 Inhibitory Network Activity during Theiler's Virus Encephalitis. *Neurosci. Lett.* 609, 210–215. doi:10.1016/j.neulet.2015.10.032

Smeal, R. M., Stewart, K.-A., Iacob, E., Fujinami, R. S., White, H. S., and Wilcox, K. S. (2012). The Activity within the CA3 Excitatory Network during Theiler's Virus Encephalitis Is Distinct from that Observed during Chronic Epilepsy. *J. Neurovirol.* 18, 30–44. doi:10.1007/s13365-012-0082-5

Steel, C. D., Stephens, A. L., Hahto, S. M., Singletary, S. J., and Ciavarra, R. P. (2008). Comparison of the Lateral Tail Vein and the Retro-Orbital Venous Sinus as Routes of Intravenous Drug Delivery in a Transgenic Mouse Model. *Lab. Anim.* 37, 26–32. doi:10.1038/laban0108-26

Stewart, K.-A. A., Wilcox, K. S., Fujinami, R. S., and White, H. S. (2010a). Development of Postinfection Epilepsy after Theiler's Virus Infection of C57BL/6 Mice. *J. Neuropathol. Exp. Neurol.* 69, 1210–1219. doi:10.1097/nen.0b013e3181ffc420

Stewart, K. A., Wilcox, K. S., Fujinami, R. S., and White, H. S. (2010b). Theiler's Virus Infection Chronically Alters Seizure Susceptibility. *Epilepsia* 51, 1418–1428. doi:10.1111/j.1528-1167.2009.02405.x

Tao, W., Chen, Q., Zhou, W., Wang, Y., Wang, L., and Zhang, Z. (2014). Persistent Inflammation-Induced Up-Regulation of Brain-Derived Neurotrophic Factor (BDNF) Promotes Synaptic Delivery of α-Amino-3-hydroxy-5-methyl-4-isoxazolepropionic Acid Receptor GluA1 Subunits in Descending Pain Modulatory Circuits. *J. Biol. Chem.* 289, 22196–22204. doi:10.1074/jbc.m114.580381

Umpierre, A. D., Remigio, G. J., Dahle, E. J., Bradford, K., Alex, A. B., Smith, M. D., et al. (2014). Impaired Cognitive Ability and Anxiety-like Behavior Following Acute Seizures in the Theiler's Virus Model of Temporal Lobe Epilepsy. *Neurobiol. Dis.* 64, 98–106. doi:10.1016/j.nbd.2013.12.015

Vezzani, A., Fujinami, R. S., White, H. S., Preux, P.-M., Blümcke, I., Sander, J. W., et al. (2016). Infections, Inflammation and Epilepsy. *Acta Neuropathol.* 131, 211–234. doi:10.1007/s00401-015-1481-5

Waltl, I., Käufer, C., Bröer, S., Chhatbar, C., Ghita, L., Gerhauser, I., et al. (2018). Macrophage Depletion by Liposome-Encapsulated Clodronate Suppresses Seizures but Not Hippocampal Damage after Acute Viral Encephalitis. *Neurobiol. Dis.* 110, 192–205. doi:10.1016/j.nbd.2017.12.001

Xu, B., Michalski, B., Racine, R. J., and Fahnestock, M. (2004). The Effects of Brain-Derived Neurotrophic Factor (BDNF) Administration on Kindling Induction, Trk Expression and Seizure-Related Morphological Changes. *Neuroscience* 126, 521–531. doi:10.1016/j.neuroscience.2004.03.044

Zhan, J., Lin, T.-H., Libbey, J. E., Sun, P., Ye, Z., Song, C., et al. (2018). Diffusion Basis Spectrum and Diffusion Tensor Imaging Detect Hippocampal Inflammation and Dendritic Injury in a Virus-Induced Mouse Model of Epilepsy. *Front. Neurosci.* 12, 77. doi:10.3389/fnins.2018.00077

Conflict of Interest: The authors declare that the research was conducted in the absence of any commercial or financial relationships that could be construed as a potential conflict of interest.

Publisher's Note: All claims expressed in this article are solely those of the authors and do not necessarily represent those of their affiliated organizations, or those of the publisher, the editors and the reviewers. Any product that may be evaluated in this article, or claim that may be made by its manufacturer, is not guaranteed or endorsed by the publisher.

frontiers | Frontiers in Cell and Developmental Biology

TYPE Review
PUBLISHED 10 August 2022
DOI 10.3389/fcell.2022.976953

OPEN ACCESS

EDITED BY
Xinjian Zhu,
Southeast University, China

REVIEWED BY
Nyzil Massey,
Iowa State University, United States
Manikandan Samidurai,
Iowa State University, United States

*CORRESPONDENCE
Manisha Patel,
Manisha.Patel@CuAnschutz.edu

SPECIALTY SECTION
This article was submitted to Signaling, a section of the journal Frontiers in Cell and Developmental Biology

RECEIVED 23 June 2022
ACCEPTED 18 July 2022
PUBLISHED 10 August 2022

CITATION
Fabisiak T and Patel M (2022), Crosstalk between neuroinflammation and oxidative stress in epilepsy.
Front. Cell Dev. Biol. 10:976953.
doi: 10.3389/fcell.2022.976953

Crosstalk between neuroinflammation and oxidative stress in epilepsy

Timothy Fabisiak and Manisha Patel*

Department of Pharmaceutical Sciences, Skaggs School of Pharmacy and Pharmaceutical Sciences, University of Colorado Anschutz Medical Center, Aurora, CO, United States

The roles of both neuroinflammation and oxidative stress in the pathophysiology of epilepsy have begun to receive considerable attention in recent years. However, these concepts are predominantly studied as separate entities despite the evidence that neuroinflammatory and redox-based signaling cascades have significant crosstalk. Oxidative post-translational modifications have been demonstrated to directly influence the function of key neuroinflammatory mediators. Neuroinflammation can further be controlled on the transcriptional level as the transcriptional regulators NF-KB and nrf2 are activated by reactive oxygen species. Further, neuroinflammation can induce the increased expression and activity of NADPH oxidase, leading to a highly oxidative environment. These factors additionally influence mitochondria function and the metabolic status of neurons and glia, which are already metabolically stressed in epilepsy. Given the implication of this relationship to disease pathology, this review explores the numerous mechanisms by which neuroinflammation and oxidative stress influence one another in the context of epilepsy. We further examine the efficacy of treatments targeting oxidative stress and redox regulation in animal and human epilepsies in the literature that warrant further investigation. Treatment approaches aimed at rectifying oxidative stress and aberrant redox signaling may enable control of neuroinflammation and improve patient outcomes.

KEYWORDS

neuroinflammation, oxidative stress, redox, epilepsy, mitochondria, NADPH oxidase

Introduction

There are 31 types of epilepsy syndromes classified by the International League Against Epilepsy (Epilepsy Syndromes, 2022) based on numerous features such as seizure type, epilepsy presentation, and etiology (Scheffer et al., 2017). This disease complexity presents a challenge in the treatment of epilepsy, where available anti-seizure medications (ASMs) that are tailored to the epilepsy syndrome generally only achieve a 30–50% responder rate (Löscher and Klein, 2021). The prevalence of drug-resistant epilepsy highlights a need to further understand underlying mechanisms in epilepsy such as neuroinflammation and consequential signaling cascades, as reviewed further elsewhere (Vezzani et al., 2019). Yet more recently, oxidative stress and redox dysregulation have

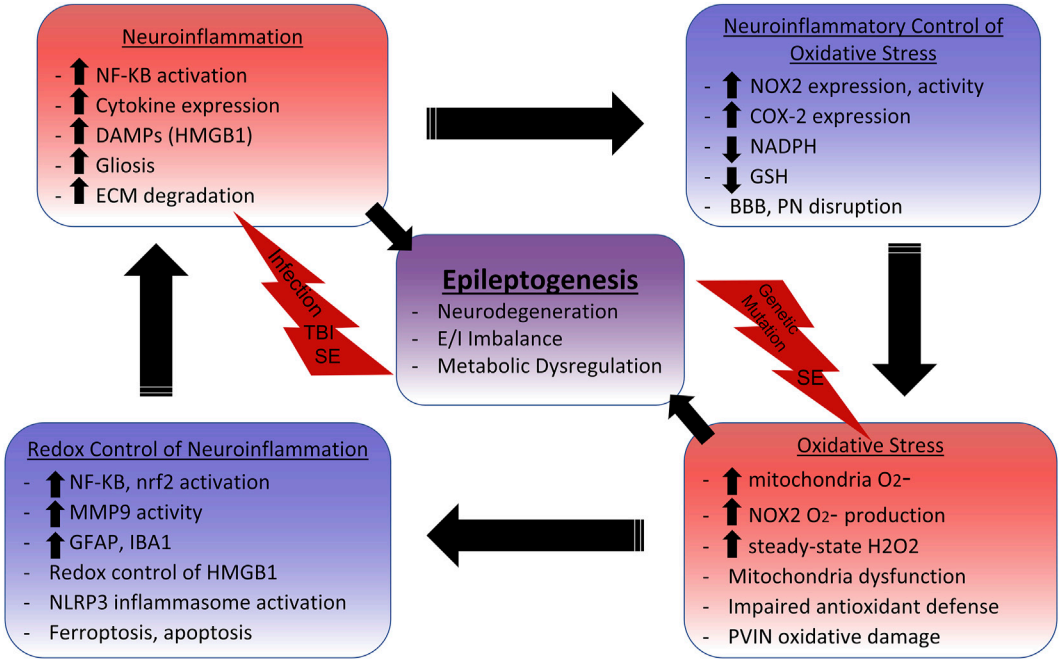

SCHEME 1
Neuroinflammation and Oxidative Stress Cycle in Epilepsy.Initial insults such as systemic infection, traumatic brain injury (TBI), status epilepticus (SE), and genetic mutations initiate inflammatory and oxidative signaling cascades. NF-KB activation leads to the production of proinflammatory cytokines such as IL-1β, TNFα, and IL-6, which have been shown to i nduce gliosis, mitochondrial dysfunction, and glutathione (GSH) depletion. GSH depletion impairs cellular and mitochondrial antioxidant defenses, enabling aberrant oxidative signaling and damage. NAPDH Oxidase 2 (NOX2) upregulation also commonly occurs with neuroinflammation. NOX2 utilizes NADPH, which is needed for the reductive abilities of antioxidant systems like thioredoxin reductase and glutathione peroxidase, to produce superoxide (O_2^-). $O_2^-$is primarily enzymatically converted to the redox-signaling reactive H_2O_2. The increased levels of steady-state H_2O_2 leads to the activation of numerous redox-sensitive pathways that influence neuroinflammation. For example, NF-KB activation and subsequent microglia activation relies on NOX2 activity, indicating that reactive oxygen species (ROS) production perpetuates neuroinflammation. Nrf2 is also activated by ROS to increase expression of the antioxidant response element (ARE) to combat oxidative damage and neuroinflammation, making it an attractive therapeutic target. The danger-associated molecular pattern (DAMP) HMGB1 is released in response to neuronal damage, which signals through TLR4 to activate NF-KB, induce gliosis, and increase NOX2 and COX-2 expression. Reduced HMGB1 has chemoattractant properties, but adjacent cysteine residues act as a redox switch where oxidation to a disulfide form increases affinity for TLR4 and induces cytokine like properties. The NLRP3 inflammasome, which activates IL-1β, can also by activated by ROS from the mitochondria and NOX. Extracellular matrix (ECM) digesting proteinases such as matrix metalloproteinases (MMPs) are also upregulated in the neuroinflammatory environment. This can lead to the disruption of the blood brain barrier (BBB) and perineuronal nets (PNs) surrounding inhibitory parvalbumin interneurons (PVINs). MMP9 has demonstrated redox-sensitive activation, which is associated with the loss of PNs and death of PVINs. Mitochondria dysfunction can result from excessive mitochondrial ROS (mtROS) which not only accounts for metabolic alterations, but can lead to inflammation-inducing events such as astrogliosis, apoptosis, and lipid peroxidase mediated death (ferroptosis). Metabolic dysfunction, excitatory/inhibitory (E/I) imbalance, and neurodegeneration can all result from these oxidative and inflammatory processes which ultimately contribute to epileptogenesis.

also emerged as hallmarks in the epilepsy literature (Patel, 2004; Pearson-Smith & Patel, 2017; Geronzi et al., 2018).

Interestingly, in human epilepsies and animal epilepsy models, various biomarkers of both oxidative stress and neuroinflammation are elevated in the brain and periphery. Neuroinflammation and reactive oxygen species (ROS) production are both prominent effectors of signaling and are therefore heavily regulated. It is not unexpected for these prominent cell signaling processes to have influence on the regulation of one another. As an evolutionarily conserved defense mechanism, inflammation in response to infection or injury promotes and utilizes ROS to kill pathogens or enact rapid, local signaling. At physiological levels, ROS is an important second messenger that modulates neuroinflammation at numerous stages through redox-sensitive mechanisms. Further, excessive ROS production or redox dysregulation under oxidative stress damages cells and produces danger signals that incite neuroinflammation. As oxidative stress and neuroinflammatory pathways have considerable crosstalk (See Scheme 1), there is an unmet need for further research exploring this relationship in the pathophysiology of epilepsy. This can enable the development of novel redox-based therapeutics, beyond traditional ASMs which primarily aim to rectify neural excitatory/inhibitor imbalances at the synapse, to control neuroinflammation and in turn, epilepsy and/or its comorbidities.

Oxidative stress in epilepsy

The brain is particularly susceptible to oxidative damage due to its high metabolic demand and per weight rate of oxygen consumption. It has long been recognized that ictal cerebral hypermetabolism is characteristic of seizure disorders, where increased cerebral oxygen (Meyer et al., 1966) and glucose consumption (Ingvar and Siesjö, 1983) are observed during seizure activity in experimental epilepsy models and in humans (During et al., 1994). These metabolic stresses lead to interictal metabolic dysfunction which is evidenced by glucose hypometabolism in chronic epilepsy (Guo et al., 2009) and mitochondrial metabolic deficits resulting from inhibition of mitochondrial enzyme complexes in animal and human epilepsies (Kunz et al., 2000, 1999). It has been demonstrated that mitochondrial reactive oxygen species (mtROS) damage mitochondrial electron transport chain complex I, subsequently decreasing mitochondrial oxidative phosphorylation (Ryan et al., 2012; Rowley et al., 2015). Further, pharmacological inhibition of mitochondrial enzyme complexes results in decreased oxidative phosphorylation and seizure activity (Fleck et al., 2004).

There are numerous indications that increased ROS production occurs across epilepsy models, as evidenced by oxidative damage and impaired redox status. In addition to Complex I inhibition in humans and animal models of temporal lobe epilepsy (TLE), the redox regulated TCA cycle enzymes aconitase and α-ketoglutarate dehydrogenase have been shown to be inactivated following status epilepticus (SE) in rats (Cock et al., 2002). Increased mitochondria oxidative phosphorylation is also shown to increase complex III mediated mtROS production (Malinska et al., 2010). Mitochondrial DNA (mtDNA) oxidative damage has also been found in the kainate model of TLE, along with increases in mitochondrial H_2O_2 (Jarrett et al., 2008a). Further, numerous other animal models and human epilepsies revealed depleted glutathione (GSH) levels, paired with increased oxidized glutathione (glutathione disulfide or GSSG) in the hippocampus or neocortex, indicative of an oxidative environment (Rumià et al., 2013; Cárdenas-Rodríguez et al., 2014; Pearson-Smith and Patel, 2017). As GSH acts as a major antioxidant in the brain, this impaired GSH redox status can lead to further oxidative damage and redox dysregulation, which is associated with cognitive deficits, neuronal death, and mortality in animal epilepsy models. Indeed, loss of glutathione peroxidase 4, a oxidation-resistant selenoprotein that utilizes GSH, leads to lipid peroxidation and subsequent ferroptosis, which is also found in epilepsy models (Ingold et al., 2018; Cai and Yang, 2021).

The NADPH oxidase (NOX) family of enzymes is another relevant major source of ROS in the context of epilepsy as evidenced by activation of NOX2 by kainate-induced SE (Patel et al., 2005). NOX enzymes utilize NADPH to produce superoxide (O_2^-), which then undergoes primarily enzymatic dismutation to H_2O_2. Interestingly, it has been demonstrated that NMDA receptor activation, which is increased due to excessive extracellular glutamate in epilepsy, increases O_2^- and subsequent H_2O_2 production via NOX induction (Brennan et al., 2009; Kovac et al., 2014). Further, NOX activation has been shown to be a sufficient trigger of seizure activity, while NOX inhibition reduced hyperactivity in multiple animal models of epilepsy (Malkov et al., 2019). It is argued that NOX2, the primary isoform in microglia, is thought to be the major contributor of SE-induced ROS production in acquired epilepsies, which has also been linked to glucose hypometabolism in epileptogenesis (Zilberter et al., 2022).

Biomarkers of oxidative stress in human epilepsies have recently received further attention. In the blood of patients with SE, lower levels of SOD, catalase, GSH, and total antioxidant capacity were found (Kalita et al., 2019). In drug-resistant complex partial seizure patient blood, there was an inverse correlation of vitamin C and positive correlation of the oxidative damage marker 3-nitrotyrosine to seizure frequency (Lorigados Pedre et al., 2018). Justifiably, therapies targeting oxidative stress are currently under investigation. In rat electrical status epilepticus, GSH increasing drug treatment was neuroprotective and reduced seizure frequency (Pauletti et al., 2019). Inhibition of KEAP1 by RTA 408 disinhibits the antioxidant transcription factor nrf2 and has neuroprotective and seizure reducing effects in the kainic model of TLE (Shekh-Ahmad et al., 2018). Treatment with a NOX inhibitor, a catalytic antioxidant, and a scavenger of reactive oxidized compounds gamma-ketoaldehydes, have all been shown to prevent experimental TLE seizure-induced neuronal death (Kim et al., 2013; Pearson et al., 2017; Pearson-Smith et al., 2017). In humans, Vitamin E in conjunction with ASMs has been shown to reduce seizure frequency and oxidative stress (Mehvari et al., 2016). Further, the high-fat low-carbohydrate ketogenic diet (KD), which shifts metabolism towards fatty acid oxidation and away from glycolysis, also has antioxidant properties which may contribute to its clinical efficacy in Dravet Syndrome (Caraballo et al., 2005). As a treatment for experimental or genetic epilepsies in rodents, this diet can reduce ROS production, activate nrf2, and increase the synthesis of GSH (Jarrett et al., 2008b; Milder and Patel, 2012).

Clearly, oxidative stress is associated with epilepsy which may be a consequence of the disease. Interestingly, there is further evidence indicating that mitochondrial dysfunction and oxidative stress contribute to epilepsy pathogenesis (Patel, 2004). The most robust links between oxidative stress or mitochondrial dysfunction and epilepsy are clear in mitochondrial encephalopathies such as myclonic epilepsy with ragged-red fibers (MERFF) and Leigh syndrome. These disorders are characterized by mtDNA mutations that impair mitochondria electron transport chain enzyme complexes, which can result in increased ROS production, oxidative damage, and decreased ATP production

(Quintana et al., 2010; Wu et al., 2010; Wojtala et al., 2017). Other genetic epilepsies such as Dravet Syndrome are further associated with mitochondrial dysfunction (Kumar et al., 2016; Banerji et al., 2021). Genetic knockouts in mice of mitochondrial superoxide dismutase (SOD2), which detoxifies O_2^- to H_2O_2, increases susceptibility to spontaneous and induced seizures (Liang and Patel, 2004; Liang et al., 2012). Further, the forebrain neuron-specific conditional knockout of SOD2 also leads to the presentation of epilepsy in mice (Rowley et al., 2015). Together, this body of work demonstrates that oxidative stress is not only a consequence of epilepsy, but also a cause.

Concomitance of neuroinflammation and oxidative stress in epilepsy

Seizure inciting events such as infection or traumatic brain injury (TBI) that initiate proinflammatory cascades are also linked to oxidative stress. Post-traumatic epilepsy (PTE) develops in as many as 50% of TBI patients, and TBI and chronic epilepsy brain tissue both display elevated markers of oxidative stress in addition to cytokines and neurodegeneration (Vezzani et al., 2008; Helmy et al., 2011; Terrone et al., 2019). NOX2 expression is additionally elevated in the brain following TBI and in epilepsy as reviewed by Ma et al., 2018. In experimental models of acquired epilepsy, such as chemically induced status epilepticus, there are clear signs of inflammation, reactive gliosis, and neurodegeneration (Loewen et al., 2016) as well as metabolic and redox dysregulation as reviewed by Pearson-Smith & Patel, 2017. In a zebrafish model of Dravet syndrome, there are metabolic irregularities (Kumar et al., 2016; Banerji et al., 2021) as well as increased astrogliosis associated gene expression (Tiraboschi et al., 2020), which is also apparent in a mouse DS model (Valassina et al., 2022). In pediatric drug-resistant epilepsy, levels of IL-1β in peripheral monocytes correlate to seizure frequency (Yamanaka et al., 2021). Further, an LPS administration model of systemic inflammation in sepsis in conjunction with convulsant PTZ treatment in mice increased seizure susceptibility, which was attenuated with NOX2 genetic ablation and inhibition (Huang et al., 2018). Theiler's murine encephalomyelitis virus (TMEV) model of temporal lope epilepsy is known to induce neuroinflammation and seizures, but also leads to oxidative stress as indicated by elevated 3-nitrotyrasine levels and reduced GSH/GSSG ratios in the hippocampus (Bhuyan et al., 2015).

Epileptic encephalopathies and genetic epilepsies such as West, Lennox-Gastaut, Dravet, Lafora, and Leigh syndromes have additionally shown evidence of gliosis and neuroinflammation in humans (Kawashima et al., 1999; You et al., 2009; Salar and Galanopoulou, 2018; Lahuerta et al., 2020; Valassina et al., 2022). There is also evidence that most of these types of epilepsies also have a metabolic dysfunction component given the efficacy of the KD in patients (Wijburg et al., 1992; Caraballo et al., 2005, 2014; You et al., 2009). As both neuroinflammation and oxidative stress or metabolic dysregulation are prevalent across the epilepsies, which are both argued to be causal and consequential to the disease, the direct interactions between neuroinflammation and oxidative stress are key components of disease pathology which deserve further evaluation.

Neuroinflammatory induction of oxidative stress

The role of NADPH oxidases in epilepsy has drawn considerable attention, with findings highlighting a link between oxidative stress production and inflammation. NOX expression of the brain isoforms 1, 2 and 4 are highly inducible, with signs of NOX2 upregulation prevalent in human and animal epilepsies. As described previously, SE can induce ROS production through NOX via NMDA receptor activation. However, NOX expression and activity is also closely linked to neuroinflammation. Pattern recognition receptor (PRR) CR3 and TLR4 signaling by damage associated molecular patterns (DAMPs), such as high mobility group box 1 (HMGB1) released by damaged neurons, is linked to NOX2 expression and activation in microglia (Pei et al., 2007; Gao et al., 2011; Bell et al., 2013; Hou et al., 2018). The inhibition of NF-KB signaling has been shown to reduce LPS induced NOX and inducible nitric oxide synthase (iNOS) expression in various peripheral cell types (Kim B et al., 2008; Al-Harbi et al., 2020; Sul and Ra, 2021). NOX-mediated aberrant ROS production in response to proinflammatory signaling is a major source of oxidative stress in epilepsy, and is further linked to interictal glucose hypometabolism (Malkov et al., 2018). It is suggested that increased NOX activity induced by SE or trauma increases steady-state levels of H_2O_2 directly and indirectly by utilizing NADPH needed for glutathione reduction, leading to the inhibition of glycolysis and increased cell susceptibility to oxidative stress. Further, other NOX2-mediated H_2O_2 redox signaling is shown to directly increase mtROS production in one of the forms of ROS-induced ROS release (Kim et al., 2017).

DAMPs, particularly HMGB1, have been implicated in epilepsy pathogenesis. HMGB1 and the PRR it can signal through, TLR4, have increased expression in human and animal epilepsies. HMGB1 released from neurons and proinflammatory microglia and has been attributed to both TBI and epilepsy pathogenesis in experimental models as reviewed by Paudel et al., 2018. In animal TLE models, HMGB1 acts through TLR-4 to increase production of cytokines such as IL-1β, TNFα, and IL-6 (Maroso et al., 2010). This TLR-4 mediated signaling cascade can activate NF-KB, leading to the production of these pro-convulsant cytokines. Cytokines like TNFα can, in turn, induce COX-2 and NOX2 gene expression (Newton et al., 1997; Li et al., 2009). Interestingly, peripheral inflammation induced by TLR-

4 activation by systemic LPS exacerbated kainic-acid induced seizures and elevated hippocampal reactive microglia, levels of IL-1β, TNFα, and IL-6, and NOX subunit expression (Ho et al., 2015). The ability of PRR-mediated inflammatory signaling to increase NOX expression in epilepsy suggests that enabling ROS production may act as a second messenger to neuroinflammation.

Tumor necrosis factor alpha (TNFα) further impacts the oxidative environment and metabolism in the brain by targeting mitochondria. In neuronal cultures, direct treatment with TNFα resulted in a time dependent decrease in mitochondrial respiration, followed by a reduction in cell viability correlated with increase cytosolic cytochrome c levels (Doll et al., 2015). In mice, systemic LPS increased brain region specific expression of IL-1β as well as mitochondrial complex II/III activity, while decreasing GSH (Noh et al., 2014). Local brain LPS administration, as well as astrocyte exposure to TNFα and IL-1β, depleted GSH (Gavillet et al., 2008; Ariza et al., 2010). These studies indicate that neuroinflammation can influence mitochondrial function, impair antioxidant defenses, and cause oxidative stress to contribute to neurodegeneration.

Neuroinflammation in epilepsy is commonly associated with blood brain barrier (BBB) disruption, allowing infiltration of the brain parenchyma by peripheral immune cells and serum albumin as reviewed in detail by Van Vliet et al. (2015). In addition to exacerbating gliosis and inflammation, BBB disruption also leads to oxidative damage such as in ischemia-reperfusion injury where SOD1 deficiency causes exacerbated neuronal damage and infarct volume (Gasche et al., 2001). Inhibition of matrix metalloproteinase 9 (MMP9), which degrades extracellular matrix around the vasculature, rescues this effect. MMP9 also contributes to parvalbumin positive inhibitory interneuron (PVIN) cell loss that is found in epilepsy. MMP9 is upregulated in epilepsy models, and this ECM proteinase has been shown to degrade the specialized ECM called perineuronal nets (PN) surrounding PVINs (Kim et al., 2009; Acar et al., 2015; Rankin-Gee et al., 2015; Dubey et al., 2017). Interestingly, PVINs are shown to be particularly susceptible to oxidative stress, and the neuroinflammatory based degradation of their neuroprotective PNs leads to oxidative damage and death of these cells (Cabungcal et al., 2013). In fact, neuronal NOX2 expression which is induced by neuroinflammation colocalizes with parvalbumin immunoreactivity in areas of PVIN loss in human TBI (Schiavone et al., 2017).

Oxidative stress and redox regulation of neuroinflammation

NOX activity may be induced by proinflammatory signaling cascades, but it is also necessary for inducing neuroinflammation. In the kainate and pilocarpine rat experimental models of TLE, ROS production through NOX activity is associated with microglial activation and is responsible for neurodegeneration in these models (Patel et al., 2005; Pestana et al., 2010). SE induced ROS production and neural cell death were attenuated by NOX inhibitors (Pestana et al., 2010; Williams et al., 2015) and overexpression of extracellular SOD (Patel et al., 2005). Interestingly, the deletion of NOX2 following mouse TBI (Dohi et al., 2010; Wang et al., 2018) or PTZ-induced SE (Huang et al., 2018) enhances neurogenesis and reduces cytokine production, indicating that the ROS production occurring following trauma is deleterious to neural recovery. A direct link between NOX activity and inflammation is apparent, as NOX2 mediated production of O_2^- and resulting increased steady-state H_2O_2 levels is necessary for NF-KB activation in macrophages (Li et al., 2018) and for microglia proliferation (Mander et al., 2006). The NOX2 inhibitor celastrol attenuated kainate-induced epileptiform activity, indicating that NOX2 is important for seizure initiation (Malkov et al., 2019). As it has been suggested that NOX2 is important for the initial oxidative burst following SE that contributes to seizures in trauma and chemically induced epilepsy models (Zilberter et al., 2022), the efficacy of NOX inhibition in chronic epilepsy and in a clinically relevant window following a seizure inciting event needs further evaluation. Chronic administration of apocynin, a NOX inhibitor antioxidant, following pilocarpine-induced SE did significantly increase neural survival (Lee et al., 2018). Despite the promise of NOX2 inhibition in epilepsy models, further efforts to develop and evaluate clinically translatable BBB permeable compounds such as GSK2795039 are needed (Hirano et al., 2015; Malkov et al., 2019).

Excessive ROS levels are toxic, but at physiological levels ROS such as H_2O_2 are important second messengers acting through redox signaling. H_2O_2 is an efficient activator of the redox-regulated proinflammatory transcription factor NF-KB, where redox-regulation activates upstream kinases P13K and NIK leading to NF-KB translocation and promotor binding. Further, NOX2 depletion and the NOX inhibitor apocynin were able to reduce NF-KB activation, demonstrating how ROS can lead to the increased expression of proinflammatory cytokines (Kim J et al., 2008). Nrf2, the redox-sensitive transcription factor controlling expression of the antioxidant response element (ARE), is an important modulator of the proinflammatory effects of ROS. For example, nrf2 depletion has been shown to increase NF-KB activation, as well as the activation of MMP3/9 and TGF-β following mouse TBI leading to neurodegeneration (Bhowmick et al., 2019). The nrf2 targets heme oxygenase 1 (HO-1), NQO1, and the GSH producing enzymes GCLC and GCLM have all been shown to exert anti-inflammatory effects as reviewed in detail by Ahmed et al., 2017. Not surprisingly, the inhibition of the nrf2 inhibitor KEAP1 with RTA 408, particularly in combination with a NOX inhibitor, prevented cell death and dramatically reduced kainate-induced

seizures (Shekh-Ahmad et al., 2019, 2018). The KD's clinical efficacy in the treatment of various epilepsies may be mediated in part due to its apparent ability to activate nrf2 (Milder et al., 2010). These inflammation modifying roles of nrf2 demonstrate redox-neuroinflammation crosstalk at the transcriptional level which highlights nrf2 as an important therapeutic target for controlling both ROS-mediated damage and activation of proinflammatory cascades.

Certain proinflammatory molecules are also directly regulated by ROS such as IL-1β, HMGB1, and MMP9. IL-1β activation is induced by caspase-1 which is activated by the DAMP-sensitive NLRP3 and NLRC4 inflammasomes (Poyet et al., 2001; Martinon et al., 2002). NLRP3 has been extensively linked to epilepsy, where heightened expression and activation is found in animal and human epilepsies as reviewed by Mohseni-Moghaddam et al., 2021. ROS can lead to NLRP3 activation through binding to thioredoxin-interacting protein (TXNIP) binding following thioredoxin oxidation (Zhou et al., 2011). Further, the crystal structure of NLRP3 revealed a disulfide bond between conserved cysteine residues in the inflammasome active site, suggesting redox-sensitive activity (Bae and Park, 2011). NLRP3 has indeed been shown to be activated by NOX2 mediated ROS production (Abais et al., 2014, 2013). Further, mtROS acts as a second messenger stimulating NLRP3 activation and localization to the mitochondria to promote IL-1β activation, thus inciting a proinflammatory signal in response to mitochondria dysfunction (Zhou et al., 2011; Subramanian et al., 2013). Interestingly, sulforaphane, an nrf2 activator, has been shown to limit mtROS generation and prevent both NLRP3 and NLRC4 activation in murine macrophages (Lee et al., 2016). Although implicated in neurodegenerative disorders but not currently in epilepsy, NLRC4 activation has also been found to be sensitive to mtROS production in astrocytes and contributes to gliosis (Freeman et al., 2017; Samidurai et al., 2020). NLRP3 activation further appears to be inhibited by the activity of the ketone body βHB produced by the KD, suggesting that the modulation of neuroinflammation contributes to KD efficacy (Youm et al., 2015). ROS-mediated inflammasome activation could explain the increased prevalence of IL-1β found in epilepsy as described above, which may in turn perpetuate cycle of oxidative stress and neuroinflammation.

HMGB1 contains three redox sensitive cysteine residues and carries out different immune system roles depending on its redox state. In the reduced state, HMGB1 acts as a chemoattractant. In the oxidized state with two nearby cysteines forming a disulfide bond and the third cysteine unmodified, HMGB1 acts as a proinflammatory cytokine (Yang et al., 2021) which can interact with TLR4 (Balosso et al., 2014). Overoxidation inhibits all HMGB1 functions. Interestingly, combinational drug treatment with sulforaphane and N-actylcysteine (NAC), a compound used to enhance GSH levels, also reduced the production of HMGB1 in the brain and blood in an electrical SE model (Pauletti et al., 2019).

Finally, MMP9 has also been found to have redox-sensitive activation, as oxidants have been shown to directly increase MMP function, contributing to BBB dysfunction (Haorah et al., 2007). IL-1β-induction of MMP9 was dependent on NOX2 activity leading to NF-KB and AP-1 transcription factor activation. Further, this enabled MMP9-dependent astrocyte migration (Yang et al., 2015). This relationship was found to be inhibited by the nrf2 activator RTA 408 (Yang et al., 2019). Incredibly, this redox-sensitive activity of MMP9 is linked to PVIN/PNN irregularities in neurons with impaired GSH synthesis ($Gclm^{-/-}$) *in vivo*. MMP9 inhibition prevented NF-KB activation and restored PVIN/PNN integrity, linking redox-controlled MMP9 to excitatory/inhibitory imbalance (Dwir et al., 2020). Rectifying redox dysregulation in epilepsy may enable the control of these proinflammatory pathways.

In the brain, the major regulator of redox status is GSH, which has also been shown to regulate inflammation. This antioxidant thiol is utilized as the electron donor by glutathione peroxidase (GPx) to convert H_2O_2 to H_2O, so the GSH/GSSG ratio is indicative of the oxidative environment. The expression of enzymes involved in this process such as GCL and GCLM is controlled by nrf2 and NF-KB. Post-translational activation of GCL by dimercaprol in cultured BV-2 microglia prevents LPS-induced production of proinflammatory cytokines and iNOS induction (McElroy et al., 2017a). Depletion of GSH with the GCL inhibitor BSO leads to gliosis and neuroinflammation in the rat brain, with a particular increase in levels of TNFα (González-Fraguela et al., 2018). In this study, this is associated with mild cognitive impairment, suggesting that impaired redox status could contribute to associated comorbidities in epilepsy. GSH in the mitochondria is protective against TNFα-induced neurotoxicity, indicating that GSH depletion in epilepsy may contribute to a vicious cycle of oxidative stress-neuroinflammation-metabolic stress (Fernandez-Checa et al., 1997). Impaired glutathione redox status also enables aberrant oxidative signaling to occur, which can influence redox sensitive ion channels, neurotransmitter receptors, and glutamate reuptake by astrocytes. Restoring GSH redox status may not only control neuroinflammation, but rectify redox based post-translational modifications that can directly influence neural excitability. The therapeutic potential of GSH increasing treatments such as NAC, Coenzyme Q10, sulforaphane, and Vitamin E has begun to be explored in epilepsy models.

Oxidative stress involves the damage to mtDNA, lipids, and proteins in the cell which can lead to neuroinflammation. Astrogliosis is prevalent in the epilepsies, and interestingly a mouse forebrain neuron-specific knockout of SOD2 resulted in seizures, oxidative stress, and marked GFAP and vimentin gene upregulation, indicative of astrogliosis resulting from increased neuronal mtROS (Fulton et al., 2021). Oxidative stress resulting from increased mtROS has significant impacts on redox signaling within neurons (Bao et al., 2009), and can lead to neuronal apoptosis as described in detail by Méndez-Armenta et al., 2014. This oxidative damage originating from neurons can induce

neuroinflammation and gliosis through the release of DAMPs. Further, oxidative damage to phospholipids can induce ferroptosis, as described earlier, which has now been directly linked to the induction of neuroinflammation (Cao Y et al., 2021; Cui et al., 2021).

Discussion

Together, these studies examining oxidative stress, redox dysregulation, metabolic alterations, and neuroinflammation suggest that these processes are all not only involved in the pathogenesis of epilepsy, but fundamentally linked (See Scheme 1). An infection or traumatic brain injury initiates proinflammatory cascades that involve the upregulation and increased activity of NOX. Excessive excitatory signaling induced by status epilepticus or genetic mutations also increase NOX activity. Seizure activity increases metabolic demand in neuronal mitochondria, which increases O_2^- production. The increased oxidative environment resulting from NOX activity and mtROS production leads to GSH depletion. Importantly, NOX utilizes NADPH to produce superoxide, thus depleting NADPH needed by antioxidant systems such as thioredoxin reductase and glutathione peroxidase. Together, these processes exacerbate neuroinflammation through oxidative damage and redox based activation of NF-KB, as well as of HMGB1, inflammasomes and IL-1β, and MMP9. NF-KB activation also increases TNFα, NOX, and COX-2 expression. Neuroinflammatory cytokines such as TNFα cause mitochondrial dysfunction when GSH is depleted, as well as induce reactive astrocytes. This can impair astrocyte regulation of the tripartite synapse, BBB, and neuronal metabolism. Damaged neurons and reactive microglia can increase NOX expression, as well as release MMP9 which degrades ECM around the BBB and PVIN neurons, leaving them susceptible to oxidative damage. Regardless of the initial insult, oxidative bursts through NOX and increased oxidative phosphorylation in the mitochondria induce metabolic alterations responsible for observed interictal glucose hypometabolism. Glycolysis further fuels the pentose phosphate pathway (PPP) which produces NADPH. Together, oxidative stress and redox dysregulation form a vicious cycle with neuroinflammation that likely underlies epileptogenesis and undermines current treatment strategies.

Developing combinational therapies that address neuronal hyperexcitability as well as oxidative stress may prevent the deleterious cycle of neuroinflammation and oxidative stress that contribute to epileptogenesis. Recent advances have identified redox-based treatment strategies that warrant further investigation (Yang et al., 2020; Parsons et al., 2022). NOX-inhibitor therapy has shown neuroprotective effects in numerous epilepsy models. However, research suggesting that NOX2 is primarily responsible for the oxidative burst immediately following SE may not allow for a wide enough treatment window in patients following their first SE event. Inhibited interictal glycolysis may contribute to a more oxidative environment due to the decreased substrate pool for the PPP. Interestingly, the KD pushes metabolism away from glycolysis, potentially removing fuel needed to trigger seizures while introducing ketone bodies. This can diminish neuroinflammation and induce Nrf2 activation to express the ARE, which has proven efficacy in treating epilepsy patients. Indeed, Nrf2 activators such as sulforaphane and hydroxylated fullerene have restored GSH levels and shown antiepileptic and neuroprotective properties in numerous epilepsy models (Wang et al., 2014; Carrasco-Pozo et al., 2015; Pauletti et al., 2019; Uddin et al., 2020; Cao H et al., 2021; Sandouka and Shekh-Ahmad, 2021). An antioxidant and metal chelator, curcumin, was able to reduce gliosis and cytokine levels in PTZ-induced epilepsy (Kaur et al., 2015). Other redox-based therapies such as AEOL10150, salicylamine, Coenzyme Q10, and NAC have also been shown to restore GSH homeostasis, which is critical to control inflammation, leading to reduction of seizure burden or comorbidities in animal models (Shin et al., 2005; Tawfik, 2011; Pearson et al., 2015; McElroy et al., 2017b). Further, in a small study of patients with refractory epilepsy, Vitamin E in combination with ASMs increased total antioxidant capacity, catalase, and glutathione and reduced seizure frequency (Mehvari et al., 2016). It is herein proposed that tempering excessive ROS production and reducing oxidative stress could thereby control neuroinflammatory processes involved in epilepsy. A comprehensive treatment strategy broadly effective in epilepsy may therefore involve a combinational approach of ASMs coupled with GSH inducing and nrf2 activating compounds.

Author contributions

TF authored the review and generated the schematic. MP provided content ideas as well as reviewing and editing of the manuscript.

Funding

The authors are grateful for the support of NIH grants R01NS039587, R01NS086423 and R01HD102071.

Conflict of interest

The authors declare that the research was conducted in the absence of any commercial or financial relationships that could be construed as a potential conflict of interest.

Publisher's note

References

Abais, J. M., Xia, M., Li, G., Chen, Y., Conley, S. M., Gehr, T. W. B., et al. (2014). Nod-like receptor protein 3 (NLRP3) inflammasome activation and podocyte injury via thioredoxin-interacting protein (TXNIP) during hyperhomocysteinemia. *J. Biol. Chem.* 289, 27159–27168. doi:10.1074/jbc.M114.567537

Abais, J. M., Zhang, C., Xia, M., Liu, Q., Gehr, T. W. B., Boini, K. M., et al. (2013). NADPH oxidase-mediated triggering of inflammasome activation in mouse podocytes and glomeruli during hyperhomocysteinemia. *Antioxid. Redox Signal.* 18, 1537–1548. doi:10.1089/ars.2012.4666

Acar, G., Tanriover, G., Acar, F., and Demir, R. (2015). Increased expression of matrix metalloproteinase-9 in patients with temporal lobe epilepsy. *Turk Neurosurg.* 25 (5), 749–756. doi:10.5137/1019-5149.JTN.10738-14.0

Ahmed, S. M. U., Luo, L., Namani, A., Wang, X. J., and Tang, X. (2017). Nrf2 signaling pathway: Pivotal roles in inflammation. *Biochim. Biophys. Acta. Mol. Basis Dis.* 1863, 585–597. doi:10.1016/j.bbadis.2016.11.005

Al-Harbi, N. O., Nadeem, A., Ahmad, S. F., AL-Ayadhi, L. Y., Al-Harbi, M. M., As Sobeai, H. M., et al. (2020). Elevated expression of toll-like receptor 4 is associated with NADPH oxidase-induced oxidative stress in B cells of children with autism. *Int. Immunopharmacol.* 84, 106555. doi:10.1016/j.intimp.2020.106555

Ariza, D., Lima, M. M. S., Moreira, C. G., Dombrowski, P. A., Avila, T. V., Allemand, A., et al. (2010). Intranigral LPS administration produces dopamine, glutathione but not behavioral impairment in comparison to MPTP and 6-OHDA neurotoxin models of Parkinson's disease. *Neurochem. Res.* 35, 1620–1627. doi:10.1007/s11064-010-0222-3

Bae, J. Y., and Park, H. H. (2011). Crystal structure of NALP3 protein pyrin domain (PYD) and its implications in inflammasome assembly. *J. Biol. Chem.* 286, 39528–39536. doi:10.1074/jbc.M111.278812

Balosso, S., Liu, J., Bianchi, M. E., and Vezzani, A. (2014). Disulfide-containing high mobility group box-1 promotes N-Methyl-d-Aspartate receptor function and excitotoxicity by activating toll-like receptor 4-dependent signaling in hippocampal neurons. *Antioxid. Redox Signal.* 21, 1726–1740. doi:10.1089/ars.2013.5349

Banerji, R., Huynh, C., Figueroa, F., Dinday, M. T., Baraban, S. C., and Patel, M. (2021). Enhancing glucose metabolism via gluconeogenesis is therapeutic in a zebrafish model of Dravet syndrome. *Brain Commun.* 3, fcab004. doi:10.1093/braincomms/fcab004

Bao, L., Avshalumov, M. V., Patel, J. C., Lee, C. R., Miller, E. W., Chang, C. J., et al. (2009). Mitochondria are the source of hydrogen peroxide for dynamic brain-cell signaling. *J. Neurosci.* 29, 9002–9010. doi:10.1523/JNEUROSCI.1706-09.2009

Bell, M. T., Puskas, F., Agoston, V. A., Cleveland, J. C., Freeman, K. A., Gamboni, F., et al. (2013). Toll-like receptor 4–dependent microglial activation mediates spinal cord ischemia–reperfusion injury. *Circulation* 128, S152–S156. doi:10.1161/CIRCULATIONAHA.112.000024

Bhowmick, S., D'Mello, V., Caruso, D., and Abdul-Muneer, P. M. (2019). Traumatic brain injury-induced downregulation of Nrf2 activates inflammatory response and apoptotic cell death. *J. Mol. Med.* 97, 1627–1641. doi:10.1007/s00109-019-01851-4

Bhuyan, P., Patel, D. C., Wilcox, K. S., and Patel, M. (2015). Oxidative stress in murine Theiler's virus-induced temporal lobe epilepsy. *Exp. Neurol.* 271, 329–334. doi:10.1016/j.expneurol.2015.06.012

Brennan, A. M., Won Suh, S., Joon Won, S., Narasimhan, P., Kauppinen, T. M., Lee, H., et al. (2009). NADPH oxidase is the primary source of superoxide induced by NMDA receptor activation. *Nat. Neurosci.* 12, 857–863. doi:10.1038/nn.2334

Cabungcal, J.-H., Steullet, P., Morishita, H., Kraftsik, R., Cuenod, M., Hensch, T. K., et al. (2013). Perineuronal nets protect fast-spiking interneurons against oxidative stress. *Proc. Natl. Acad. Sci. U. S. A.* 110, 9130–9135. doi:10.1073/pnas.1300454110

Cai, Y., and Yang, Z. (2021). Ferroptosis and its role in epilepsy. *Front. Cell. Neurosci.* 15, 696889. doi:10.3389/fncel.2021.696889

Cao, H., Zhang, L., Qu, Z., Tian, S., Wang, Z., Jiang, Y., et al. (2021). The protective effect of hydroxylated fullerene pretreatment on pilocarpine-induced status epilepticus. *Brain Res.* 1764, 147468. doi:10.1016/j.brainres.2021.147468

Cao, Y., Li, Y., He, C., Yan, F., Li, J.-R., Xu, H.-Z., et al. (2021). Selective ferroptosis inhibitor liproxstatin-1 attenuates neurological deficits and neuroinflammation after subarachnoid hemorrhage. *Neurosci. Bull.* 37, 535–549. doi:10.1007/s12264-020-00620-5

Caraballo, R. H., Cersósimo, R. O., Sakr, D., Cresta, A., Escobal, N., and Fejerman, N. (2005). Ketogenic diet in patients with Dravet syndrome. *Epilepsia* 46, 1539–1544. doi:10.1111/j.1528-1167.2005.05705.x

Caraballo, R. H., Fortini, S., Fresler, S., Armeno, M., Ariela, A., Cresta, A., et al. (2014). Ketogenic diet in patients with Lennox–Gastaut syndrome. *Seizure* 23, 751–755. doi:10.1016/j.seizure.2014.06.005

Cárdenas-Rodríguez, N., Coballase-Urrutia, E., Pérez-Cruz, C., Montesinos-Correa, H., Rivera-Espinosa, L., Sampieri, A., et al. (2014). Relevance of the glutathione system in temporal lobe epilepsy: Evidence in human and experimental models. *Oxid. Med. Cell. Longev.* 2014, e759293. doi:10.1155/2014/759293

Carrasco-Pozo, C., Tan, K. N., and Borges, K. (2015). Sulforaphane is anticonvulsant and improves mitochondrial function. *J. Neurochem.* 135, 932–942. doi:10.1111/jnc.13361

Cock, H. R., Tong, X., Hargreaves, I. P., Heales, S. J. R., Clark, J. B., Patsalos, P. N., et al. (2002). Mitochondrial dysfunction associated with neuronal death following status epilepticus in rat. *Epilepsy Res.* 48, 157–168. doi:10.1016/S0920-1211(01)00334-5

Cui, Y., Zhang, Y., Zhao, X., Shao, L., Liu, G., Sun, C., et al. (2021). ACSL4 exacerbates ischemic stroke by promoting ferroptosis-induced brain injury and neuroinflammation. *Brain Behav. Immun.* 93, 312–321. doi:10.1016/j.bbi.2021.01.003

Dohi, K., Ohtaki, H., Nakamachi, T., Yofu, S., Satoh, K., Miyamoto, K., et al. (2010). Gp91phox (NOX2) in classically activated microglia exacerbates traumatic brain injury. *J. Neuroinflammation* 7, 41. doi:10.1186/1742-2094-7-41

Doll, D. N., Rellick, S. L., Barr, T. L., Ren, X., and Simpkins, J. W. (2015). Rapid mitochondrial dysfunction mediates TNF-alpha-induced neurotoxicity. *J. Neurochem.* 132, 443–451. doi:10.1111/jnc.13008

Dubey, D., McRae, P. A., Rankin-Gee, E. K., Baranov, E., Wandrey, L., Rogers, S., et al. (2017). Increased metalloproteinase activity in the hippocampus following status epilepticus. *Epilepsy Res.* 132, 50–58. doi:10.1016/j.eplepsyres.2017.02.021

During, M. J., Fried, I., Leone, P., Katz, A., and Spencer, D. D. (1994). Direct measurement of extracellular lactate in the human hippocampus during spontaneous seizures. *J. Neurochem.* 62, 2356–2361. doi:10.1046/j.1471-4159.1994.62062356.x

Dwir, D., Giangreco, B., Xin, L., Tenenbaum, L., Cabungcal, J.-H., Steullet, P., et al. (2020). MMP9/RAGE pathway overactivation mediates redox dysregulation and neuroinflammation, leading to inhibitory/excitatory imbalance: A reverse translation study in schizophrenia patients. *Mol. Psychiatry* 25, 2889–2904. doi:10.1038/s41380-019-0393-5

Epilepsy Syndromes (2022). *EPILEPSY SYNDROMES [WWW document]*. URL: https://www.epilepsydiagnosis.org/syndrome/epilepsy-syndrome-groupoverview.html (accessed 524, 22).

Fernandez-Checa, J. C., Kaplowitz, N., Garcia-Ruiz, C., Colell, A., Miranda, M., Mari, M., et al. (1997). GSH transport in mitochondria: Defense against TNF-induced oxidative stress and alcohol-induced defect. *Am. J. Physiol.* 273, G7–G17. doi:10.1152/ajpgi.1997.273.1.G7

Fleck, J., Ribeiro, M. C. P., Schneider, C. M., Sinhorin, V. D. G., Rubin, M. A., and Mello, C. F. (2004). Intrastriatal malonate administration induces convulsive behaviour in rats. *J. Inherit. Metab. Dis.* 27, 211–219. doi:10.1023/B:BOLI.0000028769.15474.7e

Freeman, L., Guo, H., David, C. N., Brickey, W. J., Jha, S., and Ting, J. P.-Y. (2017). NLR members NLRC4 and NLRP3 mediate sterile inflammasome activation in microglia and astrocytes. *J. Exp. Med.* 214, 1351–1370. doi:10.1084/jem.20150237

Fulton, R. E., Pearson-Smith, J. N., Huynh, C. Q., Fabisiak, T., Liang, L.-P., Aivazidis, S., et al. (2021). Neuron-specific mitochondrial oxidative stress results in epilepsy, glucose dysregulation and a striking astrocyte response. *Neurobiol. Dis.* 158, 105470. doi:10.1016/j.nbd.2021.105470

Gao, H.-M., Zhou, H., Zhang, F., Wilson, B. C., Kam, W., and Hong, J.-S. (2011). HMGB1 acts on microglia Mac1 to mediate chronic neuroinflammation that drives progressive neurodegeneration. *J. Neurosci.* 31, 1081–1092. doi:10.1523/JNEUROSCI.3732-10.2011

Gasche, Y., Copin, J.-C., Sugawara, T., Fujimura, M., and Chan, P. H. (2001). Matrix metalloproteinase inhibition prevents oxidative stress-associated blood–brain barrier disruption after transient focal cerebral ischemia. *J. Cereb. Blood Flow. Metab.* 21, 1393–1400. doi:10.1097/00004647-200112000-00003

Gavillet, M., Allaman, I., and Magistretti, P. J. (2008). Modulation of astrocytic metabolic phenotype by proinflammatory cytokines. *Glia* 56, 975–989. doi:10.1002/glia.20671

Geronzi, U., Lotti, F., and Grosso, S. (2018). Oxidative stress in epilepsy. *Expert Rev. Neurother.* 18, 427–434. doi:10.1080/14737175.2018.1465410

González-Fraguela, M. E., Blanco, L., Fernández, C. I., Lorigados, L., Serrano, T., and Fernández, J. L. (2018). Glutathione depletion: Starting point of brain metabolic stress, neuroinflammation and cognitive impairment in rats. *Brain Res. Bull.* 137, 120–131. doi:10.1016/j.brainresbull.2017.11.015

Guo, Y., Gao, F., Wang, S., Ding, Y., Zhang, H., Wang, J., et al. (2009). *In vivo* mapping of temporospatial changes in glucose utilization in rat brain during epileptogenesis: An 18F-fluorodeoxyglucose–small animal positron emission tomography study. *Neuroscience* 162, 972–979. doi:10.1016/j.neuroscience.2009.05.041

Haorah, J., Ramirez, S. H., Schall, K., Smith, D., Pandya, R., and Persidsky, Y. (2007). Oxidative stress activates protein tyrosine kinase and matrix metalloproteinases leading to blood–brain barrier dysfunction. *J. Neurochem.* 101, 566–576. doi:10.1111/j.1471-4159.2006.04393.x

Helmy, A., De Simoni, M.-G., Guilfoyle, M. R., Carpenter, K. L. H., and Hutchinson, P. J. (2011). Cytokines and innate inflammation in the pathogenesis of human traumatic brain injury. *Prog. Neurobiol.* 95, 352–372. doi:10.1016/j.pneurobio.2011.09.003

Hirano, K., Chen, W. S., Chueng, A. L. W., Dunne, A. A., Seredenina, T., Filippova, A., et al. (2015). Discovery of GSK2795039, a novel small molecule NADPH oxidase 2 inhibitor. *Antioxid. Redox Signal.* 23, 358–374. doi:10.1089/ars.2014.6202

Ho, Y.-H., Lin, Y.-T., Wu, C.-W. J., Chao, Y.-M., Chang, A. Y. W., and Chan, J. Y. H. (2015). Peripheral inflammation increases seizure susceptibility via the induction of neuroinflammation and oxidative stress in the hippocampus. *J. Biomed. Sci.* 22, 46. doi:10.1186/s12929-015-0157-8

Hou, L., Wang, K., Zhang, C., Sun, F., Che, Y., Zhao, X., et al. (2018). Complement receptor 3 mediates NADPH oxidase activation and dopaminergic neurodegeneration through a Src-Erk-dependent pathway. *Redox Biol.* 14, 250–260. doi:10.1016/j.redox.2017.09.017

Huang, W.-Y., Lin, S., Chen, H.-Y., Chen, Y.-P., Chen, T.-Y., Hsu, K.-S., et al. (2018). NADPH oxidases as potential pharmacological targets against increased seizure susceptibility after systemic inflammation. *J. Neuroinflammation* 15, 140. doi:10.1186/s12974-018-1186-5

Ingold, I., Berndt, C., Schmitt, S., Doll, S., Poschmann, G., Buday, K., et al. (2018). Selenium utilization by GPX4 is required to prevent hydroperoxide-induced ferroptosis. *Cell* 172, 409–422. e21. doi:10.1016/j.cell.2017.11.048

Ingvar, M., and Siesjö, B. K. (1983). Local blood flow and glucose consumption in the rat brain during sustained bicuculline-induced seizures. *Acta Neurol. Scand.* 68, 129–144. doi:10.1111/j.1600-0404.1983.tb05339.x

Jarrett, S. G., Liang, L.-P., Hellier, J. L., Staley, K. J., and Patel, M. (2008a). Mitochondrial DNA damage and impaired base excision repair during epileptogenesis. *Neurobiol. Dis.* 30, 130–138. doi:10.1016/j.nbd.2007.12.009

Jarrett, S. G., Milder, J. B., Liang, L.-P., and Patel, M. (2008b). The ketogenic diet increases mitochondrial glutathione levels. *J. Neurochem.* 106, 1044–1051. doi:10.1111/j.1471-4159.2008.05460.x

Kalita, J., Misra, U. K., Singh, L. S., and Tiwari, A. (2019). Oxidative stress in status epilepticus: A clinical-radiological correlation. *Brain Res.* 1704, 85–93. doi:10.1016/j.brainres.2018.09.038

Kaur, H., Patro, I., Tikoo, K., and Sandhir, R. (2015). Curcumin attenuates inflammatory response and cognitive deficits in experimental model of chronic epilepsy. *Neurochem. Int.* 89, 40–50. doi:10.1016/j.neuint.2015.07.009

Kawashima, T., Adachi, T., Tokunaga, Y., Furuta, A., Suzuki, S. O., Doh-ura, K., et al. (1999). Immunohistochemical analysis in a case of idiopathic Lennox-Gastaut syndrome. *Clin. Neuropathol.* 18, 286–292.

Kim, B. H., Roh, E., Lee, H. Y., Lee, I.-J., Ahn, B., Jung, S.-H., et al. (2008). Benzoxathiole derivative blocks lipopolysaccharide-induced nuclear factor-kappaB activation and nuclear factor-kappaB-regulated gene transcription through inactivating inhibitory kappaB kinase beta. *Mol. Pharmacol.* 73, 1309–1318. doi:10.1124/mol.107.041251

Kim, G. W., Kim, H.-J., Cho, K.-J., Kim, H.-W., Cho, Y.-J., and Lee, B. I. (2009). The role of MMP-9 in integrin-mediated hippocampal cell death after pilocarpine-induced status epilepticus. *Neurobiol. Dis.* 36, 169–180. doi:10.1016/j.nbd.2009.07.008

Kim, J.-H., Na, H.-J., Kim, C.-K., Kim, J.-Y., Ha, K.-S., Lee, H., et al. (2008). The non-provitamin A carotenoid, lutein, inhibits NF-kappaB-dependent gene expression through redox-based regulation of the phosphatidylinositol 3-kinase/PTEN/akt and NF-kappaB-inducing kinase pathways: Role of H(2)O(2) in NF-kappaB activation. *Free Radic. Biol. Med.* 45, 885–896. doi:10.1016/j.freeradbiomed.2008.06.019

Kim, J. H., Jang, B. G., Choi, B. Y., Kim, H. S., Sohn, M., Chung, T. N., et al. (2013). Post-treatment of an NADPH oxidase inhibitor prevents seizure-induced neuronal death. *Brain Res.* 1499, 163–172. doi:10.1016/j.brainres.2013.01.007

Kim, Y.-M., Kim, S.-J., Tatsunami, R., Yamamura, H., Fukai, T., and Ushio-Fukai, M. (2017). ROS-induced ROS release orchestrated by Nox4, Nox2, and mitochondria in VEGF signaling and angiogenesis. *Am. J. Physiol. Cell Physiol.* 312, C749–C764. doi:10.1152/ajpcell.00346.2016

Kovac, S., Domijan, A.-M., Walker, M. C., and Abramov, A. Y. (2014). Seizure activity results in calcium- and mitochondria-independent ROS production via NADPH and xanthine oxidase activation. *Cell Death Dis.* 5, e1442. doi:10.1038/cddis.2014.390

Kumar, M. G., Rowley, S., Fulton, R., Dinday, M. T., Baraban, S. C., and Patel, M. (2016). Altered glycolysis and mitochondrial respiration in a zebrafish model of Dravet syndrome. *eNeuro* 3, 1. doi:10.1523/ENEURO.0008-16.2016

Kunz, W. S., Goussakov, I. V., Beck, H., and Elger, C. E. (1999). Altered mitochondrial oxidative phosphorylation in hippocampal slices of kainate-treated rats. *Brain Res.* 826, 236–242. doi:10.1016/s0006-8993(99)01279-2

Kunz, W. S., Kudin, A. P., Vielhaber, S., Blümcke, I., Zuschratter, W., Schramm, J., et al. (2000). Mitochondrial complex I deficiency in the epileptic focus of patients with temporal lobe epilepsy. *Ann. Neurology* 48, 766–773. doi:10.1002/1531-8249(200011)48:5<766:AID-ANA10>3.0.CO;2-M

Lahuerta, M., Gonzalez, D., Aguado, C., Fathinajafabadi, A., García-Giménez, J. L., Moreno-Estellés, M., et al. (2020). Reactive glia-derived neuroinflammation: A novel hallmark in Lafora progressive myoclonus epilepsy that progresses with age. *Mol. Neurobiol.* 57, 1607–1621. doi:10.1007/s12035-019-01842-z

Lee, J., Ahn, H., Hong, E.-J., An, B.-S., Jeung, E.-B., and Lee, G.-S. (2016). Sulforaphane attenuates activation of NLRP3 and NLRC4 inflammasomes but not AIM2 inflammasome. *Cell. Immunol.* 306 (307), 53–60. doi:10.1016/j.cellimm.2016.07.007

Lee, S. H., Choi, B. Y., Kho, A. R., Jeong, J. H., Hong, D. K., Kang, D. H., et al. (2018). Inhibition of NADPH oxidase activation by apocynin rescues seizure-induced reduction of adult hippocampal neurogenesis. *Int. J. Mol. Sci.* 19, 3087. doi:10.3390/ijms19103087

Li, H., Luo, Y.-F., Wang, Y.-S., Yang, Q., Xiao, Y.-L., Cai, H.-R., et al. (2018). Using ROS as a second messenger, NADPH oxidase 2 mediates macrophage senescence via interaction with NF-κB during *Pseudomonas aeruginosa* infection. *Oxid. Med. Cell. Longev.* 2018, e9741838. doi:10.1155/2018/9741838

Li, Q., Spencer, N. Y., Oakley, F. D., Buettner, G. R., and Engelhardt, J. F. (2009). Endosomal Nox2 facilitates redox-dependent induction of NF-kappaB by TNF-alpha. *Antioxid. Redox Signal.* 11, 1249–1263. doi:10.1089/ars.2008.2407

Liang, L.-P., and Patel, M. (2004). Mitochondrial oxidative stress and increased seizure susceptibility in Sod2−/+ mice. *Free Radic. Biol. Med.* 36, 542–554. doi:10.1016/j.freeradbiomed.2003.11.029

Liang, L.-P., Waldbaum, S., Rowley, S., Huang, T.-T., Day, B. J., and Patel, M. (2012). Mitochondrial oxidative stress and epilepsy in SOD2 deficient mice: Attenuation by a lipophilic metalloporphyrin. *Neurobiol. Dis.* 45, 1068–1076. doi:10.1016/j.nbd.2011.12.025

Loewen, J. L., Barker-Haliski, M. L., Dahle, E. J., White, H. S., and Wilcox, K. S. (2016). Neuronal injury, gliosis, and glial proliferation in two models of temporal lobe epilepsy. *J. Neuropathol. Exp. Neurol.* 75, 366–378. doi:10.1093/jnen/nlw008

Lorigados Pedre, L., Gallardo, J. M., Morales Chacón, L. M., Vega García, A., Flores-Mendoza, M., Neri-Gómez, T., et al. (2018). Oxidative stress in patients with drug resistant partial complex seizure. *Behav. Sci.* 8, 59. doi:10.3390/bs8060059

Löscher, W., and Klein, P. (2021). The pharmacology and clinical efficacy of antiseizure medications: From bromide salts to cenobamate and beyond. *CNS Drugs* 35, 935–963. doi:10.1007/s40263-021-00827-8

Ma, M. W., Wang, J., Dhandapani, K. M., Wang, R., and Brann, D. W. (2018). NADPH oxidases in traumatic brain injury – promising therapeutic targets? *Redox Biol.* 16, 285–293. doi:10.1016/j.redox.2018.03.005

Malinska, D., Kulawiak, B., Kudin, A. P., Kovacs, R., Huchzermeyer, C., Kann, O., et al. (2010). Complex III-dependent superoxide production of brain mitochondria contributes to seizure-related ROS formation. *Biochim. Biophys. Acta* 2010, 1163–1170. doi:10.1016/j.bbabio.2010.03.001

Malkov, A., Ivanov, A. I., Buldakova, S., Waseem, T., Popova, I., Zilberter, M., et al. (2018). Seizure-induced reduction in glucose utilization promotes brain hypometabolism during epileptogenesis. *Neurobiol. Dis.* 116, 28–38. doi:10.1016/j.nbd.2018.04.016

Malkov, A., Ivanov, A. I., Latyshkova, A., Bregestovski, P., Zilberter, M., and Zilberter, Y. (2019). Activation of nicotinamide adenine dinucleotide phosphate oxidase is the primary trigger of epileptic seizures in rodent models. *Ann. Neurol.* 85, 907–920. doi:10.1002/ana.25474

Mander, P. K., Jekabsone, A., and Brown, G. C. (2006). Microglia proliferation is regulated by hydrogen peroxide from NADPH oxidase. *J. Immunol.* 176, 1046–1052. doi:10.4049/jimmunol.176.2.1046

Maroso, M., Balosso, S., Ravizza, T., Liu, J., Aronica, E., Iyer, A. M., et al. (2010). Toll-like receptor 4 and high-mobility group box-1 are involved in ictogenesis and can be targeted to reduce seizures. *Nat. Med.* 16, 413–419. doi:10.1038/nm.2127

Martinon, F., Burns, K., and Tschopp, J. (2002). The inflammasome: A molecular platform triggering activation of inflammatory caspases and processing of proIL-beta. *Mol. Cell* 10, 417–426. doi:10.1016/S1097-2765(02)00599-3

McElroy, P. B., Hari, A. S., Day, B. J., and Patel, M. (2017a). Post-translational activation of glutamate cysteine ligase with dimercaprol: A novel mechanism of inhibiting neuroinflammation *in vitro*. *J. Biol. Chem.* 292, 5532–5545. doi:10.1074/jbc.M116.723700

McElroy, P. B., Liang, L.-P., Day, B. J., and Patel, M. (2017b). Scavenging reactive oxygen species inhibits status epilepticus-induced neuroinflammation. *Exp. Neurol.* 298, 13–22. doi:10.1016/j.expneurol.2017.08.009

Mehvari, J., Motlagh, F. G., Najafi, M., Ghazvini, M. R. A., Naeini, A. A., and Zare, M. (2016). Effects of Vitamin E on seizure frequency, electroencephalogram findings, and oxidative stress status of refractory epileptic patients. *Adv. Biomed. Res.* 5, 36. doi:10.4103/2277-9175.178780

Méndez-Armenta, M., Nava-Ruíz, C., Juárez-Rebollar, D., Rodríguez-Martínez, E., and Yescas Gómez, P. (2014). Oxidative stress associated with neuronal apoptosis in experimental models of epilepsy. *Oxid. Med. Cell. Longev.* 2014, e293689. doi:10.1155/2014/293689

Meyer, J. S., Gotoh, F., and Favale, E. (1966). Cerebral metabolism during epileptic seizures in man. *Electroencephalogr. Clin. Neurophysiol.* 21, 10–22. doi:10.1016/0013-4694(66)90054-X

Milder, J. B., Liang, L.-P., and Patel, M. (2010). Acute oxidative stress and systemic Nrf2 activation by the ketogenic diet. *Neurobiol. Dis.* 40, 238–244. doi:10.1016/j.nbd.2010.05.030

Milder, J., and Patel, M. (2012). Modulation of oxidative stress and mitochondrial function by the ketogenic diet. *Epilepsy Res.* 100, 295–303. doi:10.1016/j.eplepsyres.2011.09.021

Mohseni-Moghaddam, P., Roghani, M., Khaleghzadeh-Ahangar, H., Sadr, S. S., and Sala, C. (2021). A literature overview on epilepsy and inflammasome activation. *Brain Res. Bull.* 172, 229–235. doi:10.1016/j.brainresbull.2021.05.001

Newton, R., Kuitert, L. M. E., Bergmann, M., Adcock, I. M., and Barnes, P. J. (1997). Evidence for involvement of NF-kappaB in the transcriptional control of COX-2 gene expression by IL-1beta. *Biochem. Biophys. Res. Commun.* 237, 28–32. doi:10.1006/bbrc.1997.7064

Noh, H., Jeon, J., and Seo, H. (2014). Systemic injection of LPS induces region-specific neuroinflammation and mitochondrial dysfunction in normal mouse brain. *Neurochem. Int.* 69, 35–40. doi:10.1016/j.neuint.2014.02.008

Parsons, A. L. M., Bucknor, E. M. V., Castroflorio, E., Soares, T. R., Oliver, P. L., and Rial, D. (2022). The interconnected mechanisms of oxidative stress and neuroinflammation in epilepsy. *Antioxidants* 11, 157. doi:10.3390/antiox11010157

Patel, M., Li, Q.-Y., Chang, L.-Y., Crapo, J., and Liang, L.-P. (2005). Activation of NADPH oxidase and extracellular superoxide production in seizure-induced hippocampal damage. *J. Neurochem.* 92, 123–131. doi:10.1111/j.1471-4159.2004.02838.x

Patel, M. (2004). Mitochondrial dysfunction and oxidative stress: Cause and consequence of epileptic seizures. *Free Radic. Biol. Med.* 37, 1951–1962. doi:10.1016/j.freeradbiomed.2004.08.021

Paudel, Y. N., Shaikh, Mohd.F., Chakraborti, A., Kumari, Y., Aledo-Serrano, Á., Aleksovska, K., et al. (2018). HMGB1: A common biomarker and potential target for TBI, neuroinflammation, epilepsy, and cognitive dysfunction. *Front. Neurosci.* 12, 628. doi:10.3389/fnins.2018.00628

Pauletti, A., Terrone, G., Shekh-Ahmad, T., Salamone, A., Ravizza, T., Rizzi, M., et al. (2019). Targeting oxidative stress improves disease outcomes in a rat model of acquired epilepsy. *Brain* 142, e39. doi:10.1093/brain/awz130

Pearson, J. N., Rowley, S., Liang, L.-P., White, A. M., Day, B. J., and Patel, M. (2015). Reactive oxygen species mediate cognitive deficits in experimental temporal lobe epilepsy. *Neurobiol. Dis.* 82, 289–297. doi:10.1016/j.nbd.2015.07.005

Pearson, J. N., Warren, E., Liang, L.-P., Roberts, L. J., and Patel, M. (2017). Scavenging of highly reactive gamma-ketoaldehydes attenuates cognitive dysfunction associated with epileptogenesis. *Neurobiol. Dis.* 98, 88–99. doi:10.1016/j.nbd.2016.11.011

Pearson-Smith, J. N., Liang, L.-P., Rowley, S. D., Day, B. J., and Patel, M. (2017). Oxidative stress contributes to status epilepticus associated mortality. *Neurochem. Res.* 42, 2024–2032. doi:10.1007/s11064-017-2273-1

Pearson-Smith, J., and Patel, M. (2017). Metabolic dysfunction and oxidative stress in epilepsy. *Int. J. Mol. Sci.* 18, 2365. doi:10.3390/ijms18112365

Pei, Z., Pang, H., Qian, L., Yang, S., Wang, T., Zhang, W., et al. (2007). MAC1 mediates LPS-induced production of superoxide by microglia: The role of pattern recognition receptors in dopaminergic neurotoxicity. *Glia* 55, 1362–1373. doi:10.1002/glia.20545

Pestana, R. R. F., Kinjo, E. R., Hernandes, M. S., and Britto, L. R. G. (2010). Reactive oxygen species generated by NADPH oxidase are involved in neurodegeneration in the pilocarpine model of temporal lobe epilepsy. *Neurosci. Lett.* 484, 187–191. doi:10.1016/j.neulet.2010.08.049

Poyet, J. L., Srinivasula, S. M., Tnani, M., Razmara, M., Fernandes-Alnemri, T., and Alnemri, E. S. (2001). Identification of Ipaf, a human caspase-1-activating protein related to Apaf-1. *J. Biol. Chem.* 276, 28309–28313. doi:10.1074/jbc.C100250200

Quintana, A., Kruse, S. E., Kapur, R. P., Sanz, E., and Palmiter, R. D. (2010). Complex I deficiency due to loss of Ndufs4 in the brain results in progressive encephalopathy resembling Leigh syndrome. *Proc. Natl. Acad. Sci. U. S. A.* 107, 10996–11001. doi:10.1073/pnas.1006214107

Rankin-Gee, E. K., McRae, P. A., Baranov, E., Rogers, S., Wandrey, L., and Porter, B. E. (2015). Perineuronal net degradation in epilepsy. *Epilepsia* 56, 1124–1133. doi:10.1111/epi.13026

Rowley, S., Liang, L.-P., Fulton, R., Shimizu, T., Day, B., and Patel, M. (2015). Mitochondrial respiration deficits driven by reactive oxygen species in experimental temporal lobe epilepsy. *Neurobiol. Dis.* 75, 151–158. doi:10.1016/j.nbd.2014.12.025

Rumià, J., Marmol, F., Sanchez, J., Giménez-Crouseilles, J., Carreño, M., Bargalló, N., et al. (2013). Oxidative stress markers in the neocortex of drug-resistant epilepsy patients submitted to epilepsy surgery. *Epilepsy Res.* 107, 75–81. doi:10.1016/j.eplepsyres.2013.08.020

Ryan, K., Backos, D. S., Reigan, P., and Patel, M. (2012). Post-translational oxidative modification and inactivation of mitochondrial complex I in epileptogenesis. *J. Neurosci.* 32, 11250–11258. doi:10.1523/JNEUROSCI.0907-12.2012

Salar, S., and Galanopoulou, A. S. (2018). "Chapter 5 - neuroinflammation in the pathogenesis of early life epileptic encephalopathies," in *Acute encephalopathy and encephalitis in infancy and its related disorders*. Editors H. Yamanouchi, S. L. Moshé, and A. Okumura (Elsevier), 33–44. doi:10.1016/B978-0-323-53088-0.00005-1

Samidurai, M., Tarale, P., Janarthanam, C., Estrada, C. G., Gordon, R., Zenitsky, G., et al. (2020). Tumor necrosis factor-like weak inducer of apoptosis (TWEAK) enhances activation of STAT3/NLRC4 inflammasome signaling Axis through PKCδ in astrocytes: Implications for Parkinson's disease. *Cells* 9, 1831. doi:10.3390/cells9081831

Sandouka, S., and Shekh-Ahmad, T. (2021). Induction of the Nrf2 pathway by sulforaphane is neuroprotective in a rat temporal lobe epilepsy model. *Antioxidants* 10, 1702. doi:10.3390/antiox10111702

Scheffer, I. E., Berkovic, S., Capovilla, G., Connolly, M. B., French, J., Guilhoto, L., et al. (2017). ILAE classification of the epilepsies: Position paper of the ILAE commission for classification and terminology. *Epilepsia* 58, 512–521. doi:10.1111/epi.13709

Schiavone, S., Neri, M., Trabace, L., and Turillazzi, E. (2017). The NADPH oxidase NOX2 mediates loss of parvalbumin interneurons in traumatic brain injury: Human autoptic immunohistochemical evidence. *Sci. Rep.* 7, 8752. doi:10.1038/s41598-017-09202-4

Shekh-Ahmad, T., Eckel, R., Dayalan Naidu, S., Higgins, M., Yamamoto, M., Dinkova-Kostova, A. T., et al. (2018). KEAP1 inhibition is neuroprotective and suppresses the development of epilepsy. *Brain* 141, 1390–1403. doi:10.1093/brain/awy071

Shekh-Ahmad, T., Lieb, A., Kovac, S., Gola, L., Christian Wigley, W., Abramov, A. Y., et al. (2019). Combination antioxidant therapy prevents epileptogenesis and modifies chronic epilepsy. *Redox Biol.* 26, 101278. doi:10.1016/j.redox.2019.101278

Shin, E.-J., Suh, S. K., Lim, Y. K., Jhoo, W.-K., Hjelle, O. P., Ottersen, O. P., et al. (2005). Ascorbate attenuates trimethyltin-induced oxidative burden and neuronal degeneration in the rat hippocampus by maintaining glutathione homeostasis. *Neuroscience* 133, 715–727. doi:10.1016/j.neuroscience.2005.02.030

Subramanian, N., Natarajan, K., Clatworthy, M. R., Wang, Z., and Germain, R. N. (2013). The adaptor MAVS promotes NLRP3 mitochondrial localization and inflammasome activation. *Cell* 153, 348–361. doi:10.1016/j.cell.2013.02.054

Sul, O.-J., and Ra, S. W. (2021). Quercetin prevents LPS-induced oxidative stress and inflammation by modulating NOX2/ROS/NF-kB in lung epithelial cells. *Molecules* 26, 6949. doi:10.3390/molecules26226949

Tawfik, M. K. (2011). Coenzyme Q10 enhances the anticonvulsant effect of phenytoin in pilocarpine-induced seizures in rats and ameliorates phenytoin-induced cognitive impairment and oxidative stress. *Epilepsy Behav.* 22, 671–677. doi:10.1016/j.yebeh.2011.09.018

Terrone, G., Frigerio, F., Balosso, S., Ravizza, T., and Vezzani, A. (2019). Inflammation and reactive oxygen species in status epilepticus: Biomarkers and implications for therapy. *Epilepsy Behav.* 101, 106275. doi:10.1016/j.yebeh.2019.04.028

Tiraboschi, E., Martina, S., van der Ent, W., Grzyb, K., Gawel, K., Cordero-Maldonado, M. L., et al. (2020). New insights into the early mechanisms of epileptogenesis in a zebrafish model of Dravet syndrome. *Epilepsia* 61, 549–560. doi:10.1111/epi.16456

Uddin, Md.S., Mamun, A. A., Jakaria, Md., Thangapandiyan, S., Ahmad, J., Rahman, Md.A., et al. (2020). Emerging promise of sulforaphane-mediated Nrf2 signaling cascade against neurological disorders. *Sci. Total Environ.* 707, 135624. doi:10.1016/j.scitotenv.2019.135624

Valassina, N., Brusco, S., Salamone, A., Serra, L., Luoni, M., Giannelli, S., et al. (2022). Scn1a gene reactivation after symptom onset rescues pathological phenotypes in a mouse model of Dravet syndrome. *Nat. Commun.* 13, 161. doi:10.1038/s41467-021-27837-w

Van Vliet, E. A., Aronica, E., and Gorter, J. A. (2015). Blood–brain barrier dysfunction, seizures and epilepsy. *Semin. Cell Dev. Biol.* 38, 26–34. doi:10.1016/j.semcdb.2014.10.003

Vezzani, A., Balosso, S., and Ravizza, T. (2019). Neuroinflammatory pathways as treatment targets and biomarkers in epilepsy. *Nat. Rev. Neurol.* 15, 459–472. doi:10.1038/s41582-019-0217-x

Vezzani, A., Balosso, S., and Ravizza, T. (2008). The role of cytokines in the pathophysiology of epilepsy. *Brain Behav. Immun.* 22, 797–803. doi:10.1016/j.bbi.2008.03.009

Wang, J., Ma, M. W., Dhandapani, K. M., and Brann, D. W. (2018). NADPH oxidase 2 deletion enhances neurogenesis following traumatic brain injury. *Free Radic. Biol. Med.* 123, 62–71. doi:10.1016/j.freeradbiomed.2018.05.069

Wang, W., Wu, Y., Zhang, G., Fang, H., Wang, H., Zang, H., et al. (2014). Activation of Nrf2-ARE signal pathway protects the brain from damage induced by epileptic seizure. *Brain Res.* 1544, 54–61. doi:10.1016/j.brainres.2013.12.004

Wijburg, F. A., Barth, P. G., Bindoff, L. A., Birch-Machin, M. A., Blij, J. F. V. D., Ruitenbeek, W., et al. (1992). Leigh syndrome associated with a deficiency of the pyruvate dehydrogenase complex: Results of treatment with a ketogenic diet. *Neuropediatrics* 23, 147–152. doi:10.1055/s-2008-1071331

Williams, S., Hamil, N., Abramov, A. Y., Walker, M. C., and Kovac, S. (2015). Status epilepticus results in persistent overproduction of reactive oxygen species, inhibition of which is neuroprotective. *Neuroscience* 303, 160–165. doi:10.1016/j.neuroscience.2015.07.005

Wojtala, A., Karkucinska-Wieckowska, A., Sardao, V. A., Szczepanowska, J., Kowalski, P., Pronicki, M., et al. (2017). Modulation of mitochondrial dysfunction-related oxidative stress in fibroblasts of patients with Leigh syndrome by inhibition of prooxidative p66Shc pathway. *Mitochondrion* 37, 62–79. doi:10.1016/j.mito.2017.07.002

Wu, S.-B., Ma, Y.-S., Wu, Y.-T., Chen, Y.-C., and Wei, Y.-H. (2010). Mitochondrial DNA mutation-elicited oxidative stress, oxidative damage, and altered gene expression in cultured cells of patients with MERRF syndrome. *Mol. Neurobiol.* 41, 256–266. doi:10.1007/s12035-010-8123-7

Yamanaka, G., Takamatsu, T., Morichi, S., Yamazaki, T., Mizoguchi, I., Ohno, K., et al. (2021). Interleukin-1β in peripheral monocytes is associated with seizure frequency in pediatric drug-resistant epilepsy. *J. Neuroimmunol.* 352, 577475. doi:10.1016/j.jneuroim.2021.577475

Yang, C.-C., Lin, C.-C., Jou, M.-J., Hsiao, L.-D., and Yang, C.-M. (2019). RTA 408 inhibits interleukin-1β-induced MMP-9 expression via suppressing protein kinase-dependent NF-κB and AP-1 activation in rat brain astrocytes. *Int. J. Mol. Sci.* 20, 2826. doi:10.3390/ijms20112826

Yang, C.-M., Hsieh, H.-L., Yu, P.-H., Lin, C.-C., and Liu, S.-W. (2015). IL-1β induces MMP-9-dependent brain astrocytic migration via transactivation of PDGF receptor/NADPH oxidase 2-derived reactive oxygen species signals. *Mol. Neurobiol.* 52, 303–317. doi:10.1007/s12035-014-8838-y

Yang, H., Lundbäck, P., Ottosson, L., Erlandsson-Harris, H., Venereau, E., Bianchi, M. E., et al. (2021). Redox modifications of cysteine residues regulate the cytokine activity of HMGB1. *Mol. Med.* 27, 58. doi:10.1186/s10020-021-00307-1

Yang, N., Guan, Q.-W., Chen, F.-H., Xia, Q.-X., Yin, X.-X., Zhou, H.-H., et al. (2020). Antioxidants targeting mitochondrial oxidative stress: Promising neuroprotectants for epilepsy. *Oxid. Med. Cell. Longev.* 2020, e6687185. doi:10.1155/2020/6687185

You, S. J., Kim, H. D., and Kang, H.-C. (2009). Factors influencing the evolution of west syndrome to lennox-gastaut syndrome. *Pediatr. Neurol.* 41, 111–113. doi:10.1016/j.pediatrneurol.2009.03.006

Youm, Y.-H., Nguyen, K. Y., Grant, R. W., Goldberg, E. L., Bodogai, M., Kim, D., et al. (2015). The ketone metabolite β-hydroxybutyrate blocks NLRP3 inflammasome–mediated inflammatory disease. *Nat. Med.* 21, 263–269. doi:10.1038/nm.3804

Zhou, R., Yazdi, A. S., Menu, P., and Tschopp, J. (2011). A role for mitochondria in NLRP3 inflammasome activation. *Nature* 469, 221–225. doi:10.1038/nature09663

Zilberter, Y., Popova, I., and Zilberter, M. (2022). Unifying mechanism behind the onset of acquired epilepsy. *Trends Pharmacol. Sci.* 43, 87–96. doi:10.1016/j.tips.2021.11.009

frontiers | Frontiers in Cell and Developmental Biology

TYPE Original Research
PUBLISHED 13 September 2022
DOI 10.3389/fcell.2022.969364

OPEN ACCESS

EDITED BY
Jianxiong Jiang,
University of Tennessee Health Science Center (UTHSC), United States

REVIEWED BY
Xiaoming Jin,
Indiana University–Purdue University Indianapolis, United States
Yunfei Huang,
Albany Medical College, United States

*CORRESPONDENCE
Sookyong Koh,
skoh@childrensomaha.org

†These authors have contributed equally to this work

SPECIALTY SECTION
This article was submitted to Signaling, a section of the journal Frontiers in Cell and Developmental Biology

RECEIVED 14 June 2022
ACCEPTED 03 August 2022
PUBLISHED 13 September 2022

CITATION
Erisken S, Nune G, Chung H, Kang JW and Koh S (2022), Time and age dependent regulation of neuroinflammation in a rat model of mesial temporal lobe epilepsy: Correlation with human data. *Front. Cell Dev. Biol.* 10:969364. doi: 10.3389/fcell.2022.969364

Time and age dependent regulation of neuroinflammation in a rat model of mesial temporal lobe epilepsy: Correlation with human data

Sinem Erisken[1,2†], George Nune[1,3†], Hyokwon Chung[1,4], Joon Won Kang[4,5] and Sookyong Koh[1,4*]

[1]Department of Pediatrics, Stanley Manne Children's Research Institute, Ann & Robert H. Lurie Children's Hospital of Chicago, Northwestern University School of Medicine, Chicago, IL, United States, [2]Department of Biomedical Engineering, McCormick School of Engineering, Northwestern University, Evanston, IL, United States, [3]Department of Neurology, University of Southern California, Los Angeles, CA, United States, [4]Department of Pediatrics, Children's Hospital & Medical Center, University of Nebraska, Omaha, NE, United States, [5]Department of Pediatrics & Medical Science, Brain Research Institute, College of Medicine, Chungnam National University, Daejeon, South Korea

Acute brain insults trigger diverse cellular and signaling responses and often precipitate epilepsy. The cellular, molecular and signaling events relevant to the emergence of the epileptic brain, however, remain poorly understood. These multiplex structural and functional alterations tend also to be opposing - some homeostatic and reparative while others disruptive; some associated with growth and proliferation while others, with cell death. To differentiate pathological from protective consequences, we compared seizure-induced changes in gene expression hours and days following kainic acid (KA)-induced status epilepticus (SE) in postnatal day (P) 30 and P15 rats by capitalizing on age-dependent differential physiologic responses to KA-SE; only mature rats, not immature rats, have been shown to develop spontaneous recurrent seizures after KA-SE. To correlate gene expression profiles in epileptic rats with epilepsy patients and demonstrate the clinical relevance of our findings, we performed gene analysis on four patient samples obtained from temporal lobectomy and compared to four control brains from NICHD Brain Bank. Pro-inflammatory gene expressions were at higher magnitudes and more sustained in P30. The inflammatory response was driven by the cytokines IL-1β, IL-6, and IL-18 in the acute period up to 72 h and by IL-18 in the subacute period through the 10-day time point. In addition, a panoply of other immune system genes was upregulated, including chemokines, glia markers and adhesion molecules. Genes associated with the mitogen activated protein kinase (MAPK) pathways comprised the largest functional group identified. Through the integration of multiple ontological databases, we analyzed genes belonging to 13 separate pathways linked to Classical MAPK ERK, as well as stress activated protein kinases (SAPKs) p38 and JNK. Interestingly, genes belonging to the Classical MAPK pathways were mostly transiently activated within the first 24 h, while genes in the SAPK pathways had divergent time courses of expression, showing sustained activation only in P30. Genes in P30 also had different

regulatory functions than in P15: P30 animals showed marked increases in positive regulators of transcription, of signaling pathways as well as of MAPKKK cascades. Many of the same inflammation-related genes as in epileptic rats were significantly upregulated in human hippocampus, higher than in lateral temporal neocortex. They included glia-associated genes, cytokines, chemokines and adhesion molecules and MAPK pathway genes. Uniquely expressed in human hippocampus were adaptive immune system genes including immune receptors CDs and MHC II HLAs. In the brain, many immune molecules have additional roles in synaptic plasticity and the promotion of neurite outgrowth. We propose that persistent changes in inflammatory gene expression after SE leads not only to structural damage but also to aberrant synaptogenesis that may lead to epileptogenesis. Furthermore, the sustained pattern of inflammatory genes upregulated in the epileptic mature brain was distinct from that of the immature brain that show transient changes and are resistant to cell death and neuropathologic changes. Our data suggest that the epileptogenic process may be a result of failed cellular signaling mechanisms, where insults overwhelm the system beyond a homeostatic threshold.

KEYWORDS

epileptogenesis, inflammation, gene expression, microarray, status epilepticus, MAPK, glia

1 Introduction

Epileptogenesis is a theoretical construct whereby concerted cascades of molecular, cellular and network changes precipitate spontaneous recurrent seizures, or epilepsy. Etiology is known for roughly half of diagnosed epilepsies; these symptomatic or acquired epilepsies are often triggered by brain injury (Hauser and Hesdorffer, 1990; Hauser, 1997; Engel, 2006). Up to 53% of patients who experience severe traumatic brain injury (TBI) and between 2% and 5% of patients who experience ischemic stroke will develop epilepsy (Salazar et al., 1985; Menon and Shorvon, 2009). Additionally, epilepsy develops in up to 43% of patients who experience refractory status epilepticus (SE), a prolonged seizure lasting over 30 min (Hesdorffer et al., 1998). Once seizures begin, epilepsy can worsen over time and are frequently accompanied by declining cognitive function (Engel and International League Against Epilepsy, 2001; Briellmann et al., 2002; Sayin et al., 2004; Thompson and Duncan, 2005; Engel, 2006).

Mesial temporal lobe epilepsy (MTLE) is the most common type of focal epilepsy and is often resistant to currently available pharmacotherapy (Loscher, 2002). One of the primary identified risk factors for developing MTLE in adulthood is prolonged febrile seizures in childhood (Baulac et al., 2004). The pathologic process that occurs between the initial insult and the development of frank epilepsy is of great interest in designing therapeutic strategies to prevent epileptogenesis.

A number of hippocampal changes have been proposed to lead to epileptogenesis. One of the classic neuropathologic changes is mossy fiber sprouting from dentate granule cells (Blumcke et al., 1999). Many of these fibers display an aberrant growth pattern that leads them back into the inner molecular layer of the dentate gyrus instead of the CA3 area of the hippocampus, forming recurrent excitatory loops (Tauck and Nadler, 1985; Sutula et al., 1989; Babb et al., 1991). MTLE also displays a specific pattern of neuronal loss in the hippocampal subfields and a dense gliosis that has led to the description of this pathologic pattern as hippocampal sclerosis (Blumcke et al., 2007). In animal models, excitatory interneurons in the dentate gyrus seem to be particularly vulnerable to cell death (Sloviter, 1987). These neurons normally project onto inhibitory interneurons and their loss may therefore lead to decreased inhibition. Furthermore, seizure activity in animal models leads to increased mitotic activity, producing new dentate granule cells which may become abnormally integrated into neuronal circuit (Parent et al., 1997; Scharfman et al., 2000). On a molecular level, there are also changes in the expression and components of different receptors, such as γ-aminobutyric acid A (GABAA) (Brooks-Kayal et al., 1998).

The systemic administration of kainic acid (KA), a glutamate agonist, is frequently used in animal models of MTLE. KA leads to prolonged seizures, status epilepticus, and to the generation of spontaneous seizures after a latent period. These seizures originate from the hippocampus in a similar manner to MTLE (Tremblay et al., 1984). Seizure activity has been shown to alter the expression of a variety of genes for neurotransmitters, ion channels, receptors, transcription factors, intracellular messengers, inflammatory mediators, and neurotrophic factors (Jamali et al., 2006). These changes in gene expression may lead to the pathologic phenomena observed in

MTLE. In order to link neuronal activity during seizures with the long-term changes which lead to epilepsy, focus has been primarily on the mechanisms of synaptic plasticity and inflammation.

An increasing amount of evidence indicates that seizures result in activation of the inflammatory responses (Oprica et al., 2003; Vezzani and Granata, 2005). Recent work implicates innate as well as adaptive immunity in the generation of this inflammatory responses (Ravizza et al., 2008). Seizures cause marked glial activation similar to that proposed to contribute to the neuronal damage observed in Alzheimer's disease (Mrak and Griffin, 2005). The neuroinflammation seen in response to seizures may result in cell death as well as more subtle changes that lead to epileptogenesis. The KA model of MTLE elicits multi-faceted immune responses. KA-induced status epilepticus (KA-SE) causes prolonged astrocyte activation and a microglial activation of shorter duration (Somera-Molina et al., 2007). A strong pattern of astrogliosis has also been classically demonstrated in human MTLE, while animal models show a variety of functional changes in astrocytes (Binder and Steinhauser, 2006). Seizures seems to affect the expression of a wide variety of inflammatory cytokines, particularly IL-1β, chemokines, adhesion molecules, extracellular proteinases, complement components, immune receptors, heat shock proteins, and other immune regulatory molecules (De Simoni et al., 2000; van Gassen et al., 2008).

Reflecting the wide range of functional and anatomical changes observed during epileptogenesis, numerous studies examining the gene expression profiles in epilepsy and its models have previously identified an overwhelming array of transcriptional changes (Jamali et al., 2006; Lukasiuk et al., 2006; Wang et al., 2010; Dixit et al., 2016; Pfisterer et al., 2020). Alongside mechanisms of inflammation and synaptic plasticity, some of these studies have drawn attention to mitogen activated protein kinase (MAPK) activity and MAPK signaling pathways (Okamoto et al., 2010; Hansen et al., 2014; Dixit et al., 2016; Salman et al., 2017; Kalozoumi et al., 2018; Fu et al., 2020; Bencurova et al., 2021). These ubiquitous and highly conserved molecules have evolved to transduce environmental and developmental signals into a wide range of programmed and adaptive cellular responses (Zhang et al., 2002; Arthur and Ley, 2013; Peti and Page, 2013). As MAPK pathways transduce extracellular signals into cellular modifications by means of transcriptional (Whitmarsh, 2007), translational (Kelleher et al., 2004) and epigenetic control (Suganuma and Workman, 2012), misregulation could ostensibly underlie maladaptive cellular responses observed during epileptogenesis.

Our first goal was to identify main categories of genes and their important constituents that contribute to the inflammatory responses in an experimental model of MTLE. By comparing the gene expression profile in tissue samples of human brain removed for intractable MTLE with that of the KA rat model of the disease, we aimed to demonstrate a similar pathologic process and highlight the relevance of animal data to human disease. Second, we aimed to elucidate the temporal pattern of immune gene expression following KA-SE in rats at P15 and P30. While both P15 and P30 animals experience acute SE in response to KA injection, only the P30 animals develop spontaneous recurrent seizures. P15 animals show no cell death and no spontaneous recurrent seizures while P30 animals develop chronic epileptic state (Albala et al., 1984; Stafstrom et al., 1992; Williams et al., 2009; Mlsna & Koh, 2013). Studying the age-dependent changes following KA-SE, therefore, offers a strategy for understanding pathogenesis of epilepsy. By comparing time and age-dependent gene expression in P15 and P30 rats, we sought to differentiate pathological from protective consequences of KA-SE and gain insight into the process of epileptogenesis. Third, we investigated the time course for the expression of various functional groups of genes concentrating on pathway interactions and the implications for pathogenesis of epilepsy. Additionally, we confirmed the validity of microarray gene profiling results by real-time (quantitative) reverse transcriptase polymerase chain reaction (qRT-PCR) and immunohistochemistry and assessed the translational significance of our findings through microarray analysis and qRT-PCR of hippocampal tissue collected from patients diagnosed with MTLE.

2 Materials and methods

2.1 Seizure induction

Intraperitoneal (IP) injections of KA dissolved in phosphate-buffered saline (PBS) were administered to P15 (3 mg/kg) and P30 (10 mg/kg) Long-Evans male rats (Wilson et al., 2005). Age-specific doses of KA have been determined previously to result in <25% mortality while inducing acute seizures in >60% of animals. Control littermates received equal IP volume of PBS. Only animals with nearly continuous seizures for more than 30 min (KA-SE) were included in the study. P15 is considered roughly equivalent to human infancy/early childhood (Romijn et al., 1991; Avishai-Eliner et al., 2002; Haut et al., 2004; Baek et al., 2016). Likewise, P30 animals were chosen because their response to KA injection is adult-like with neuronal injury and the occurrence of spontaneous seizures. However, P30 might be more accurately considered pubescence rather than adulthood (Nitecka et al., 1984; Stafstrom et al., 1992).

2.2 Selection of patients and controls

From our database of surgical pathology samples, we identified four patients who received surgical treatment for MTLE between January 2006 and February 2008 at Children's Memorial Hospital and Northwestern Memorial Hospital in

TABLE 1 Clinical information of temporal lobe epilepsy cases.

Patient ID	Tissue analyzed	Sex	Age at operation (years)	Age of seizure onset (years)	History of febrile seizures	Family history of epilepsy
A14	Neocortex	F	9	7	Yes	No
A16	Neocortex, Hipp	F	68	42	Yes	Yes—2 children
A17	Neocortex, Hipp	M	39	7	No	No
A21	Neocortex, Hipp	M	34	1.5	No	Yes—Maternal uncle

ID, identification; Hipp, hippocampus.

TABLE 2 Clinical information of control cases.

Patient ID	Age at death (years)	Sex	Cause of death	Post-mortem interval (hours)
C1	15	F	Chest injuries—MVA	5
C2	13	M	Asphyxia	5
C3	8	M	Cardiac arrythmia	6
C4	32	F	Seroquel/alcohol intoxication	5

ID, identification; MVA, motor vehicle accident.

Chicago (Table 1). These patients all had intractable seizures despite best medical therapy. Seizure semiology consisted of focal impaired awareness seizures and bilateral secondarily generalized tonic-clonic seizures. The diagnosis of MTLE was confirmed by neuropathology and all patients received a full pre-operative workup including magnetic resonance imaging (MRI), electroencephalogram (EEG) or video EEG, and neuropsychiatry testing. Tissue samples of the hippocampus and temporal lobe neocortex were extracted from the anterior temporal lobectomy surgical specimens. The sample from one patient did not contain enough hippocampal tissue for qRT-PCR, leaving only three hippocampal tissues.

The control group was selected based on cause of death and post-mortem interval (Table 2). The cause of death in all cases was an acute, non-infectious, extracranial process. In order to ensure good ribonucleic acid (RNA) quality, we used tissue only from subjects with post-mortem intervals less than 10 h. Four control tissue samples were obtained from the National Institute of Child Health and Human Development (NICHD) Brain and Tissue Bank for Developmental Disorders at the University of Maryland, Baltimore. Tissues were collected and prepared according to the protocols described on the NICHD Brain and Tissue Bank website.

2.3 Hippocampal dissection and preparation of RNA

Rats were sacrificed at 1, 6, 24, 72, and 240 h after seizure induction (n = 12/time point per age group). Animals were deeply anesthetized with isoflurane, decapitated, and the brains were removed. Both hippocampi from each animal were rapidly dissected, frozen in isopentane cooled with dry ice, and stored at −80°C. Individual hippocampal tissues (0.15–0.2 g) were homogenized in Trizol reagent® (Invitrogen, Carlsbad, CA, United States) using a glass homogenizer (Wheaton Industries, Millville, NJ, United States), and total RNA was isolated following the manufacturer's protocol. RNA concentration and purity was determined spectrophotometrically by Gene QuantPro® (Amersham Biosciences GE, Piscataway, NJ, United States). For microarray analysis, equimolar quantities of RNAs were pooled from four animals for each sample. Individual RNA sample for qRT-PCR was treated with RNase-free DNase I (Roche Diagnostics, Indianapolis, IN, United States) for 20 min at room temperature, followed by inactivation for 10 min at 75°C. All of the RNA samples for microarray and qRT-PCR were further purified using RNA Easy Kit (Qiagen, Valencia, CA, United States), according to the manufacturer's instructions, in order to remove any remaining genomic DNA and salts.

Human samples were collected intra-operatively. The hippocampus and temporal neocortex were immediately dissected and frozen in isopentane cooled with dry ice. RNA was extracted and prepared using the same technique described above with the sole difference that RNA for microarray studies consisted of samples from individual patients rather than pooled RNA from several animals. For each MTLE patient, temporal neocortex and hippocampal samples were processed separately.

2.4 Microarray analysis

For the rat microarray experiments, we used the RG34A high-density oligonucleotide Affymetrix Genechip arrays. Three independent hybridizations were performed per condition: Control, KA; 1, 6, 24, 72, and 240 h; P15, P30, total of 60 profiles. Preparation of cRNA, array hybridization, and scanning were performed by Microarray Consortium (NINDS/NIMH) at TGEN (Phoenix, AZ). Affymetrix Microarray Suite (v. 5.0) was used for probe-level analysis. The analysis relies on the interpretation of probe set hybridization performance (pairs of 16 perfect match and mismatch 25-mer oligonucleotides per probe set) as a measure of whether signal intensities are significantly above background and specific to the gene of interest. A signal value is produced that represents the relative level of expression of a transcript. Additionally, the detection algorithm uses probe pair intensities and assigns a present, marginal, or absent call, after comparing with a predefined threshold.

We included in our data analysis only those probe sets that were present in at least two out of three samples in either control or KA. In each time point, the selected genes are >4,000 out of 8,799. This stringent threshold effectively eliminated genes with low precision or those with expression levels too close to the background. We used GeneSpring (v. 5.03) for normalizing data, selecting genes for fold change and performing statistical group comparison between control and KA to generate the p value. We also used Significance Analysis of Microarrays (SAM v. 1.21, Stanford University) for additional statistical analysis, which generates a q value that reflects the false discovery rate (Storey and Tibshirani, 2003). Select genes are considered significant if $p < 0.05$ and $q < 0.05$ in at least one time point.

For the human microarray experiments, we used the Human Genome U133 Plus 2.0 Array. For each patient, individual hybridizations were performed for each tissue type, hippocampus and temporal neocortex. Three hippocampal MTLE tissues, four temporal cortex MTLE tissues, and four control neocortical tissues were analyzed. The preparation of cRNA, array hybridization, and scanning were performed by the Microarray Consortium at TGEN as described above.

The same probe-level analysis was applied to human data. However, due to the fact that human arrays contain more probe sets and that more sensitive algorithm was used for detecting lower signal intensities, we included in our data analysis only those probe sets that were present in all samples. Still, more than 20,000 probe sets (out of 54,675) passed the criteria in each comparison against control. The genes were selected both by fold change (1.5) and by t-test ($p < 0.05$).

2.5 Real time reverse transcriptase polymerase chain reaction

qRT-PCR was used for validation of both rat and human microarray results. The levels of gene expression of 84 inflammatory factors and MAPK related genes [including MAPK kinase (MAPKK) and MAP kinase kinase (MKK)], five housekeeping genes, three positive controls, and three reverse transcription controls were measured using the RT2Profiler™PCRArray (SuperArray Bioscience Corp., Frederick, MD, United States). In addition to genes related to the MAPK signaling pathway, this array profiles the expression of transcription factors, Raf regulating proteins, MEK kinase 1 (MEKK1) interacting proteins, cell cycle proteins regulated by the extracellular-signal regulated kinase (ERK) 1/2 pathway, and genes whose expression is induced by MAPK.

RT2Profiler™PCRArray is a qRT-PCR based and performed in a 96-well plate. The RNA samples from animals and patients were placed into individual RT2Profiler™PCRArrays. First, 1 μg of each RNA sample was converted to first strand cDNAs using the RT2 First Strand Kit following the manufacturer's user manual. The cDNA was added to the RT2 qPCR Master Mixes containing SYBR Green. The mixtures were aliquoted into 96-well plate containing pretreated gene specific primer sets. The PCR reactions were performed using ABI Prism 7,500 system (Applied Biosystems, Foster City, CA, United States) with the following parameters; cycle 1 (1 repeat), 10 min at 95°C; and cycle 2 (40 repeats), 15 s at 95°C and followed by 1 min at 60°C, and the data were collected at 60°C.

The cycle threshold values (CT) for genes of interest were first normalized to that of housekeeping genes, β-actin and/or GAPDH, in the same sample and expressed as percentage of controls. This normalized Ct (ΔCt) was used to compare control vs. treated samples (ΔΔCt), which is then expressed as fold change of gene amplification. The Student's t-test (unpaired) was used with the standard significance level of $p < 0.05$. Analysis was performed using GraphPad Prism 4 (GraphPad Software, LaJolla, CA, United States).

2.6 Database integration and classification of genes

Several gene ontology databases were used to investigate the functional importance of differentially expressed genes. Functional analysis was performed in Mathematica 6.0.1 and Mathematica 7.0.0 (Wolfram Research, Champaign, IL, United States) using pattern matching capabilities and nine online databases: Affymetrix NetAffxTM at www.affymetrix.com/analysis/index.affx (Liu et al., 2003), GeneCards—human only at www.genecards.org (Safran et al., 2002; Stelzer et al., 2008), NCBI Entrez Gene at http://www.ncbi.nlm.nih.gov/gene/

(Maglott et al., 2005), KEGG pathway at http://www.genome.jp/kegg/pathway.html (Kanehisa et al., 2002), Gene Ontology at http://www.geneontology.org/ (Ashburner et al., 2000), AmiGO at http://amigo.geneontology.org/cgi-bin/amigo/go.cgi, the Rat Genome Database at http://rgd.mcw.edu/ (Twigger et al., 2007), Panther at http://www.pantherdb.org/ (Thomas et al., 2003), and the Pathway Interactions Database at http://pid.nci.nih.gov/ (Schaefer et al., 2009).

After retrieving the database information, Mathematica was used to create a composite functional and pathway-related database for significantly expressed genes and their aliases. Human gene aliases and homologues were identified primarily using GeneCards and secondarily using the Rat Genome Database and NCBI Entrez Gene. Mathematica's pattern matching capabilities were then used to identify functional and pathway groupings of the genes involved.

The composite database was created with code that searched through various database files by gene name and alias and integrated all unique ontological descriptions for each gene across databases. Important functional and pathway ontologies were identified by two consecutive methods: first, consistently reappearing ontological terms were identified and the occurrence of each ontological term in the composite database was then counted. Functional and pathway-related gene groupings were then created with code that searched through the ontological descriptions by user-defined key words (i.e. "inflammation," "inflammatory response").

The gene expression data analyzed through GeneSpring and SAM was then transferred into Mathematica. Mathematica then reorganized the data by group (P15, P30, Controls), gene name, time-point of expression, and functionality. Programming code also generated line graphs and tables to reflect the data. Line graphs of gene expression levels were fitted using second order interpolation for ease of visualization.

2.7 Pathway analysis

Initial results and data analysis pointed to a significant role of MAPKs in KA-SE. Consequently, pathways involving MAPK genes were analyzed from several perspectives. MAPK pathways have been described as continuously variable switches dependent on various factors with multiple upstream and downstream pathways feeding into the primary MAPKs: ERK, p38 and Jun N-terminal kinase (JNK). A single gene may be implicated in multiple pathways, therefore one association may not be more "correct" than the other. We picked our pathways in the spirit of "modular biology" (Hartwell et al., 1999; Bruggeman et al., 2002; Ingolia and Murray, 2007), still acknowledging that canonical representations of discrete and linear signaling transduction systems may not be suitable models, especially in response to highly deleterious stimuli.

We analyzed MAPK related cascades into 13 component pathways: ERK, Growth Factor Signaling, Ras/Rab, p38, Rho/Rac/Cdc42, JNK, p53, TGF-β, TNF-α, JAK/STAT, Wnt, NF-κB, and PI3K/AKT. Although genes differentially expressed in P15 or P30 were annotated with numerous pathways, only pathways with uniquely expressed genes were selected. Each gene was assigned a pathway set—i.e., according to the databases, a gene was associated with the regulation and/or transduction of one or more of the 13 component pathways. Single-pathway associated genes were organized and analyzed separately from multiple-pathway associated genes. Genes classified as transcription factors and/or co-factors or transcriptional regulators were analyzed as well. Finally, genes associated with regulation of pathways, MAPKKKs, phosphatase, and kinase activity were identified and analyzed.

2.8 Immunohistochemistry

Immunohistochemistry was performed on horizontal sections of rat brain using antibodies to CD74 or Hsp70 (DAKO, Glostrup, Denmark). Sections were mounted on premium microscope slides (Fisher Scientific, Pittsburgh, PA), fixed in paraformaldehyde and incubated with anti-CD74 or anti-Hsp70 at 4°C overnight, followed by a biotinylated secondary anti-IgG, using a previously published method (Koh et al., 1999). The sections were then treated with HRP-conjugated streptavidin. Specimens were then examined under light microscopy.

3 Results

3.1 Higher magnitude and longer duration of gene expression in response to KA-SE at P30

A total of 517 genes were differentially expressed (>2-fold change, $p < 0.05$, $q > 0.05$ or <0.5-fold change, $p < 0.05$, $q > 0.05$) in P15 ($n = 198$) and P30 ($n = 454$) hippocampi at 1, 6, 24, 72 and 240 h after seizure induction compared to PBS injected control littermates (Figure 1A). More genes were differentially expressed at higher magnitudes in P30 compared P15 (Figure 1B); 135 genes were commonly expressed in P15 and P30 (Figure 1C). Differential gene expression remained below 50-fold change in P15 while it exceeded 100-fold in P30. By 72 h, only three genes (S100a4, Ccnc, Kcna4) were above baseline in P15, while marked gene upregulation persisted in P30 ($n = 48$, 72 h; $n = 43$, 240 h) throughout the 10 days. At each time point, more genes were upregulated in P30 ($n = 57$, 1 h; $n = 155$, 6 h; $n = 196$, 24 h; $n = 48$, 72 h; $n = 43$, 240 h) than P15 ($n = 31$, 1 h; $n = 99$, 6 h; $n = 92$, 24 h; $n = 3$, 72 h).

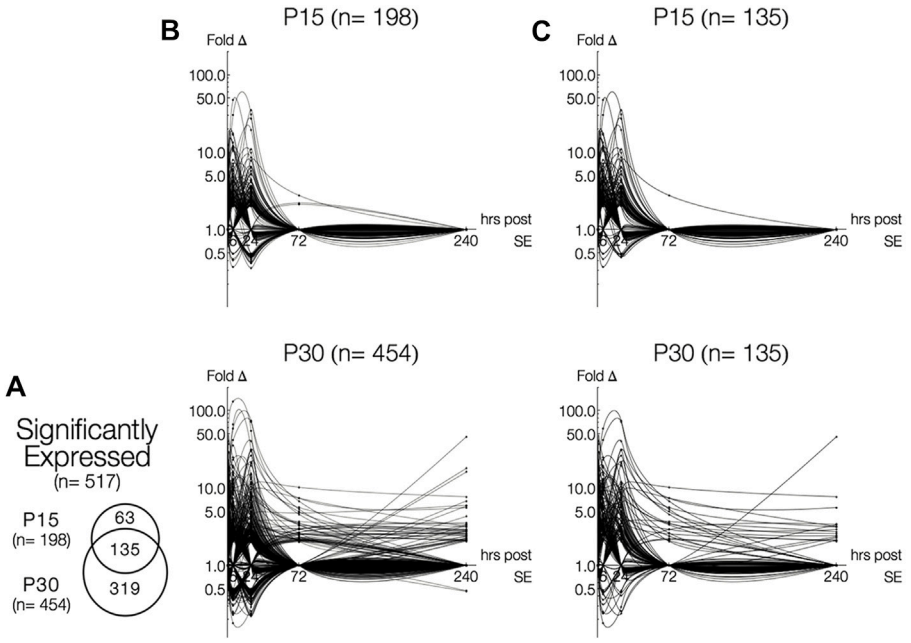

FIGURE 1
Time-and age-dependent gene regulation in rat hippocampus after KA-SE. **(A)** Venn Diagrams of all differentially expressed genes (fold change > 2, $p < 0.05$, $q < 0.05$). While majority of genes (135/198, 68%) in P15 are also expressed in P30, many genes (319/454, 70%) are expressed only in P30. **(B)** Log-linear plots of differential gene expression (fold change) of all significant genes 1–240 h after KA. Data points are indicated by black circles. Lines, each representing a single gene, were fitted using second order interpolation for ease of visualization. **(C)** Log-linear plots of differential gene expression of common genes between P15 and P30.

Although many genes were upregulated at only a single time point in both age groups ($n = 118$, P15; $n = 186$, P30), more genes were upregulated for a longer time in P30 compared to P15. In P15, only five genes have extended time-courses of upregulation: Ania-2, Ania-4, Bdnf and Nptx2 were upregulated 1–24 h, and S100a4 was upregulated at 24 and 72 h. In P30, 41 genes were upregulated for an extended time (3 or more time points) and 28 genes were upregulated at both 24 and 72 h. Remarkably, Mt2a, Hspb1, Lgals3, Lox, and Spp1 are all upregulated 6–240 h.

A similar pattern was observed in downregulated genes ($n = 31$, P15; $n = 137$, P30). In P15, downregulation took place only at 6 ($n = 6$) and 24 h ($n = 25$), while downregulation in P30 occurred at 1, 6, 24, and 240 h ($n = 4$, 1 h; $n = 71$, 6 h; $n = 71$, 24 h; $n = 2$, 240 h). In P15, all genes were downregulated for only a single time point. For P30 animals, nine genes (Adra1d, Dbp, Dcn, Gucy1a, Hnmt, Htr5b, Kit, Neurod1, Pk1b) were downregulated at 6 and 24 h.

3.2 Microarray findings of inflammatory response

Figure 2A compares fold change in expression between the microarray and quantitative RT-PCR results among a few representative genes in rats at P30. The relative expression levels between the various genes are preserved between microarray and RT-PCR. Similarly, Figure 2B compares fold changes in expression for a selected group of genes between the same two methods of amplification. Gene expression is shown for both temporal neocortex and hippocampal tissues. Fold changes were often higher in the qRT-PCR than in microarray, likely reflecting a greater linear dynamic range afforded by qRT-PCR. Marked differences in fold change between microarray and RT-PCR may also be due to sampling differences. Each value in microarray represents an average of 12 animals (pooled RNAs from four animals, three independent hybridizations) whereas only an individual sample was run in qRT-PCR (RNA samples were not pooled).

Figure 2C shows all genes significantly upregulated in the P30 animals at 10 days after KA-SE. A large proportion of upregulated genes at this time point are inflammatory in nature and many of these are expressed at high levels, highlighting the importance of the immune response in the brain's response to seizures.

In order to compare the seizure-induced inflammatory response in P15 with that of P30, all inflammatory genes were graphed over time (Figure 2D). Many more genes are upregulated to significant levels in P30 compared to P15. Furthermore, P30 also shows more prolonged and higher levels of expression of inflammatory genes.

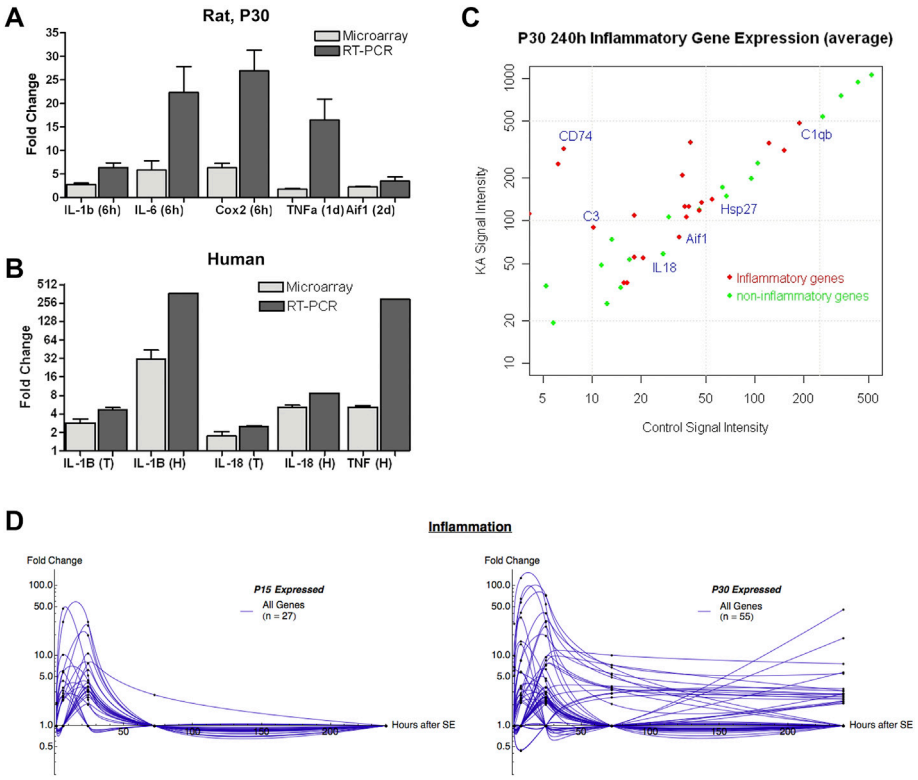

FIGURE 2
Time- and age-dependent expression of inflammatory genes after KA-SE: qRT-PCR validation and human data correlation. **(A)** Fold change in expression in select inflammatory genes: comparison between the microarray and qRT-PCR results in rats at P30. **(B)** Fold change in expression in select inflammatory genes: comparison between the microarray and quantitative RT-PCR results in human. T, temporal lobe; H, hippocampus. **(C)** Inflammatory genes comprised a significant proportion of persistently upregulated genes at 240 h after KA-SE in P30. Red dots represent inflammatory genes. Green dots represent non-inflammatory genes. **(D)** Summary graph of the time course of fold change in inflammatory genes. Note the inflammatory genes remain significantly elevated at 240 h only in P30 rats.

3.3 Time and age dependent regulation of inflammatory markers

3.3.1 Microglial and astrocyte activation

To understand the differential pattern of activation among different CNS cell types, we focused our attention to cell-specific markers (Figure 3A). GFAP and vimentin are intermediate filaments that have traditionally been used to investigate astrocyte activation (Eng and Ghirnikar, 1994). The S100 group of proteins bind calcium and are involved in a large number of cellular functions. S100B is classically used as an astrocyte marker but S100a4 has been found to be involved in cellular migration and is upregulated specifically in white matter astrocytes after CNS injury (Kozlova and Lukanidin, 2002). We found that astrocyte activation in P30 rats peaked at 24 h after KA-SE and remained elevated through the 10-day time point. In contrast, P15 rats have lower levels of astrocyte activation at all time points and the upregulation of astrocyte markers was largely complete by 72 h.

Aif-1 is a marker of microglial activation, which is upregulated in response to CNS injury (Schwab et al., 2001). Osteopontin (Spp-1) is secreted by a subpopulation of activated microglia in response to a variety of insults, including stroke and systemic KA administration (Ellison et al., 1998; Kim et al., 2002). In the P15 animals, Spp-1 expression is only significantly upregulated at the 24 h time point, while Aif-1 is not significantly upregulated at any time point. In the P30 animals, Spp-1 upregulation peaks at 24 h after KA-SE but is significantly upregulated from 6 to 240 h. Aif-1 upregulation in P30 animals is delayed, with increased expression only at 72 and 240 h.

3.3.2 Cytokines and eicosanoid pathways

Cytokine genes are significantly elevated only in the P30 animals (Figure 3B). IL-1β and IL-6 gene expression are increased at 6 h after KA-SE. The IL-18 gene is upregulated in a biphasic manner, with significant increase at 24 and 240 h after KA-SE. Lipopolysaccharide-induced TNF factor, LITAF, is a transcription factor for TNF-α. It is upregulated to modest

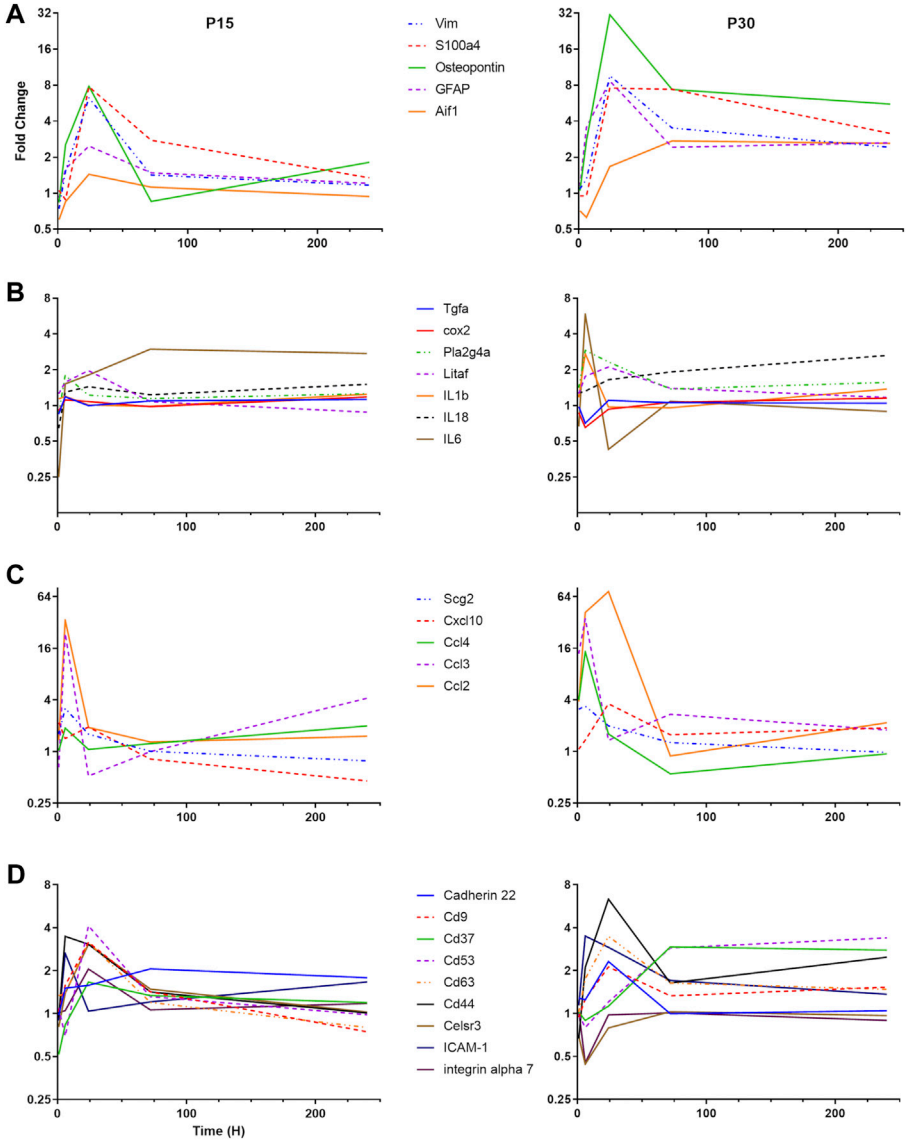

FIGURE 3
Differential time course of various groups of inflammatory genes in P15 and P30. **(A)** Microglial and astrocyte markers (Aif1, GFAP, Osteopontin, S100a4, and VIM). **(B)** Cytokines and eicosanoid pathways (IL-1β, IL-6, IL-18, LITAF, TGF-β R1, TNF R1, PLA2G4A, and COX2). **(C)** Chemokines (CCL2, CCL3, CCL4, CXCL10, and Scg2). **(D)** Adhesion molecules (Cadherin 22, CD9, CD37, CD 53, CD63, CD44, Celsr3, ICAM-1, and Integrin α7).

levels at 24 h. The TNF receptor type 1 and the TGF-β receptor type 1 are also upregulated to modest levels in the P30 animals at 24 h after KA-SE.

Eicosanoid production begins with the conversion of phospholipids or diacylglycerol into arachidonic acid by Phospholipase A2. Downstream, COX-2 catalyzes the conversion of arachidonic acid into an intermediate, which results in the production of Prostacyclin, Thromboxane A2 and a variety of prostaglandins. We saw upregulation of PLA2G4A, a cytosolic phospholipase A2 isozyme, at 6 and 24 h only in P30 rats. However, COX2 is upregulated in both P15 and P30 animals. In the P15 group, COX2 expression is increased 1 and 6 h after KA-SE while in the P30 group, COX2 expression is of higher intensity and longer duration, peaking at 1 h but persisting through 24 h.

3.3.3 Chemokines

There was a dramatic upregulation of chemokine expression in both P15 and P30 (Figure 3C). In P15 rats, Ccl2 is only significantly upregulated at the 6 and 24 h time points, peaking at 6 h. However, in P30 rats it is upregulated at all but 240 h, peaking at 24 h. Cxcl10, Ccl3 and Ccl4 are upregulated in the

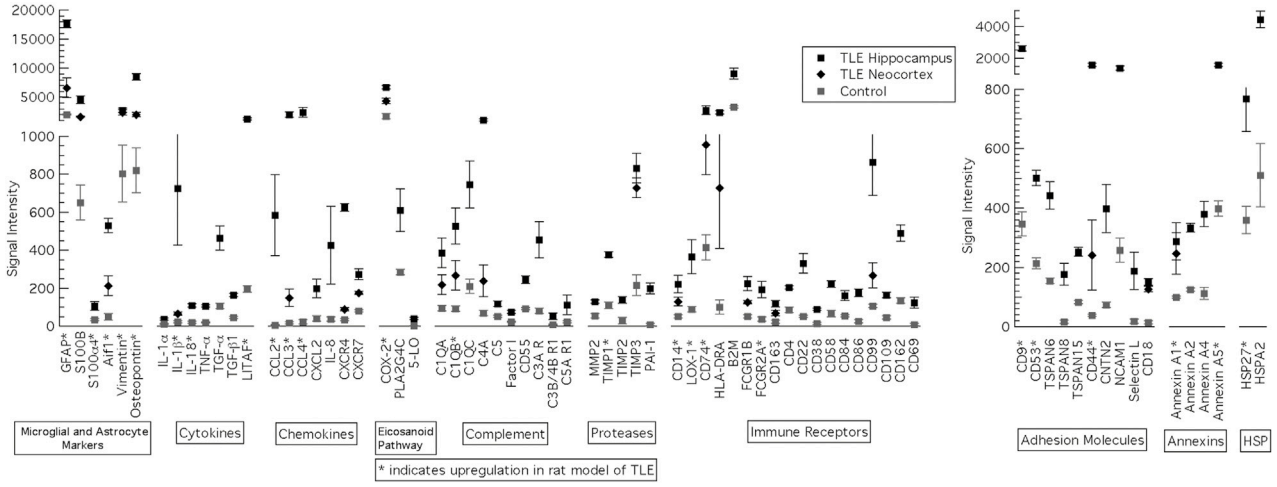

FIGURE 4
Genes significantly upregulated in the hippocampus and lateral temporal neocortex of patients with MTLE. Inflammatory genes were classified into 10 groups: microglia and astrocyte markers, Cytokines, Chemokines, Eicsanoid Pathway, Complement, Proteases, Immune Receptors, Adhesion Molecules, Annexins and heat shock proteins (HSP). *Genes also upregulated in the rat KA model of MTLE. Reproduced with the permission from the author (SK), J Child Neurology 2018. vol 33 (1) 64–72.

P30 animals at 6 h after KA-SE. The product of the gene Scg2 is a neuropeptide which can be modified to produce secretoneurin. Scg2 is upregulated only at 6 h after KA-SE in P15 animals, while in P30 animals Scg2 is upregulated at both 1 and 6 h.

3.3.4 Adhesion molecules

The tetraspanins are a large family of scaffolding membrane proteins that function in cell adhesion, motility, activation, and proliferation (Figure 3D). This group includes CD9, CD37, CD53, and CD63. In P15 rats, the tetraspanins CD9, CD53, and CD63 are upregulated at 24 h. P30 animals also show an increase in the expression of CD9 and CD62 at 24 h after KA-SE followed by a late upregulation of CD37 and CD53 at 72 and 240 h after KA-SE.

Cadherin 22, an adhesion molecule which is primarily expressed in brain tissue, is only upregulated in the P30 group at 24 h. Celsr3 is a seven-pass transmembrane cadherin primarily involved in neuron-neuron adhesion and the inhibition of neurite outgrowth (Shima et al., 2007). This molecule, along with integrin α7, show an interesting pattern of expression. They are upregulated at 24 h in P15 animals while downregulated at 6 h after KA-SE in the P30 group.

Other adhesion molecules are also known to function in leukocyte recruitment and extravasation. ICAM-1 is transiently expressed in the P15 group only at 6 h. However, in the P30 group, ICAM-1 showed a prolonged upregulation, reaching significance at 6 and 24 h. CD44 expression is increased to significant levels in both P15 and P30 animals at the 6 and 24 h time points but it reaches much higher levels of expression in P30 animals at 24 h after KA-SE.

3.4 Mesial temporal lobe epilepsy in humans

Several genes were significantly upregulated in the hippocampus and lateral temporal neocortex of patients with MTLE (Figure 4). Many of the same genes are upregulated in the KA-SE rat model of MTLE and hippocampal tissue from patients with MTLE. With the exception of HSPs, the human hippocampus data generally includes a larger number of significantly upregulated genes than the rats within each category. A particularly glaring difference between our human and rat data is the upregulation of a large number of genes involved in the activation of the adaptive immune system only in MTLE patients. This includes immune receptors such as CD4, CD22, CD38, CD58, CD69, CD84, CD86, CD99, CD109, and CD162. Of note, only HLA-DRA is graphed as a member of the MHC II group of gene but we also find significant upregulation of HLA-DQA1/2, HLA-DPA1, HLA-DPB1, HLA-G, HLA-DOA, HLA-C, HLA-DMB, HLA-DRB1/3/4, HLA-DMA, HLA-B, and HLA-A. A smaller subset of genes from each category is also upregulated in the lateral temporal neocortex in addition to the hippocampus. In all these cases, expression in the neocortex was lower than in the hippocampus.

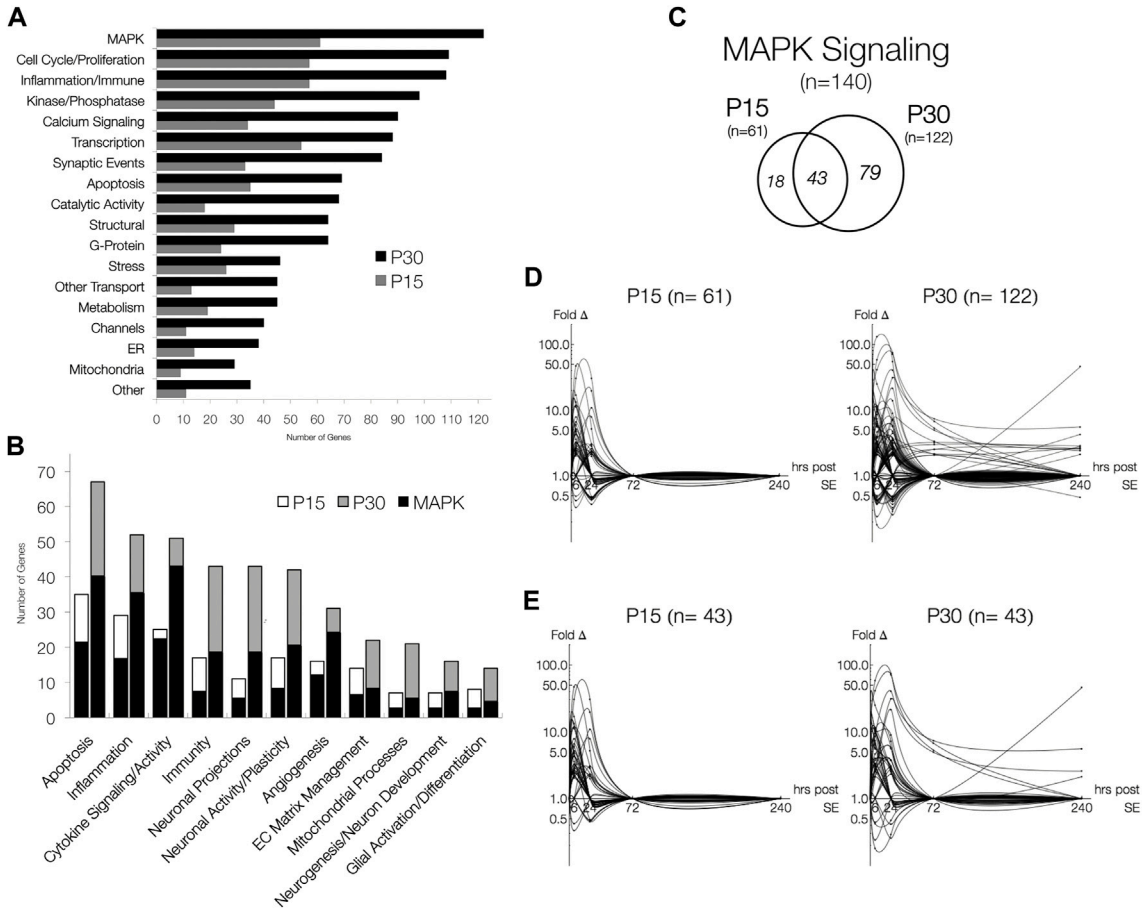

FIGURE 5
Functional Distribution of Differentially Expressed Genes and MAPK Signaling pathway, the most abundant functional groups. **(A)** Genes involved in processes associated with the latent period and MAPK signaling. Genes were categorized in agreement with databases. **(B)** The number of genes associated with MAPK signaling in P15 and P30 animals across all time points. Significantly expressed genes are more numerous in P30 than in P15, but relative MAPK co-categorization is comparable. MAPK overlaps most with cytokine signaling/activity (24/25, P15; 46/51, P30) and least with mitochondrial processes (3/7, P15; 6/21, P30) and glial activation/differentiation (3/8, P15; 5/14, P30). **(C)** Venn Diagrams of differentially expressed genes belonging to MAPK Signaling (fold change > 2, $p < 0.05$, $q < 0.05$). While majority (70.5%) of genes in P15 are also expressed in P30, most (64.8%) genes are only expressed in P30. **(D)** Log-linear plots of differential gene expression (fold change) of MAPK genes 1–240 h after KA-SE. Data points are indicated by black circles. Lines, each representing a single gene, were fitted using second order interpolation for ease of visualization. **(E)** Log-linear plots of differential gene expression (fold change) of common MAPK genes between P15 and P30.

3.5 Functional distribution of differentially expressed genes and MAPK signaling pathway: The most abundant functional groups

After database integration (see Section 2.6), we performed an inclusive ontological survey of all differentially expressed genes in both age groups across all 5 times points (Figure 5A). MAPK signaling (n = 61, P15; n = 122, P30), comprising a total of 140 differentially expressed genes, was the largest functional group identified. The next largest groups of genes differentially expressed are associated with inflammation, immune responses (n = 57, P15; n = 108, P30), and cell cycle and proliferation (n = 57, P15; n = 109, P30). Genes related to transcription (n = 54, P15; n = 88, P30), synaptic events (n = 33, P15; n = 84, P30), calcium signaling (n = 34, P15; n = 90, P30) and apoptosis (n = 35, P15; n = 69, P30), were also differentially expressed in both P15 and P30 animals. Although none of these groups are as large in MAPK, they have all been previously implicated as potential epileptogenic alterations (Pitkanen et al., 2007; Pitkanen et al., 2009).

We next investigated the overlap between MAPK signaling and putative epileptogenic events such as inflammation, neuronal activity, and glial activation. Within functionally relevant genes, we identified those associated with MAPK signaling (Figure 5B). Although all groups identified are present in both P15 and P30, P30 differentially expressed more genes across all functional groups. Many genes

associated with each process are also involved in MAPK signaling.

Figure 5C summarizes the number of genes associated with MAPK signaling in P15 and P30 animals across all time points. Again, more genes were differentially expressed at higher magnitudes for longer time courses after KA in P30 compared to P15 (Figure 5D). All MAPK genes returned to baseline by 72 h in P15 while they remained upregulated ($n = 13$, 72 h; $n = 10$, 240 h) in P30. MAPK genes differentially expressed in both age groups ($n = 43$) were expressed at higher magnitudes over longer time courses in P30 (Figure 5E). Notable examples included: Ccl2 (peak = 47.2 fc, 6 h), Timp1 (peak = 30.6 fc, 24 h), Spp1 (peak = 7.8 fc, 24 h), and Hspb1 (peak = 40.4 fc, 24 h) were all upregulated only at 6 and 24 h in P15 animals. In P30, however, Ccl2 (peak = 74.0 fc, 24 h) and Timp1 (peak = 71.4 fc, 24 h) were upregulated 1–72 h, and Spp1 (peak = 31.0 fc, 24 h) and Hspb1 (peak = 41.3 fc, 24 h) were upregulated 6–240 h. Similarly, Ret (2.88 fc, 6 h) and Cd74 (10.85 fc, 24 h) were both upregulated at single time points in P15, while in P30, Ret (peak = 5.68 fc, 6 h) was upregulated at 6, 24 and 240 h and Cd74 (peak = 45.6 fc, 240 h) was upregulated at 24 and 240 h.

The age-dependent nature of our study introduced a risk that our results were confounded by developmental differences. To account for this possibility, we compared the gene expression profiles of P30 controls (treated with PBS instead of KA) with P15 controls (see Section 2.4). 117 genes were differentially expressed between age groups (fold change >2, $p < 0.05$, $q < 0.05$) 1–24 h after PBS injection; 35 of these genes were also differentially expressed in either P15 or P30 at 1, 6, 24, 72 or 240 h after KA-SE (data not shown). Amongst the 117 genes differentially expressed between PBS injected P15 and P30, 23 were associated with MAPK signaling. Only 9 of the 23 MAPK genes differentially expressed between P15 and P30 controls were also differentially expressed in response to KA-SE in either P15 or P30. This is in stark contrast to the 140 genes differentially expressed in P15 or P30 after KA-SE.

To investigate how baseline differences in gene expression may affect gene expression after seizure induction, we examined the relative abundance of mRNA for these 9 genes in P15 and P30 controls and compared them to seizure-induced changes in expression in P15 and P30 (Table 3). Changes in gene expression in response to seizure were diverse in both age groups and independent of baseline differences in relative mRNA signal. This suggested that differences in changes observed in MAPK gene expression profiles between P15 and P30 (after KA-SE) were age-dependent differences in seizure response rather than an artifact of development.

3.6 Pathway-based distribution of differentially expressed MAPK genes

Genes are annotated in online databases by pathways as well as functions such as "apoptosis." Annotations include both pathways (e.g. "p53 signaling pathway") as well as regulatory schemes (e.g. "positive regulation of I-κB kinase/NF-κB cascade").

Many pathways were associated with the differentially expressed genes found in our study. For simplicity, we reduced MAPK signaling networks into 13 pathways: ERK, Growth Factor Signaling, Ras/Rab, p38, Rho/Cdc42/Rac, JNK, p53, TGF-β, TNF-α, JAK/STAT, Wnt, NF-κB, and PI3K/AKT. These 13 were chosen according to a single criterion: each pathway contained least one unique gene differentially expressed in P15 or P30 after KA-SE (see Section 2.7). Reduction of MAPK signaling into 13 component pathways excluded 6 genes which were not annotated with any specific pathway in the databases. 5 of these genes were differentially expressed in P15 and 5 were differentially expressed in P30. Although these 6 genes were expressed differently in P15 and P30, additional inclusion of these genes (data not shown) did not affect the overall patterns of the data presented below.

A total of 134 genes in P15 ($n = 56$) or P30 ($n = 117$) are annotated with the 13 pathways, and 80 of these genes ($n = 33$, P15; $n = 69$, P30) are annotated with only a single pathway. Even though single-pathway annotated genes constitute the majority of the genes expressed in P15 and P30, the majority of genes annotated within a given pathway (in P15 and P30) are annotated with multiple pathways (Table 4).

Although cellular signaling pathways are traditionally characterized as discrete and separate, the vast amount of crosstalk among them makes separation into causal relationships difficult. Whether crosstalk between pathways is the rule or the exception still remains unclear. Furthermore, an emerging idea of signaling pathways comprising a network, which together is responsible for cellular decisions, is starting to eclipse the prior understanding of discrete, linear, and separate pathways. Against this backdrop, we examined different kinds of associations and considered single-pathway annotated and multiple-pathway annotated genes separately.

3.7 Single-pathway associated genes

The most studied MAPK families are ERK, p38 and JNK (Morrison, 2012). While these MAPKs respond to a variety of stimuli and there is a considerable amount of crosstalk between them (Shen et al., 2003; Fey et al., 2012), they initiate exquisitely specific cellular responses and have traditionally been split between the classical (the first discovered) MAPK ERK and the stress activated protein kinases (SAPKs), p38 and JNK. With regard to epileptogenesis, ERK has been associated with synaptic remodeling and plasticity while p38 and JNK tend to be associated with immune and inflammatory responses (Gautam et al., 2021). It should be noted that these delineations are oversimplifications and cellular responses may often involve concerted action across interacting pathways (Liu, 2011;

TABLE 3 Relative baselines of mRNA signal and qualitative changes in gene expression amongst MAPK genes differentially expressed between P15 and P30 controls and differentially expressed in P15 or P30 after kainic acid induced status epilepticus (KA-SE).

Gene	Phosphate-buffered saline	Kainic acid	
	Relative mRNA signal	P15	P30
Bdnf	P15 > P30	Upregulated	Upregulated
Hmgcr	P15 > P30	Upregulated	Upregulated
Gadd45a	P15 > P30	Upregulated	Upregulated
Prkaa2	P15 > P30	Downregulated	
Fkbp1b	P15 > P30		Downregulated
Cat	P15 > P30		Downregulated
Camk2a	P30 > P15		Downregulated
Itpr1	P30 > P15		Downregulated
Pdk1	P30 > P15	Upregulated	

RNA, ribonucleic acid; MAPK, mitogen-activated protein kinase; BDNF, brain-derived neurotrophic factor; HMGCR, 3-hydroxy-3-methylglutaryl-CoA reductase; GADD45A, growth arrest and DNA damage inducible α; PRKAA2, protein kinase AMP-activated catalytic subunit α2; FKBP1B, FKBP prolyl isomerase 1B; CAT, catalase; CAMK2A, calcium/calmodulin dependent protein kinase IIα; ITPR1, inositol 1,4,5-trisphosphate receptor type 1; PDK1, pyruvate dehydrogenase kinases 1; P, postnatal.

TABLE 4 Thirteen representative pathways for differentially expressed genes in P15 and P30 after KA-SE.

Pathway	P15		P30	
	All genes	Single pathway	All genes	Single pathway
ERK 1/2	9	3	14	5
Growth Factor	18	9	25	9
Ras/Rab	10	3	19	5
P38	12	1	19	5
Rho/Cdc42/Rac	4	0	11	4
JNK	8	0	16	3
P53	12	3	25	5
TGF-β	17	3	23	6
TNF-α	0	0	8	4
NF-κB	13	5	20	8
Wnt	6	2	22	5
JAK/STAT	5	3	10	5
PI3K/AKT	5	1	13	5

P, postnatal; ERK, extracellular signal-regulated kinase; JNK, Jun NH_2-terminal kinase; TGF-β, transforming growth factor-β; TNF-α, tumor necrosis factor α; NF-κB, Nuclear factor kappa B; JAK/STAT, janus kinase-signal transducer and activator of transcription; PI3K, phosphoinositide 3-kinases.

Kyriakis and Avruch, 2012; Gautam et al., 2021). Stress related pathways had a different distribution in P15: there were no TNF-α annotated genes and almost no single-pathway annotated genes for p38, JNK, and Rho/Cdc42/Rac (Table 4). To investigate this further, we grouped the single-pathway annotated genes based on their MAPK families: Classical (ERK1/2, Growth Factor, Ras/Rab), SAPK (p38, Rho/Cdc42/Rac, JNK, p53, TGF-β, TNF-α), and Other (NF-κB, Wnt, JAK/STAT, PI3K/AKT).

There were more single-pathway annotated genes within the Classical ($n = 15$) or Other ($n = 11$) families than SAPK ($n = 7$) in P15 animals. This was in contrast to P30, where more SAPK genes ($n = 27$) were expressed than either Classical ($n = 19$) or Other ($n = 23$) families. Among genes differentially expressed in both P15 and P30, there were less SAPK ($n = 4$) genes differentially than Classical ($n = 11$) or Other ($n = 7$).

Figure 6 plots the single-pathway annotated gene expression profiles of P15 (left column) and P30 (right column) by Classical, SAPK, and Other family groupings. To discriminate between 1 and 6 h, time is presented in log scale. Genes differentially expressed in both age groups are traced in gray, while genes solely in P15 are traced in blue and in P30 traced in red. More genes were differentially expressed at more time points with higher

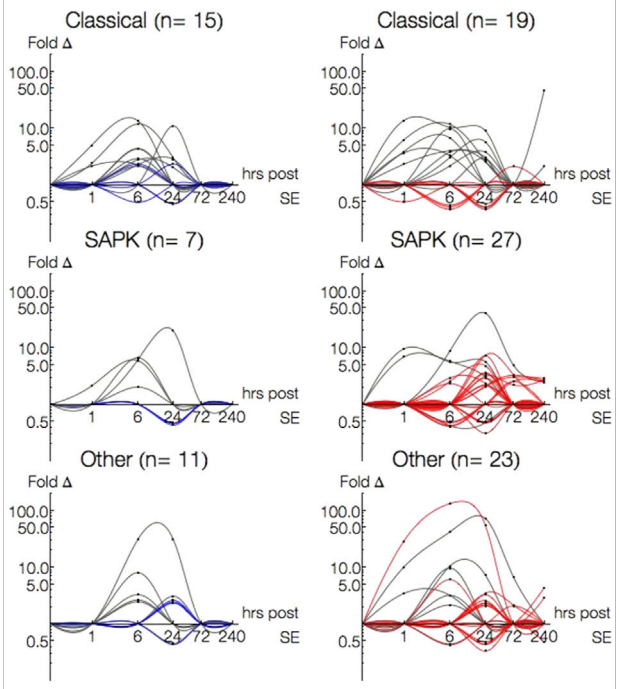

FIGURE 6
Log-Log plots of differential gene expression (fold change) of single-pathway associated genes amongst Classical, SAPK and Other family groupings. Data points are indicated by black circles. Lines, each representing a single gene, were fitted using second order interpolation for ease of visualization. Genes differentially expressed in both P15 (left column) and P30 (right column) are indicated in gray; Genes differentially expressed only in P15 are blue and only in P30 are red.

magnitudes in P30 than P15 across all three family groupings. This difference was most striking amongst Other families. In P15 animals, Classical (Cyr62, Bdnf, Rasl11b) and SAPK (Ptgs2) began to be activated 1 h after KA-SE and all genes returned to baseline by 72 h, while Other genes were differentially expressed at 6 and 24 h alone.

Classical, SAPK and Other were all differentially expressed 1–240 h in P30 animals. Most Classical genes were upregulated within 24 h (n = 5, 1 h; n = 9, 6 h; n = 7, 24 h) and most SAPK genes were upregulated 24 h and beyond (n = 15, 24 h; n = 7, 72 h; n = 5, 240 h). Additionally, most Classical genes upregulated within 24 h in P30 were also upregulated in P15, while most SAPK genes upregulated at 24 h and beyond in P30 were not differentially expressed in P15. To investigate what kinds of interactions may be accompanying the overactivation of single-pathway annotated genes in SAPK and Other groupings in P30, we turned our attention to multiple-pathway annotated genes.

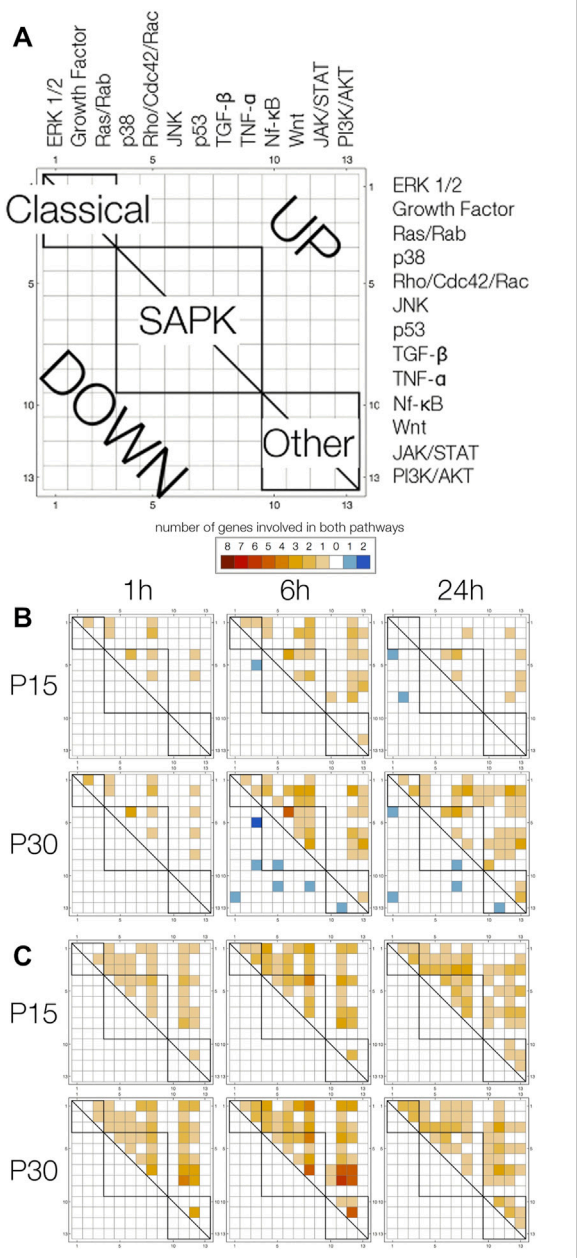

FIGURE 7
Pathway array plots for multiple-pathway annotated genes plot the number of genes annotated with any two pathways. **(A)** General label for all plots. Pathways are arranged (1 = ERK1/2... 13 = PI3K/AKT) by Classical, SAPK and Other families, and boxes are drawn to indicate pathways are in the same family (intra-family v. inter-family). Upregulated genes are filled in on the upper triangle in a shade of orange, and downregulated genes are filled in on the lower triangle in a shade of blue. **(B)** Pathway array plots for (4 or less)—pathway annotated genes differentially expressed at 1, 6 and 24 h in P15 and P30 animals. **(C)** Pathway array plots for (5 or more)—pathway annotated genes differentially expressed at 1,6 and 24 h in P15 and P30 animals.

3.8 Multiple-pathway annotated genes

Forty one percent of both P15 (n = 23/56) and P30 (n = 48/117) pathway-annotated genes were associated with a variable number (2–7) of multiple pathways. For example, NF-κB1, upregulated in P15 (2.15 fc, 6 h), is annotated with both "TGF-β signaling pathway" and "NF-κB cascade." Fos, upregulated in both P15 (6.87 fc, 1 h; 16.8 fc, 6 h) and P30 (29.1 fc, 1 h; 24.8 fc, 6 h; 5.82 fc, 24 h), is annotated with four different pathways: "activated by p38 MAPK signaling," "activated by classical MAPK signaling" (also known as ERK), "TGF-β signaling pathway," and growth factor signaling ("nerve growth factor pathway (NGF)" and "PDGF signaling pathway," "PDGFR-α signaling pathway").

In both age groups, multiple-pathway annotated genes were downregulated only 6 (n = 1, P15; n = 5, P30) and 24 h (n = 2, P15; n = 5, P30), and upregulated 1 (n = 7, P15; n = 11, P30), 6 (n = 15, P15; n = 25, P30) and 24 (n = 7, P15; n = 21, P30) hours after KA-SE. Only Ccl2 (5.31 fc, 72 h) and Spp1 (7.37 fc, 72 h; 5.56 fc, 240 h) were differentially expressed after 24 h in P30 (plots not shown). All downregulated genes in P15 and 9 out of 10 downregulated genes in P30 are annotated with only 2 pathways.

To use pathway annotations as a window into possible pathway interactions, we devised pathway array plots (Figure 7A). These display the number of upregulated (upper triangle) and downregulated (lower triangle) genes annotated with any two pathways (1 = ERK1/2. . . 13 = PI3K/AKT). Since the array plot is two-dimensional, a single gene associated with 2 pathways fills in 1 square, 3 pathways fill in 3 squares, 4 pathways fills in 6 squares, and n pathways fills in n choose 2 squares. Due to the large number of squares filled in for a single gene annotated with 5, 6 or 7 pathways (n = 7, P15; n = 10, P30) compared to genes annotated with 2 (n = 10, P15; n = 23, P30), 3 (n = 2, P15; n = 8, P30) or 4 (n = 4, P15; n = 7, P30) pathways, we looked at them separately (Figures 7B,C).

Differences between P15 and P30 are clearer amongst genes annotated with 4 or less pathways (Figure 7B). Particularly, in P30 animals, downregulation of genes annotated with multiple pathways at 6 h was followed by increased upregulation at 24 h. At 1 h, P15 and P30 pathway plots are comparable. At 6 h, the major difference between the age groups is that downregulated genes in P30 (Dact2_predicted, Kit, Mtch2_predicted, Plcb4, Ralbp1, RGD1565616_predicted) are annotated with pathways spanning Classical, SAPK and Other families; in contrast, the number of downregulated genes spanning more than 1 pathway is limited to one coordinate for P15. By 24 h, P15 pathway array plot is sparser for upregulated genes compared to P15 6 h. Downregulated genes (Agt, Inha) are still in the Classical and SAPK region. This is in contrast to P30, where downregulated genes (Agt, Faim2, Kit, Plcb1, Prkcc) continue to span all three families. Although upregulated genes in the array plot are sparser within the SAPK box, they are denser for the Other regions. Within the first 24 h, all 5, 6, or 7-pathway annotated genes were upregulated in both age groups. Pathway array plots of P15 and P30 are both dense and comparable: at 1 h, only TNF-α, JAK/STAT and PI3K/AKT have no annotations, and by 24 h, only TNF-α has no annotations (Figure 7C).

3.9 Regulation of pathways—Kinases and phosphatases

Next, we were interested in how the MAPK pathways may be regulated differently between P15 and P30 animals. As mentioned earlier (Section 2.4), pathway annotations will sometimes include regulatory schemes. We isolated genes annotated to regulate the 13 pathways (e.g. "regulation of Wnt receptor signaling pathway," "regulation of Ras protein signal transduction"), and separated those explicitly annotated as "positive" or "negative" (e.g. "negative regulation of JNK cascade") regulators. Genes annotated as both positive and negative regulators of the same pathway were not included as "positive" or "negative" regulators and, instead, were grouped as "general" regulatory genes (Figure 8A).

Nearly a third of all pathway-annotated genes in both P15 (n = 18/56) and P30 (n = 39/119) were regulatory. Most of these regulatory genes only regulated a single pathway (n = 16, P15; n = 35, P30), even amongst multiple-pathway associated genes. Like the expression patterns for previous groupings, genes annotated as regulating pathways were more numerous and expressed for longer time courses with higher magnitudes in P30 animals. The robust gene induction occurs within 72 h, while a few genes persist at 240 h. This expression pattern is especially evident amongst genes classified as positively regulating a pathway. In P15 animals, positive regulators were upregulated only at 6 h (Cited2, 6.57 fc; Hmox1, 2.43 fc; Jak2, 5.23 fc; Ret, 2.88 fc; Sgk, 2.62 fc) and 24 h (Cd74, 10.85 fc; Tbk1, 2.41 fc), while in P30 animals, positive regulators were upregulated throughout all 10 days of the study. In addition, all genes upregulated in P15 at 6 h were also upregulated in P30, and remained so for longer time courses. For example, Hmox1 is upregulated at 6 (10.3 fc) and 24 h (7.26 fc), and Ret is upregulated at 6 (2.99 fc), 24 (5.68 fc) and 240 h (2.12 fc) after KA-SE.

Rgs4 (2.11 fc, 6 h), which negatively regulates ERK signaling, was the only negative regulator differentially expressed in P15 and the only such negative regulator upregulated in P30 (3.83 fc, 1 h; 6.69 fc, 6 h). Interestingly, this earlier activation of a negative regulator of ERK in P30 (compared to P15) precedes later activation at 240 h of positive regulators of ERK, Ret (2.12 fc) and Cd74 (45.6 fc).

Additionally, we found four genes (n = 2, P15; n = 4, P30), which regulate multiple pathways (Figure 8B): Agt ("positive regulation of p38" and "positive regulation of classical MAPK"), Scg2 ("negative regulation of JNK cascade" and "positive regulation of TGF-β receptor signaling pathway"), IL-1β

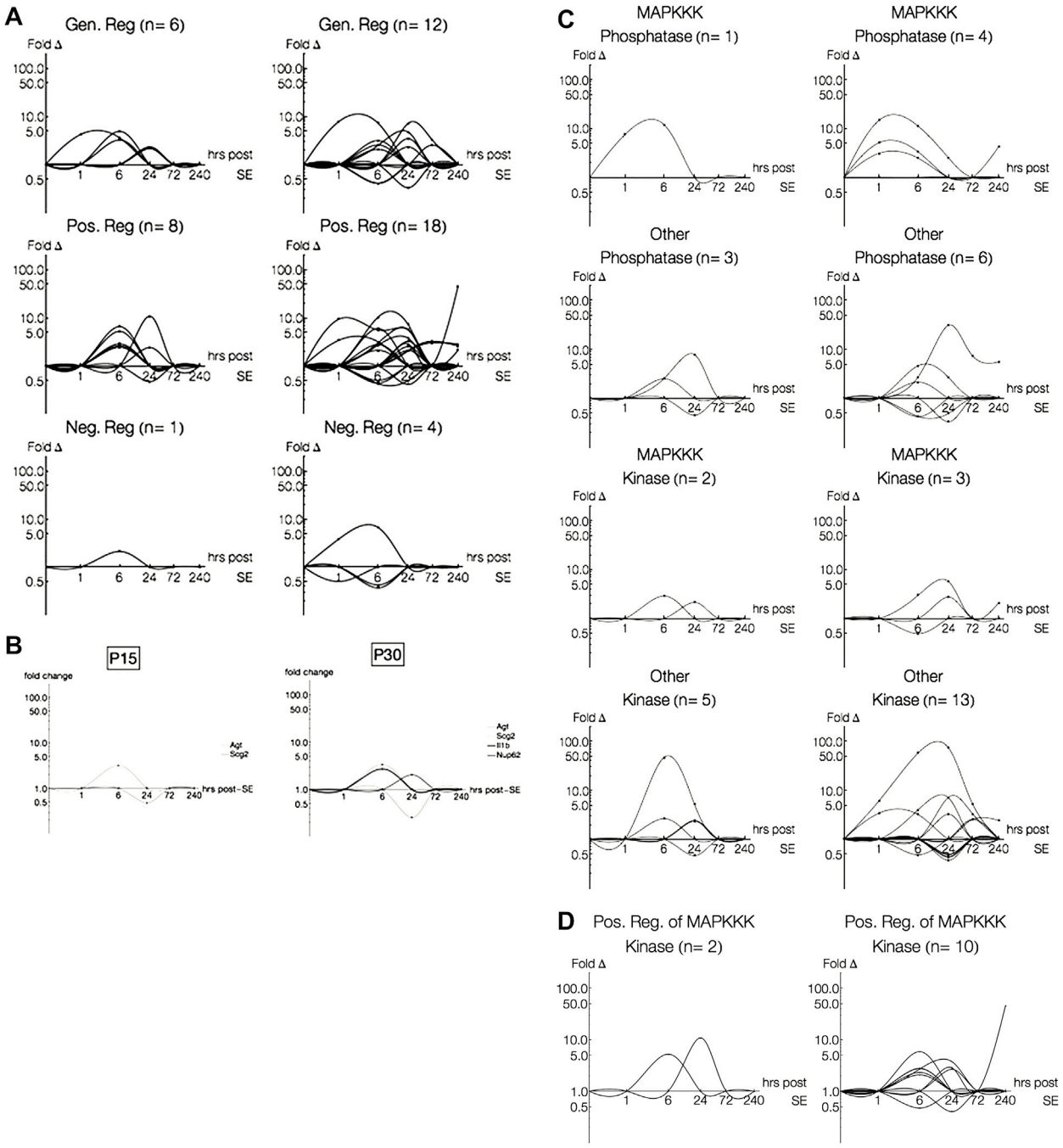

FIGURE 8
Log-Log plots of differential gene expression (fold change). Lines, each representing a single gene, were fitted using second order interpolation for ease of visualization. **(A)** Log-Log plots of differential gene expression (fold change) of genes regulating pathways. Most genes differentially expressed in P15 (left) and P30 (right) only regulate a single pathway, even amongst multiple-pathway annotated genes. **(B)** Log-Log plots of differential gene expression (fold change) of genes regulating pathways. Only four genes differentially expressed in P15 or P30 were annotated as regulating multiple pathways. **(C)** Log-Log plots of differential gene expression (fold change) of phosphatases and kinases in P15 (left) and P30 (right). **(D)** Log-Log plots of differential gene expression (fold change) of positive regulators of phosphatases and kinases.

("positive regulation of p38 MAPK cascade" and "positive regulation of JNK cascade") and Nup62 ("regulation of Ras protein signal transduction," "positive regulation of epidermal growth factor receptor signaling pathway," "positive regulation of i-κB kinase/NF-κB cascade"). Of the genes regulating multiple pathways, those differentially expressed in both P15 and P30 were expressed at lower levels than those that were only expressed in P15 or P30.

We were surprised to find that dual specificity protein phosphatases (Dusps), which are key inactivators of MAPK cascades, were not included as negative regulators of any of our pathways. To pursue the question of how phosphatases and kinases may be expressed and regulated differently among all MAPK signaling genes ($n = 140$), we isolated genes involved with phosphatase and kinase activity (Figures 8C,D). Within these genes, we found that 1) some were regulators of kinase and phosphatase activity and 2) some were associated specifically with MAPKKK cascades. All of the MAPKKK associated phosphatases were dual specificity protein phosphatases (Dusp1, P15; Dusp1, Dusp5 and Dusp6, P30).

Although most differentially expressed genes coding for phosphatases and kinases were not associated with MAPKKKs, we see an interesting temporal relationship in both age groups (Figure 8C): Dusps are activated before MAPKKK-related kinases (Ret and Mapk14, P15; Ret, Mapkapk3, Map3k12, P30) and other phosphatases. Similar to what we saw in the array plots and within our pathway regulators, increased Dusp activation earlier in P30 is followed by increased MAPKKK-related kinase activation later (Ret).

The greatest difference between P15 and P30 is across the non-MAPKKK kinases. These kinases are activated earlier and span 1–240 h in P30 but are restricted to 6 and 24 h in P15. However, when we look at the regulators of kinases and phosphatases, we see that the most striking difference between P15 and P30 is across the positive regulators of MAPKKK-annotated kinases (Figure 8D).

3.10 Verification

We verified our microarray data in several ways. First, we performed qRT-PCR. Second, we stained for proteins (HSP70 and CD74) coded by two highly expressed genes in P30. Lastly, we performed microarray analysis on tissue collected from hippocampi of human patients with medically intractable MTLE.

3.10.1 Real time reverse transcriptase polymerase chain reaction verifies microarray data for P30 at 24 h

Out of the 84 genes present in the Superarray qRT-PCR array, 61 were also present in the Affymetrix Microarray. Nineteen out of these 61 genes were significantly regulated in P30 microarray data at 24 h ($p < 0.05$, $q < 0.05$). 15 out of these 19 genes also showed a similar trend in the qRT-PCR data, and 7 of these reached statistical significance, 5 of which were over 2-fold change (Figure 9A).

An additional 16 genes showed statistical significance in our qRT-PCR data, which were not present in our microarray. These included cyclins (Ccna1, Ccna2, Ccnb1, Ccnb2) and cyclin dependent kinase and inhibitors (Cdk2, Cdkn1a, Cdkn2c). Also, we saw MAP2Ks, their activators (Map2k1ip1, Map2k2, Map2k6) and Map3k4. Furthermore, ERK5 showed differential expression at 24 h, suggesting that the fourth prototypical MAPK pathway is also differentially regulated after seizures. Finally, there were Stratifin (which activates MMP1 through p38 and c-fos), Smad4 (which is involved in TGF-β signaling), Rp1p1 and E2f1.

3.10.2 Immunohistochemistry

Hsp70 immunohistochemistry in the rat hippocampus paralleled expression profiles of Hsp 70 in microarray analysis. No difference in Hsp 70 immunoreactive cells are noted between KA and PBS controls in P15 animals, whereas Hsp 70 immunoreactive cells are clearly visible only 24 h after KA-SE in P30 animals (Figure 9B). There appears to be developmental upregulation of Hsp 70 at P15 with subsequent downregulation of Hsp gene expression at P30. Thus, there was no significant changes in Hsp 70 gene expression after KA-SE in P15 at any time point sampled, while Hsp70 (Hspa1a, Hspa1b) was differentially expressed in P30 animals at 1 (28.5 fc), 6 (129.6 fc), and 24 (54.8 fc) hours after KA-SE. It is worth noting that Hsp70 was one of the most upregulated genes, likely reflecting gene induction, at all 3 time points sampled in P30 animals.

We stained for CD74 in P15 and P30 animals at both 24 and 240 h after PBS or KA injection. Immunohistochemistry for CD74 also paralleled changes seen in microarray. 24 h after KA-SE, but not in PBS controls, P15 hippocampi showed staining for CD74. There were some CD74 immunoreactive cells in P30 hippocampi in PBS controls and there appeared more staining in KA-SE animals (Figure 9C). No immunoreactive cells were found 240 h (10 days) after KA-SE and PBS in P15 animals (P25 at the time of sacrifice). In contrast, P30 animals injected with KA showed considerable CD74 staining 240 h after KA-SE (Figure 9D). Although only the hippocampi are pictured in Figure 9, we saw marked increases in CD74 staining throughout all cortical areas 240 h after KA-SE in P30 animals. CD74 is differentially expressed in P15 (10.85 fc) exclusively 24 h after KA-SE. CD74 is slightly upregulated at 24 h (2.84 fc) but it is one of the most highly upregulated genes 240 h after KA-SE in P30 animals (45.6 fc).

3.10.3 Human microarray data on MAPK pathway

Microarray analysis of transcriptional regulation in the hippocampus of human patients diagnosed with temporal lobe

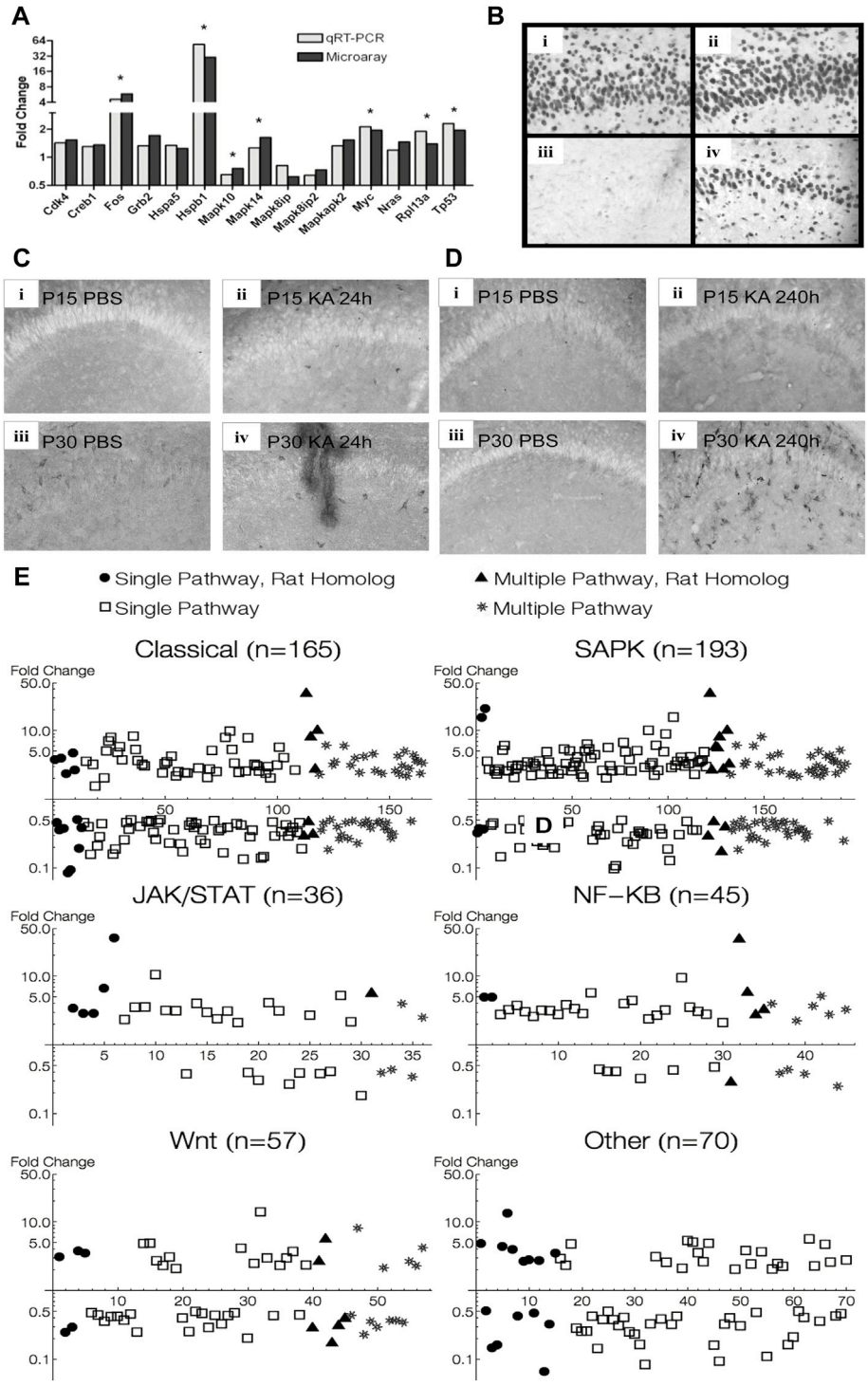

FIGURE 9
Verification of MAPK pathway genes found in animal experiments. **(A)** qRT-PCR verification of microarray data of some differentially expressed MAPK pathway genes 24 h after KA-SE in P30 animals. **(B)** Hippocampal sections stained for Hsp70. High magnification (×20) view of CA1 subfield 24 h after KA-SE at P15 and P30 [**(i)** P15 PBS; **(ii)** P15 KA; **(iii)** P30 PBS; **(iv)** P30 KA]. Notice robust Hsp 70 immunoreactivity in P15, undetectable in control P30, and induction by KA-SE at 24 h in P30. **(C)** Hippocampal sections stained for CD74 24 h after KA-SE [**(i)** P15 PBS; **(ii)** P15 KA; **(iii)** P30 PBS; **(iv)** P30 KA]. **(D)** Hippocampal sections stained for CD74 240 h after KA-SE [**(i)** P15 PBS; **(ii)** P15 KA; **(iii)** P30 PBS; **(iv)**P30 KA]. CD74 immunoreactive cells are most notable in P30 240 h after KA-SE. **(E)** MAPK pathway genes found in microarray analysis of hippocampus from patients with MTLE superimposed on MAPK pathway genes found in rats after KA-SE. Human genes: open square = single-pathway associated gene; star = multiple-pathway associated gene. Rat genes: filled circle = single-pathway associated gene; filled triangle = multiple-pathway associated gene.

epilepsy showed several similar changes in expression of the MAPK associated pathways analyzed in rats (Figure 9E). Several common genes were differentially regulated in both human and rat, with overlap between Classical, SAPK, JAK/STAT, NF-KB, and WNT groupings. The Classical and MAPK groupings showed the most notable changes. Most of the genes differentially regulated (particularly >5-fold change) belonged to either Classical or SAPK groupings. NF-κB, JAK/STAT, and WNT also showed changes, with NF-κB showing the highest proportion of upregulated genes among those differentially expressed. Notably, all pathways were both up and down regulated.

4 Discussion

Our first goal was to elucidate the multifaceted immune responses induced by seizures in KA-SE rat models of MTLE and in patients treated surgically for intractable MTLE. We found many common proinflammatory genes upregulated in both rat and human tissue. Some significant differences exist likely because we are comparing temporally discrete gene expressions changes after KA-SE in rats with chronic changes in the MTLE patients who have been exposed to recurrent seizures over many years. It should also be noted that our human control tissues were neocortical tissue while the experimental tissues consist of epileptogenic hippocampal tissue and lateral temporal neocortex. Many of the same genes were upregulated in the temporal neocortex and the hippocampus but to a higher level in epileptogenic hippocampus, lending support to the idea that many of the same inflammatory processes occur in both areas after exposure to chronic seizures. Similarly, higher, and sustained levels of inflammatory genes were expressed in P30 rat hippocampi while lower and transient inflammatory responses were noted in P15 rat hippocampi. Temporal pattern of changes in immune gene regulation provided important information. Acute early changes were activity-regulated transcription factors and immediate-early genes (IEGs) capable of modulating signaling cascade, pathways and protein networks downstream. These transcriptional changes in inflammatory genes in the mature brain (twice more compared to the immature brain) initiate genomic responses that may underlie long-term modification of neuronal physiology. Thus, prolonged seizure activity is translated via gene expression regulation into lasting cellular changes underlying epileptogenic process.

Many immune molecules in the brain have dual functions—acute inflammatory responses and long-term modulation of synaptic activity. The nonspecific inflammatory damage and the more specific modulation of synaptic strengths both have potential to increase cortical excitability. This process seems to be driven primarily by glial cells. The activation of microglia and astrocytes in response to seizure activity is well documented in rats (Shapiro et al., 2008) and gliosis is one of the classic neuropathologic findings in human MTLE. We confirm that glial activation persists over 10 days after status epilepticus in mature rats (Somera-Molina et al., 2007), and demonstrate a similar robust glial activation in both the hippocampi and the lateral temporal neocortex of MTLE patients. We saw persistently high levels of GFAP, Vimentin, and S100B, (astrocyte markers) as well as marked upregulation of both osteopontin and Aif-1, the markers of microglial activation.

IL-1β has been considered the main mediator of innate immune system activation in response to seizures. IL-1β and its receptor are found in neurons, astrocytes, and microglia. Both activated microglia and astrocytes produce IL-1β within hours of seizures, but prolonged production is maintained by astrocytes (Ravizza et al., 2008). In addition to IL-1β, we identified several other cytokines that may propagate the cycle of glial activation. Cytokine upregulation in rats peaked between 6 and 24 h after KA-SE correlating with the peak of glial activation. It is interesting to note that IL-18 expression increased again at the 10-day time point in P30 rats, likely a result of continued microglial activation. IL-1β and IL-18 were also upregulated in the human hippocampus while IL-6 expression was only increased in rats. IL-1β is the only cytokine also upregulated in the lateral temporal neocortex, highlighting its central role in epilepsy. IL-18 is a cytokine of the IL-1β family which is expressed by microglia after KA-induced excitotoxic damage (Jeon et al., 2008). IL-6 is produced by a variety of cells but astrocytes are the dominant source. It has both protective and damaging action including neuroprotection from glutamate toxicity and induction of neurotrophic, inflammatory, and other immune molecules (Van Wagoner and Benveniste, 1999). TNF-α functions in synaptic scaling in addition to promoting inflammation (Stellwagen and Malenka, 2006). It is produced by glia in response to changes in synaptic activity and is necessary for increasing synaptic strength by stimulating cell-surface expression and clustering of AMPA receptors. LITAF is a transcription factor that positively regulates the NF-κB pathway and increases expression of TNF-α. LITAF and TNF-α were upregulated in both rats and human tissue.

The chemokine-mediated recruitment of astrocytes, microglia, monocytes, and other immune cells also plays a central role in the inflammatory response to seizures. We demonstrated extremely high levels of chemokine expression, which generally peaked at 6 h after KA-SE in rats, with the exception of Ccl2, was complete by 24 h. These genes seem to play important roles in the innate as well as the adaptive immunity. The alpha chemokines include Cxcl10, IL-8, and Cxcl2. Cxcl10 was only upregulated in rats while IL-8, and Cxcl2 were only upregulated in our human tissue. Cxcl10 is produced by a variety of cell types, including neurons (Klein et al., 2005), astrocytes, and microglia (Ren et al., 1998). In addition to its functions in the chemotaxis of T-lymphocytes, natural killer cells, and monocytes, Cxcl10 causes astrocyte

chemotaxis when upregulated in response to cortical ischemia (Wang et al., 1998). The other two significantly upregulated alpha chemokines in human tissue, IL-8 and Cxcl2, function primarily to stimulate neutrophil chemotaxis and extravasation (Zhang et al., 2001). The beta chemokines, which include Ccl2, Ccl3, and Ccl4, are produced by astrocytes and microglia. They work to increase the migratory response of microglia and monocytes (Peterson et al., 1997). When Ccl2 is overexpressed in the CNS of transgenic mice, it also seems to recruit peripheral monocytes and T lymphocytes (Bennett et al., 2003). To summarize, rats exposed to status epilepticus primarily upregulate the beta chemokines, which function in the chemotaxis of monocytes, microglia, and lymphocytes. However, CXCL10 also shows a modest upregulation. Human hippocampal tissue showed the upregulation of both alpha and beta chemokines, including chemokines with activity on neutrophils and astrocytes. Some of these genes were also upregulated in the lateral temporal neocortex. The broader chemokine profile of the human tissues may be due to continued seizure-induced damage over long periods of time.

Secretoneurin is produced by endoproteolytic processing of Secretogranin II and is found in a variety of neuroendocrine tissues. Its functions include promoting the chemotaxis and extravasation of neutrophils and monocytes (Kahler et al., 2002). In addition, secretoneurin is a chemoattractant protein for endothelial cells, promotes angiogenesis, and stimulates neurite growth in cerebellar granule cells (Fischer-Colbrie et al., 2005). It is also upregulated in the cortical tissue of mice in response to experimentally induced ischemia and seems to have neuroprotective properties (Shyu et al., 2008). Secretogranin II was upregulated in our rat hippocampal tissue with a similar temporal profile as the chemokines.

COX-2 is the rate-limiting enzyme in the production of thromboxane A2 and a variety of prostaglandins. It is one of the key molecules bridging synaptic plasticity and inflammation. A variety of studies have found that COX-2 is expressed at high levels in the normal cortex and hippocampus but also upregulated in response to synaptic activity and seizures (Yang and Chen, 2008). The expression of COX-2 is regulated by NMDA receptor-dependent synaptic activity (Yamagata et al., 1993) and its function is necessary for the induction of long-term potentiation in hippocampal dentate granule cells (Chen et al., 2002). We demonstrate high levels of COX-2 expression in human and rats acutely after seizures. In the human tissue, there was significant upregulation in both hippocampal tissue and the temporal neocortex. The COX-2 produced by cortical tissue in response to seizure activity may induce subsequent inflammatory responses, which in turn may cause increased cortical excitability and further inflammation. Different forms of Phospholipase A2, which also function in promoting inflammation through the eicosanoid pathway, were also upregulated in both the human and rats but their function in the CNS has not been thoroughly investigated.

A wide variety of adhesion molecules were upregulated in both our human and rat tissue. These seem to fall broadly into two categories, those that affect neurite outgrowth and those that have more general immune functions. CD44 binds hyaluronan and is thought to be involved in a variety of inflammatory processes (Pure and Cuff, 2001). It is ubiquitously expressed on leukocytes as well as parenchymal cells and functions in leukocyte recruitment, cell-matrix interactions, cell migration, and induction of inflammatory gene expression. In addition to these roles in immunity, CD44 also functions in axonal pathfinding during development (Lin and Chan, 2003) and high levels of expression have been correlated to mossy fiber sprouting after status epilepticus in mice (Borges et al., 2004). Inhibition of CD44 activity seems to inhibit mossy fiber sprouting in organotypic hippocampal slices exposed to kainite (Bausch, 2006). CD44 was strongly upregulated in the rat hippocampus, peaking at 24 h after KA-SE, a similar time course to mossy fiber sprouting. It was also upregulated in the human TLE hippocampus and temporal lobe neocortex. Celsr proteins are neuron-neuron adhesion molecules that also function in axonal pathfinding during development (Tissir et al., 2005). Gene silencing experiments demonstrate that Celsr3 inhibits neurite outgrowth, while Celsr2 stimulates it (Shima et al., 2007). In adult rats, Celsr3 is one of the few molecules to be significantly downregulated in the period up to 24 h after KA-SE, suggesting the therapeutic potential of Celsr3 in preventing the formation of aberrant synaptic connections. Contactin 2, also called TAG-1, is an immunoglobulin superfamily member expressed by neurons, which promotes neurite outgrowth (Furley et al., 1990). It is anchored onto the neuronal membrane, and also secreted into the extracellular space where it may function as a substrate adhesion molecule. Expression of Contactin 2 was only significantly increased in the human MTLE patients. The tetraspanins, a group of cell-surface adhesion molecules, have a multitude of roles in cell motility, integrin-dependent cell adhesion, cell proliferation, apoptosis, tumor metastasis, and in organizing cell surface signal transducing complexes, or microdomains (Hemler, 2005). Leukocytes contain up to 20 different tetraspanins, which interact with a variety of immune molecules, including CD4, CD8, Fc receptors, MHC I, and MHC II molecules (Tarrant et al., 2003). The tetraspanins upregulated in rat, CD9, CD37, CD53, and CD63 are found in B-cells, T-cells, monocytes/macrophages, and granulocytes. These molecules showed an interesting pattern of expression. CD37 and CD53 are upregulated primarily at the late 72 h and 240 h time points while the other tetraspanins peaked at 24 h, suggesting a multiphasic immune response. Our human MTLE data also demonstrates upregulation of CD9 and CD53 in addition to Tetraspanins 6, 8, and 15. This group of molecules may also contribute the tissue-leukocyte interactions that lead to immune system activation.

Other adhesion molecules found to be expressed in rats and human function in leukocyte extravasation. They tend to be upregulated in response to inflammatory cytokines and are found either on leukocyte membranes or endothelial surfaces. These include L-selectin, ICAM-1, and the integrins. Recent studies demonstrate that molecules such as ICAM-1, VCAM-1, and selectins are upregulated in response to seizure activity and that disruption of their interactions with leukocyte receptors such as integrins prevents BBB breakdown and leukocyte extravasation (Fabene et al., 2008). Further highlighting the therapeutic potential of disrupting the inflammatory response to seizures, disruption of leukocyte extravasation led to decreased frequency of seizures after pilocarpine-induced SE. A number of receptors that function in the adaptive immune system were also upregulated in our experiments. This may suggest a breakdown in the BBB and infiltration of peripheral leukocytes. Indeed, chronic expression of IL-1β in the mouse brain leads to blood brain barrier breakdown, expression of CCL-2, and a dramatic infiltration of neutrophils, T-cells, macrophages, and dendritic cells (Shaftel et al., 2007; Xu et al., 2018). Chronic IL-1β expression leads to neutrophil infiltration of the hippocampus persisting up to 1 year due to activation of the CXCR2 receptor. Histopathologic examination of surgical specimens from children with intractable epilepsy also shows BBB disruption due to an angiopathy of capillaries and arterioles (Hildebrandt et al., 2008).

Another important goal of our research was to delineate some of the differences in status epilepticus-induced gene expression changes between mature and immature rats. P15 rats have increased seizure susceptibility in response to electrical stimulation (Moshe and Albala, 1983). Similarly, systemic injections of KA causes more severe seizures and a higher rate of death in immature rats but they are paradoxically less susceptible to the development of convulsions later in life (Okada et al., 1984). Furthermore, immature rats are much more resistant to neuronal death, mossy fiber sprouting, and the synaptic reorganization that alters the electrophysiological properties of the hippocampus (Haas et al., 2001). Our data showed a peak in expression of both astrocyte and microglial markers at 24 h after KA-SE in mature as well as immature rats. However, the upregulation of these markers in immature rats was largely terminated by 72 h, whereas the mature rats have higher peak expression levels and upregulation is significantly prolonged, lasting through the 240 h time point. We propose that temporal expression difference may be responsible for the increased damage and epileptogenesis seen in mature animals. We also observed a dramatic discrepancy between cytokine, chemokine, complement, and protease expression between these groups. The increased seizure susceptibility seen in immature animals may be due to active synaptogenesis and synaptic plasticity in young nervous system, but seizures without the prolonged inflammatory responses do not seem to produce the long-term changes seen in mature animals.

MAPK signaling comprised the largest functional grouping for genes differentially expressed in P30 and for genes differentially expressed in P15 (Figure 5A). These genes were also associated with other processes (e.g., inflammation, synaptic plasticity) previously observed to change during the latent period, suggesting that differential regulation of MAPK signaling may underlie such functional alterations in older animals (Figure 5B). Using online databases, we found that MAPK genes differentially expressed in response to seizures in P15 or P30 fell into numerous canonical signaling schemes, which we reduced to 13 component pathways (Growth Factor, Ras/Rab, ERK, p38, JNK, Rho/Rac/Cdc42, TGF-β, TNF-α, NF-κB, Wnt, JAK/STAT, PI3K/AKT) based on the criterion that each pathway contained a unique gene. After this simplification, most genes expressed in P30 or P15 were associated with only a single pathway. However, most genes within any given pathway were still associated with multiple pathways, suggesting that genes differentially expressed in response to seizures (P15) and during the latent period (P30) can participate in multiple canonical signaling cascades. This may allow such genes to act as central regulatory hubs, whose dysregulation can have propagating effects across the signal transduction network. Compared to P15, P30 animals also showed marked increases in genes participating in positive regulation at multiple levels of signal transduction: at the level of pathways (Figures 8A,B), at the level of transcription (Figure 6) and at the level of MAPKKK cascades (Figure 8D). Additionally, increases in downregulation at P30 precede increases in upregulation of multiple-pathway annotated genes (Figure 7B), and increases in negative regulation of ERK signaling precede increases in positive regulation of ERK signaling (Figures 8A,B). This is consistent with the idea that transcriptional feedback into MAPK signaling during the latent period produces a positive feed-forward loop, as we see drastic increases in positive regulation coupled with negative regulatory elements precipitating positive regulation.

Another striking difference between the age groups was unmasked by splitting up our pathway related genes based on MAPK family groupings (i.e., SAPK and Classical). We found that most of the genes in both P30 and P15 animals that belonged exclusively to one of the Classical pathways (ERK, Ras/Rab, Growth Factor) were commonly expressed across age groups and expressed within the first 24 h (Figure 6). At around 24 h, genes belonging exclusively to one of the SAPK pathways (p38, JNK, Rho/Rac/Cdc42, TGF-β, TNF-α), on the other hand, act differently between the age groups. Particularly, we saw genes exclusively expressed in P30 animals were upregulated and remained upregulated for the entire sampled period of 10 days. This, coupled with the late and persistent activation of genes which serve as glial markers and glial activators (S1004a, Ccl2, Spp1, Aif-1), may suggest a network disturbance spanning multiple signaling schemes across multiple cell types, which together propagate a persistent over-activation of transcription in epileptic P30 animals.

Our data support that chronic epileptic state and spontaneous recurrent seizures after KA-SE emerge from a systemic disruption of signal transduction networks across multiple canonical pathways. At the level of transcription, our data suggests this disturbance is propagated by over activation in the direction of feed-forward loops onto MAPK signaling pathways. Studies looking at phosphorylation of p38, JNK and ERK signaling have described different time courses of expression from each other as well as across cell types and hippocampal regions (Gass, 1999; Mielke et al., 1999; Jeon et al., 2000; Berkeley et al., 2002; Brisman et al., 2002; Ferrer et al., 2002; Choi et al., 2003; Kim S. H. et al., 2004; Kim S. W. et al., 2004; Jiang et al., 2005; Houser et al., 2008). However, the results of these experiments have been inconsistent across different models of epilepsy, and even in the same model. Though attributed to methodological differences, this may suggest that seizure-induced directional changes in the regulation of MAPK pathways are not consistently predictable. It is plausible that widespread dysregulation across dynamically modular networks with emergent nonlinear properties may rely more on changes in network dynamics, and less on specific genes or species. We propose that chronic spontaneous recurrent seizures after KA-SE result from a systemic disruption of signal transduction networks across multiple pathways affecting multiple cell types.

MAPK pathways are composed of several different families with different signaling motifs and crosstalk between pathways which can activate or deactivate each other in a context dependent manner (Shen et al., 2003; Aksamitiene et al., 2012; Fey et al., 2012). All of our 13 pathways have previously been linked to various models of epilepsy, and the potential crosstalk between them has been discussed elsewhere (Gautam et al., 2021). Though the role of interaction and crosstalk between pathways still are not well understood, studies suggest that under non-pathological conditions one way of gaining signal specificity and maintaining robustness in signaling transduction systems is through molecular species acting to mutually inhibit one another (Natarajan et al., 2006; McClean et al., 2007), and that most potential interactions between molecules are not realized, limiting cellular responses to discrete subsets of ligands and pathways to enhance specific cellular functions (Hsueh et al., 2009). Our data suggests that in P30 animals, the crosstalk between pathways as well as the pathways themselves are overactivated. Particularly, in comparison to P15 animals, P30 animals have sustained overactivation and further expression of genes specific to P30 across all pathway families (Figures 6–8). We propose sustained overactivation of multiple crosstalking pathways, especially those in our SAPK grouping, may be recruiting instead of inhibiting crosstalking species. This "leakage," instead of maintaining signal specificity, results in a diverse array of cellular responses, culminating in epileptogenesis.

Single-cell transcriptomics have identified cell-specific changes related to plasticity and inflammation, particularly in interneuron and glial populations (Pfisterer et al., 2020; Kumar et al., 2022). Potential central regulators explaining glial genes expressed during epileptogenesis are directly upstream and regulate several MAPK pathways (Kalozoumi et al., 2018). Interestingly, reports of MAPK related changes in the extracellular matrix (Han et al., 2019) may also suggest that signaling transduction networks perturbed during epileptogenesis operate across cells, especially in neuron-glial interactions. For example, microglia in the dentate gyrus, shortly after SE, have increased IGF-1 expression, mediated by CREB (Choi et al., 2008) and likely MAPK signaling (Labandeira-Garcia et al., 2017; Wu et al., 2018). Two days post SE, reactive microglia near the subgranular zone (SGZ) drop IGF-1 to drive cellular proliferation via ERK in the SGZ (Choi et al., 2008).

There are limitations when comparing gene expression profiles in an acute rat model to human epileptic brains. While we emphasized the commonality between rat and human data, showing that the same inflammatory genes are persistently upregulated in P30 hippocampi and human epileptic tissue, distinct classes of genes uniquely expressed in rats or humans are noteworthy. Heat shock proteins were uniquely upregulated in rats during the first 24 h after KA-SE. Conversely, adaptive immune system activation is noted only in human tissue. These differences reflect acute reactive changes in gene expression in the rat KA-SE model compared to the chronic epileptic state in humans. The body responds to recurrent seizures over time: breakdown of blood brain barrier occurs and immune cells from periphery infiltrate into the brain in chronic epilepsy (Xu et al., 2018). Given this limitation of comparing an acute epileptogenic insult model (KA-SE) to chronic epilepsy, it is remarkable to see many inflammation-related genes and the same MAPK pathway genes altered in parallel in both rats and humans. Our findings thus provide clinical relevance and credence to our preclinical time-course gene expression profiling.

In summary, we demonstrated significant changes in hippocampal gene expression in MAPK signaling pathways after prolonged seizures and identified potential role of dysregulated SAPK and p38 MAPK in pathogenesis unique to P30. We also demonstrated significantly higher levels of inflammatory gene upregulation in the epileptogenic hippocampus compared to the lateral temporal neocortex of patients with MTLE. Age- and time-dependent differential regulation of inflammatory genes after KA-SE further demonstrated that chronic, persistent and active inflammation occur only in epileptic P30 animals while transient inflammation

is observed in P15 animals that show no cell death and no spontaneous recurrent seizures. This observation suggests a critical role of chronic active neuroinflammation in epileptogenesis. Under normal physiologic conditions, the immune system likely subserves many of the functions necessary for proper synaptic scaling and so must be responsive to synaptic activity. When appropriately activated and deactivated, inflammation benefits the host defense response by removing damaged cells and promoting repair and recovery. However, prolonged seizures appear to inappropriately activate the immune system leading to sustained, out of control inflammation. This uncontrolled inflammation can exacerbate neuronal injury and cause immediate damage to the brain and long-term changes in brain structure by stimulating neurite outgrowth and the formation of aberrant synapses, thus promoting epileptogenic process.

Data availability statement

The datasets generated for this study are available upon request to the corresponding author.

The datasets are also available at the Microarray Consortium (https://www.ncbi.nlm.nih.gov/), accession numbers GSE1834 and GSE1831, and at TGEN (Phoenix, AZ).

Ethics statement

The studies involving human participants were reviewed and approved by the Northwestern University, Feinberg School of Medicine. Written informed consent to participate in this study was provided by the participants' legal guardian/next of kin. The animal study was reviewed and approved by the Northwestern University, Feinberg School of Medicine.

Author contributions

SK conceived and designed the study. GN and SE drafted the manuscript. JK performed breakpoints verification. GN, SE, and HC participated in the data analysis. SE, GN, HC, JK, and SK reviewed and edited the manuscript and contributed to the discussions. GN and SK participated in clinical data collection. SK supervised the study. All authors reviewed and approved this submission.

Acknowledgments

We thank Ms. Minjung Kim for her technical support.

Funding

This study was supported by NIH/NINDS R01NS073768.

Conflict of interest

The authors declare that the research was conducted in the absence of any commercial or financial relationships that could be construed as a potential conflict of interest.

Publisher's note

References

Aksamitiene, E., Kiyatkin, A., and Kholodenko, B. N. (2012). Cross-talk between mitogenic Ras/MAPK and survival PI3K/Akt pathways: a fine balance. *Biochem. Soc. Trans.* 40, 139–146. doi:10.1042/BST20110609

Albala, B. J., Moshe, S. L., and Okada, R. (1984). Kainic-acid-induced seizures: a developmental study. *Brain Res.* 315, 139–148. doi:10.1016/0165-3806(84)90085-3

Arthur, J. S., and Ley, S. C. (2013). Mitogen-activated protein kinases in innate immunity. *Nat. Rev. Immunol.* 13, 679–692. doi:10.1038/nri3495

Ashburner, M., Ball, C. A., Blake, J. A., Botstein, D., Butler, H., Cherry, J. M., et al. (2000). Gene ontology: tool for the unification of biology. The gene ontology Consortium. *Nat. Genet.* 25, 25–29. doi:10.1038/75556

Avishai-Eliner, S., Brunson, K. L., Sandman, C. A., and Baram, T. Z. (2002). Stressed-out, or in (utero)? *Trends Neurosci.* 25, 518–524. doi:10.1016/s0166-2236(02)02241-5

Babb, T. L., Kupfer, W. R., Pretorius, J. K., Crandall, P. H., and Levesque, M. F. (1991). Synaptic reorganization by mossy fibers in human epileptic fascia dentata. *Neuroscience* 42, 351–363. doi:10.1016/0306-4522(91)90380-7

Baek, H., Yi, M. H., Pandit, S., Park, J. B., Kwon, H. H., Zhang, E., et al. (2016). Altered expression of KCC2 in GABAergic interneuron contributes prenatal stress-induced epileptic spasms in infant rat. *Neurochem. Int.* 97, 57–64. doi:10.1016/j.neuint.2016.05.006

Baulac, S., Gourfinkel-An, I., Nabbout, R., Huberfeld, G., Serratosa, J., Leguern, E., et al. (2004). Fever, genes, and epilepsy. *Lancet. Neurol.* 3, 421–430. doi:10.1016/S1474-4422(04)00808-7

Bausch, S. B. (2006). Potential roles for hyaluronan and CD44 in kainic acid-induced mossy fiber sprouting in organotypic hippocampal slice cultures. *Neuroscience* 143, 339–350. doi:10.1016/j.neuroscience.2006.07.037

Bencurova, P., Baloun, J., Hynst, J., Oppelt, J., Kubova, H., Pospisilova, S., et al. (2021). Dynamic miRNA changes during the process of epileptogenesis in an infantile and adult-onset model. *Sci. Rep.* 11, 9649. doi:10.1038/s41598-021-89084-9

Bennett, J. L., Elhofy, A., Canto, M. C., Tani, M., Ransohoff, R. M., and Karpus, W. J. (2003). CCL2 transgene expression in the central nervous system directs diffuse infiltration of CD45(high)CD11b(+) monocytes and enhanced Theiler's murine encephalomyelitis virus-induced demyelinating disease. *J. Neurovirol.* 9, 623–636. doi:10.1080/13550280390247551

Berkeley, J. L., Decker, M. J., and Levey, A. I. (2002). The role of muscarinic acetylcholine receptor-mediated activation of extracellular signal-regulated kinase

1/2 in pilocarpine-induced seizures. *J. Neurochem.* 82, 192–201. doi:10.1046/j.1471-4159.2002.00977.x

Binder, D. K., and Steinhauser, C. (2006). Functional changes in astroglial cells in epilepsy. *Glia* 54, 358–368. doi:10.1002/glia.20394

Blumcke, I., Zuschratter, W., Schewe, J. C., Suter, B., Lie, A. A., Riederer, B. M., et al. (1999). Cellular pathology of hilar neurons in Ammon's horn sclerosis. *J. Comp. Neurol.* 414, 437–453. doi:10.1002/(sici)1096-9861(19991129)414:4<437::aid-cne2>3.0.co;2-3

Blumcke, I., Pauli, E., Clusmann, H., Schramm, J., Becker, A., Elger, C., et al. (2007). A new clinico-pathological classification system for mesial temporal sclerosis. *Acta Neuropathol.* 113, 235–244. doi:10.1007/s00401-006-0187-0

Borges, K., Mcdermott, D. L., and Dingledine, R. (2004). Reciprocal changes of CD44 and GAP-43 expression in the dentate gyrus inner molecular layer after status epilepticus in mice. *Exp. Neurol.* 188, 1–10. doi:10.1016/j.expneurol.2004.03.019

Briellmann, R. S., Berkovic, S. F., Syngeniotis, A., King, M. A., and Jackson, G. D. (2002). Seizure-associated hippocampal volume loss: A longitudinal magnetic resonance study of temporal lobe epilepsy. *Ann. Neurol.* 51, 641–644. doi:10.1002/ana.10171

Brisman, J. L., Rees Cosgrove, G., and Cole, A. J. (2002). Phosphorylation of P42/P44 MAP kinase and DNA fragmentation in the rat perforant pathway stimulation model of limbic epilepsy. *Brain Res.* 933, 50–59. doi:10.1016/s0006-8993(02)02304-1

Brooks-Kayal, A. R., Shumate, M. D., Jin, H., Rikhter, T. Y., and Coulter, D. A. (1998). Selective changes in single cell GABA(A) receptor subunit expression and function in temporal lobe epilepsy. *Nat. Med.* 4, 1166–1172. doi:10.1038/2661

Bruggeman, F. J., Westerhoff, H. V., Hoek, J. B., and Kholodenko, B. N. (2002). Modular response analysis of cellular regulatory networks. *J. Theor. Biol.* 218, 507–520. doi:10.1016/s0022-5193(02)93096-1

Chen, C., Magee, J. C., and Bazan, N. G. (2002). Cyclooxygenase-2 regulates prostaglandin E2 signaling in hippocampal long-term synaptic plasticity. *J. Neurophysiol.* 87, 2851–2857. doi:10.1152/jn.2002.87.6.2851

Choi, J. S., Kim, S. Y., Park, H. J., Cha, J. H., Choi, Y. S., Kang, J. E., et al. (2003). Upregulation of gp130 and differential activation of STAT and p42/44 MAPK in the rat hippocampus following kainic acid-induced seizures. *Brain Res. Mol. Brain Res.* 119, 10–18. doi:10.1016/j.molbrainres.2003.08.010

Choi, Y. S., Cho, H. Y., Hoyt, K. R., Naegele, J. R., and Obrietan, K. (2008). IGF-1 receptor-mediated ERK/MAPK signaling couples status epilepticus to progenitor cell proliferation in the subgranular layer of the dentate gyrus. *Glia* 56, 791–800. doi:10.1002/glia.20653

De Simoni, M. G., Perego, C., Ravizza, T., Moneta, D., Conti, M., Marchesi, F., et al. (2000). Inflammatory cytokines and related genes are induced in the rat hippocampus by limbic status epilepticus. *Eur. J. Neurosci.* 12, 2623–2633. doi:10.1046/j.1460-9568.2000.00140.x

Dixit, A. B., Banerjee, J., Srivastava, A., Tripathi, M., Sarkar, C., Kakkar, A., et al. (2016). RNA-seq analysis of hippocampal tissues reveals novel candidate genes for drug refractory epilepsy in patients with MTLE-HS. *Genomics* 107, 178–188. doi:10.1016/j.ygeno.2016.04.001

Ellison, J. A., Velier, J. J., Spera, P., Jonak, Z. L., Wang, X., Barone, F. C., et al. (1998). Osteopontin and its integrin receptor alpha(v)beta3 are upregulated during formation of the glial scar after focal stroke. *Stroke* 29, 1698–1706. discussion 1707. doi:10.1161/01.str.29.8.1698

Eng, L. F., and Ghirnikar, R. S. (1994). GFAP and astrogliosis. *Brain Pathol.* 4, 229–237. doi:10.1111/j.1750-3639.1994.tb00838.x

Engel, J., Jr.International League Against Epilepsy ILAE (2001). A proposed diagnostic scheme for people with epileptic seizures and with epilepsy: report of the ILAE task force on classification and terminology. *Epilepsia* 42, 796–803. doi:10.1046/j.1528-1157.2001.10401.x

Engel, J. J. (2006). Report of the ILAE classification core group. *Epilepsia* 47, 1558–1568. doi:10.1111/j.1528-1167.2006.00215.x

Fabene, P. F., Navarro Mora, G., Martinello, M., Rossi, B., Merigo, F., Ottoboni, L., et al. (2008). A role for leukocyte-endothelial adhesion mechanisms in epilepsy. *Nat. Med.* 14, 1377–1383. doi:10.1038/nm.1878

Ferrer, I., Blanco, R., Carmona, M., Puig, B., Dominguez, I., and Vinals, F. (2002). Active, phosphorylation-dependent MAP kinases, MAPK/ERK, SAPK/JNK and p38, and specific transcription factor substrates are differentially expressed following systemic administration of kainic acid to the adult rat. *Acta Neuropathol.* 103, 391–407. doi:10.1007/s00401-001-0481-9

Fey, D., Croucher, D. R., Kolch, W., and Kholodenko, B. N. (2012). Crosstalk and signaling switches in mitogen-activated protein kinase cascades. *Front. Physiol.* 3, 355. doi:10.3389/fphys.2012.00355

Fischer-Colbrie, R., Kirchmair, R., Kahler, C. M., Wiedermann, C. J., and Saria, A. (2005). Secretoneurin: A new player in angiogenesis and chemotaxis linking nerves, blood vessels and the immune system. *Curr. Protein Pept. Sci.* 6, 373–385. doi:10.2174/1389203054546334

Fu, Y., Wu, Z., Guo, Z., Chen, L., Ma, Y., Wang, Z., et al. (2020). Systems-level analysis identifies key regulators driving epileptogenesis in temporal lobe epilepsy. *Genomics* 112, 1768–1780. doi:10.1016/j.ygeno.2019.09.020

Furley, A. J., Morton, S. B., Manalo, D., Karagogeos, D., Dodd, J., and Jessell, T. M. (1990). The axonal glycoprotein TAG-1 is an immunoglobulin superfamily member with neurite outgrowth-promoting activity. *Cell* 61, 157–170. doi:10.1016/0092-8674(90)90223-2

Gass, P. (1999). Expression of inducible transcription factors after experimental limbic seizures. *Adv. Neurol.* 81, 347–355.

Gautam, V., Rawat, K., Sandhu, A., Kumari, P., Singh, N., and Saha, L. (2021). An insight into crosstalk among multiple signaling pathways contributing to epileptogenesis. *Eur. J. Pharmacol.* 910, 174469. doi:10.1016/j.ejphar.2021.174469

Haas, K. Z., Sperber, E. F., Opanashuk, L. A., Stanton, P. K., and Moshe, S. L. (2001). Resistance of immature hippocampus to morphologic and physiologic alterations following status epilepticus or kindling. *Hippocampus* 11, 615–625. doi:10.1002/hipo.1076

Han, C. L., Zhao, X. M., Liu, Y. P., Wang, K. L., Chen, N., Hu, W., et al. (2019). Gene expression profiling of two epilepsy models reveals the ECM/integrin signaling pathway is involved in epiletogenesis. *Neuroscience* 396, 187–199. doi:10.1016/j.neuroscience.2018.10.021

Hansen, K. F., Sakamoto, K., Pelz, C., Impey, S., and Obrietan, K. (2014). Profiling status epilepticus-induced changes in hippocampal RNA expression using high-throughput RNA sequencing. *Sci. Rep.* 4, 6930. doi:10.1038/srep06930

Hartwell, L. H., Hopfield, J. J., Leibler, S., and Murray, A. W. (1999). From molecular to modular cell biology. *Nature* 402, C47–C52. doi:10.1038/35011540

Hauser, W. A., and Hesdorffer, D. C. (1990). *Epilepsy : frequency, causes, and consequences*. New York, NY: Demos.

Hauser, W. A. (1997). "Incidence and prevalence," in *Epilepsy: a comprehensive textbook*. Editors J. J. Engel and T. Pedley (Philadelphia: Lippincott-Raven), 47–57.

Haut, S. R., Veliskova, J., and Moshe, S. L. (2004). Susceptibility of immature and adult brains to seizure effects. *Lancet. Neurol.* 3, 608–617. doi:10.1016/S1474-4422(04)00881-6

Hemler, M. E. (2005). Tetraspanin functions and associated microdomains. *Nat. Rev. Mol. Cell Biol.* 6, 801–811. doi:10.1038/nrm1736

Hesdorffer, D. C., Logroscino, G., Cascino, G., Annegers, J. F., and Hauser, W. A. (1998). Risk of unprovoked seizure after acute symptomatic seizure: effect of status epilepticus. *Ann. Neurol.* 44, 908–912. doi:10.1002/ana.410440609

Hildebrandt, M., Amann, K., Schroder, R., Pieper, T., Kolodziejczyk, D., Holthausen, H., et al. (2008). White matter angiopathy is common in pediatric patients with intractable focal epilepsies. *Epilepsia* 49, 804–815. doi:10.1111/j.1528-1167.2007.01514.x

Houser, C. R., Huang, C. S., and Peng, Z. (2008). Dynamic seizure-related changes in extracellular signal-regulated kinase activation in a mouse model of temporal lobe epilepsy. *Neuroscience* 156, 222–237. doi:10.1016/j.neuroscience.2008.07.010

Hsueh, R. C., Natarajan, M., Fraser, I., Pond, B., Liu, J., Mumby, S., et al. (2009). Deciphering signaling outcomes from a system of complex networks. *Sci. Signal.* 2, ra22. doi:10.1126/scisignal.2000054

Ingolia, N. T., and Murray, A. W. (2007). Positive-feedback loops as a flexible biological module. *Curr. Biol.* 17, 668–677. doi:10.1016/j.cub.2007.03.016

Jamali, S., Bartolomei, F., Robaglia-Schlupp, A., Massacrier, A., Peragut, J. C., Regis, J., et al. (2006). Large-scale expression study of human mesial temporal lobe epilepsy: evidence for dysregulation of the neurotransmission and complement systems in the entorhinal cortex. *Brain.* 129, 625–641. doi:10.1093/brain/awl001

Jeon, S. H., Kim, Y. S., Bae, C. D., and Park, J. B. (2000). Activation of JNK and p38 in rat hippocampus after kainic acid induced seizure. *Exp. Mol. Med.* 32, 227–230. doi:10.1038/emm.2000.37

Jeon, G. S., Park, S. K., Park, S. W., Kim, D. W., Chung, C. K., and Cho, S. S. (2008). Glial expression of interleukin-18 and its receptor after excitotoxic damage in the mouse hippocampus. *Neurochem. Res.* 33, 179–184. doi:10.1007/s11064-007-9434-6

Jiang, W., Van Cleemput, J., Sheerin, A. H., Ji, S. P., Zhang, Y., Saucier, D. M., et al. (2005). Involvement of extracellular regulated kinase and p38 kinase in hippocampal seizure tolerance. *J. Neurosci. Res.* 81, 581–588. doi:10.1002/jnr.20566

Kahler, C. M., Kaufmann, G., Kahler, S. T., and Wiedermann, C. J. (2002). The neuropeptide secretoneurin stimulates adhesion of human monocytes to arterial

and venous endothelial cells *in vitro*. *Regul. Pept.* 110, 65–73. doi:10.1016/s0167-0115(02)00161-1

Kalozoumi, G., Kel-Margoulis, O., Vafiadaki, E., Greenberg, D., Bernard, H., Soreq, H., et al. (2018). Glial responses during epileptogenesis in *Mus musculus* point to potential therapeutic targets. *PLoS One* 13, e0201742. doi:10.1371/journal.pone.0201742

Kanehisa, M., Goto, S., Kawashima, S., and Akihiro, N. (2002). The KEGG databases at GenomeNet. *Nucleic Acids Res.* 30, 42–46. doi:10.1093/nar/30.1.42

Kelleher, R. J., 3rd, Govindarajan, A., Jung, H. Y., Kang, H., and Tonegawa, S. (2004). Translational control by MAPK signaling in long-term synaptic plasticity and memory. *Cell* 116, 467–479. doi:10.1016/s0092-8674(04)00115-1

Kim, S. Y., Choi, Y. S., Choi, J. S., Cha, J. H., Kim, O. N., Lee, S. B., et al. (2002). Osteopontin in kainic acid-induced microglial reactions in the rat brain. *Mol. Cells* 13, 429–435.

Kim, S. H., Smith, C. J., and Van Eldik, L. J. (2004a). Importance of MAPK pathways for microglial pro-inflammatory cytokine IL-1 beta production. *Neurobiol. Aging* 25, 431–439. doi:10.1016/S0197-4580(03)00126-X

Kim, S. W., Yu, Y. M., Piao, C. S., Kim, J. B., and Lee, J. K. (2004b). Inhibition of delayed induction of p38 mitogen-activated protein kinase attenuates kainic acid-induced neuronal loss in the hippocampus. *Brain Res.* 1007, 188–191. doi:10.1016/j.brainres.2004.02.009

Klein, R. S., Lin, E., Zhang, B., Luster, A. D., Tollett, J., Samuel, M. A., et al. (2005). Neuronal CXCL10 directs CD8+ T-cell recruitment and control of West Nile virus encephalitis. *J. Virol.* 79, 11457–11466. doi:10.1128/JVI.79.17.11457-11466.2005

Koh, S., Storey, T. W., Santos, T. C., Mian, A. Y., and Cole, A. J. (1999). Early-life seizures in rats increase susceptibility to seizure-induced brain injury in adulthood. *Neurology* 53, 915–921. doi:10.1212/wnl.53.5.915

Kozlova, E. N., and Lukanidin, E. (2002). Mts1 protein expression in the central nervous system after injury. *Glia* 37, 337–348. doi:10.1002/glia.10045

Kumar, P., Lim, A., Hazirah, S. N., Chua, C. J. H., Ngoh, A., Poh, S. L., et al. (2022). Single-cell transcriptomics and surface epitope detection in human brain epileptic lesions identifies pro-inflammatory signaling. *Nat. Neurosci.* 25, 956–966. doi:10.1038/s41593-022-01095-5

Kyriakis, J. M., and Avruch, J. (2012). Mammalian MAPK signal transduction pathways activated by stress and inflammation: a 10-year update. *Physiol. Rev.* 92, 689–737. doi:10.1152/physrev.00028.2011

Labandeira-Garcia, J. L., Costa-Besada, M. A., Labandeira, C. M., Villar-Cheda, B., and Rodriguez-Perez, A. I. (2017). Insulin-like growth factor-1 and neuroinflammation. *Front. Aging Neurosci.* 9, 365. doi:10.3389/fnagi.2017.00365

Lin, L., and Chan, S. O. (2003). Perturbation of CD44 function affects chiasmatic routing of retinal axons in brain slice preparations of the mouse retinofugal pathway. *Eur. J. Neurosci.* 17, 2299–2312. doi:10.1046/j.1460-9568.2003.02686.x

Liu, G., Loraine, A., Shigeta, R., Cline, M., Cheng, J., Valmeekam, V., et al. (2003). NetAffx: Affymetrix probesets and annotations. *Nucleic Acids Res.* 31, 82–86. doi:10.1093/nar/gkg121

Liu, J. S. (2011). Molecular genetics of neuronal migration disorders. *Curr. Neurol. Neurosci. Rep.* 11, 171–178. doi:10.1007/s11910-010-0176-5

Loscher, W. (2002). Animal models of drug-resistant epilepsy. *Novartis Found. Symp.* 243, 149–159. discussion 159-166, 180-145.

Lukasiuk, K., Dabrowski, M., Adach, A., and Pitkanen, A. (2006). Epileptogenesis-related genes revisited. *Prog. Brain Res.* 158, 223–241. doi:10.1016/S0079-6123(06)58011-2

Maglott, D., Ostell, J., Pruitt, K. D., and Tatusova, T. (2005). Entrez gene: gene-centered information at NCBI. *Nucleic Acids Res.* 33, D54–D58. doi:10.1093/nar/gki031

McClean, M. N., Mody, A., Broach, J. R., and Ramanathan, S. (2007). Cross-talk and decision making in MAP kinase pathways. *Nat. Genet.* 39, 409–414. doi:10.1038/ng1957

Menon, B., and Shorvon, S. D. (2009). Ischaemic stroke in adults and epilepsy. *Epilepsy Res.* 87, 1–11. doi:10.1016/j.eplepsyres.2009.08.007

Mielke, K., Brecht, S., Dorst, A., and Herdegen, T. (1999). Activity and expression of JNK1, p38 and ERK kinases, c-Jun N-terminal phosphorylation, and c-jun promoter binding in the adult rat brain following kainate-induced seizures. *Neuroscience* 91, 471–483. doi:10.1016/s0306-4522(98)00667-8

Mlsna, L. M., and Koh, S. (2013). Maturation-dependent behavioral deficits and cell injury in developing animals during the subacute postictal period. *Epilepsy Behav.* 29, 190–197. doi:10.1016/j.yebeh.2013.07.018

Morrison, D. K. (2012). MAP kinase pathways. *Cold Spring Harb. Perspect. Biol.* 4, a011254. doi:10.1101/cshperspect.a011254

Moshe, S. L., and Albala, B. J. (1983). Maturational changes in postictal refractoriness and seizure susceptibility in developing rats. *Ann. Neurol.* 13, 552–557. doi:10.1002/ana.410130514

Mrak, R. E., and Griffin, W. S. (2005). Glia and their cytokines in progression of neurodegeneration. *Neurobiol. Aging* 26, 349–354. doi:10.1016/j.neurobiolaging.2004.05.010

Natarajan, M., Lin, K. M., Hsueh, R. C., Sternweis, P. C., and Ranganathan, R. (2006). A global analysis of cross-talk in a mammalian cellular signalling network. *Nat. Cell Biol.* 8, 571–580. doi:10.1038/ncb1418

Nitecka, L., Tremblay, E., Charton, G., Bouillot, J. P., Berger, M. L., and Ben-Ari, Y. (1984). Maturation of kainic acid seizure-brain damage syndrome in the rat. II. Histopathological sequelae. *Neuroscience* 13, 1073–1094. doi:10.1016/0306-4522(84)90289-6

Okada, R., Moshe, S. L., and Albala, B. J. (1984). Infantile status epilepticus and future seizure susceptibility in the rat. *Brain Res.* 317, 177–183. doi:10.1016/0165-3806(84)90095-6

Okamoto, O. K., Janjoppi, L., Bonone, F. M., Pansani, A. P., Da Silva, A. V., Scorza, F. A., et al. (2010). Whole transcriptome analysis of the hippocampus: toward a molecular portrait of epileptogenesis. *BMC Genomics* 11, 230. doi:10.1186/1471-2164-11-230

Oprica, M., Eriksson, C., and Schultzberg, M. (2003). Inflammatory mechanisms associated with brain damage induced by kainic acid with special reference to the interleukin-1 system. *J. Cell. Mol. Med.* 7, 127–140. doi:10.1111/j.1582-4934.2003.tb00211.x

Parent, J. M., Yu, T. W., Leibowitz, R. T., Geschwind, D. H., Sloviter, R. S., and Lowenstein, D. H. (1997). Dentate granule cell neurogenesis is increased by seizures and contributes to aberrant network reorganization in the adult rat hippocampus. *J. Neurosci.* 17, 3727–3738. doi:10.1523/jneurosci.17-10-03727.1997

Peterson, P. K., Hu, S., Salak-Johnson, J., Molitor, T. W., and Chao, C. C. (1997). Differential production of and migratory response to beta chemokines by human microglia and astrocytes. *J. Infect. Dis.* 175, 478–481. doi:10.1093/infdis/175.2.478

Peti, W., and Page, R. (2013). Molecular basis of MAP kinase regulation. *Protein Sci.* 22, 1698–1710. doi:10.1002/pro.2374

Pfisterer, U., Petukhov, V., Demharter, S., Meichsner, J., Thompson, J. J., Batiuk, M. Y., et al. (2020). Author Correction: Identification of epilepsy-associated neuronal subtypes and gene expression underlying epileptogenesis. *Nat. Commun.* 11, 5988. doi:10.1038/s41467-020-19869-5

Pitkanen, A., Kharatishvili, I., Karhunen, H., Lukasiuk, K., Immonen, R., Nairismagi, J., et al. (2007). Epileptogenesis in experimental models. *Epilepsia* 48, 13–20. doi:10.1111/j.1528-1167.2007.01063.x

Pitkanen, A., Immonen, R. J., Grohn, O. H., and Kharatishvili, I. (2009). From traumatic brain injury to posttraumatic epilepsy: what animal models tell us about the process and treatment options. *Epilepsia* 50, 21–29. doi:10.1111/j.1528-1167.2008.02007.x

Pure, E., and Cuff, C. A. (2001). A crucial role for CD44 in inflammation. *Trends Mol. Med.* 7, 213–221. doi:10.1016/s1471-4914(01)01963-3

Ravizza, T., Gagliardi, B., Noe, F., Boer, K., Aronica, E., and Vezzani, A. (2008). Innate and adaptive immunity during epileptogenesis and spontaneous seizures: evidence from experimental models and human temporal lobe epilepsy. *Neurobiol. Dis.* 29, 142–160. doi:10.1016/j.nbd.2007.08.012

Ren, L. Q., Gourmala, N., Boddeke, H. W., and Gebicke-Haerter, P. J. (1998). Lipopolysaccharide-induced expression of IP-10 mRNA in rat brain and in cultured rat astrocytes and microglia. *Brain Res. Mol. Brain Res.* 59, 256–263. doi:10.1016/s0169-328x(98)00170-3

Romijn, H. J., Hofman, M. A., and Gramsbergen, A. (1991). At what age is the developing cerebral cortex of the rat comparable to that of the full-term newborn human baby? *Early Hum. Dev.* 26, 61–67. doi:10.1016/0378-3782(91)90044-4

Safran, M., Solomon, I., Shmueli, O., Lapidot, M., Shen-Orr, S., Adato, A., et al. (2002). GeneCards 2002: towards a complete, object-oriented, human gene compendium. *Bioinformatics* 18, 1542–1543. doi:10.1093/bioinformatics/18.11.1542

Salazar, A., Jabbari, B., Vance, S., Grafman, J., Amin, D., and Dillon, J. (1985). Epilepsy after penetrating head injury. I. Clinical correlates: A report of the vietnam head injury study. *Neurology* 35, 1406–1414. doi:10.1212/wnl.35.10.1406

Salman, M. M., Sheilabi, M. A., Bhattacharyya, D., Kitchen, P., Conner, A. C., Bill, R. M., et al. (2017). Transcriptome analysis suggests a role for the differential expression of cerebral aquaporins and the MAPK signalling pathway in human temporal lobe epilepsy. *Eur. J. Neurosci.* 46, 2121–2132. doi:10.1111/ejn.13652

Sayin, U., Sutula, T. P., and Stafstrom, C. E. (2004). Seizures in the developing brain cause adverse long-term effects on spatial learning and anxiety. *Epilepsia* 45, 1539–1548. doi:10.1111/j.0013-9580.2004.54903.x

Schaefer, C. F., Anthony, K., Krupa, S., Buchoff, J., Day, M., Hannay, T., et al. (2009). PID: the pathway interaction database. *Nucleic Acids Res.* 37, D674–D679. doi:10.1093/nar/gkn653

Scharfman, H. E., Goodman, J. H., and Sollas, A. L. (2000). Granule-like neurons at the hilar/CA3 border after status epilepticus and their synchrony with area CA3 pyramidal cells: functional implications of seizure-induced neurogenesis. *J. Neurosci.* 20, 6144–6158. doi:10.1523/jneurosci.20-16-06144.2000

Schwab, J. M., Frei, E., Klusman, I., Schnell, L., Schwab, M. E., and Schluesener, H. J. (2001). AIF-1 expression defines a proliferating and alert microglial/macrophage phenotype following spinal cord injury in rats. *J. Neuroimmunol.* 119, 214–222. doi:10.1016/s0165-5728(01)00375-7

Shaftel, S. S., Carlson, T. J., Olschowka, J. A., Kyrkanides, S., Matousek, S. B., and O'banion, M. K. (2007). Chronic interleukin-1beta expression in mouse brain leads to leukocyte infiltration and neutrophil-independent blood brain barrier permeability without overt neurodegeneration. *J. Neurosci.* 27, 9301–9309. doi:10.1523/JNEUROSCI.1418-07.2007

Shapiro, L. A., Wang, L., and Ribak, C. E. (2008). Rapid astrocyte and microglial activation following pilocarpine-induced seizures in rats. *Epilepsia* 49, 33–41. doi:10.1111/j.1528-1167.2008.01491.x

Shen, Y. H., Godlewski, J., Zhu, J., Sathyanarayana, P., Leaner, V., Birrer, M. J., et al. (2003). Cross-talk between JNK/SAPK and ERK/MAPK pathways: sustained activation of JNK blocks ERK activation by mitogenic factors. *J. Biol. Chem.* 278, 26715–26721. doi:10.1074/jbc.M303264200

Shima, Y., Kawaguchi, S. Y., Kosaka, K., Nakayama, M., Hoshino, M., Nabeshima, Y., et al. (2007). Opposing roles in neurite growth control by two seven-pass transmembrane cadherins. *Nat. Neurosci.* 10, 963–969. doi:10.1038/nn1933

Shyu, W. C., Lin, S. Z., Chiang, M. F., Chen, D. C., Su, C. Y., Wang, H. J., et al. (2008). Secretoneurin promotes neuroprotection and neuronal plasticity via the Jak2/Stat3 pathway in murine models of stroke. *J. Clin. Invest.* 118, 133–148. doi:10.1172/JCI32723

Sloviter, R. S. (1987). Decreased hippocampal inhibition and a selective loss of interneurons in experimental epilepsy. *Science* 235, 73–76. doi:10.1126/science.2879352

Somera-Molina, K. C., Robin, B., Somera, C. A., Anderson, C., Stine, C., Koh, S., et al. (2007). Glial activation links early-life seizures and long-term neurologic dysfunction: evidence using a small molecule inhibitor of proinflammatory cytokine upregulation. *Epilepsia* 48, 1785–1800. doi:10.1111/j.1528-1167.2007.01135.x

Stafstrom, C. E., Thompson, J. L., and Holmes, G. L. (1992). Kainic acid seizures in the developing brain: status epilepticus and spontaneous recurrent seizures. *Brain Res. Dev. Brain Res.* 65, 227–236. doi:10.1016/0165-3806(92)90184-x

Stellwagen, D., and Malenka, R. C. (2006). Synaptic scaling mediated by glial TNF-alpha. *Nature* 440, 1054–1059. doi:10.1038/nature04671

Stelzer, G., Harel, A., Rosen, N., Shmoish, M., Iny Stein, T., Sirota, A., et al. (2008). "GeneCards: One stop site for human gene research," in 5th Congress of the Federation of the Israel Societies for Experimental Biology.

Storey, J. D., and Tibshirani, R. (2003). Statistical significance for genomewide studies. *Proc. Natl. Acad. Sci. U. S. A.* 100, 9440–9445. doi:10.1073/pnas.1530509100

Suganuma, T., and Workman, J. L. (2012). MAP kinases and histone modification. *J. Mol. Cell Biol.* 4, 348–350. doi:10.1093/jmcb/mjs043

Sutula, T., Cascino, G., Cavazos, J., Parada, I., and Ramirez, L. (1989). Mossy fiber synaptic reorganization in the epileptic human temporal lobe. *Ann. Neurol.* 26, 321–330. doi:10.1002/ana.410260303

Tarrant, J. M., Robb, L., Van Spriel, A. B., and Wright, M. D. (2003). Tetraspanins: Molecular organisers of the leukocyte surface. *Trends Immunol.* 24, 610–617. doi:10.1016/j.it.2003.09.011

Tauck, D. L., and Nadler, J. V. (1985). Evidence of functional mossy fiber sprouting in hippocampal formation of kainic acid-treated rats. *J. Neurosci.* 5, 1016–1022. doi:10.1523/jneurosci.05-04-01016.1985

Thomas, P. D., Campbell, M. J., Kejariwal, A., Mi, H., Karlak, B., Daverman, R., et al. (2003). PANTHER: A library of protein families and subfamilies indexed by function. *Genome Res.* 13, 2129–2141. doi:10.1101/gr.772403

Thompson, P. J., and Duncan, J. S. (2005). Cognitive decline in severe intractable epilepsy. *Epilepsia* 46, 1780–1787. doi:10.1111/j.1528-1167.2005.00279.x

Tissir, F., Bar, I., Jossin, Y., De Backer, O., and Goffinet, A. M. (2005). Protocadherin Celsr3 is crucial in axonal tract development. *Nat. Neurosci.* 8, 451–457. doi:10.1038/nn1428

Tremblay, E., Nitecka, L., Berger, M. L., and Ben-Ari, Y. (1984). Maturation of kainic acid seizure-brain damage syndrome in the rat. I. Clinical, electrographic and metabolic observations. *Neuroscience* 13, 1051–1072. doi:10.1016/0306-4522(84)90288-4

Twigger, S. N., Shimoyama, M., Bromberg, S., Kwitek, A. E., and Jacob, H. J.RGD Team (2007). The Rat Genome Database, update 2007--easing the path from disease to data and back again. *Nucleic Acids Res.* 35, D658–D662. doi:10.1093/nar/gkl988

van Gassen, K. L., De Wit, M., Koerkamp, M. J., Rensen, M. G., Van Rijen, P. C., Holstege, F. C., et al. (2008). Possible role of the innate immunity in temporal lobe epilepsy. *Epilepsia* 49, 1055–1065. doi:10.1111/j.1528-1167.2007.01470.x

Van Wagoner, N. J., and Benveniste, E. N. (1999). Interleukin-6 expression and regulation in astrocytes. *J. Neuroimmunol.* 100, 124–139. doi:10.1016/s0165-5728(99)00187-3

Vezzani, A., and Granata, T. (2005). Brain inflammation in epilepsy: experimental and clinical evidence. *Epilepsia* 46, 1724–1743. doi:10.1111/j.1528-1167.2005.00298.x

Wang, X., Ellison, J. A., Siren, A. L., Lysko, P. G., Yue, T. L., Barone, F. C., et al. (1998). Prolonged expression of interferon-inducible protein-10 in ischemic cortex after permanent occlusion of the middle cerebral artery in rat. *J. Neurochem.* 71, 1194–1204. doi:10.1046/j.1471-4159.1998.71031194.x

Wang, Y. Y., Smith, P., Murphy, M., and Cook, M. (2010). Global expression profiling in epileptogenesis: does it add to the confusion? *Brain Pathol.* 20, 1–16. doi:10.1111/j.1750-3639.2008.00254.x

Whitmarsh, A. J. (2007). Regulation of gene transcription by mitogen-activated protein kinase signaling pathways. *Biochim. Biophys. Acta* 1773, 1285–1298. doi:10.1016/j.bbamcr.2006.11.011

Williams, P. A., White, A. M., Clark, S., Ferraro, D. J., Swiercz, W., Staley, K. J., et al. (2009). Development of spontaneous recurrent seizures after kainate-induced status epilepticus. *J. Neurosci.* 29, 2103–2112. doi:10.1523/JNEUROSCI.0980-08.2009

Wilson, D. N., Chung, H., Elliott, R. C., Bremer, E., George, D., and Koh, S. (2005). Microarray analysis of postictal transcriptional regulation of neuropeptides. *J. Mol. Neurosci.* 25, 285–298. doi:10.1385/JMN:25:3:285

Wu, H. Y., Tang, X. Q., Liu, H., Mao, X. F., and Wang, Y. X. (2018). Both classic Gs-cAMP/PKA/CREB and alternative Gs-cAMP/PKA/p38β/CREB signal pathways mediate exenatide-stimulated expression of M2 microglial markers. *J. Neuroimmunol.* 316, 17–22. doi:10.1016/j.jneuroim.2017.12.005

Xu, D., Robinson, A. P., Ishii, T., Duncan, D. S., Alden, T. D., Goings, G. E., et al. (2018). Peripherally derived T regulatory and γδ T cells have opposing roles in the pathogenesis of intractable pediatric epilepsy. *J. Exp. Med.* 215, 1169–1186. doi:10.1084/jem.20171285

Yamagata, K., Andreasson, K. I., Kaufmann, W. E., Barnes, C. A., and Worley, P. F. (1993). Expression of a mitogen-inducible cyclooxygenase in brain neurons: regulation by synaptic activity and glucocorticoids. *Neuron* 11, 371–386. doi:10.1016/0896-6273(93)90192-t

Yang, H., and Chen, C. (2008). Cyclooxygenase-2 in synaptic signaling. *Curr. Pharm. Des.* 14, 1443–1451. doi:10.2174/138161208784480144

Zhang, X. W., Liu, Q., Wang, Y., and Thorlacius, H. (2001). CXC chemokines, MIP-2 and KC, induce P-selectin-dependent neutrophil rolling and extravascular migration *in vivo*. *Br. J. Pharmacol.* 133, 413–421. doi:10.1038/sj.bjp.0704087

Zhang, X., Cui, S. S., Wallace, A. E., Hannesson, D. K., Schmued, L. C., Saucier, D. M., et al. (2002). Relations between brain pathology and temporal lobe epilepsy. *J. Neurosci.* 22, 6052–6061. doi:10.1523/JNEUROSCI.22-14-06052.2002

frontiers | Frontiers in Neurology

TYPE Original Research
PUBLISHED 14 September 2022
DOI 10.3389/fneur.2022.902157

OPEN ACCESS

EDITED BY
Xinjian Zhu,
Southeast University, China

REVIEWED BY
Izumi Kawachi,
Niigata University, Japan
Thashi Chang,
University of Colombo, Sri Lanka

*CORRESPONDENCE
Riki Matsumoto
matsumot@med.kobe-u.ac.jp
Akio Ikeda
akio@kuhp.kyoto-u.ac.jp

†These authors have contributed equally to this work

SPECIALTY SECTION
This article was submitted to Epilepsy, a section of the journal Frontiers in Neurology

RECEIVED 22 March 2022
ACCEPTED 19 July 2022
PUBLISHED 14 September 2022

CITATION
Sakamoto M, Matsumoto R, Shimotake A, Togawa J, Takeyama H, Kobayashi K, Leypoldt F, Wandinger K-P, Kondo T, Takahashi R and Ikeda A (2022) Diagnostic value of an algorithm for autoimmune epilepsy in a retrospective cohort. *Front. Neurol.* 13:902157. doi: 10.3389/fneur.2022.902157

Diagnostic value of an algorithm for autoimmune epilepsy in a retrospective cohort

Mitsuhiro Sakamoto[1,2], Riki Matsumoto[1,3*†], Akihiro Shimotake[1], Jumpei Togawa[4], Hirofumi Takeyama[4,5], Katsuya Kobayashi[1], Frank Leypoldt[6], Klaus-Peter Wandinger[7], Takayuki Kondo[8], Ryosuke Takahashi[1] and Akio Ikeda[9*†]

[1]Department of Neurology, Kyoto University Graduate School of Medicine, Kyoto, Japan, [2]Department of Neurology, Rakuwakai Otowa Hospital, Kyoto, Japan, [3]Division of Neurology, Kobe University Graduate School of Medicine, Kobe, Japan, [4]Department of Respiratory Care and Sleep Control Medicine, Kyoto University Graduate School of Medicine, Kyoto, Japan, [5]Department of Neurology, Japanese Red Cross Otsu Hospital, Otsu, Japan, [6]Neuroimmunology, Institute of Clinical Chemistry, University Hospital Schleswig-Holstein, Kiel, Germany, [7]Neuroimmunology, Institute of Clinical Chemistry, University Hospital Schleswig-Holstein, Lübeck, Germany, [8]Department of Neurology, Kansai Medical University Medical Center, Moriguchi, Japan, [9]Department of Epilepsy, Movement Disorders and Physiology, Kyoto University Graduate School of Medicine, Kyoto, Japan

Purpose: This study aims to propose a diagnostic algorithm for autoimmune epilepsy in a retrospective cohort and investigate its clinical utility.

Methods: We reviewed 60 patients with focal epilepsy with a suspected autoimmune etiology according to board-certified neurologists and epileptologists. To assess the involvement of the autoimmune etiology, we used the patients' sera or cerebrospinal fluid (CSF) samples to screen for antineuronal antibodies using rat brain immunohistochemistry. Positive samples were analyzed for known antineuronal antibodies. The algorithm applied to assess the data of all patients consisted of two steps: evaluation of clinical features suggesting autoimmune epilepsy and evaluation using laboratory and imaging findings (abnormal CSF findings, hypermetabolism on fluorodeoxyglucose-positron emission tomography, magnetic resonance imaging abnormalities, and bilateral epileptiform discharges on electroencephalography). Patients were screened during the first step and classified into five groups according to the number of abnormal laboratory findings. The significant cutoff point of the algorithm was assessed using a receiver-operating characteristic curve analysis.

Results: Fourteen of the 60 patients (23.3%) were seropositive for antineuronal antibodies using rat brain immunohistochemistry. Ten patients had antibodies related to autoimmune epilepsy/encephalitis. The cutoff analysis of the number of abnormal laboratory and imaging findings showed that the best cutoff point was two abnormal findings, which yielded a sensitivity of 78.6%, a specificity of 76.1%, and an area under the curve of 0.81.

Conclusion: The proposed algorithm could help predict the underlying autoimmune etiology of epilepsy before antineuronal antibody test results are available.

KEYWORDS

observational study, epilepsy, focal seizures, autoimmune disease, diagnostic test assessment

Introduction

As a result of advancements in antibody detection technology since the 2000s, antibodies against antineuronal cell-surface antigens have been discovered (1, 2), and many types of autoimmune encephalitis associated with these antibodies have been reported. The existence of epilepsy syndrome associated with an autoimmune etiology was proposed in the early twenty-first century (3), and it has also been demonstrated that antineuronal antibodies are present in patients with classical focal epilepsy syndromes (4). In the latest International League Against Epilepsy (ILAE) classification of epilepsy in 2017, immunity was adopted for the first time as one of the etiologies of epilepsy (5). It has been reported that immunotherapy is successful in treating antineuronal antibody-positive refractory epilepsy and that early treatment improves the patient prognosis (6, 7). However, in real-world medical practice, antibody testing may be inaccessible, thereby rendering an early diagnosis of autoimmune epilepsy difficult worldwide. Additionally, patients may have epilepsy associated with an autoimmune etiology despite negative antineuronal antibody results. Recently, clinical features suggestive of autoimmune epilepsy have been proposed (7), and a clinical approach to the diagnosis of autoimmune encephalitis has been presented (8). The antibody prevalence in epilepsy (APE) score and the antibodies contributing to focal epilepsy signs and symptoms (ACES) score may be helpful when selecting patients who require antibody testing (9, 10). However, definitive diagnostic criteria have not been established. Herein, we propose and validate a diagnostic algorithm for autoimmune epilepsy in a cohort of patients who underwent antineuronal antibody testing. We adopted this algorithm approach without antibody testing because this follows the real-life medical process that ranges from assessing the clinical history and symptoms to laboratory examinations.

Materials and methods

Standard protocol approvals, registrations, and patient consent

This study was approved by the ethics committee of the Kyoto University Graduate School of Medicine (no. C-0588). All patients provided written informed consent.

The cohort consisted of 60 patients with focal epilepsy suspected of having an autoimmune etiology according to board-certified neurologists and epileptologists at the clinic of Kyoto University Hospital. All patients were admitted to the hospital from January 2012 to March 2017, and underwent comprehensive evaluations for epilepsy. We included 40 out of 70 patients from the preliminary cohort (11) whose serum or CSF samples were available to check the rat brain immunohistochemistry and comprehensive antibody testing, and added 20 patients who were admitted after the previous study had been completed. When patients had other obvious neurological diseases, such as paraneoplastic neurological syndrome and multiple sclerosis (MS), they were excluded from the present study. Two patients were excluded. The first patient was diagnosed as having paraneoplastic neurological syndrome because of typical symptoms, and he suddenly died from advanced gastric cancer after being diagnosed. The second one was diagnosed with tumefactive MS in light of the MRI findings.

Immunological analysis

The cerebrospinal fluid (CSF) or serum samples were initially screened for reactivity with rat brain through immunohistochemistry as reported elsewhere (12, 13). In brief, fresh rat brains were split, briefly fixed in 4°C paraformaldehyde in PBS for 30 min, and then dehydrated in 40% sucrose in PBS at 4°C overnight. Brains were frozen in liquid nitrogen and cut into 7 μm sections on a cryostat and transferred onto coverslips. After thawing, coverslips were washed in PBS, treated with 0.3% H_2O_2 in PBS, and blocked with 5% goat serum followed by incubation with serum at 1:200 or CSF at 1:4 in blocking solution overnight at 4°C. After washing, coverslips were then incubated with a goat anti-human IgG (H+L) biotinylated antibody (Vector, BA-3000) followed by staining with ABC Elite Kit (Vector PK6100) according to the manufacturer's instructions. Sections were analyzed using a Zeiss Axioscope by at least two experienced investigators blinded to the experimental conditions. Positive samples were further investigated for reactivity against specific known antigens in a sequential manner (14). First, we investigated the levels of proteins related to autoimmune epilepsy/limbic encephalitis using standardized commercially available test kits (immunofluorescence tests with tissue and fixed transfected cells, enzyme-linked immunosorbent assay, and immunoblotting [EUROIMMUN, Lubeck, Germany]). The following proteins were targeted: N-methyl-D-aspartate receptor (NMDAR); α-amino-3-hydroxy-5-methyl-4-isoxazole propionic acid receptor (AMPAR); LGI1; contactin-associated protein-like 2 (CASPR2); Delta/Notch-like epidermal growth factor-related receptor (DNER); Zic4; dipeptidyl-peptidase-like protein 6 (DPPX); γ-aminobutyric acid type B receptor (GABABR); Hu, Yo, Ri, Ma, and collapsin response mediator protein 5 (CRMP-5/CV2); and amphiphysin. Immunoreactivity for GAD65 was tested using an enzyme-linked immunosorbent assay and immunofluorescence with tissue sections. Thereafter, the negative samples were tested for the presence of antibodies against rarely occurring antigens [that is, metabotropic glutamate receptor 1 and metabotropic glutamate receptor 5 (mGluR1 and mGluR5)] (15, 16), γ-aminobutyric acid type A receptor (GABAAR), and IgLON 5 (17, 18) using specifically transfected cells. Additionally, we assessed the

myelin-oligodendrocyte glycoprotein (MOG) titers with a full-length human MOG construct transfected into HEK293T cells using indirect immunofluorescence on live, non-permeabilized cells for 12 patients whose serum was available (19). All samples that tested positive with cell-based assays, either commercial or in-house, were characterized using end-point dilutions.

We reported samples as positive if they had staining of hippocampal neuropil or GAD-typical staining (as positive GAD). We considered the nuclear stains sample to be positive, but there was no sample in this study. We considered the patients with antibodies to detectable known target antigens, that is, known antineuronal antibodies, to have "definite autoimmune epilepsy." Patients whose CSF samples showed positive reactivity in rat brain immunohistochemistry but were negative for known antineuronal antibodies were considered to have "probable seropositive autoimmune epilepsy." When the serum samples had positive rat brain immunohistochemistry but the CSF samples were negative, or when CSF samples were not available, we considered these patients to have "possible seropositive autoimmune epilepsy."

Thereafter, we retrospectively applied the diagnostic algorithm to our cohort. To analyze our algorithm, we considered patients with seropositivity for antineuronal antibodies according to an assessment using rat brain immunohistochemistry (herein referred to as seropositive) to have autoimmune epilepsy with a definite, probable, or possible seropositive status and validated the usefulness of the diagnostic algorithm.

Algorithm

In a real-world clinical environment, the medical history is first assessed, followed by laboratory tests, evaluation of these test results, and the final diagnosis. We previously proposed such a diagnostic algorithm for autoimmune epilepsy and evaluated its clinical utility (11). In this preliminary investigation, the diagnostic algorithm followed the "real-world" practical procedures, from assessing medical history/clinical symptoms to laboratory examinations, taking into account the "clinical features suggesting autoimmune epilepsy" (7). Based on

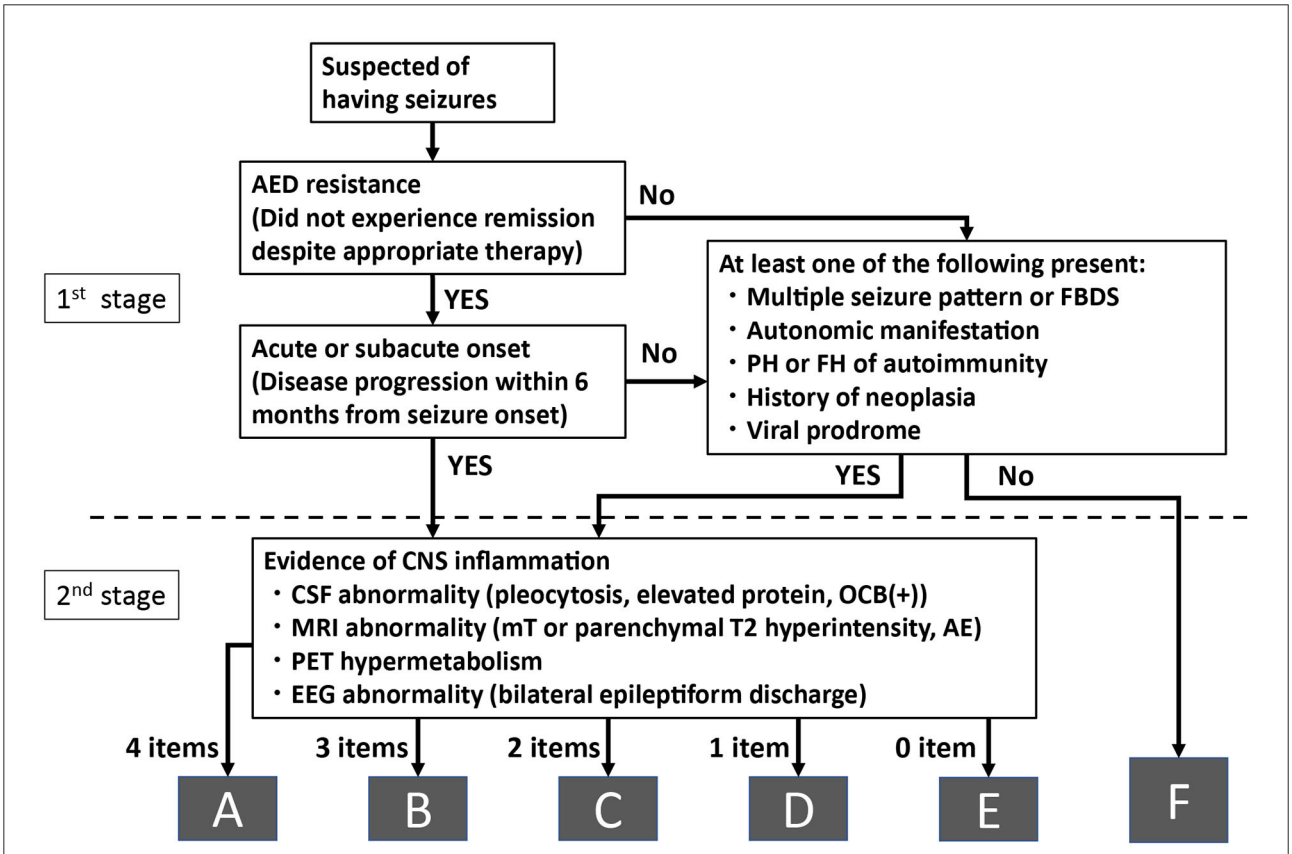

FIGURE 1
Algorithm for diagnosing autoimmune epilepsy without evaluating antineuronal antibodies. AE, amygdala enlargement; AED, antiepileptic drugs; CNS, central nervous system; CSF, cerebrospinal fluid; EEG, electroencephalography; FBDS, faciobrachial dystonic seizure; FH, family history; MRI, magnetic resonance imaging; mT, medial temporal; OCB, oligoclonal bands; PET, positron emission tomography; PH, past history.

our preliminary investigation, which included several false-negative results, we revised the diagnostic algorithm by adding peri-ictal autonomic symptoms and electroencephalography (EEG) findings and evaluated its utility in a larger cohort who underwent comprehensive antineuronal antibody testing (Figure 1) (8, 20, 21). The algorithm consisted of two stages. During the first stage, we assessed the clinical information, such as the medical history and ictal symptoms. Specifically, we assessed "refractory seizure to appropriate drug therapy" and "acute or subacute onset (disease progression within 6 months from seizure onset)" or having one of the following characteristic clinical features: "multiple seizure types or facial brachial dystonic seizures (FBDS)," "ictal autonomic manifestations," "past or family history of autoimmune disease," "history of malignancy," and "virus prodrome" (22). Regarding the ictal autonomic manifestations, we included cardiovascular, respiratory, gastrointestinal, thermoregulatory, vasomotor, pilomotor, sensory, genital, and urinary manifestations; however, we excluded epigastric rising sensation, nausea, and urinary incontinence because these symptoms are commonly observed with typical mesial temporal lobe epilepsy, such as hippocampal sclerosis.

When applying this algorithm to the retrospective cohort, we considered the patients to have acute or subacute onset when they were admitted to the hospital for evaluation and treated within 6 months of their seizure onset.

When the patients satisfied any of these conditions, we considered that they had a high possibility of autoimmune epilepsy based on clinical reasons and recommended that they proceed to the second stage for further laboratory analyses. When the patients did not satisfy the first stage of the algorithm, they were classified into the group with a low possibility of autoimmune epilepsy (group F).

During the second stage, we evaluated the results of four examinations listed below:

1) "Abnormal CSF finding:" elevated cell count (>5 cells per μL), elevated protein levels (> 40 mg / dl), or positive oligoclonal band.
2) "Abnormal brain magnetic resonance imaging (MRI) findings" (medial temporal or parenchymal including white matter lesions hyperintense signal on T2-weighted image (T2WI) or fluid-attenuated inversion recovery sequence (FLAIR) and/or amygdala enlargement).
3) "Hypermetabolism on fluorodeoxyglucose-positron emission tomography (FDG-PET)."
4) "EEG with bilateral epileptiform discharge (independently recorded either ictally or interictally)."

Patients who had positive findings in all the four examinations during the second stage were classified into group A. Similarly, when patients had three, two, one, or none of the positive findings in four examinations during the second stage, they were classified into groups B, C, D, and E, respectively.

Abnormal MRI and FDG-PET findings were determined by visual inspection. Amygdala enlargement was defined as a unilateral or bilateral enlargement of the amygdala on FLAIR or T2WI, irrespective of signal changes. The findings were judged by three board-certified neurologists or radiologists to reach a consensus. We considered the findings significant when two or more evaluators observed abnormal findings. We only evaluated the MRI results obtained at our hospital. We included bilateral epileptiform discharges and EEG seizure patterns (including periodic patterns) as abnormal EEG findings in this article, and we did not mention the specific EEG findings for autoimmune encephalitis, such as extreme delta brush.

Comparison with other scores

To compare the diagnostic value of the algorithm with that of the previously published APE score (9) and ACES score (10), we applied these scores to the patients in our cohort and calculated the sensitivity and specificity of each score. We then compared the diagnostic value of our algorithm with that of the scores.

Statistical analysis

Univariate analyses of nominal and interval variables were performed using the Fisher exact test and the Wilcoxon test, respectively. To evaluate this diagnosis algorithm, we conducted a receiver operating characteristic (ROC) curve analysis (23). The optimal cutoff was determined by "the closest to (0, 1) criteria": the point on the curve closest to the point which implies the perfect scenario, 100% sensitivity, and 100% specificity.

Results

The algorithm was applied to 60 patients. Thirty-four patients (57%) were female and the median age at onset was 55 years (range: 9–83 years) (Table 1). MRI and EEG were performed for all patients, but the CSF and FDG-PET examinations were performed for 55 and 58 patients, respectively (Table 2). Fourteen patients had CSF or serum reactivity with rat brain immunohistochemistry [CSF: 9/49 patients (18%); serum: 5/11 patients (45%)]. Among 14 patients with positive immunohistochemistry results, monospecific cell-based assays against the specific antigens related to autoimmune epilepsy/limbic encephalitis revealed that 10 patients had antibodies against a specific antigen (LGI1, 5 patients; GAD, 4 patients; N-methyl-D-aspartate receptor: 1 patient). We considered them to have "definite autoimmune epilepsy." The

10.3389/fneur.2022.902157

TABLE 1 Demographic clinical data of the patients.

	Seropositive patients	Seroneative patients	*P*-Value
Age at onset, median (range)	39 y (9–83)	55 y (14–73)	0.44
Time to admission, median (range)	5.5 mo (1–172)	11 mo (1–420)	0.38
Female sex	11 (79%)	23 (50%)	0.07
History of febrile seizures	0	4 (8.7%)	0.56
Cognitive symtoms	10 (71%)	13 (28%)	0.005
Admission within 6 months (subacute)	8 (57%)	16 (35%)	0.21
AED resistance	12 (86%)	26 (56%)	0.06
Multiple seizure types or FBDS	3 (21%)	0	0.01
Personal history of autoimmunity	4 (29%)	6 (13%)	0.22
Neoplasm or ovarian cyst	0	3 (7%)	1.00
Viral prodrome	1 (7%)	1 (2%)	0.23
Autonomic manifestation	6 (43%)	9 (15%)	0.003

AED, antiepileptic drugs; FBDS, faciobrachial dystonic seizure; mo, month.

TABLE 2 Laboratory data of the patients.

	Seropositive patients	Seronegative patients	*P*-Value
CSF abnormality[a]	7/14 (50%)	22/41 (54%)	1.00
MRI abnormality[b]	11 (79%)	24 (52%)	0.12
T2WI/FLAIR HIA in the temporal lobes	9 (64%)	16 (34%)	0.07
T2WI/FLAIR HIA in the extratemporal lobes	4 (29%)	4 (8.7%)	0.08
Amygdala enlargement	5 (36%)	10 (22%)	0.31
FDG-PET hypermetabolism[a]	9/14 (64%)	10/44 (23%)	0.007
Bilateral EEG epileptiform discharge	8 (57%)	15 (32%)	0.12
LGI1	5 (36%)		
GAD	4 (29%)		
NMDAR	1 (7%)		
Seropositive but not specified	4 (29%)		

[a]Examinations of a limited number of patients. The percentage was calculated based on the results of these patients.
[b]MRI abnormalities included T2-weighted/FLAIR hyperintense lesions and/or amygdala enlargement.
CSF, cerebrospinal fluid; EEG, electroencephalography; FDG-PET, fluorodeoxyglucose-positron emission tomography; FLAIR, fluid-attenuated inversion recovery; GAD, glutamic acid decarboxylase; HIA, high-intensity area; LGI1, leucine-rich glioma-inactivated 1; MRI, magnetic resonance imaging; NMDAR, N-methyl-D-aspartate receptor.

findings are summarized in Table 2. Regarding the remaining four patients, one was classified as having "probable seropositive autoimmune epilepsy" and three were classified as having "possible seropositive autoimmune epilepsy."

In terms of classifications according to the diagnostic algorithm among 60 patients, 31 (52%) fulfilled the criteria during the first stage and were considered to have possible autoimmune epilepsy; therefore, they underwent further laboratory evaluations. The remaining 29 patients were classified as having a low possibility of autoimmune epilepsy (group F). During the second stage, 5 patients were classified into group A (8%), 6 were classified into group B (10%), 11 were classified into group C (18%), 7 were classified into group D (12%), and 2 were classified into group E (3%) (Supplementary Figure 1). Among the 14 seropositive patients, 13 proceeded to the second stage and one patient with LGI1-positive antibodies in CSF did not (group F). That one patient had a single generalized tonic-clonic seizure that was controlled by an antiepileptic drug and showed slowly progressive memory impairment and irritability. The EEG results indicated frequent subclinical independent seizures in the bilateral temporal regions, and the MRI and FDG-PET results suggested inflammation of the medial temporal area, including the amygdala, as reported elsewhere (24).

The findings of all patients are summarized in Tables 1, 2, and the clinical and laboratory features of seropositive patients are shown in the Supplementary Table. Abnormalities were observed in seven patients (50%) during the CSF examination, in 11 patients (79%) during the MRI examination, in nine patients (64%) during the FDG-PET examination, and in eight patients (57%) during the EEG examination. Regarding the MRI findings, T2WI/FLAIR high-intensity areas were found in 11 patients; nine were in the temporal lobe and four were in the extratemporal lobe. Amygdala enlargement was observed in five patients. In contrast, three seropositive patients had normal MRI findings.

Regarding MRI abnormalities, 29 patients had temporal lesions, 8 had extratemporal lesions, and 2 had both types of lesions (Table 2). Among the 29 patients with temporal lesions, 25 had T2WI/FLAIR high-intensity lesions and 15 had amygdala enlargement. Eleven patients had both high-signal-intensity lesions and amygdala enlargement. Among the 15 patients with amygdala enlargement, 5 were seropositive and 10 were seronegative. One antibody-positive patient (the aforementioned patient) and six seronegative patients were allocated to group F (24).

The ROC analysis indicated that the area under the curve of ROC curve was 0.81 (Figure 2) and the most optimal cutoff was identified between groups C and D (sensitivity, 0.79; specificity,

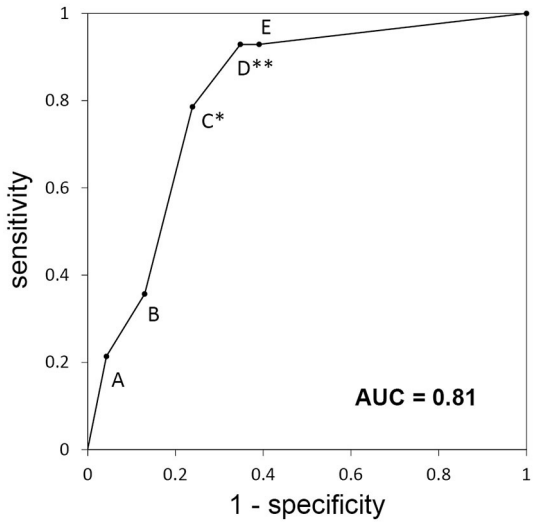

FIGURE 2
Receiver-operating characteristic curve for the categories of the diagnostic algorithm used for the retrospective cohort. Each alphabet means the sensitivity and specificity when the patients classified A to X are diagnosed with "autoimmune epilepsy." *Best optimal cutoff; **second optimal cutoff; AUC, area under the curve.

0.76). The second optimal cutoff point was located between groups D and E (sensitivity, 0.93; specificity, 0.65).

A comparison of the diagnostic value of this algorithm with that of the previously published scores (AEP score, ACES score) demonstrated that the APE score showed a sensitivity of 0.93 and specificity of 0.52, and the ACES score showed a sensitivity of 0.86 and a specificity of 0.74.

Discussion

During this study, we proposed a diagnostic algorithm without antibody testing for autoimmune epilepsy and verified its clinical utility by retrospectively applying it to a cohort who underwent a comprehensive antineuronal antibody work-up. The use of this algorithm showed the possibility of diagnosing autoimmune epilepsy without waiting for the results of antineuronal antibody testing when patients have clinical features suggestive of autoimmune epilepsy and laboratory examination results indicating two or more positive findings (groups A, B, and C). Compared with the preliminary study (11), the revised algorithm had higher sensitivity, and the use of immunohistochemistry improved the accuracy of the diagnosis of autoimmune epilepsy.

The diagnostic criteria for autoimmune limbic encephalitis have been extensively described (8); however, those for autoimmune epilepsy have been rarely reported. To the best of our knowledge, the clinical features suggestive of autoimmune epilepsy and the scoring systems for diagnosing autoimmune epilepsy have been proposed (7, 9, 10). The proposed diagnostic algorithm has two advantages over the scoring systems. First, by using this algorithm, it is possible to follow the actual clinical decision-making process of using clinical features to determine if patients should undergo laboratory examinations. This procedure would help avoid unnecessary examinations (25). Second, the second step of this algorithm incorporates laboratory findings of the CSF, MRI, PET, and EEG examinations more comprehensively. The diagnostic value of EEG findings, that is, bilateral epileptiform discharges, was not evaluated during the two aforementioned studies related to autoimmune epilepsy (8–10). Subclinical seizures detected on EEG (20) or other characteristics, such as dynamic evolution and the involvement of the perisylvian region, have been reported for autoimmune encephalitis, including anti-LGI1 antibody-positive encephalitis (21, 26), indicating the utility of EEG for diagnosing autoimmune epilepsy. Bilateral epileptiform discharges were noted in 39% of the recruited patients. On the other hand, specific EEG findings for autoimmune encephalitis, such as extreme delta brush, were not evaluated in this study. Extreme delta brush is an important EEG finding for anti-NMDAR encephalitis. However, as this is not the case for autoimmune epilepsy, how to handle these EEG findings should be thoroughly discussed.

Although this algorithm focused on the characteristics of autoimmune epilepsy, it did not evaluate psychiatric symptoms or memory impairment, which may occur because of inflammation, especially of the medial temporal structures. Some studies have shown that clinical findings of encephalitis are more associated with antibody positivity than laboratory findings (10, 27). Another report indicated that encephalitis findings are associated with good responsiveness to immunotherapy (27). One LGI1 antibody-positive patient was allocated to group F even though he had both symptoms. This patient fulfilled the diagnostic criteria for definite autoimmune limbic encephalitis but not the criteria of the present diagnostic algorithm or the scoring system for autoimmune epilepsy (8, 9). A forme fruste of limbic encephalitis could manifest as autoimmune epilepsy, but the patient may not be diagnosable by the algorithm/scoring system when the seizure is mild or is not the predominant clinical feature.

The ROC analysis showed that the optimal cutoff point between groups C and D had a sensitivity of 0.79 and a specificity of 0.76. With this cutoff, the algorithm misses approximately one-fifth of autoimmune epilepsy cases. From the viewpoint of treatment, we could choose the second optimal cutoff point between groups D and E (one or more positive findings according to laboratory examinations) that provides higher sensitivity (0.93). This cutoff point is not optimal from a more accurate diagnostic point of view (specificity of 0.65), but it would be beneficial for determining the treatment for autoimmune epilepsy refractive to antiepileptic medications but

responsive to first-line immunotherapies, such as intravenous methylprednisolone (28). This is especially true when full antibody testing is unavailable and the patient does not have contraindications for intravenous methylprednisolone.

In our cohort, we included patients who showed positive reactivity for rat brain immunohistochemistry but negative reactivity for antibodies against known or identified antigens, that is, those patients positive for antibodies against unidentified antigens. We defined these patients as having "probable seropositive autoimmune epilepsy" or "possible seropositive autoimmune epilepsy," depending on the positive results of serum and CSF testing. We should have tested the sera of "possible seropositive autoimmune epilepsy" patients using live neurons to confirm the autoimmune etiology, but it was not feasible to do so because of the limited amount of pretreatment sera available during the present study.

Four patients who had clinical features consistent with autoimmune epilepsy were identified and they underwent evaluations during the second stage. Notably, three patients had examination scores higher than the cutoff point, indicating that they would benefit from immunotherapy. The efficacy of immunotherapy has been reported for patients with suspected autoimmune limbic encephalitis but had negative test results for known antibodies (29). The absence of seizures and improvements in MRI findings, cognition, and mood were observed (14–57%); unidentified antibodies could have been associated with successful immunotherapy.

During this study, 25% of patients tested positive for immunohistochemistry; this value was higher than that reported by previous studies (9, 30). This could be attributed to our hospital being a tertiary epilepsy center where epilepsy specialists are actively diagnosing possible autoimmune epilepsy and performing further evaluations.

Regarding MRI abnormalities, the relationship between amygdala enlargement and epilepsy has recently been highlighted (31, 32). We considered amygdala enlargement as a finding suggestive of autoimmune epilepsy. A total of 15 patients had amygdala enlargement, and five were seropositive. Except for the patient whose predominant clinical features were memory impairment and psychosis (24), all seropositive patients proceeded to the second stage of the algorithm. Regarding the remaining 10 seronegative patients, one patient was allocated to group A, one patient was allocated to group B, one patient was allocated to group C, one patient was allocated to group D, and six patients were allocated to group F. Those in group F may have had pathologies, such as focal cortical dysplasia, hamartomatous lesions, and low-grade glioma, as previously reported (31, 33–35).

When amygdala enlargement occurs in the context of autoimmunity, the enlargement may remit during the clinical course (31). In our cohort, three seropositive but MRI abnormality-negative patients were observed. The amygdala volume of these patients may have been normalized during their clinical course. If available, it is important to obtain previous MRI data, especially when patients have "smoldering" autoimmune epilepsy/limbic encephalitis.

We also included extratemporal lesions as positive MRI finding in our algorithm. Autoimmune encephalitis is often related to limbic encephalitis (9). In our cohort, most patients were considered to have temporal lobe epilepsy with MRI abnormalities in the temporal lobe. However, extratemporal lesions including white matter lesions on MRI are also reported to be frequent in autoimmune epilepsy patients (36). As such, we considered these extratemporal MRI lesions in our algorithm. In this retrospective cohort, extratemporal lesions were observed in eight patients; of these eight patients, four were seropositive. This algorithm successfully detected these seropositive patients. Therefore, it would be more clinically beneficial to include extratemporal abnormalities as positive MRI findings to improve the ability to detect seropositive patients.

When comparing the diagnostic values between this algorithm and previously published scores, the sensitivity and specificity were not very different, taking into account the small size of our cohort. Especially when the second cutoff was used, this algorithm and the APE score showed very similar sensitivity and specificity. It was probably due to the overlap of the factors used in our algorithm and the APE score.

This study had some limitations. First, we applied the proposed algorithm to a retrospective and relatively small cohort and proposed a cutoff value for examinations. The patients were highly selected. In particular, as we included only inpatients, some kind of selection bias could have occurred, including, but not limited to, healthcare access bias (our hospital is a tertiary medical institution for epilepsy) and spectrum bias (the included patients were selected by board-certified neurologists and epileptologists). These facts may have artificially increased the performance of the algorithm. This algorithm should be validated for patients with focal epilepsy and not those with epilepsy with a suspected autoimmune cause. Second, this algorithm involves the potential risk of oversight for patients with other predominant symptoms of autoimmune encephalitis and mild or rare seizures. Whether we should classify these patients as having autoimmune epilepsy should be carefully discussed. Third, anti-NMDA receptor encephalitis is the most common autoimmune encephalitis (37); however, the antibody most frequently detected was the anti-LGI1 antibody and only one patient tested positive for the anti-NMDA receptor antibody during this study. This is in agreement with the finding of a previous study performed at an outpatient clinic (30). Further validation is needed to clarify the antibody that is more associated with autoimmune epilepsy, which is a form of forme fruste of autoimmune encephalitis and may have a smoldering course. Therefore, further immunohistological clarification of unidentified antibodies is also important. Fourth, we evaluated the utility of FDG-PET, but this is only accessible at tertiary

epilepsy centers. Single-photon emission computed tomography could be an alternative method because it is more accessible at several hospitals. Some case reports argued the utility of single-photon emission computed tomography hyperperfusion for autoimmune or paraneoplastic encephalitis (38–40). Fifth, anti-MOG antibodies and anti-glycine antibodies are possible causes of autoimmune epilepsy. A broad spectrum of associated clinical phenotypes that can be addressed with anti-MOG antibodies has been shown, and some cases of encephalitis with seizures have been reported (41). In our cohort, we were able to evaluate the sera of only 12 patients for anti-MOG antibodies, and all patients had negative results. This number is too low to evaluate the relevance of MOG antibodies. Anti-glycine antibodies have also been postulated in autoimmune epilepsy (42). However, testing for these antibodies needs to be interpreted carefully, since there are no confirmatory test systems and the syndrome specificity—especially of glycine antibodies—is broad. Nevertheless, anti-MOG and anti-glycine assays should be included in a prospective cohort study in the future. Finally, validation of the cutoff value and modification of the algorithm using a larger prospective cohort are warranted to establish the diagnostic algorithm for autoimmune epilepsy.

Conclusion

We proposed a diagnostic algorithm without antibody testing for autoimmune epilepsy that followed real-world practical procedures ranging from assessing the medical history/clinical symptoms to performing laboratory examinations. We verified its clinical utility by retrospectively applying the algorithm to a cohort who underwent a comprehensive antineuronal antibody work-up. This study provides Class IV evidence that this algorithm improves the diagnostic accuracy when autoimmune epilepsy is suspected, when patients have clinical features suggestive of autoimmune epilepsy, and when patients have two or more positive laboratory examination results.

Data availability statement

The data that support the findings of this study are available on request from the corresponding authors (RM and AI). The data are not publicly available because they contain information that could compromise the privacy of the research participants.

Ethics statement

The studies involving human participants were reviewed and approved by Kyoto University Graduate School and Faculty of Medicine, Ethics Committee. Written informed consent to participate in this study was provided by the participants and/or their legal guardian/next of kin.

Author contributions

Conceptualization was performed by RM, TK, RT, and AI. Methodology was created by MS, RM, FL, K-PW, TK, and AI. Formal analysis and investigation were performed by MS, RM, FL, and K-PW. Resources were arranged by RM, JT, HT, KK, AS, FL, K-PW, and AI. The manuscript was written by MS and reviewed and edited by RM, AS, FL, and AI. RM, FL, K-PW, and AI were responsible for funding acquisition. RT and AI supervised this research. All authors contributed to the article and approved the submitted version.

Funding

This work was partly supported by JSPS KAKENHI (15H05874), a research grant from the Japan Epilepsy Research Foundation (JERF TENKAN 20010), and the German Ministry of Education and Research (BMBF, 01GM1908A, Leypoldt).

Acknowledgments

We would like to thank our patients for participating in this study, as well as Mr. Hiroyasu Abe from the Department of Biomedical Statistics and Bioinformatics, Kyoto University Graduate School of Medicine, for assistance with statistical analysis.

Conflict of interest

Department of Epilepsy, Movement Disorders, and Physiology was an endowment department supported by a grant from GlaxoSmithKline K.K., NIHON KOHDEN CORPORATION, Otsuka Pharmaceutical Co., and UCB Japan Co., Ltd. until May 2018. Since 1 June 2018, this department has changed to Industry-Academia Collaboration Courses supported by a grant from Eisai Co., Ltd., NIHON KOHDEN CORPORATION, Otsuka Pharmaceutical Co., and UCB Japan Co., Ltd. Author AI is a current member of this department, and Authors RM and AS are previous members of this department. Department of Respiratory Care and Sleep Control Medicine is funded by endowments from Philips Japan, ResMed, Fukuda Denshi, and Fukuda Lifetec Keiji to Kyoto University. Author JT is a current member of this department, and author HT is a previous member of this department. Authors K-PW and FL report speakers honoraria from Bayer, Roche, Novartis, and Fresenius, have received travel funding from Merck, Grifols, and Bayer, and serve on the advisory boards for Roche, Biogen, and Alexion.

The remaining authors declare that the research was conducted in the absence of any commercial or financial relationships that could be construed as a potential conflict of interest.

Publisher's note

All claims expressed in this article are solely those of the authors and do not necessarily represent those of their affiliated organizations, or those of the publisher, the editors and the reviewers. Any product that may be evaluated in this article, or claim that may be made by its manufacturer, is not guaranteed or endorsed by the publisher.

Supplementary material

The Supplementary Material for this article can be found online at: https://www.frontiersin.org/articles/10.3389/fneur.2022.902157/full#supplementary-material

References

1. Dalmau J, Gleichman AJ, Hughes EG, Rossi JE, Peng X, Lai M, et al. Anti-NMDA-receptor encephalitis: case series and analysis of the effects of antibodies. *Lancet Neurol.* (2008) 7:1091–8. doi: 10.1016/S1474-4422(08)70224-2

2. Irani SR, Alexander S, Waters P, Kleopa KA, Pettingill P, Zuliani L, et al. Antibodies to Kv1 potassium channel-complex proteins leucine-rich, glioma inactivated 1 protein and contactin-associated protein-2 in limbic encephalitis, Morvan's syndrome and acquired neuromyotonia. *Brain.* (2010) 133:2734–48. doi: 10.1093/brain/awq213

3. Levite M. Autoimmune epilepsy. *Nat Immunol.* (2002) 3:500. doi: 10.1038/ni0602-500

4. Ekizoglu E, Tuzun E, Woodhall M, Lang B, Jacobson L, Icoz S, et al. Investigation of neuronal autoantibodies in two different focal epilepsy syndromes. *Epilepsia.* (2014) 55:414-22. doi: 10.1111/epi.12528

5. Scheffer IE, Berkovic S, Capovilla G, Connolly MB, French J, Guilhoto L, et al. ILAE classification of the epilepsies: position paper of the ILAE commission for classification and terminology. *Epilepsia.* (2017) 58:512–21. doi: 10.1111/epi.13709

6. Quek AM, Britton JW, McKeon A, So E, Lennon VA, Shin C, et al. Autoimmune epilepsy: clinical characteristics and response to immunotherapy. *Arch Neurol.* (2012) 69:582–93. doi: 10.1001/archneurol.2011.2985

7. Toledano M, Britton JW, McKeon A, Shin C, Lennon VA, Quek AM, et al. Utility of an immunotherapy trial in evaluating patients with presumed autoimmune epilepsy. *Neurology.* (2014) 82:1578–86. doi: 10.1212/WNL.0000000000000383

8. Graus F, Titulaer MJ, Balu R, Benseler S, Bien CG, Cellucci T, et al. A clinical approach to diagnosis of autoimmune encephalitis. *Lancet Neurol.* (2016) 15:391–404. doi: 10.1016/S1474-4422(15)00401-9

9. Dubey D, Alqallaf A, Hays R, Freeman M, Chen K, Ding K et al. Neurological autoantibody prevalence in epilepsy of unknown etiology. *JAMA Neurol.* (2017) 74:397–402. doi: 10.1001/jamaneurol.2016.5429

10. de Bruijn MAAM, Bastiaansen AEM, Mojzisova H, van Sonderen A, Thijs RD, Majoie MJM, et al. Antibodies contributing to focal epilepsy signs and symptoms score. *Ann Neurol.* (2021) 89:698–710. doi: 10.1002/ana.26013

11. Sakamoto M, Matsumoto R, Togawa J, Hashi Y, Takeyama H, Kobayashi K, et al. Proposal of a diagnostic algorithm for autoimmune epilepsy: preliminary investigation of its utility. *Rinsho Shinkeigaku.* (2018) 58:609–16. doi: 10.5692/clinicalneurol.cn-001180

12. Dalmau J. NMDA receptor encephalitis and other antibody-mediated disorders of the synapse: the 2016 cotzias lecture. *Neurology.* (2016) 87:2471–82. doi: 10.1212/WNL.0000000000003414

13. Ances BM, Vitaliani R, Taylor RA, Liebeskind DS, Voloschin A, Houghton DJ, et al. Treatment-responsive limbic encephalitis identified by neuropil antibodies: MRI and PET correlates. *Brain.* (2005) 128:1764–77. doi: 10.1093/brain/awh526

14. Wandinger KP, Leypoldt F, Junker R. Autoantibody-mediated encephalitis. *Dtsch Arztebl Int.* (2018) 115:666–73. doi: 10.3238/arztebl.2018.0666

15. Marignier R, Chenevier F, Rogemond V, Sillevis Smitt P, Renoux C, Cavillon G, et al. Metabotropic glutamate receptor type 1 autoantibody–associated cerebellitis: a primary autoimmune disease? *Arch Neurol.* (2010) 67:627–30. doi: 10.1001/archneurol.2010.51

16. Spatola M, Sabater L, Planagumà J, Martínez-Hernandez E, Armangué T, Prüss H, et al. Encephalitis with mGluR5 antibodies: symptoms and antibody effects. *Neurology.* (2018) 90:e1964–72. doi: 10.1212/WNL.0000000000005614

17. Petit-Pedrol M, Armangue T, Peng X, Bataller L, Cellucci T, Davis R, et al. Encephalitis with refractory seizures, status epilepticus, and antibodies to the GABAA receptor: a case series, characterisation of the antigen, and analysis of the effects of antibodies. *Lancet Neurol.* (2014) 13:276–86. doi: 10.1016/S1474-4422(13)70299-0

18. Sabater L, Gaig C, Gelpi E, Bataller L, Lewerenz J, Torres-Vega E, et al. A novel non-rapid-eye movement and rapid-eye-movement parasomnia with sleep breathing disorder associated with antibodies to IgLON5: a case series, characterisation of the antigen, and post-mortem study. *Lancet Neurol.* (2014) 13:575–86. doi: 10.1016/S1474-4422(14)70051-1

19. Titulaer MJ, Höftberger R, Iizuka T, Leypoldt F, McCracken L, Cellucci T, et al. Overlapping demyelinating syndromes and anti–N-methyl-D-aspartate receptor encephalitis. *Ann Neurol.* (2014) 75:411–28. doi: 10.1002/ana.24117

20. Baysal-Kirac L, Tuzun E, Erdag E, Ulusoy C, Vanli-Yavuz EN, Ekizoglu E, et al. Neuronal autoantibodies in epilepsy patients with peri-ictal autonomic findings. *J Neurol.* (2016) 263:455–66. doi: 10.1007/s00415-015-8002-2

21. Steriade C, Mirsattari SM, Murray BJ, Wennberg R. Subclinical temporal EEG seizure pattern in LGI1-antibody–mediated encephalitis. *Epilepsia.* (2016) 57:e155–60. doi: 10.1111/epi.13436

22. Irani SR, Michell AW, Lang B, Pettingill P, Waters P, Johnson MR, et al. Faciobrachial dystonic seizures precede Lgi1 antibody limbic encephalitis. *Ann Neurol.* (2011) 69:892–900. doi: 10.1002/ana.22307

23. Akobeng AK. Understanding diagnostic tests 3: receiver operating characteristic curves. *Acta Paediatr.* (2007) 96:644–7. doi: 10.1111/j.1651-2227.2006.00178.x

24. Kanazawa K, Matsumoto R, Shimotake A, Kinoshita M, Otsuka A, Watanabe O, et al. Persistent frequent subclinical seizures and memory impairment after clinical remission in smoldering limbic encephalitis. *Epileptic Disord.* (2014) 16:312–7. doi: 10.1684/epd.2014.0664

25. Jang Y, Kim DW, Yang KI, Byun JI, Seo JG, et al. Clinical approach to autoimmune epilepsy. *J Clin Neurol.* (2020) 16:519–29. doi: 10.3988/jcn.2020.16.4.519

26. Steriade C, Moosa ANV, Hantus S, Prayson RA, Alexopoulos A, Rae-Grant A. Electroclinical features of seizures associated with autoimmune encephalitis. *Seizure.* (2018) 60:198–204. doi: 10.1016/j.seizure.2018.06.021

27. McGinty RN, Handel A, Moloney T, Ramesh A, Fower A, Torzillo E, et al. Clinical features which predict neuronal surface autoantibodies in new-onset focal epilepsy: implications for immunotherapies. *J Neurol Neurosurg Psychiatry.* (2021) 92:291–4. doi: 10.1136/jnnp-2020-325011

28. Lancaster E. The diagnosis and treatment of autoimmune encephalitis. *J Clin Neurol.* (2016) 12:1–13. doi: 10.3988/jcn.2016.12.1.1

29. von Rhein B, Wagner J, Widman G, Malter MP, Elger CE, Helmstaedter C. Suspected antibody negative autoimmune limbic encephalitis: outcome of immunotherapy. *Acta Neurol Scand.* (2017) 135:134–41. doi: 10.1111/ane.12575

30. Dubey D, Singh J, Britton JW, Pittock SJ, Flanagan EP, Lennon VA, et al. Predictive models in the diagnosis and treatment of autoimmune epilepsy. *Epilepsia.* (2017) 58:1181–9. doi: 10.1111/epi.13797

31. Mitsueda-Ono T, Ikeda A, Inouchi M, Takaya S, Matsumoto R, Hanakawa T, et al. Amygdalar enlargement in patients with temporal lobe epilepsy. *J Neurol Neurosurg Psychiatry.* (2011) 82:652–7. doi: 10.1136/jnnp.2010.206342

32. Malter MP, Widman G, Galldiks N, Stoecker W, Helmstaedter C, Elger CE, et al. Suspected new-onset autoimmune temporal lobe epilepsy with amygdala enlargement. *Epilepsia.* (2016) 57:1485–94. doi: 10.1111/epi.13471

33. Bower SP, Vogrin SJ, Morris K, Cox I, Murphy M, Kilpatrick CJ, et al. Amygdala volumetry in "imaging-negative" temporal lobe epilepsy. *J Neurol Neurosurg Psychiatry.* (2003) 74:1245–9. doi: 10.1136/jnnp.74.9.1245

34. Takaya S, Ikeda A, Mitsueda-Ono T, Matsumoto R, Inouchi M, Namiki C, et al. Temporal lobe epilepsy with amygdala enlargement: a morphologic and functional study. *J Neuroimaging.* (2014) 24:54–62. doi: 10.1111/j.1552-6569.2011.00694.x

35. Minami N, Morino M, Uda T, Komori T, Nakata Y, Arai N, et al. Surgery for amygdala enlargement with mesial temporal lobe epilepsy: pathological findings and seizure outcome. *J Neurol Neurosurg Psychiatry.* (2015) 86:887–94. doi: 10.1136/jnnp-2014-308383

36. Guerin J, Watson RE, Carr CM, Liebo GB, Kotsenas AL. Autoimmune epilepsy: findings on MRI and FDG-PET. *Br J Radiol.* (2019) 92:20170869. doi: 10.1259/bjr.20170869

37. Geis C, Planagumà J, Carreño M, Graus F, Dalmau J. Autoimmune seizures and epilepsy. *J Clin Invest.* (2019) 129:926–40. doi: 10.1172/JCI125178

38. Heine J, Prüss H, Bartsch T, Ploner CJ, Paul F, Finke C. Imaging of autoimmune encephalitis – relevance for clinical practice and hippocampal function. *Neuroscience.* (2015) 309:68–83. doi: 10.1016/j.neuroscience.2015.05.037

39. Iizuka T, Sakai F, Ide T, Monzen T, Yoshii S, Iigaya M, et al. Anti-NMDA receptor encephalitis in Japan: long-term outcome without tumor removal. *Neurology.* (2008) 70:504–11. doi: 10.1212/01.wnl.0000278388.90370.c3

40. Vitaliani R, Mason W, Ances B, Zwerdling T, Jiang Z, Dalmau J. Paraneoplastic encephalitis, psychiatric symptoms, and hypoventilation in ovarian teratoma. *Ann Neurol.* (2005) 58:594–604. doi: 10.1002/ana.20614

41. Hegen H, Reindl M. Recent developments in MOG-IgG associated neurological disorders. *Ther Adv Neurol Disord.* (2020) 13:1756286420945135. doi: 10.1177/1756286420945135

42. Piquet AL, Khan M, Warner JEA, Wicklund MP, Bennett JL, Leehey MA, et al. Novel clinical features of glycine receptor antibody syndrome: a series of 17 cases. *Neurol Neuroimmunol Neuroinflamm.* (2019) 6:e592. doi: 10.1212/NXI.0000000000000592

frontiers | Frontiers in Neurology

TYPE Original Research
PUBLISHED 21 September 2022
DOI 10.3389/fneur.2022.993405

OPEN ACCESS

EDITED BY
Xinjian Zhu,
Southeast University, China

REVIEWED BY
Ayoob Sabaghi,
Razi University, Iran
Alex Cleber Improta Caria,
University of São Paulo, Brazil

*CORRESPONDENCE
Yonghua Ji
yhji@staff.shu.edu.cn
Jie Tao
jietao_putuo@foxmail.com
Yudan Zhu
yudanzhu_putuo@foxmail.com

†These authors share first authorship

SPECIALTY SECTION
This article was submitted to Epilepsy, a section of the journal Frontiers in Neurology

RECEIVED 13 July 2022
ACCEPTED 30 August 2022
PUBLISHED 21 September 2022

CITATION
Jia Y, Tang L, Yao Y, Zhuo L, Qu D, Chen X, Ji Y, Tao J and Zhu Y (2022) Low-intensity exercise combined with sodium valproate attenuates kainic acid-induced seizures and associated co-morbidities by inhibiting NF-κB signaling in mice.
Front. Neurol. 13:993405.
doi: 10.3389/fneur.2022.993405

Low-intensity exercise combined with sodium valproate attenuates kainic acid-induced seizures and associated co-morbidities by inhibiting NF-κB signaling in mice

Yuxiang Jia[1†], Lele Tang[2†], Yu Yao[1], Limin Zhuo[1], Dongxiao Qu[2], Xingxing Chen[2], Yonghua Ji[1*], Jie Tao[2*] and Yudan Zhu[2*]

[1]School of Medicine, Shanghai University, Shanghai, China, [2]Department of Neurology and Neurosurgery, Putuo Hospital, Shanghai University of Traditional Chinese Medicine, Shanghai, China

Sodium valproate (VPA) is a broad-spectrum anticonvulsant that is effective both in adults and children suffering from epilepsy, but it causes psychiatric and behavioral side effects in patients with epilepsy. In addition, 30% of patients with epilepsy develop resistance to VPA. At present, regular physical exercise has shown many benefits and has become an effective complementary therapy for various brain diseases, including epilepsy. Therefore, we wondered whether VPA combined with exercise would be more effective in the treatment of seizures and associated co-morbidities. Here, we used a mouse model with kainic acid (KA)-induced epilepsy to compare the seizure status and the levels of related co-morbidities, such as cognition, depression, anxiety, and movement disorders, in each group using animal behavioral experiment and local field potential recordings. Subsequently, we investigated the mechanism behind this phenomenon by immunological means. Our results showed that low-intensity exercise combined with VPA reduced seizures and associated co-morbidities. This phenomenon seems to be related to the Toll-like receptor 4, activation of the nuclear factor kappa B (NF-κB), and release of interleukin 1β (IL-1β), tumor necrosis factor α (TNF-α), and IL-6. In brief, low-intensity exercise combined with VPA enhanced the downregulation of NF-κB-related inflammatory response, thereby alleviating the seizures, and associated co-morbidities.

KEYWORDS

seizures, low-intensity exercise, sodium valproate, co-morbidities, TLR4/NF-κB pathway, inflammatory factors

Introduction

Epilepsy is a brain disorder that affects over 70 million people worldwide. This disorder is characterized by the abnormal discharge of neurons (1, 2). Currently, antiepileptic drugs, such as sodium valproate (VPA), are the most common form of treatment. After more than a century from its discovery, as a result of its anticonvulsant effects, VPA is still a drug of choice for epilepsy in children and adults with either general or focal seizures (3). However, antiepileptic drugs cause psychiatric and behavioral side effects (4, 5) and drug resistance in ∼ 30% of patients with epilepsy (6). Therefore, it is urgent to find a non-pharmacological intervention that can reduce the development rate of drug-resistant epilepsy and the side effects associated with antiepileptic drugs. Noteworthily, physical exercise is a complementary therapy with beneficial effects for epilepsy (7–9). The beneficial effects of low-intensity physical exercise on the brain have been demonstrated in mouse models of disorders like Alzheimer's disease (AD), stroke, and depression (10–13). Clinical studies have found that more than half of the patients never experience a seizure during or after physical exercise, including 10% of patients who have frequent seizures (14); therefore, physical exercise seems to reduce the severity of seizures. Therefore, we evaluated whether low-intensity physical exercise combined with VPA (LE-VPA) would be more effective for treating seizures and other epilepsy-associated co-morbidities in mice.

Epilepsy pathogenesis is complex, but evidence suggests an increased number of microglial cells in the Cornu Ammonis 1 (CA1) and Cornu Ammonis 3 (CA3) layers of the hippocampus in patients with epilepsy (15–17). Therefore, microglial-mediated neuroinflammation may be involved in its pathogenesis (18, 19). Microglial cells are brain-resident immune cells that regulate mechanisms essential for cognitive functions. A variety of receptors are distributed on the surface or in the cytoplasm of microglial cells (20, 21), including Toll-like receptor 4 (TLR4). TLR4 belongs to one of the subfamilies of pattern recognition receptors that recognize invading pathogens and endogenous harmful stimuli, thus, activating the transcription factor nuclear factor κB (NF)-κB pathway (22), and releasing large amounts of inflammatory proteins (e.g., interleukin 1-β [IL-1β], interleukin 6 [IL-6], tumor necrosis factor α [TNF-α], and chemokines) (23–25). VPA induces epigenetic signaling that involves NF-κB-related inflammatory responses in the frontal cortex and hippocampus (26, 27). Meanwhile, it has been reported that physical exercise alleviates inflammatory lung injury (28) and osteoarthritis (29) by inhibiting NF-κB signaling. Therefore, we studied whether LE-VPA alleviates seizures and associated co-morbidities by inhibiting TLR4/NF-κB-related inflammatory responses.

In this study, we aimed to examine whether LE-VPA exerted an ameliorative effect in a kainic acid (KA) mouse model for seizures and associated co-morbidities (i.e., cognitive dysfunction, motor impairment, depression, and anxiety). In addition, we hypothesized that the positive effects of LE-VPA were associated with the inhibition of TLR4/ NF-κB and lower expression levels of IL-1β, TNF-α, and IL-6.

Materials and methods

Animals

Eighty male, 2-month-old C57BL/6 mice (Jiesijie Laboratory Animal, Shanghai, China), weighing 20–25 g, were used. Except for a control group of eight mice, epilepsy was induced in the remaining mice by intraperitoneal injection of kainic acid (KA; 30 mg/kg) according to body weight. The symptoms of injected mice were judged according to the Racine scale, and the mice that were successfully modeled were divided into four groups (30), with eight mice in each group: model group, drug group, runner group, and running combined with drug treatment group (combination group). In our experiment, out of the 60 mice that received KA injection, 32 survived, with a death rate of around 50% due to KA. All animal experiments were performed according to the National Institutes of Health (NIH) Guide for the Care and Use of Laboratory Animals (NIH Publication No. 80–23, revised 1996) and were approved by the Institutional Animal Care and Use Committee of Shanghai University of Traditional Chinese Medicine.

Treatment program

In this study, the mice performed low-intensity physical exercise on treadmills (SANS, SA 101). It has been proven that the average maximal speed of young mice is 70 cm/s (42 m/min), and low-intensity exercise is defined as around 35–40% (14.7 m/min−16.8 m/min) of the maximal capacity (31). In addition, we observed that the mice ran at 15 m/min without any discomfort. Therefore, the maximal intensity of the mouse treadmill was set to 15 m/min. Runners were assigned to run 5 m/min for 10 min on the first day, and the running speed was gradually increased to 15 m/min for 20 min from second to seventh day and 15 m/min for 60 min from eighth to 28th day. The treadmill exercise was performed 5 days per week.

The drug group and the combination group received an intraperitoneal injection of VPA (Sigma, St Louis, MO, USA) dissolved in 0.9% NaCl, at 30 mg/kg per day, for 28 days. The model group were injected with the same volume of normal saline daily for 4 weeks (Table 1).

Video monitoring

Cameras were used to monitor the mice moving freely in an observation bucket. Each mouse was placed in a

TABLE 1 Exercise and treatment program.

Group	Pretreatment	Exercise	VPA (ip)	Saline (ip)	Duration (day)
Control	-	-	-	+	28
Model group	KA, ip	-	-	+	28
Drug group	KA, ip	-	+	-	28
Runner group	KA, ip	+	-	-	28
Combination group	KA, ip	+	+	-	28

transparent observation bucket equipped with a surveillance camera (Shanghai JiLian Web Tech Ltd., Shanghai, China) for 9 h for continuous observation. Using the Racine scale, the duration and frequency of epileptic seizures in each mouse during this period were analyzed and recorded.

Morris water maze

The Morris water maze (MWM) (32) is a circular pool with a diameter of 120 cm and a height of 60 cm, a water level of 35 cm, and a temperature of 22–24 °C. The mice were trained on the MWM with one trial per day for 6 days. A platform was hidden 1 cm below the surface of the water, which was made opaque with white non-toxic paint. Each trial lasted until the mouse found the platform or for a maximum of 60 s. At the end of each trial, mice were allowed to rest on the platform for 60 s. The time to reach the platform (latency), length of the swim path, and swim speed were recorded semi-automatically using a video tracking system (Shanghai JiLian Web Tech Ltd.).

Y maze

The Y maze (Shanghai JiLian Web Tech Ltd.) has three arms in total, with a 120° angle between the two arms (33). An infrared camera tracking system was installed above the maze to record the process, using supporting software. In the experiment, the mice were placed toward the center of the Y maze from the end of one arm and were allowed to explore freely for 10 min. In the spontaneous alternation reaction, the complete entry of the body of the mouse into the arm was recorded as a standard entry, and the continuous entry of the animal into the three different arms was defined as successful exploration.

Alternation rate (%) = correct entry time / (total entry times-2) × 100.

Open-field testing

The open-field test is used to measure anxiety-like behavior in animals. This test used a camera to measure the movement of the test animal in the peripheral and central zones (20 × 20 × 20 cm) of a 42 × 42 × 42 cm polyvinyl chloride box for 10 min. A video tracking program (Stoelting Co., Wood Dale, IL, USA) was used to record and measure the total distance traveled, the time spent in the center of the open-field arena, and the distance moved in the center of the open-field arena in each trial. The time spent in the center and distance traveled in the center of the arena were used as measures of anxiety-like behavior (34, 35).

Catwalk gait analysis

The Catwalk System (Catwalk XT, Noldus Information Technology, Wageningen, Netherlands) consists of an enclosed walkway (glass plate) illuminated by fluorescent light. The system was equipped with a high-speed color camera connected to a computer using appropriate detection software (CatwalkXT9.1). Animals were individually placed on the walkway, and each animal was allowed to move freely in both directions. To detect all parameters used in the experiments, the camera gain was set to 20, and the detection threshold was set to 0.1. All runs with a run duration between 0.50 and 5.00 s for a complete walkway and a maximum allowed speed variation of 60% were considered as successful runs. For each animal, three compliant runs were performed per trial. Compliant runs were classified for all limbs and were statistically analyzed. The software can detect several dynamic parameters of an animal's walk (36): we focused on swing speed (average stride time), body speed (distance traveled/time), print area (measurements of complete paw prints), and mean intensity (average pressure applied by single-paw contact with the floor).

Local field potential

Mice were deeply anesthetized and placed in a stereotaxic frame (Narishige, Tokyo, Japan). Multi-channel electrodes were inserted into the hippocampus of mice based on a mouse brain map (anteroposterior: −2.0 mm posterior to bregma, ventral: 1.5 mm ventral to the dura surface, and lateral: 1.5 mm lateral to the skull midline). After the mice woke up from anesthesia and moved freely, the local field potential (LFP) recordings were obtained. Data were collected using an *in vivo* multi-channel

recording system, amplified 1,000 times by a preamplifier, with a wave amplitude range of −2 to +2V and a filtering range of 1.6–100 Hz. The LFP recording frequency was 1,000 Hz, and the recording time was not <30 min. LFP was exported in Pl2 format, and the Offline Sorter V4 software was used for visual previews. The LFP analysis selected the same channel using MATLAB (MathWorks, Natick, MO, USA) to export data. Five different frequencies of circadian rhythms were decomposed: δ (0.4–4 Hz), θ (4–8 Hz), α (8–15 Hz), β (15–30 Hz), and γ (> 30 Hz). The Welch Hamming window and fast Fourier transform methods were used to calculate the frequency domain information of the LFP. The power spectral density (PSD) was calculated as follows:

$$\int_{-\infty}^{+\infty} x^2(t)\,dt = \frac{1}{2\pi}\int_{-\infty}^{+\infty} \left|X(jw)\right|^2 d\omega \quad (1)$$

$$P = \frac{1}{2T}\int_{-T}^{T} x^2(t)\,dt = \frac{1}{2\pi}\int_{-\infty}^{+\infty} \frac{1}{2T}\left|X_T(\omega)\right|^2 d\omega \quad (2)$$

Immunofluorescence and immunohistochemistry

After acute anesthesia with chloral hydrate, mice were transcardially perfused with ice-cold 4% paraformaldehyde (PFA). The dissected brains were post-fixed overnight in 4% PFA and were then transferred to 30% sucrose buffer for 48 h. Subsequently, the brains were frozen in Tissue-Tek OCT compound (Sakura Finetek, Torrance, CA, USA) and sliced at 20 μm using a cryostat (Leica Biosystems, Nußloch, Germany). The sections were washed with phosphate-buffered saline (PBS, pH 7.4), incubated with 0.3% Triton in PBS at room temperature for 0.5 h, and incubated with blocking solution (Beyotime Biotech, Shanghai, China) at room temperature for 1 h. Then, the sections were treated with appropriate primary antibodies at a suitable concentration in blocking solution at 4°C for overnight. After washing with PBS three times, the sections were incubated with secondary antibody at 37°C for 1 h. After washing again with PBS three times, the sections were incubated with DAPI (Beyotime, 1:1) at room temperature for 10 min. The sections were then washed, mounted, and covered with a lid. The images were analyzed using Image-Pro Plus 6.0 software (Media Cybernetics).

The steps of immunohistochemical procedure on the first day of experiment were equivalent to those of immunofluorescence. On the next day, the steps of immunohistochemical procedure were different. First, brain slices were incubated with secondary antibodies and stained with 3, 3'-diaminobenzidine (DAB) using the SABC and DAB staining kit (Wellbio, Shanghai, China), according to the instructions. Then, hematoxylin was used for counterstaining. The differentiation solution was terminated. Finally, dehydration, transparency, sealing, and observation were performed. A light microscope (ECLIPSE E600; Nikon, Tokyo, Japan) was used to observe the sections, and at least five panoramic images of the hippocampus were taken from each group. Image-pro Plus 6.0 software was used to analyze the intensity of staining areas in each group (Media Cybernetics, MD, USA).

The primary antibodies used in this study were rabbit anti-IL-1β antibody (Abcam, Cambridge, MA, USA; EPR23851-127; 1:100), rabbit anti-TNF-α (Abcam, EPR20972; 1:100), mouse anti-iba1 (Abcam, EPR16589; 1:100), rabbit anti-IL-6 (Abmart, Shanghai, China; P05231; 1:100), rabbit anti-NLRP3 (Affinity, Shanghai, China; DF7438; 1:100), rabbit anti-TLR4 (Affinity, Shanghai, China; AF7017; 1:100), and rabbit anti-NF-Kb-p65 (Affinity, Shanghai, China; AF5006; 1:100). The secondary antibodies used were Alexa Fluor 488 goat anti-mouse (Abcam, 1:200) and Alexa Fluor 647 goat anti-rabbit (Abcam,1:200).

Enzyme-linked immunosorbent assay

The mouse brains were dissected, and hippocampal tissues were quickly removed on ice. Blood was washed away with pre-cooled fresh PBS. Hippocampal tissues were homogenized in PBS and centrifuged at 45,000 × *g* for 30 min at 4°C. We used enzyme-linked immunosorbent assay (ELISA) kits to measure cytokines including IL-1β, TNF-α, and IL-6, according to the manufacturer's protocols. The results were obtained using a multifunction microplate meter.

Statistical analysis

Data were expressed as mean ± standard error of the mean. Statistical differences were analyzed using two-way analysis of variance or three-way analysis of variance (followed by Tukey's multiple comparison test). For multiple comparisons, we selected "simple effect within row" or "main column effect," respectively, depending on the purpose, and compared each column mean with every other column mean. Data were considered significant at $P < 0.05$. Statistical analyses were performed using GraphPad Prism (version 6.07, GraphPad, San Diego, USA), Excel 2016 (Microsoft, WA), and Adobe Photoshop CC 2018 (Adobe Systems, San José, CA, USA).

Results

Experimental design

Mice were assigned to five groups ($n = 8$) according to the experimental protocol. The animals were maintained under

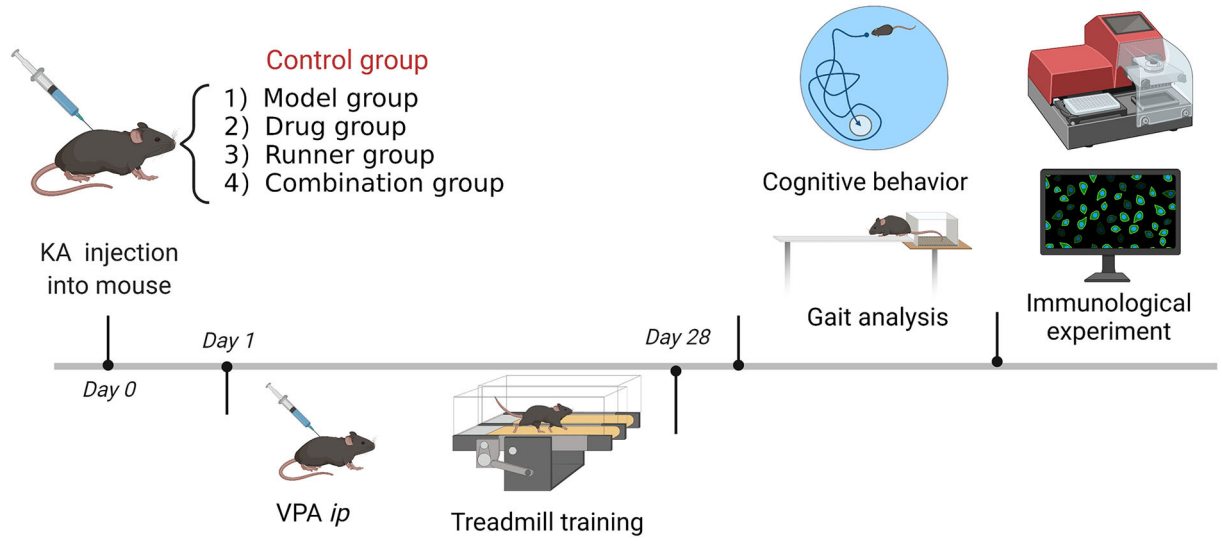

FIGURE 1
Flowchart of the experiment.

their respective experimental conditions for 28 days. Mice were tested in behavioral experiments, and LFP recordings were made between days 29 and 37. After sacrificing the mice, we collected brain tissue for immunological experiments (Figure 1).

LE-VPA provided better control of mild seizures

Mice were intraperitoneally injected with KA and presented with status epilepticus (SE) 15–30 min later. After a latency of 14–21 days, mice presented with spontaneous epilepsy (37). We used video cameras to track the number of seizures and the latency of tonic–clonic seizures in each group for the continuous 9-h video monitoring (Figure 2A). In the statistics, the number of mild seizures (stages 2–3) (Figure 2B) in the three treated groups showed different degrees of improvement (drug: $P < 0.001$, runner: $P < 0.01$, combination: $P < 0.001$, $n = 8$), and LE-VPA had greater advantages than VPA alone ($P < 0.05$). The number of severe seizures (stages 4–5) (Figure 2C) showed remission in only two groups that are treated with VPA (drug: $P < 0.001$, combination: $P < 0.001$), and the effect of running appeared to be modest ($P > 0.05$). The statistics of seizure latency (Figure 2D) also showed a significant difference among VPA-treated groups (drug: $P < 0.001$, combination: $P < 0.001$), but there was no significant difference between LE-VPA and VPA alone group ($P > 0.05$). Taken together, LE-VPA therapy significantly reduced the number of mild seizures in KA mice.

LE-VPA improved epilepsy and associated co-morbidities like cognitive impairment, depression, and anxiety

We also evaluated whether LE-VPA could alleviate the cognitive impairment, depression, and anxiety that are associated with epilepsy.

Mice in each group received the corresponding treatment for 28 days, followed by MWM that was conducted for 6 days (Figure 3A). During the first 5 days of the training period, the software recorded the latency for each mouse which provided evidence for spatial learning. The 6th day was the test period, and the time to find the platform for the first time was recorded as the latency on day 6. The time spent in the correct quadrant represented memory retention. The latency of healthy mice shortened over training, indicating that mice had a normal spatial learning ability, while the latency of mice in the KA model group remained unchanged or was not significantly shortened, indicating that epileptic mice had a spatial learning ability disorder (Figure 3B). After 5 days of training, the experimental performance of each group of mice on the last day was as follows: The time to find the platform was approximately 20 s shorter in the drug group than in the model group ($P < 0.05$, $n = 6$), while that in the LE-VPA group was about 30 s shorter ($P < 0.001$, $n = 6$). The difference between the drug and LE-VPA groups was also significant ($P < 0.05$). We then compared the duration that each group spent in the correct quadrant on day 6 (Figure 3C). The model mice spent a shorter time in the quadrant as compared to control mice, indicating memory dysfunction ($P < 0.001$, $n = 6$). This could be improved by 5

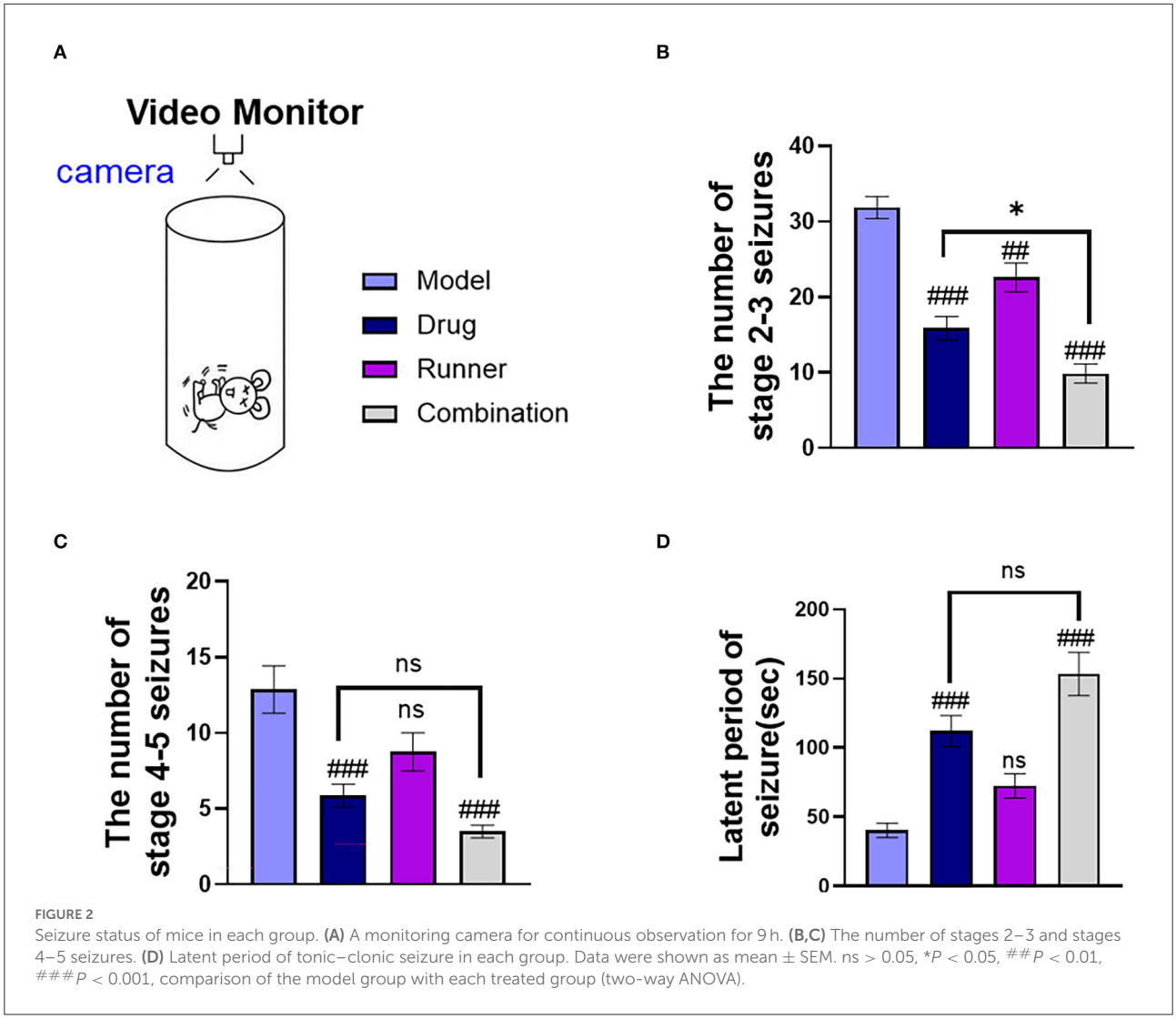

FIGURE 2
Seizure status of mice in each group. **(A)** A monitoring camera for continuous observation for 9 h. **(B,C)** The number of stages 2–3 and stages 4–5 seizures. **(D)** Latent period of tonic–clonic seizure in each group. Data were shown as mean ± SEM. ns > 0.05, *$P < 0.05$, ##$P < 0.01$, ###$P < 0.001$, comparison of the model group with each treated group (two-way ANOVA).

% after drug therapy alone ($P < 0.05$, $n = 6$). The improvement effect of the LE-VPA therapy was more obvious: The time was increased by 20% ($P < 0.001$). The effect of LE-VPA also differed significantly from that of VPA alone in this respect ($P < 0.05$).

In the Y-maze task (Figure 3D), based on the mouse's movements, the software automatically calculated the rate of alternation for each group, which represents the mouse's working memory (Figure 3E). Compared to control mice, the spontaneous alternation rate was lower in the model group ($P < 0.001$, $n = 6$). With drug alone and running alone therapy, mice showed a 10% (both $P < 0.05$, $n = 6$) increase in spontaneous alternation rates, respectively, whereas combination group seemed to have a better effect ($P < 0.001$). In addition, there was no significant difference between LE-VPA and VPA alone ($P > 0.05$).

Next, the mice were subjected to an open-field test (Figure 3F). Compared with control mice, KA mice moved significantly less distance ($P < 0.05$, $n = 8$) and had depression-like behavior (Figure 3G). After different ways of treatment, this condition has been alleviated in runner and combination groups (both $P < 0.001$, $n = 8$), showing LE-VPA is more effective than VPA therapy alone ($P < 0.05$, $n = 8$). We counted the movement time and distance of each group in the central area. We found that the movement time ($P < 0.00$) and distance ($P < 0.01$) in the center of the model group were significantly shorter than healthy mice, indicating that epilepsy could cause anxiety-like behavior in mice (Figures 3H,I). After different treatments, the time (runner: $P < 0.01$, combination: $P < 0.001$, $n = 7$) and distance (drug: $P < 0.05$, runner: $P < 0.001$, combination: $P < 0.001$, $n = 7$) of movement in the center of each group increased significantly. There were significant differences between the LE-VPA group and VPA group in center distance ($P < 0.05$).

In conclusion, compared with drug alone treatment, LE-VPA was more effective in improving the learning ability and

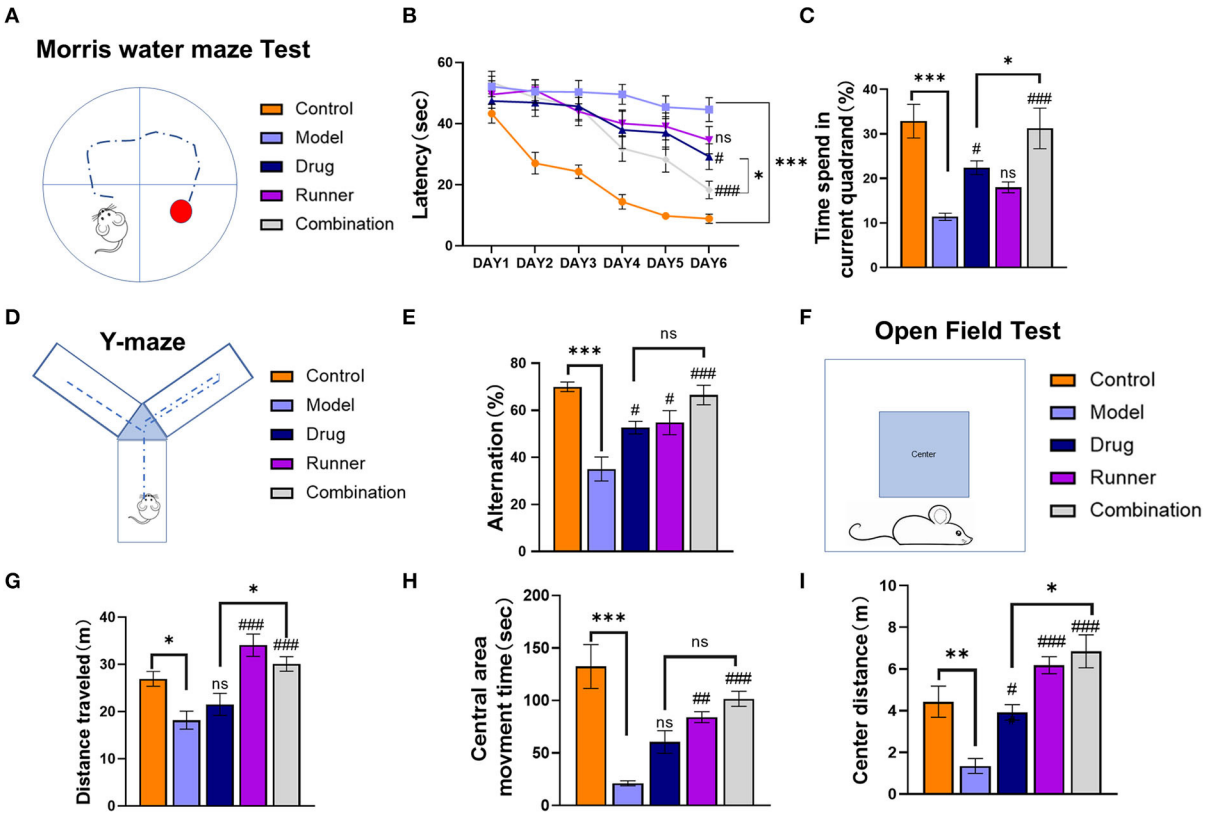

FIGURE 3
Cognitive impairment, anxiety, and depression in mice of each group. **(A)** Schematic of the Morris water maze task. **(B,C)** The 6-day latency of each group and time spent in the current quadrant on day 6. **(D)** Schematic of the Y-maze test task. **(E)** The spontaneous alternation in behavior of each group. **(F–I)** The open-field test was performed to record the total distance traveled throughout the open-field arena, entries into the center zone, duration spent within the center zone, and distance traveled within the center zone. Data were shown as mean ± SEM. ns > 0.05, $^{*}P < 0.05$, $^{**}P < 0.01$, $^{***}P < 0.001$; $^{\#}P < 0.05$, $^{\#\#}P < 0.01$, $^{\#\#\#}P < 0.001$, comparison of the model group with each treated group (B: three-way ANOVA or two-way ANOVA was used for the rest of the data).

memory retention as well as ameliorating epileptic-induced depression and anxiety-like behavior in KA mice.

Dyskinesia of epilepsy was ameliorated by LE-VPA

Motor skill deficits are nearly universal to all neurodevelopmental disorders, and epilepsy is no exception (38). To assess these deficits, mice were exposed to Catwalk analysis. After habituation to the new surroundings, the animals had to perform a minimum of three non-stop runs that qualified for Catwalk XT® analysis. The same calibration parameters were used for each experimental group. To improve data quality, automated footprint recognition was manually reviewed. Catwalk XT® software separately analyzed a combination of 24 dynamic and static parameters for each paw. In addition, the print positions of the left and right paws, as well as the base of the support of the front and hind paws, were analyzed (Figure 4A). In the Catwalk gait analysis, print area and mean intensity indicated the paw force, which may reflect the weight-bearing capability of the limbs; swing speed and body speed indicated the thrust force of the limbs, where shorter swing speed or body speed indicated that the thrust force of the limbs was reduced (Figures 4E–H). Compared with the model group, only the footprint area was significantly increased in the drug group (Figure 4B, $P < 0.001$, $n = 6$). On the contrary, all parameters, print area ($P < 0.05$, $n = 6$), swing speed (Figure 4C, $P < 0.001$, $n = 6$), and body speed (Figure 4D, $P < 0.01$, $n = 6$), were significantly increased in the runner group. Mice in the combination group showed improvement in all three parameters ($P < 0.001$, $n = 6$). In addition, compared with the drug group, the combination group showed a more significant effect on swing speed ($P < 0.001$) and body speed ($P < 0.001$). Therefore, compared with VPA treatment, LE-VPA can significantly improve movement disorders such as discoordination of limbs and slow movement caused by epilepsy.

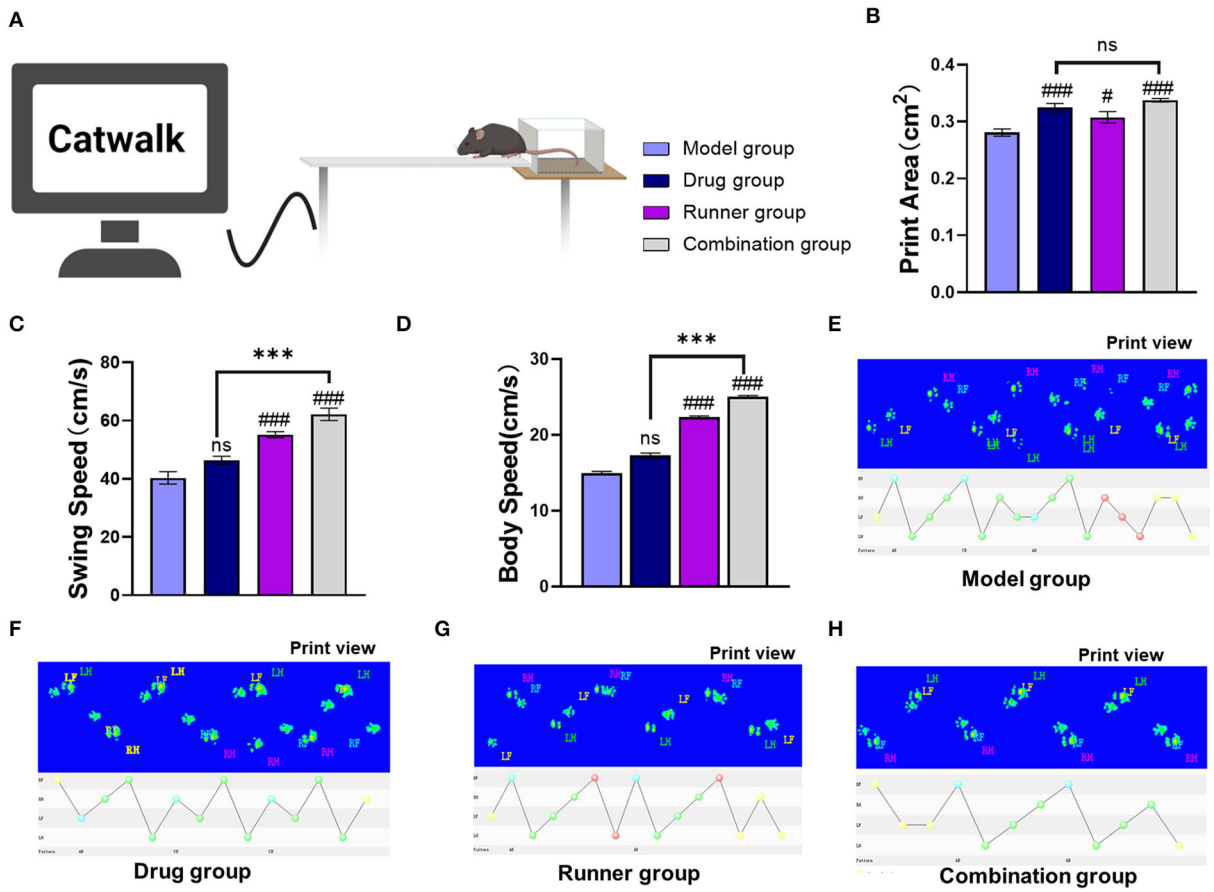

FIGURE 4
Effect of LE-VPA on the gait parameters after KA. **(A)** Diagram of gait analysis. The Catwalk gait analysis demonstrated that auxiliary running could improve the gait posture as reflected by the increased print area **(B)**, swing speed **(C)**, and body speed **(D)** compared with the model group. **(E–H)** Displayed the footprints picture and the marching patterns of the groups. Data were expressed as mean ± SEM. ns > 0.05, $^{***}P < 0.001$; $^{\#}P < 0.05$, $^{\#\#\#}P < 0.001$, comparison of the model group with each treated group (two-way ANOVA).

Inhibitory effects of LE-VPA on LFP responses

Subsequently, to determine whether LE-VPA could reduce the intensity of epileptic seizures, the effects of running on the power spectral density (PSD) of LFP during KA-induced seizures were directly tested (Figure 5A). In the recording, which was not <30 min, 10 min of data were randomly selected for statistical analysis. The LFP of control mice showed normal rhythms with low-frequency amplitude, and there was no abnormal epileptic rhythm. The electroencephalogram of model mice showed an explosive polyspike rhythm with high frequency and large amplitude, while the LFP frequency and amplitude were decreased in both the drug and runner groups. On the contrary, the LFP frequency and amplitude in the combination group were almost like those in healthy control mice (Figure 5B). The energy intensity of five common rhythms collected by LFP was statistically analyzed, as shown in Figure 5C. The δ rhythms (0.5–4 Hz) are slow rhythm of the sleep state in mice that can convert early long-term potentiation (LTP) to long-lasting LTP (39). The energy intensity of δ- rhythms of KA mice was significantly increased ($P < 0.001$, $n = 3$). Compared with the model group, the energy intensity of δ rhythms of the drug ($P < 0.05$, $n = 3$), runner ($P < 0.001$, $n = 3$), and combination groups ($P < 0.001$, $n = 3$) decreased by 50 and 70%. The θ rhythms (4–7 Hz) are like δ rhythms and occur during sleep. The KA model group exhibited a higher θ- rhythm energy intensity ($P < 0.001$, $n = 3$). Compared with the KA group, the energy intensity of θ rhythms of the drug group ($P < 0.05$, $n = 3$), runner group ($P < 0.01$, $n = 3$), and combination group ($P < 0.001$, $n = 3$) was decreased by 50%. The α rhythms (8–13 Hz) are normal brain rhythms in mice. The α rhythm energy intensity was significantly increased in the model group ($P < 0.001$, $n = 3$). Compared with the model group, the energy intensity of α rhythms of the drug, running, and combination groups (all $P < 0.001$, $n = 3$) was significantly decreased. The θ and α frequency

bands are usually collectively referred to as the low-frequency (LF) range (40, 41). LF oscillations have been widely studied in cognitive and emotional fields, including memory consolidation (42), attention and consciousness (43), and depressive mood (44, 45). There is some evidence that LF oscillations are related to the message of self-movement (46) and sequential dependencies during spatial planning (47). The β rhythms (15–30 Hz) are the main rhythms of the brain during excitation, which seem to focus more on associative memory and ability to predict object locations based on environmental cues (48, 49). The energy intensity of the β rhythms was significantly increased in the model group as compared with the control group ($P < 0.05$, $n = 3$), while the other groups showed no significant difference from the model group. The γ rhythms (> 30 Hz) are fast rhythms occurring in the rapid eye movement sleep period, in which oscillations in entorhinal cortex-hippocampus circuits play crucial roles in memory function in a healthy animal's brain (50). The energy intensity of the γ rhythms was significantly increased in the model group ($P < 0.05$, $n = 3$), while the other groups showed no significant difference as compared with the model group. Figure 5D shows that the PSD of the model group was increased, while it was inhibited to a certain extent after drug therapy, running therapy, and combination therapy. In addition, the combination group showed more effective inhibition of abnormal LFP signals than the drug group for the δ ($P < 0.05$), θ ($P < 0.05$), and α rhythms ($P < 0.001$). These results also support our hypothesis that LE-VPA therapy is more potent in suppressing neuroexcitability, especially low-frequency rhythm.

Suppressive effect of LE-VPA on neuroinflammatory response induced by epilepsy

In mammals, epilepsy can be caused by a large number of inflammatory factors that activate microglial cells (15). We used ELISA (Figures 6A–C) and immunofluorescence (Figures 6D–G), to verify the expression levels of the inflammatory cytokines IL-1β, TNF-α, and IL-6 in the hippocampus of mice. High levels of IL-1β ($P < 0.001$, $n = 6$), TNF-α ($P < 0.001$, $n = 6$), and IL-6 ($P < 0.05$, $n = 6$) were expressed in the hippocampal tissues of model mice, while running reduced the expression levels of IL-1β ($P < 0.05$, $n = 6$) and TNF-α ($P < 0.05$, $n = 6$). Drug treatment alone was effective in reversing the hyperinflammatory state of the hippocampus (IL-1β and TNF-α: $P < 0.001$, IL-6: $P < 0.05$, $n = 6$), but the advantage of the combination group was more prominent (all $P < 0.01$, $n = 6$) and significantly different from that of the drug group in TNF-α and IL-6 expression (both $P < 0.05$, $n = 6$). To verify this conclusion, we performed immunofluorescence staining of IBA1 (M1 microglial marker), IL-1β, TNF-α, and IL-6 in the CA3 region (51) and found that microglial cells were activated and IL-1β, TNF-α, and IL-6 levels were high in model mice (all $P < 0.001$, $n = 6$). We determined the average percentage of positive areas of $IBA1^+$ IL-1β, $IBA1^+$ TNF-α, or $IBA1^+$ IL-6 in each group. Compared to the model group, the levels of all three inflammatory factors in the hippocampus decreased after treatment with VPA alone (IL-1β and TNF-α: $P < 0.01$, IL-6: $P < 0.05$, $n = 6$). In the combination group, the mean positive area related to IL-1β, TNF-α, and IL-6 was decreased by 60% ($P < 0.001$, $n = 6$), 50% ($P < 0.001$, $n = 6$), and 50% ($P < 0.001$, $n = 6$), respectively. Compared with the drug group, LE-VPA has more obvious inhibitory effect on the TNF-α ($P < 0.05$) and IL-6 ($P < 0.05$).

LE-VPA inhibited NF-κB activation in the hippocampus

In the attempt to define the underlying molecular mechanisms by which LE-VPA suppressed microglial inflammatory response, we monitored expression levels of TLR4 and the activation of the transcription factor NF-κB, which occurs in response of proinflammatory stimuli and results in increased expression of many cytokines and chemokines (52). To this end, we quantified the expression level of NF-κB p65 subunit as an indicator of NF-κB activation (Figures 7A–C). TLR4 ($P < 0.001$, $n = 6$) and p65 ($P < 0.001$, $n = 6$) are abundant in the hippocampus of KA mice, and the levels of these two factors decreased in the runner group (TLR4: $P < 0.05$, P65: $P < 0.01$, $n = 6$) and combination group (both $P < 0.01$, $n = 6$) after exercise, but drug group only reversed the expression of p65 ($P < 0.05$, $n = 6$) and has no effect on TLR4 ($P > 0.05$, $n = 6$). Thus, the combination treatment significantly reduced the expression of TLR4 and inhibited NF-κB activation compared with the drug alone treatment ($P < 0.05$), suggesting that inhibition of NF-κB activation may contribute to the anti-inflammatory effect of the microglial cells.

Discussion

First, our results of animal behavioral experiments and LFP show that compared with conventional drug treatment, LE-VPA can better control mild seizures and ease epilepsy-associated co-morbidities, such as cognitive dysfunction, depression, anxiety-like behaviors, and movement disorders (Figures 2–4). In addition, we found that LE-VPA had a larger significant effect on the abnormal LFP signal at low-frequency waves (Figure 5). This result is consistent with the literature, since LFP is used to understand the relationship between brain oscillations within different frequency ranges and cognitive and motor processes (53). Next, we explored the mechanism of action of the LE-VPA treatment of seizures and epilepsy-associated co-morbidities. We performed immunohistochemistry to examine the activation

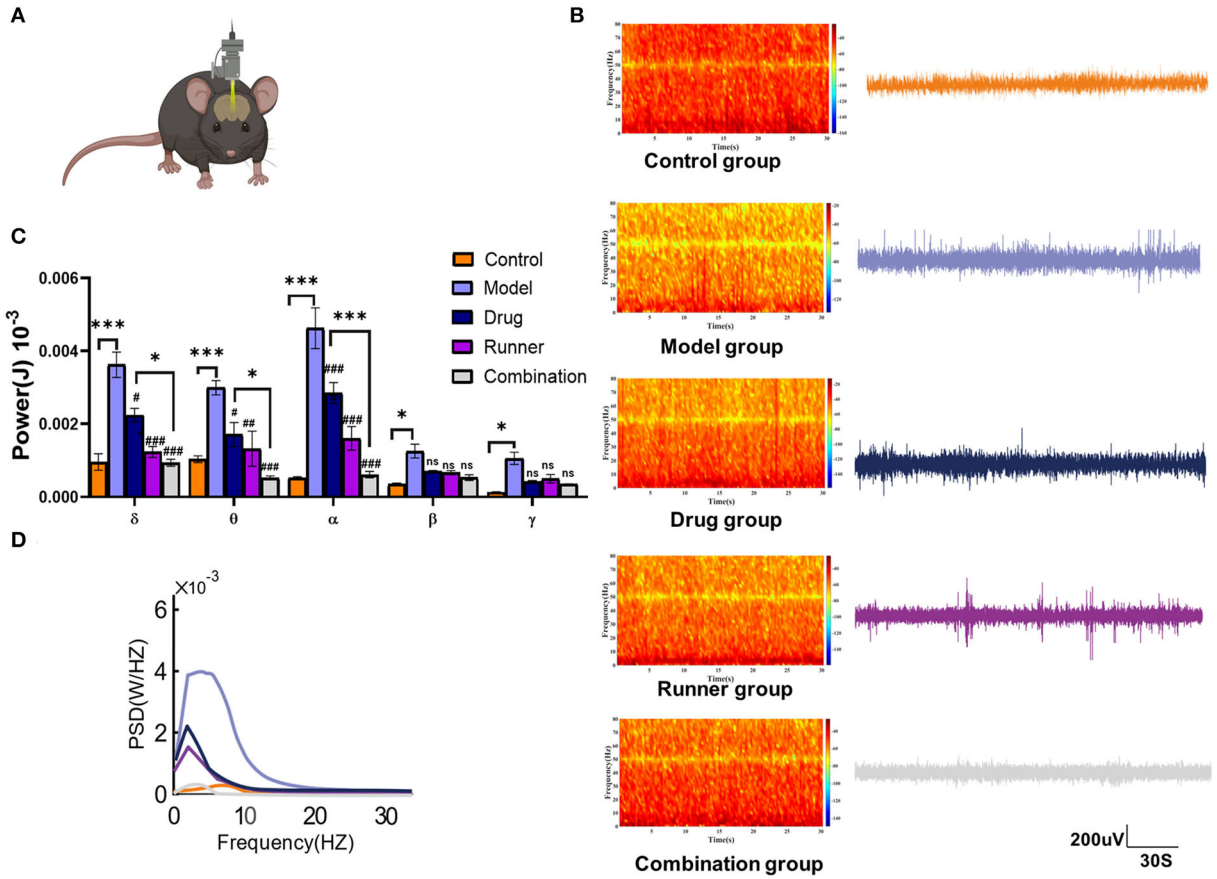

FIGURE 5
LFP spectral characteristics and PSD in each group. **(A)** Diagram of local field potential recording in mice. **(B)** LFP signals and spectral heat maps from representative seizure mice treated with control (orange), model (lavender), drug (blue), runner (amaranth), and combination (gray) groups were displayed, respectively. **(C)** Spectral plots and cumulative distribution curves from model mice with no treatment, VPA, treadmill, and combination treatment were shown, respectively. **(D)** Spectral analysis on PSD values of δ, θ, α, β, and γ rhythm in each group. Data in **(C)** were shown as mean ± SEM. ns > 0.05, *$P < 0.05$, ***$P < 0.001$; $^{\#}P < 0.05$, $^{\#\#}P < 0.01$, $^{\#\#\#}P < 0.001$, compared with model group (two-way ANOVA).

of TLR4/ NF-κB and the downstreaming IL-1β, TNF-α, and IL-6 signaling in the hippocampus. LE-VPA reduced TLR4 expression, inhibiting NF-κB signaling and, in turn, inhibiting the increase in expression levels of IL-1β, TNF-α, and IL-6. Therefore, this novel therapeutic approach was more effective in attenuating seizures and associated co-morbidities (Figure 8).

The pathogenesis of epilepsy is complex and has not been fully elucidated; consequently, there is a limited clinical cure rate. Recent studies have suggested that a variety of signaling pathways may be associated with epilepsy (54). These pathways include the Phosphatidylinositol-3-kinase (PI3K) / protein kinase B (Akt) / mammalian target of rapamycin (mTOR) signaling pathway that regulates the autophagy process in neurodegenerative diseases (55), the Wnt/β-catenin signaling pathway (56), mitogen-activated protein kinase (MAPK) signaling pathway (57) and the TLR4/ NF-κB pathway (58) that is associated with neurogenesis and neuronal death. Different inflammatory factors are closely related to these signaling pathways. Studies have shown that an increase in the BBB permeability is directly associated with seizure generation and severity (18, 59). Activated macrophages produce IL-1, IL-6, and TNF-α; these cytokines can alter the permeability of the blood–brain barrier (BBB) and allow peripheral proinflammatory factors to enter the circumventricular brain regions and cause seizures (60), followed by the activation of NF-κB pathway. IL-1β then triggers the breakdown of the BBB and activates glial cells (61). NF-κB then recruits other proteins (coactivators and RNA polymerase), which finally lead to the expression of proinflammatory cytokines (e.g., IL-1, IL-2, IL-6, and TNF-α) that exacerbates and perpetuates the seizures (62). In addition, TNF-α can control the glutamate receptor transport *via* TNF receptor 1 and the TNF receptor 2, and these receptors promote neuron firing by increasing glutamate levels in the synaptic cleft; therefore, TNF-α plays a role in epilepsy (63). During acute and

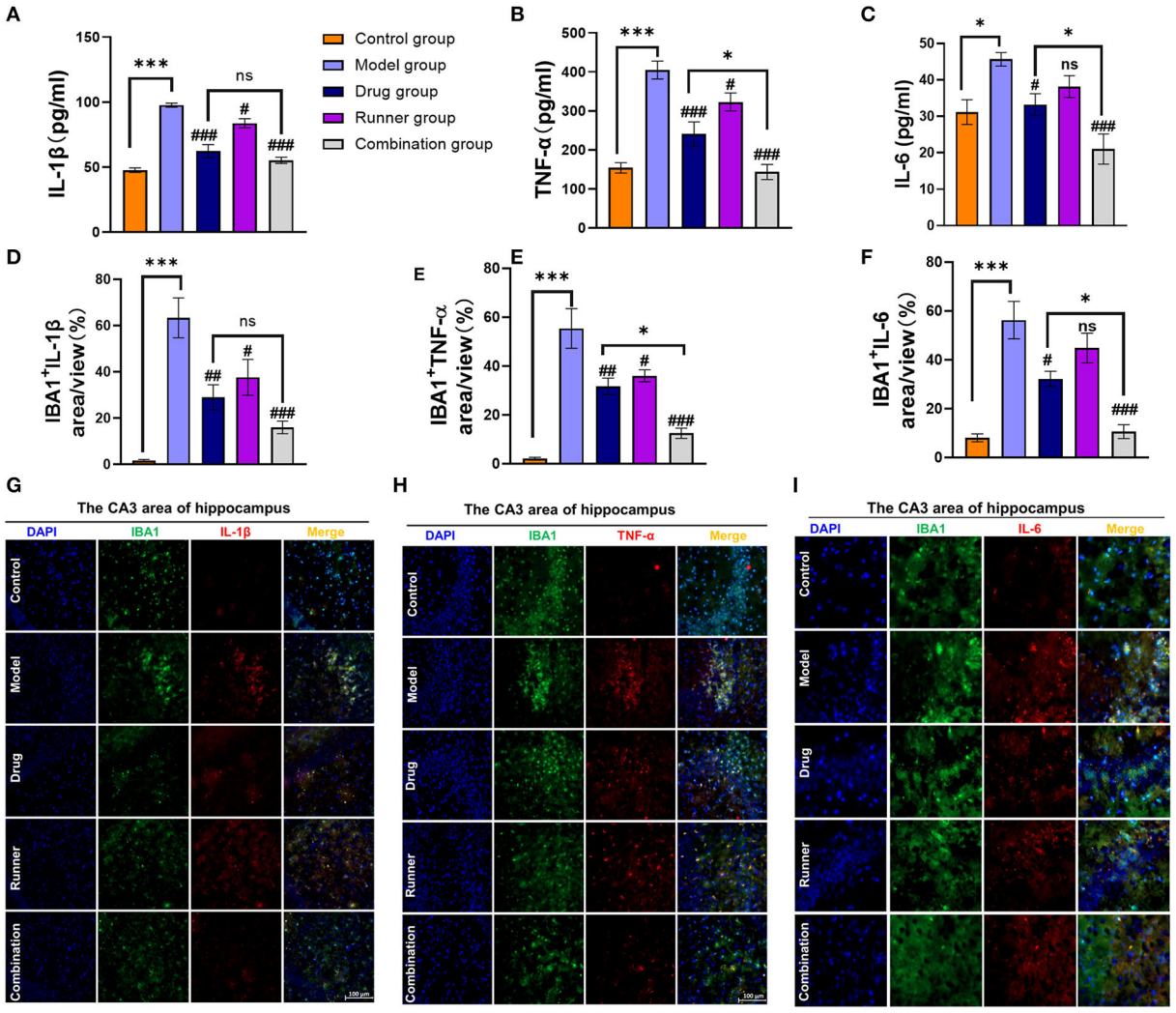

FIGURE 6
LE-VPA blocked the activation of microglial cells and the release of inflammatory factors. **(A–C)** ELISA analysis of secreted TNF-α, IL-1β, and IL-6 levels in control and four different treatment groups with epilepsy. **(D–F)** Quantitative analysis of percentage of IBA1$^+$ IL-1β-, IBA1$^+$ TNF-α-, and IBA1$^+$ IL-6-positive area. **(G–I)** Immunofluorescent staining of IBA1 and IL-1β, IBA1$^+$ TNF-α, and IBA1$^+$ IL-6 in the hippocampal CA3 area (scale bar, 100 μm). The data were expressed as the mean ± SEM. ns > 0.05, $^*P < 0.05$, $^{***}P < 0.001$; $^{\#}P < 0.05$, $^{\#\#}P < 0.01$, $^{\#\#\#}P < 0.001$, compared with model group (two-way ANOVA).

chronic seizures, IL-1β is highly expressed and its binding to IL-1β receptors (IL-1R1) activates NF-κB in target cells amplifying the inflammatory response (64). Previous studies have shown that following seizures, the IL-6 receptor mRNA is upregulated only in the hippocampus (65, 66). However, in recent years, there have been conflicting reports on the role of IL-6 in seizures. Although IL-6 is necessary for the nervous system normal development (67), high levels of IL-6 in the brain can lead to neurotoxic and proconvulsive effects (68, 69). The inhibition of the histone deacetylase (HDAC) and the modulation of brain-derived neurotrophic factor (BDNF) play a key role in regulating the main pathways that modulate the VPA epigenetic effects (70). Therefore, VPA may inhibit PI3K/Akt/ Mouse double minute 2 (MDM2) signaling pathway (71), inhibit NF-κB, p65-dependent transcriptional activation (71), and promote the tropomyosin receptor kinase B (TrkB)/BDNF signaling pathway (70) that reduces neuroinflammation and regulate synaptic plasticity.

In recent years, the relationship between VPA and cognitive function has been controversial (72–74). Our results of the water maze and the Y maze align with the evidence that shows VPA-induced cognition improvement in KA mice. There was no significant difference between the VPA-treated mice and the control group in total distance traveled in the Y maze (Figure 3G); this result could be explained by the diminished motor state of the mice resulting from the

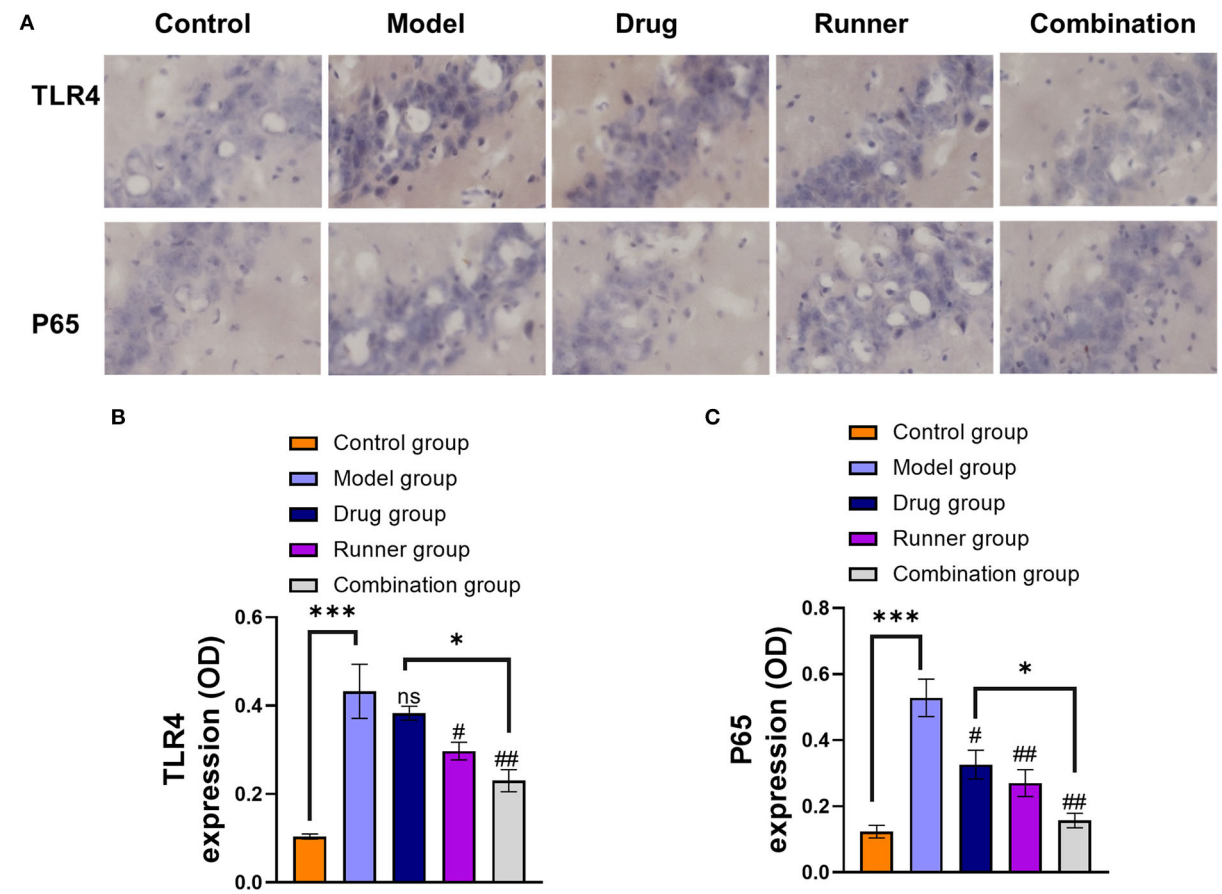

FIGURE 7
Effect of LE-VPA on TLR4/ NF-kB activation in the hippocampus. **(A)** Five brain slices were processed for TLR4 and NF-κB p65 immunohistochemical staining. Experiments were performed three times, and the staining of the cells under a 20x microscope was shown. **(B,C)** Comparison of the IODs of TLR4 and p65 using immunohistochemical staining in the hippocampus from each group. The data were expressed as the mean ± SEM. ns > 0.05, $^{*}P < 0.05$, $^{***}P < 0.001$; $^{\#}P < 0.05$, $^{\#\#}P < 0.01$, compared with model group (two-way ANOVA).

continuous intraperitoneal drug injection for 4 weeks. The gait analysis showed that VPA increased the print area during walking, but not the swing speed or body speed (Figure 4). This result suggests VPA might improve walking stability in patients with epilepsy without changing their physical flexibility. In addition, the immunohistochemistry showed that VPA did not reduce the expression levels of TLR4 in the hippocampus but significantly inhibited NF-κB p65-dependent transcriptional activation (Figure 6). We speculate that VPA may inhibit NF-κB activation through a pathway other than TLR4.

There is vast evidence for the beneficial effects of physical exercise on epilepsy in animals models and at the clinical level (75). For instance, it improves cognitive function and alleviates depression and anxiety in patients with epilepsy, which is consistent with our experimental results. The exact mechanism has not been elucidated. Nevertheless, researchers have adopted different strategies to explain the phenomenon. First, in chronic epilepsy, aerobic exercise improves regional cerebral glucose metabolism and an increase in adenosine content in the brain gray matter associated with motor, sensory, and autonomic functions. Thus, aerobic exercise has an anticonvulsant effect by affecting brain metabolism (76). Second, physical exercise exerted positive effects on hippocampal synaptic plasticity, including increasing hippocampal neurogenesis and restoring the LTP-induced damage in epileptic rats (77). Particularly, physical exercise alters BDNF/TrkB (78) and Akt/ mTOR signaling pathways (79). Finally, physical exercise can improve the hyperinflammatory state in the hippocampus (80). It has been shown that swimming exercise stimulates IGF1/PI3K/Akt and AMPK/SIRT1/PGC1α survival signals to suppress inflammation (81).

Most studies suggest that physical exercise can boost serotonin (82), norepinephrine (83), dopamine synthesis and release (84), increase BDNF, and reduce the activity of the hypothalamus–pituitary–adrenal (85). Consequently, there is a reduction in epilepsy co-morbidities. In addition, studies have

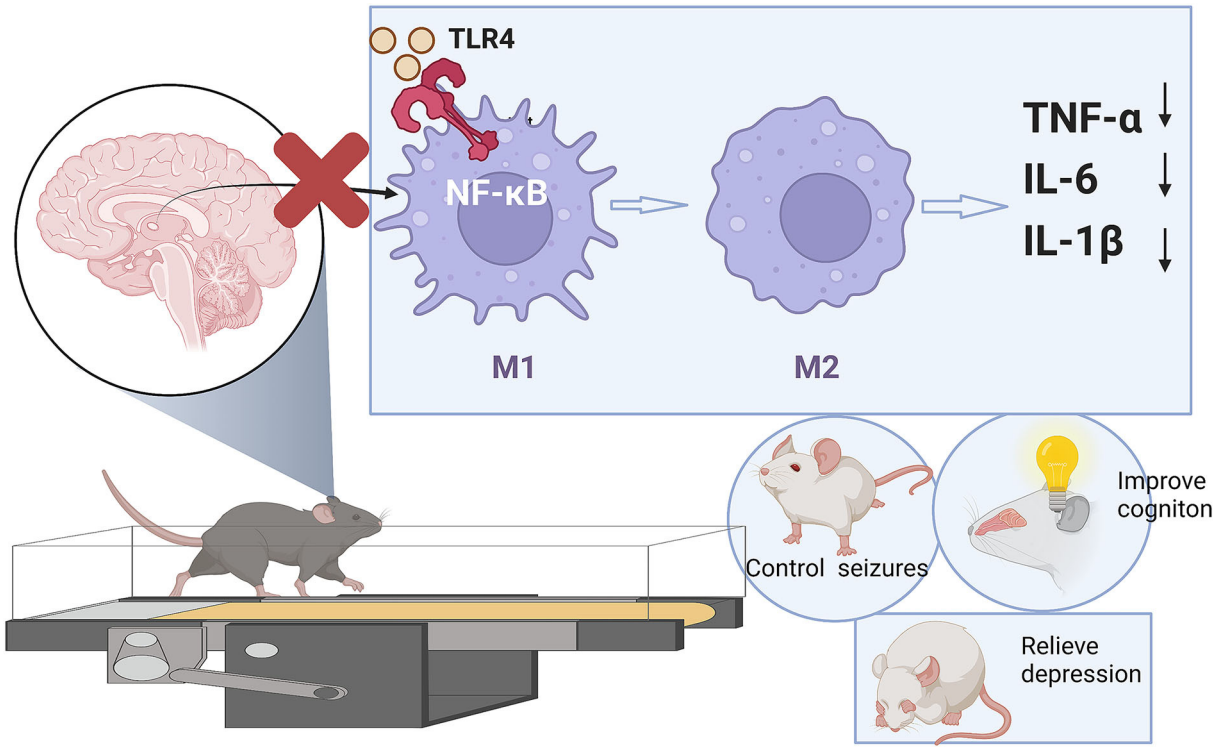

FIGURE 8
Summary of the article.

shown that moderate physical exercise could reduce the levels of IL-1β and TNF-α in the hippocampus or serum (86, 87) in interventions for brain disorders, although the effect on IL-6 is subject to specific discussion. To illustrate, physical exercise can reduce IL-6 levels in the hippocampus and cerebellum (88, 89). By contrast, during physical exercise, skeletal muscle produces large amounts of IL-6 to induce hepatic glucose export and induce lipolysis (90).

Altogether, our experiments showed that VPA plays a leading role in improving the frequency of severe seizures; however, physical exercise alone has little effect as a treatment (Figures 2C,D). Moreover, the effects of physical exercise alone on working memory tests (Figure 3E) and hippocampal IL-6 expression levels (Figures 6C,F) were also limited. Considering previous studies, we speculate that the physical exercise intensity may not be the optimal intensity for KA mice. Therefore, the next step is to determine the optimal intensity for the KA mice. To this end, we will divide the physical exercise intensity by gradient. Here, we showed that low-intensity physical exercise may be inhibiting the TLR4/ NF-κB pathway. Nonetheless, the mechanism in which the physical exercise-generated force is affecting the TLR4 expression in the brain needs to be further explored. For instance, physical exercise activates the mechanical sensor Piezo1 (91) which leads to enhanced expression of the bone-derived growth factor osteocalcin (OCN) (92). Subsequently, OCN can regulate cognition through G protein-coupled receptors (GPR) (93, 94). Furthermore, it has been shown that activation of GPR30 on microglial cells can reduce ischemic injury by inhibiting TLR4-mediated microglial inflammation. We need more evidence on whether microglial cells have receptors for OCN, thus, possibly playing a role in seizures and its co-morbidities by regulating the TLR4-mediated signaling pathway. These results suggest the LE-VPA treatment is a promising novel therapeutic avenue with translational application.

Data availability statement

The original contributions presented in the study are included in the article/supplementary material, further inquiries can be directed to the corresponding authors.

Ethics statement

The animal study was reviewed and approved by Shanghai University of Traditional Chinese Medicine.

Author contributions

YJi, JT, and YJia designed the research. YJia and LT performed the data analysis work. YJia, LT, YY, XC, and LZ conducted experiments. YJia wrote and revised the manuscript. LT and DQ drew the figures. YZ was responsible for the statistical analyses. All authors read and approved the final manuscript.

Funding

This work was supported by grants from National Key Research and Development Program (No. 2020YFA0803800), National Natural Science Foundation of China (Nos. 82274344, 82074162, and 81903995), Science, Technology Innovation Project of Putuo District Health System (No. ptkwws202107), Research Project (2020336B), and the One Hundred Talents Project of Putuo Hospital, Shanghai University of Traditional Chinese Medicine (No. 2022LH002).

Conflict of interest

The authors declare that the research was conducted in the absence of any commercial or financial relationships that could be construed as a potential conflict of interest.

Publisher's note

References

1. Thijs RD, Surges R, O'Brien TJ, Sander JW. Epilepsy in adults. *Lancet.* (2019) 393:689–701. doi: 10.1016/S0140-6736(18)32596-0

2. Beghi E, Giussani G, Sander JW. The natural history and prognosis of epilepsy. *Epileptic Disord.* (2015) 17:243–53. doi: 10.1684/epd.2015.0751

3. Löscher W. Basic pharmacology of valproate: a review after 35 years of clinical use for the treatment of epilepsy. *CNS Drugs.* (2002) 16:669–94. doi: 10.2165/00023210-200216100-00003

4. Chen B, Choi H, Hirsch LJ, Katz A, Legge A, Buchsbaum R, et al. Psychiatric and behavioral side effects of antiepileptic drugs in adults with epilepsy. *Epilepsy Behav.* (2017) 76:24–31. doi: 10.1016/j.yebeh.2017.08.039

5. Fricke-Galindo I, Jung-Cook H, Llerena A, López-López M. Farmacogenética de reacciones adversas a fármacos antiepilépticos. *Neurología.* (2018) 33:165–76. doi: 10.1016/j.nrl.2015.03.005

6. Cardenas-Rodriguez N, Huerta-Gertrudis B, Rivera-Espinosa L, Montesinos-Correa H, Bandala C, Carmona-Aparicio L, et al. Role of oxidative stress in refractory epilepsy: evidence in patients and experimental models. *Int J Mol Sci.* (2013) 14:1455–76. doi: 10.3390/ijms14011455

7. Nuzum H, Stickel A, Corona M, Zeller M, Melrose RJ, Wilkins SS. Potential benefits of physical activity in MCI and dementia. *Behav Neurol.* (2020) 2020:7807856. doi: 10.1155/2020/7807856

8. Posadzki P, Pieper D, Bajpai R, Makaruk H, Könsgen N, Neuhaus AL, et al. Exercise/physical activity and health outcomes: an overview of Cochrane systematic reviews. *BMC Public Health.* (2020) 20:1724. doi: 10.1186/s12889-020-09855-3

9. Kelly RS, Kelly MP, Kelly P. Metabolomics, physical activity, exercise and health: a review of the current evidence. *Biochim Biophys Acta Mol Basis Dis.* (2020) 1866:165936. doi: 10.1016/j.bbadis.2020.165936

10. Lourenco MV, Frozza RL, de Freitas GB, Zhang H, Kincheski GC, Ribeiro FC, et al. Exercise-linked FNDC5/irisin rescues synaptic plasticity and memory defects in Alzheimer's models. *Nat Med.* (2019) 25:165–75. doi: 10.1038/s41591-018-0275-4

11. Al Shoyaib A, Alamri FF, Biggers A, Karamyan ST, Arumugam TV, Ahsan F, et al. Delayed exercise-induced upregulation of angiogenic proteins and recovery of motor function after photothrombotic stroke in mice. *Neuroscience.* (2021) 461:57–71. doi: 10.1016/j.neuroscience.2021.02.023

12. Hong M, Kim M, Kim TW, Park SS, Kim MK, Park YH, et al. Treadmill exercise improves motor function and short-term memory by enhancing synaptic plasticity and neurogenesis in photothrombotic stroke mice. *Int Neurourol J.* (2020) 24:S28–38. doi: 10.5213/inj.2040158.079

13. Morgan JA, Singhal G, Corrigan F, Jaehne EJ, Jawahar MC, Baune BT. The effects of aerobic exercise on depression-like, anxiety-like, and cognition-like behaviours over the healthy adult lifespan of C57BL/6 mice. *Behav Brain Res.* (2018) 337:193–203. doi: 10.1016/j.bbr.2017.09.022

14. Nakken KO. Physical exercise in outpatients with epilepsy. *Epilepsia.* (1999) 40:643–51. doi: 10.1111/j.1528-1157.1999.tb05568.x

15. Hiragi T, Ikegaya Y, Koyama R. Microglia after seizures and in epilepsy. *Cells.* (2018) 7:26. doi: 10.3390/cells7040026

16. Morin-Brureau M, Milior G, Royer J, Chali F, Le Duigou C, Savary E, et al. Microglial phenotypes in the human epileptic temporal lobe. *Brain.* (2018) 141:3343–60. doi: 10.1093/brain/awy276

17. Feng L, Murugan M, Bosco DB, Liu Y, Peng J, Worrell GA, et al. Microglial proliferation and monocyte infiltration contribute to microgliosis following status epilepticus. *Glia.* (2019) 67:1434–48. doi: 10.1002/glia.23616

18. Vezzani A, French J, Bartfai T, Baram TZ. The role of inflammation in epilepsy. *Nat Rev Neurol.* (2011) 7:31–40. doi: 10.1038/nrneurol.2010.178

19. Devinsky O, Vezzani A, Najjar S, De Lanerolle NC, Rogawski MA. Glia and epilepsy: excitability and inflammation. *Trends Neurosci.* (2013) 36:174–84. doi: 10.1016/j.tins.2012.11.008

20. De Nardo D. Activation of the innate immune receptors: guardians of the micro galaxy: activation and functions of the innate immune receptors. *Adv Exp Med Biol.* (2017) 1024:1–35. doi: 10.1007/978-981-10-5987-2_1

21. Labzin LI, Heneka MT, Latz E. Innate immunity and neurodegeneration. *Annu Rev Med.* (2018) 69:437–49. doi: 10.1146/annurev-med-050715-104343

22. Liu B, Gu Y, Pei S, Peng Y, Chen J, Pham LV, et al. Interleukin-1 receptor associated kinase (IRAK)-M -mediated type 2 microglia polarization ameliorates the severity of experimental autoimmune encephalomyelitis (EAE). *J Autoimmun.* (2019) 102:77–88. doi: 10.1016/j.jaut.2019.04.020

23. Cerri C, Caleo M, Bozzi Y. Chemokines as new inflammatory players in the pathogenesis of epilepsy. *Epilepsy Res.* (2017) 136:77–83. doi: 10.1016/j.eplepsyres.2017.07.016

24. Iori V, Frigerio F, Vezzani A. Modulation of neuronal excitability by immune mediators in epilepsy. *Curr Opin Pharmacol.* (2016) 26:118–23. doi: 10.1016/j.coph.2015.11.002

25. Klein P, Dingledine R, Aronica E, Bernard C, Blümcke I, Boison D, et al. Commonalities in epileptogenic processes from different acute brain insults: do they translate? *Epilepsia.* (2018) 59:37–66. doi: 10.1111/epi.13965

26. Ichiyama T, Okada K, Lipton JM, Matsubara T, Hayashi T, Furukawa S. Sodium valproate inhibits production of TNF-alpha and IL-6 and activation of NF-kappaB. *Brain Res.* (2000) 857:246–51. doi: 10.1016/S0006-8993(99)02439-7

27. Eissa N, Azimullah S, Jayaprakash P, Jayaraj RL, Reiner D, Ojha SK, et al. The dual-active histamine H3 receptor antagonist and acetylcholine esterase inhibitor E100 ameliorates stereotyped repetitive behavior and neuroinflammmation in sodium valproate induced autism in mice. *Chem Biol Interact.* (2019) 312:108775. doi: 10.1016/j.cbi.2019.108775

28. Tang J, Xu L, Zeng Y, Gong F. Effect of gut microbiota on LPS-induced acute lung injury by regulating the TLR4/NF-kB signaling pathway. *Int Immunopharmacol.* (2021) 91:107272. doi: 10.1016/j.intimp.2020.107272

29. Chen L, Lou Y, Pan Z, Cao X, Zhang L, Zhu C, et al. Treadmill and wheel exercise protect against JNK/NF-κB induced inflammation in experimental models of knee osteoarthritis. *Biochem Biophys Res Commun.* (2020) 523:117–22. doi: 10.1016/j.bbrc.2019.12.014

30. Racine RJ. Modification of seizure activity by electrical stimulation. II motor seizure. *Electroencephalogr Clin Neurophysiol.* (1972) 32:281–94. doi: 10.1016/0013-4694(72)90177-0

31. Lai Z, Shan W, Li J, Min J, Zeng X, Zuo Z. Appropriate exercise level attenuates gut dysbiosis and valeric acid increase to improve neuroplasticity and cognitive function after surgery in mice. *Mol Psychiatry.* (2021) 26:7167–87. doi: 10.1038/s41380-021-01291-y

32. Morris R. Developments of a water-maze procedure for studying spatial learning in the rat. *J Neurosci Methods.* (1984) 11:47–60. doi: 10.1016/0165-0270(84)90007-4

33. Kraeuter AK, Guest PC, Sarnyai Z. The Y-maze for assessment of spatial working and reference memory in mice. *Methods Mol Biol.* (2019) 1916:105–11. doi: 10.1007/978-1-4939-8994-2_10

34. Kraeuter AK, Guest PC, Sarnyai Z. The open field test for measuring locomotor activity and anxiety-like behavior. *Methods Mol Biol.* (2019) 1916:99–103. doi: 10.1007/978-1-4939-8994-2_9

35. Zimcikova E, Simko J, Karesova I, Kremlacek J, Malakova J. Behavioral effects of antiepileptic drugs in rats: are the effects on mood and behavior detectable in open-field test? *Seizure.* (2017) 52:35–40. doi: 10.1016/j.seizure.2017.09.015

36. Hamers FP, Lankhorst AJ, van Laar TJ, Veldhuis WB, Gispen WH. Automated quantitative gait analysis during overground locomotion in the rat: its application to spinal cord contusion and transection injuries. *J Neurotrauma.* (2001) 18:187–201. doi: 10.1089/08977150150502613

37. Rusina E, Bernard C, Williamson A. The kainic acid models of temporal lobe epilepsy. *eNeuro.* (2021) 8:2. doi: 10.1523/ENEURO.0337-20.2021

38. de Gusmão CM, Garcia L, Mikati MA, Su S, Silveira-Moriyama L. Paroxysmal genetic movement disorders and epilepsy. *Front Neurol.* (2021) 12:648031. doi: 10.3389/fneur.2021.648031

39. Poe GR, Walsh CM, Bjorness TE. Cognitive neuroscience of sleep. *Prog Brain Res.* (2010) 185:1–19. doi: 10.1016/B978-0-444-53702-7.00001-4

40. Mazzoni A, Rosa M, Carpaneto J, Romito LM, Priori A, Micera S. Subthalamic neural activity patterns anticipate economic risk decisions in gambling. *eNeuro.* (2018) 5:1. doi: 10.1523/ENEURO.0366-17.2017

41. Wojtecki L, Elben S, Vesper J, Schnitzler A. The rhythm of the executive gate of speech: subthalamic low-frequency oscillations increase during verbal generation. *Eur J Neurosci.* (2017) 45:1200–11. doi: 10.1111/ejn.13429

42. Miller J, Watrous AJ, Tsitsiklis M, Lee SA, Sheth SA, Schevon CA, et al. Lateralized hippocampal oscillations underlie distinct aspects of human spatial memory and navigation. *Nat Commun.* (2018) 9:2423. doi: 10.1038/s41467-018-04847-9

43. Palva S, Palva JM. New vistas for alpha-frequency band oscillations. *Trends Neurosci.* (2007) 30:150–8. doi: 10.1016/j.tins.2007.02.001

44. Brücke C, Kupsch A, Schneider GH, Hariz MI, Nuttin B, Kopp U, et al. The subthalamic region is activated during valence-related emotional processing in patients with Parkinson's disease. *Eur J Neurosci.* (2007) 26:767–74. doi: 10.1111/j.1460-9568.2007.05683.x

45. Huebl J, Schoenecker T, Siegert S, Brücke C, Schneider GH, Kupsch A, et al. Modulation of subthalamic alpha activity to emotional stimuli correlates with depressive symptoms in Parkinson's disease. *Mov Disord.* (2011) 26:477–83. doi: 10.1002/mds.23515

46. Shin J. The interrelationship between movement and cognition: θ rhythm and the P300 event-related potential. *Hippocampus.* (2011) 21:744–52. doi: 10.1002/hipo.20792

47. Kaplan R, Tauste Campo A, Bush D, King J, Principe A, Koster R, et al. Human hippocampal theta oscillations reflect sequential dependencies during spatial planning. *Cogn Neurosci.* (2020) 11:122–31. doi: 10.1080/17588928.2019.1676711

48. Wang D, Huang Z, Ren L, Liu J, Wang X, Yu T, et al. Amygdalar and hippocampal beta rhythm synchrony during human fear memory retrieval. *Acta Neurochir.* (2020) 162:2499–507. doi: 10.1007/s00701-020-04276-y

49. Iwasaki S, Sasaki T, Ikegaya Y. Hippocampal beta oscillations predict mouse object-location associative memory performance. *Hippocampus.* (2021) 31:503–11. doi: 10.1002/hipo.23311

50. Nakazono T, Jun H, Blurton-Jones M, Green KN, Igarashi KM. Gamma oscillations in the entorhinal-hippocampal circuit underlying memory and dementia. *Neurosci Res.* (2018) 129:40–6. doi: 10.1016/j.neures.2018.02.002

51. Bando SY, Bertonha FB, Pimentel-Silva LR, de Oliveira JGM, Carneiro MAD, Oku MHM, et al. Hippocampal CA3 transcriptional modules associated with granule cell alterations and cognitive impairment in refractory mesial temporal lobe epilepsy patients. *Sci Rep.* (2021) 11:10257. doi: 10.1038/s41598-021-89802-3

52. Liu G, Fan G, Guo G, Kang W, Wang D, Xu B, et al. FK506 Attenuates the inflammation in rat spinal cord injury by inhibiting the activation of NF-κB in microglia cells. *Cell Mol Neurobiol.* (2017) 37:843–55. doi: 10.1007/s10571-016-0422-8

53. Einevoll GT, Kayser C, Logothetis NK, Panzeri S. Modelling and analysis of local field potentials for studying the function of cortical circuits. *Nat Rev Neurosci.* (2013) 14:770–85. doi: 10.1038/nrn3599

54. Zhang S, Chen F, Zhai F, Liang S. Role of HMGB1/TLR4 and IL-1β/IL-1R1 signaling pathways in epilepsy. *Front Neurol.* (2022) 13:904225. doi: 10.3389/fneur.2022.904225

55. Romero-Leguizamon CR, Ramirez-Latorre JA, Mora-Munoz L, Guerrero-Naranjo A. [Signaling pathways mTOR and AKT in epilepsy]. *Rev Neurol.* (2016) 63:33–41. doi: 10.33588/rn.6301.2015459

56. Gupta K, Schnell E. Neuronal network remodeling and Wnt pathway dysregulation in the intra-hippocampal kainate mouse model of temporal lobe epilepsy. *PLoS ONE.* (2019) 14:e0215789. doi: 10.1371/journal.pone.0215789

57. Wu DM, Zhang YT, Lu J, Zheng YL. Effects of microRNA-129 and its target gene c-Fos on proliferation and apoptosis of hippocampal neurons in rats with epilepsy via the MAPK signaling pathway. *J Cell Physiol.* (2018) 233:6632–43. doi: 10.1002/jcp.26297

58. Dong J, Liao Y, Wu B. TAK-242 ameliorates epileptic symptoms in mice by inhibiting the TLR4/NF-κB signaling pathway. *Ann Transl Med.* (2022) 10:795. doi: 10.21037/atm-22-2707

59. Sanchez-Munoz F, Dominguez-Lopez A, Yamamoto-Furusho JK. Role of cytokines in inflammatory bowel disease. *World J Gastroenterol.* (2008) 14:4280–8. doi: 10.3748/wjg.14.4280

60. Wilson CJ, Finch CE, Cohen HJ. Cytokines and cognition–the case for a head-to-toe inflammatory paradigm. *J Am Geriatr Soc.* (2002) 50:2041–56. doi: 10.1046/j.1532-5415.2002.50619.x

61. Choi J, Koh S. Role of brain inflammation in epileptogenesis. *Yonsei Med J.* (2008) 49:1–18. doi: 10.3349/ymj.2008.49.1.1

62. Karunaweera N, Raju R, Gyengesi E, Münch G. Plant polyphenols as inhibitors of NF-κB induced cytokine production-a potential anti-inflammatory treatment for Alzheimer's disease? *Front Mol Neurosci.* (2015) 8:24. doi: 10.3389/fnmol.2015.00024

63. Shandra AA, Godlevsky LS, Vastyanov RS, Oleinik AA, Konovalenko VL, Rapoport EN, et al. The role of TNF-alpha in amygdala kindled rats. *Neurosci Res.* (2002) 42:147–53. doi: 10.1016/S0168-0102(01)00309-1

64. Webster KM, Sun M, Crack P, O'Brien TJ, Shultz SR, Semple BD. Inflammation in epileptogenesis after traumatic brain injury. *J Neuroinflammation.* (2017) 14:10. doi: 10.1186/s12974-016-0786-1

65. Lehtimäki KA, Peltola J, Koskikallio E, Keränen T, Honkaniemi J. Expression of cytokines and cytokine receptors in the rat brain after kainic acid-induced seizures. *Brain Res Mol Brain Res.* (2003) 110:253–60. doi: 10.1016/S0169-328X(02)00654-X

66. Rosell DR, Nacher J, Akama KT, McEwen BS. Spatiotemporal distribution of gp130 cytokines and their receptors after status epilepticus: comparison with neuronal degeneration and microglial activation. *Neuroscience.* (2003) 122:329–48. doi: 10.1016/S0306-4522(03)00593-1

67. Nakashima K, Taga T. Mechanisms underlying cytokine-mediated cell-fate regulation in the nervous system. *Mol Neurobiol.* (2002) 25:233–44. doi: 10.1385/MN:25:3:233

68. Kalueff AV, Lehtimaki KA, Ylinen A, Honkaniemi J, Peltola J. Intranasal administration of human IL-6 increases the severity of chemically induced seizures in rats. *Neurosci Lett.* (2004) 365:106–10. doi: 10.1016/j.neulet.2004.04.061

69. Campbell IL, Abraham CR, Masliah E, Kemper P, Inglis JD, Oldstone MB, et al. Neurologic disease induced in transgenic mice by cerebral overexpression of interleukin 6. *Proc Natl Acad Sci U S A.* (1993) 90:10061–5. doi: 10.1073/pnas.90.21.10061

70. Ghiglieri V, Sgobio C, Patassini S, Bagetta V, Fejtova A, Giampà C, et al. TrkB/BDNF-dependent striatal plasticity and behavior in a genetic model of epilepsy: modulation by valproic acid. *Neuropsychopharmacology.* (2010) 35:1531–40. doi: 10.1038/npp.2010.23

71. Jambalganiin U, Tsolmongyn B, Koide N, Odkhuu E, Naiki Y, Komatsu T, et al. A novel mechanism for inhibition of lipopolysaccharide-induced proinflammatory cytokine production by valproic acid. *Int Immunopharmacol.* (2014) 20:181–7. doi: 10.1016/j.intimp.2014.02.032

72. Verma T, Mallik SB, Ramalingayya GV, Nayak PG, Kishore A, Pai KSR, et al. Sodium valproate enhances doxorubicin-induced cognitive dysfunction in Wistar rats. *Biomed Pharmacother.* (2017) 96:736–41. doi: 10.1016/j.biopha.2017.09.150

73. Wu P, Hong S, Zhong M, Guo Y, Chen H, Jiang L. Effect of sodium valproate on cognitive function and hippocampus of rats after convulsive status epilepticus. *Med Sci Monit Int Med J Exp Clin Res.* (2016) 22:5197–205. doi: 10.12659/MSM.898859

74. Li B, Wu Y, He Q, Zhou H, Cai J. The effect of complicated febrile convulsion on hippocampal function and its antiepileptic treatment significance. *Transl Pediatr.* (2021) 10:394–405. doi: 10.21037/tp-20-458

75. Arida RM. Physical exercise and seizure activity. *Biochim Biophys Acta Mol Basis Dis.* (2021) 1867:165979. doi: 10.1016/j.bbadis.2020.165979

76. Arida RM, da Silva Fernandes MJ, Scorza FA, Preti SC, Cavalheiro EA. Physical training does not influence interictal LCMRglu in pilocarpine-treated rats with epilepsy. *Physiol Behav.* (2003) 79:789–94. doi: 10.1016/S0031-9384(03)00204-X

77. Arida RM, Sanabria ERG, da Silva AC, Faria LC, Scorza FA, Cavalheiro EA. Physical training reverts hippocampal electrophysiological changes in rats submitted to the pilocarpine model of epilepsy. *Physiol Behav.* (2004) 83:165–71. doi: 10.1016/S0031-9384(04)00338-5

78. Iqbal M, Xiao XL, Zafar S, Yang PB Si KW, Han H, et al. Forced physical training increases neuronal proliferation and maturation with their integration into normal circuits in pilocarpine induced status epilepticus mice. *Neurochem Res.* (2019) 44:2590–605. doi: 10.1007/s11064-019-02877-3

79. de Almeida AA, Gomes da. Silva S, Lopim GM, Vannucci Campos D, Fernandes J, Cabral FR, et al. Physical exercise alters the activation of downstream proteins related to BDNF-TrkB signaling in male Wistar rats with epilepsy. *J Neurosci Res.* (2018) 96:911–20. doi: 10.1002/jnr.24196

80. Erickson KI, Voss MW, Prakash RS, Basak C, Szabo A, Chaddock L, et al. Exercise training increases size of hippocampus and improves memory. *Proc Natl Acad Sci U S A.* (2011) 108:3017–22. doi: 10.1073/pnas.1015950108

81. Lin JY, Kuo WW, Baskaran R, Kuo CH, Chen YA, Chen WS, et al. Swimming exercise stimulates IGF1/ PI3K/Akt and AMPK/SIRT1/PGC1α survival signaling to suppress apoptosis and inflammation in aging hippocampus. *Aging.* (2020) 12:6852–64. doi: 10.18632/aging.103046

82. Roth DL, Goode KT, Williams VL, Faught E. Physical exercise, stressful life experience, and depression in adults with epilepsy. *Epilepsia.* (1994) 35:1248–55. doi: 10.1111/j.1528-1157.1994.tb01796.x

83. Epps SA, Kahn AB, Holmes PV, Boss-Williams KA, Weiss JM, Weinshenker D. Antidepressant and anticonvulsant effects of exercise in a rat model of epilepsy and depression comorbidity. *Epilepsy Behav.* (2013) 29:47–52. doi: 10.1016/j.yebeh.2013.06.023

84. de Lima C, de Lira CA, Arida RM, Andersen ML, Matos G, de Figueiredo Ferreira Guilhoto LM, et al. Association between leisure time, physical activity, and mood disorder levels in individuals with epilepsy. *Epilepsy Behav.* (2013) 28:47–51. doi: 10.1016/j.yebeh.2013.03.016

85. Arida RM, Cavalheiro EA, Scorza FA. From depressive symptoms to depression in people with epilepsy: Contribution of physical exercise to improve this picture. *Epilepsy Res.* (2012) 99:1–13. doi: 10.1016/j.eplepsyres.2011.10.012

86. Paolucci EM, Loukov D, Bowdish DME, Heisz JJ. Exercise reduces depression and inflammation but intensity matters. *Biol Psychol.* (2018) 133:79–84. doi: 10.1016/j.biopsycho.2018.01.015

87. Gilak-Dalasm M, Peeri M, Azarbayjani MA. Swimming exercise decreases depression-like behaviour and inflammatory cytokines in a mouse model of type 2 diabetes. *Exp Physiol.* (2021) 106:1981–91. doi: 10.1113/EP089501

88. Bashiri H, Enayati M, Bashiri A, Salari AA. Swimming exercise improves cognitive and behavioral disorders in male NMRI mice with sporadic Alzheimer-like disease. *Physiol Behav.* (2020) 223:113003. doi: 10.1016/j.physbeh.2020.113003

89. Chennaoui M, Drogou C, Gomez-Merino D. Effects of physical training on IL-1beta, IL-6 and IL-1ra concentrations in various brain areas of the rat. *Eur Cytokine Netw.* (2008) 19:8–14. doi: 10.1684/ecn.2008.0115

90. Pedersen BK, Steensberg A, Schjerling P. Exercise and interleukin-6. *Curr Opin Hematol.* (2001) 8:137–41. doi: 10.1097/00062752-200105000-00002

91. Beech DJ. Endothelial Piezo1 channels as sensors of exercise. *J Physiol.* (2018) 596:979–84. doi: 10.1113/JP274396

92. Xing Y, Yang B, He Y, Xie B, Zhao T, Chen J. Effects of mechanosensitive ion channel Piezo1 on proliferation and osteogenic differentiation of human dental follicle cells. *Ann Anat.* (2022) 239:151847. doi: 10.1016/j.aanat.2021.151847

93. Chiappe A, Gonzalez G, Fradinger E, Iorio G, Ferretti JL, Zanchetta J. Influence of age and sex in serum osteocalcin levels in thoroughbred horses. *Arch Physiol Biochem.* (1999) 107:50–4. doi: 10.1076/apab.107.1.50.4357

94. Khrimian L, Obri A, Ramos-Brossier M, Rousseaud A, Moriceau S, Nicot AS, et al. Gpr158 mediates osteocalcin's regulation of cognition. *J Exp Med.* (2017) 214:2859–73. doi: 10.1084/jem.20171320

frontiers | Frontiers in Neurology

TYPE Original Research
PUBLISHED 18 October 2022
DOI 10.3389/fneur.2022.1019121

OPEN ACCESS

EDITED BY
Xinjian Zhu,
Southeast University, China

REVIEWED BY
Zucai Xu,
Affiliated Hospital of Zunyi Medical College, China
Wei Shan,
Beijing Tiantan Hospital, Capital Medical University, China

*CORRESPONDENCE
Qinglan Chen
chenqinglan1992@sina.com

SPECIALTY SECTION
This article was submitted to Epilepsy, a section of the journal Frontiers in Neurology

RECEIVED 14 August 2022
ACCEPTED 21 September 2022
PUBLISHED 18 October 2022

CITATION
Min J, Chen Q, Wu W, Zhao J and Luo X (2022) Identification of mRNA expression biomarkers associated with epilepsy and response to valproate with co-expression analysis. *Front. Neurol.* 13:1019121. doi: 10.3389/fneur.2022.1019121

Identification of mRNA expression biomarkers associated with epilepsy and response to valproate with co-expression analysis

Jun Min, Qinglan Chen*, Wenyue Wu, Jing Zhao and Xinming Luo

Department of Neurology, The Second Affiliated Hospital of Nanchang University, Nanchang, China

Purpose: Valproate (VPA) resistance was reported to be an important predictor of intractable epilepsy. We conducted this study to identify candidate biomarkers in peripheral blood correlated with VPA resistance.

Methods: The microarray dataset (GSE143272) was downloaded from the Gene Expression Omnibus database. Weighted gene co-expression network analysis (WGCNA) was performed to construct co-expression modules and obtain the most prominent module associated with VPA resistance. Differentially expressed genes (DEGs) between VPA-responsive and VPA-resistant patients were obtained using the "Limma" package in R. The intersections between the most prominent module and DEGs were identified as target genes. Metascape was performed to discover the possible involved pathways of the target genes. GeneCards database was used to know the function of each target gene.

Results: All genes in the GSE143272 were divided into 24 different modules. Among these modules, the darkred module showed a pivotal correlation with VPA resistance. A total of 70 DEGs between VPA-responsive and VPA-resistant patients were identified. After taking the intersection, 25 target genes were obtained. The 25 target genes were significantly enriched in T cell receptor recognition, T cell receptor signaling pathway, regulation of T cell activation, cytokine–cytokine receptor interaction, and *in utero* embryonic development. Half of the target genes (*CD3D*, *CD3G*, *CXCR3*, *CXCR6*, *GATA3*, *GZMK*, *IL7R*, *LIME1*, *SIRPG*, *THEMIS*, *TRAT1*, and *ZNF683*) were directly involved in the T cell development, migration, and activation signaling pathway.

Conclusion: We identified 25 target genes prominently associated with VPA resistance, which could be potential candidate biomarkers for epilepsy resistance in peripheral blood. The peripheral blood T cells may play a crucial role in VPA resistance. Those genes and pathways might become therapeutic targets with clinical usefulness in the future.

KEYWORDS

epilepsy, valproate, drug resistance, WGCNA, T cells, biomarker

Introduction

Epilepsy is characterized as a predisposition of the brain to generate epileptic seizures accompanied by neurobiological, cognitive, and psychosocial consequences (1). About 65 million people around the world suffer from epilepsy (2). One-third of patients with epilepsy fail to achieve sustained seizure freedom in spite of appropriately choosing and taking antiepileptic drugs (3). Pharmacoresistant epilepsy is associated with increased cognitive and psychiatric disorders, decreased quality of life, and even high risk of premature death (4, 5). The mechanisms of drug resistance in epilepsy remain elusive. Searching hematological diagnostic markers of drug resistance in epilepsy contributes to early diagnosis and treatment of refractory epilepsy.

Valproate (VPA) is the most commonly prescribed antiepileptic drug which is suitable for various epilepsy types including partial and generalized epilepsy (6). VPA can prevent seizures in 66% of patients with convulsive status epilepticus (7). However, almost one-third of patients are resistant to VPA treatment (7). Gesche et al. (8) revealed that VPA resistance is an important predictor of refractory idiopathic generalized epilepsy. The specificity and predictive value of VPA resistance in determining patients with epilepsy resistance is 100%, which is strongly associated with adverse social outcome and high seizure burden (8). Exploring the biomarker and mechanisms of VPA resistance is of great value for the study of epilepsy resistance.

Expression microarrays and high-throughput sequencing play an important role in promoting the research on drug resistance, identifying novel therapeutic targets, and accelerating drug discovery, and have been widely used in the study on drug resistance to chemotherapy and antibiotics (9–11). Previously, Wang et al. detected the differentially expressed genes (DEGs) in the peripheral blood of VPA-responsive and non-responsive pediatric patients with epilepsy and showed that specific cytokines and chemokines might participate in processes associated with VPA resistance (12). Compared with traditional expression profile analysis focusing on several DEGs, weighted gene co-expression network analysis (WGCNA) divides thousands of genes into dozens of gene modules with similar expression patterns and obtains the significant relationships between gene modules and specific phenotypes (13). WGCNA has been successfully applied to identify candidate biomarkers or therapeutic targets in various diseases and biological contexts (14–16).

In this study, we performed WGCNA analysis in peripheral blood expression profiles of patients with VPA-sensitive and VPA-resistant epilepsy and identified the mRNA expression biomarkers of VPA resistance. Our results revealed that the activation of peripheral blood T cells might have important pathophysiological significance in VPA resistance.

Abbreviations: VPA, valproate; WGCNA, weighted gene co-expression network analysis; DEGs, differentially expressed genes; BBB, blood brain barrier; TLE, temporal lobe epilepsy.

Materials and methods

Data collection

The microarray dataset (GSE143272) was downloaded from the Gene Expression Omnibus database (http://www.ncbi.nlm.nih.gov/geo/). This dataset consisted of 34 drug-naïve patients with epilepsy, 57 patients with different responses to antiepileptic drug monotherapy (phenytoin, VPA, and carbamazepine) during a follow-up, and 50 healthy control subjects. The peripheral blood samples were obtained and detected using an expression profiles array. In this article, only data from patients responsive and resistant to VPA were collected for further co-expression network analysis. In the GSE143272 dataset, patients on VPA therapy were followed-up over a period of 1 year for drug, dose, and serum drug concentrations and response to treatment after enrolment (17). During the course, patients who remained seizure-free were categorized as "VPA responsive" and who experienced at least 3 seizures were categorized as "VPA resistant" (17).

Weighted gene co-expression network analysis

Before co-expression network construction, all samples were clustered to observe whether there were outliers. Two outlier samples (GSM4255896 and GSM4255845) were deleted. The WGCNA R package was used to construct a gene co-expression network. The expression matrix of all the genes was converted into an adjacency matrix, which was then converted into a topological dissimilarity matrix. To ensure that the weighted co-expression network conformed to the scale-free network in this process, a soft threshold of 7 was chosen. Then, a dynamic tree-cutting algorithm was used to cluster gene modules on the basis of topological matrix. The module-trait relationship was obtained by estimating the correlation between the module eigengene and the phenotype (gender, age, and VPA resistance). The module highly related to VPA resistance was selected. For each expression profile, gene significance was calculated as the absolute value of the correlation between expression profile and each trait; module membership was defined as the correlation of expression profile and each module eigengene. The significant module genes were denoted as genes with a p-value of gene significance in VPA resistance less than 0.05 and were used for subsequent analysis.

Identification of DEGs

The "Limma" package in R was conducted to obtain DEGs between VPA-responsive and VPA-resistant patients, drug-naïve patients with epilepsy and healthy controls, and drug-naïve patients with epilepsy and patients taking VPA. If multiple probes matched the same gene, the mean signal intensity was computed. Genes with a p-value of < 0.05 and the $|\log2\ FC|$ of > 0.5 were considered robust DEGs.

Bio-function analysis

The Venn diagram was used to intersect the significant genes in the darkred module and the DEGs of VPA resistance obtained by Limma to identify target genes. The intersected genes were uploaded to Metascape (http://metascape.org/gp/index.html) to perform functional annotation analysis (18). GeneCards database (https://www.genecards.org/) was used to know the function of each target gene (19).

Specificity verification of the target genes

To determine whether the target genes were related to VPA resistance rather than VPA or epilepsy, we intersected the target genes with the DEGs between drug-naïve patients with epilepsy and patients taking VPA. The same method was used to obtain the intersection of the target genes with DEGs between drug-naïve patients with epilepsy and healthy controls.

Results

Construction of weighted co-expression network and modules

The workflow of this article is shown in Figure 1. A total of 9 VPA-resistant and 16 VPA-responsive samples were included for co-expression network analysis. Two outlier samples (GSM4255896 and GSM4255845) were deleted after sample cluster analysis (Figure 2A). To conform to the scale-free network, the soft-thresholding power of 7 was selected to attain the balanced scale independence (Figure 2B) and mean connectivity (Figure 2C). All genes were hierarchically clustered using the dynamic hybrid tree cut method and the highly similar modules were merged. All genes were finally divided into 24 different modules according to the connectivity, as shown in Figure 3. The genes that could not be included in any modules were classified into the gray module, which was removed in the subsequent analysis.

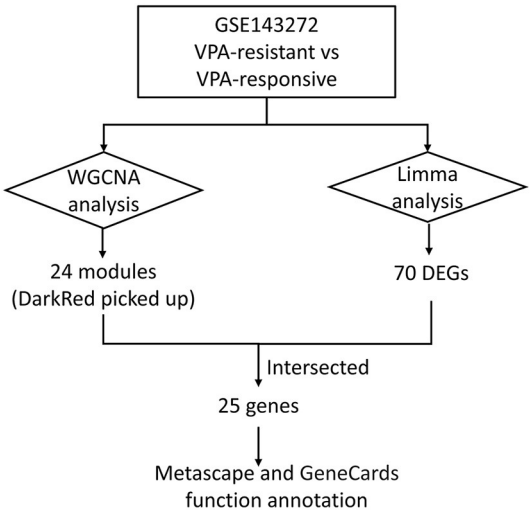

FIGURE 1
The workflow of this article.

Correlation between modules and identification of key modules

Among the 24 different modules, the interaction association (Figure 4A) and eigengene adjacency (Figure 4B) were analyzed and plotted. The results showed that modules were independent of each other, which indicated a high-degree independence of gene expression in different modules. Furthermore, we obtained modules related to VPA resistance, age, and gender through the module-traits correlation analysis. The results are shown in Figure 5A. The darkred, lightpink4, purple, darkorange, and floralwhite modules revealed a high correlation with disease type (responsive or resistant to VPA) compared with other modules (Figure 5A). None of the 24 modules showed a significant correlation with age and gender. The darkred module was the most significant module related to the VPA resistance. The gene significance and module membership in the darkred module were calculated, as shown in Figure 5B and Supplementary Table S1. In the darkred module, genes with a p-value of gene significance in VPA resistance less than 0.05 were recognized as significant module genes, and 562 genes were screened out accordingly for subsequent analysis (Supplementary Table S1).

Identification of DEGs

A total of 70 genes were found to be differentially expressed between VPA-responsive and VPA-resistant patients (Supplementary Table S2). Among these DEGs, 47 were downregulated and 23 were upregulated. There were 26 genes identified to be differentially expressed between patients with

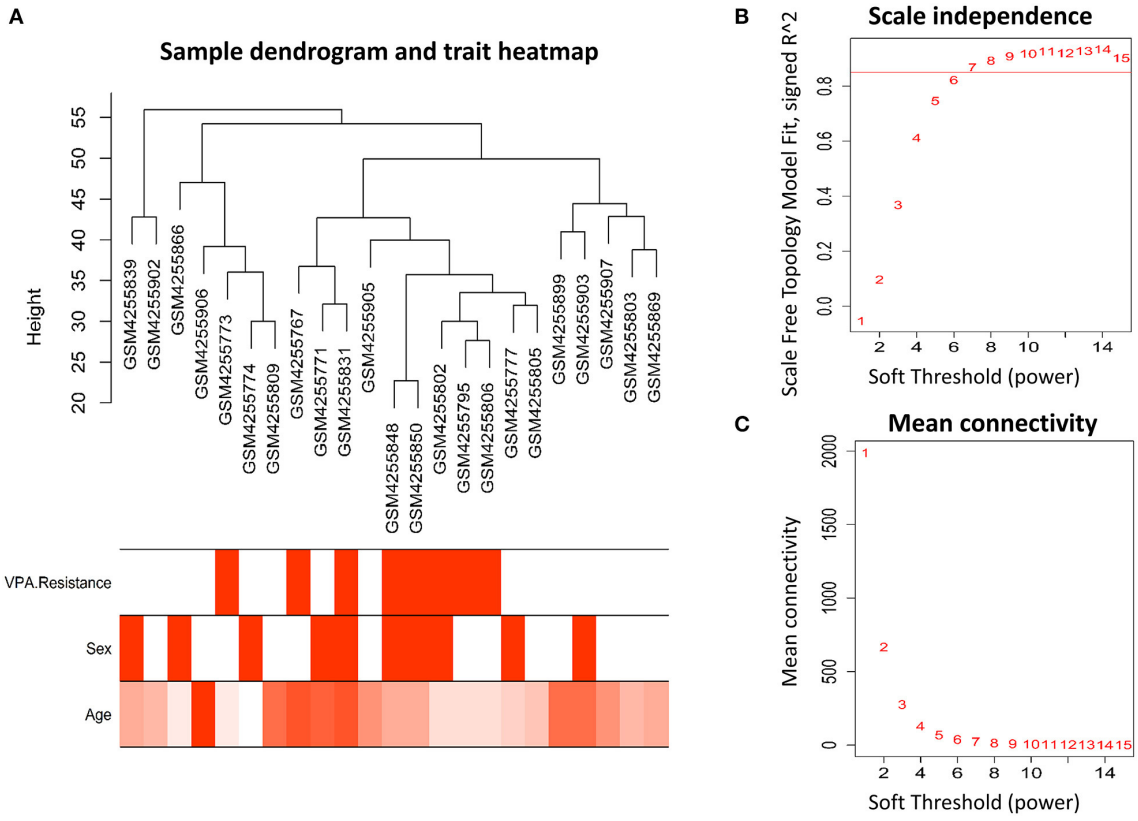

FIGURE 2
Clustering of samples and identification of soft-thresholding power. **(A)** The microarray dataset GSE143272 contained 9 VPA-resistant and 16 VPA-responsive samples. After clustering and removing two outliers, the remaining 23 samples were analyzed. The different color below denoted different disease status (VPA resistance, gender, and age). **(B)** The scale-independence and **(C)** mean connectivity for different soft threshold powers were calculated, and 7 was selected as the most fit power value to construct scale-free networks (VPA, valproate).

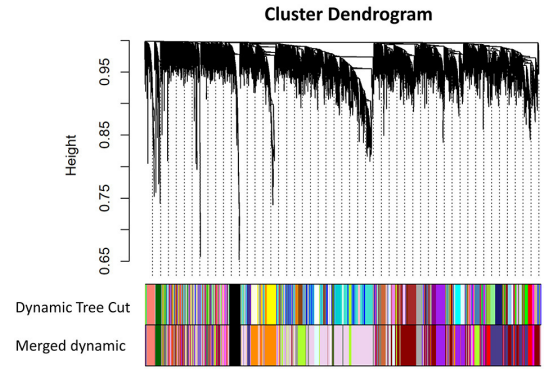

FIGURE 3
Cluster dendrogram of all genes and construction of co-expression modules by WGCNA in GSE143272. Each branch represented one gene, and every color bar below corresponded to one co-expression module. All genes were finally divided into 24 different modules after merging modules with high similarity (WGCNA, weighted gene co-expression network analysis).

naïve epilepsy and healthy control samples. Among these DEGs, 15 were downregulated and 11 were upregulated (Supplementary Table S3). A total of 74 genes were differentially expressed between patients with naive epilepsy and patients taking VPA. Among these DEGs, 28 were downregulated and 46 were upregulated (Supplementary Table S4).

Identification of target gene and bio-function analysis

We used the Venn diagram to intersect the 562 significant genes in the darkred module with the 70 DEGs between VPA-responsive and VPA-resistant patients, and a total of 25 genes (*ATP23*, *C17orf97*, *CBS*, *CD3D*, *CD3G*, *CDR2*, *CRYZ*, *CXCR3*, *CXCR6*, *GATA3*, *GZMK*, *IL7R*, *IMPA1*, *LIME1*, *RBBP6*, *RPS26*, *RPS26P11*, *SF1*, *SIRPG*, *SNORA28*, *STMN3*, *THEMIS*, *TRAT1*, *ZNF683*, and *ZNF816*) were obtained (Figure 6A, Supplementary Table S5). Among the 25 target genes, 23 genes

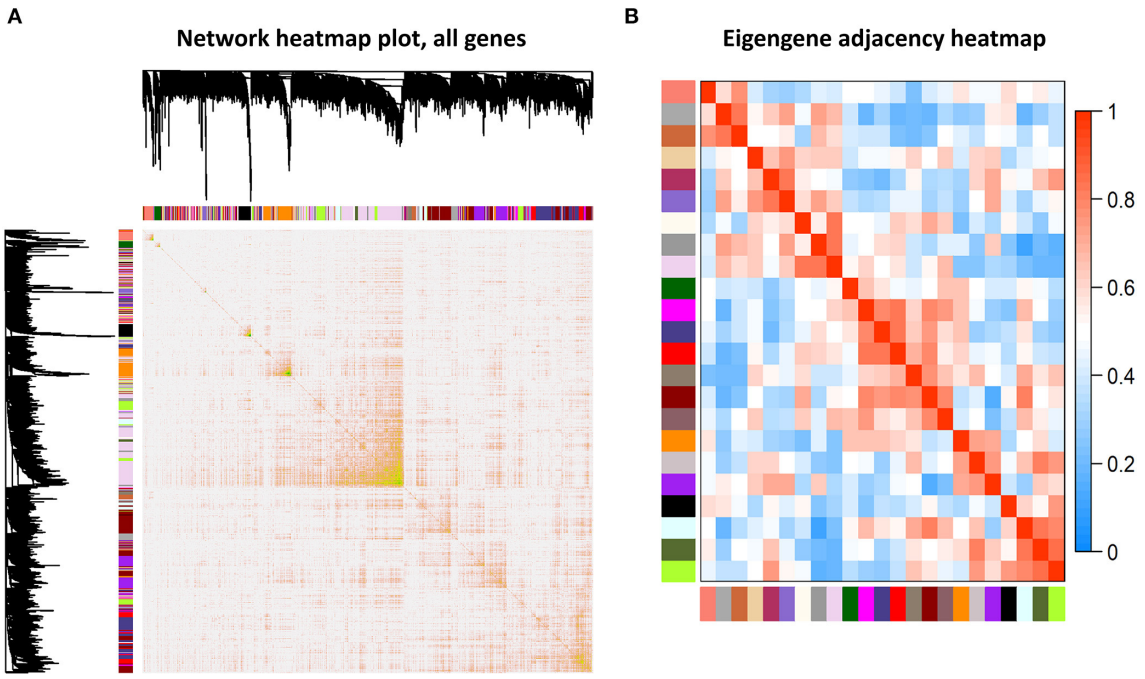

FIGURE 4
Association analysis of modules. **(A)** Different colored bars represented different modules. The depth of color represented the tightness of the connection among different modules. Significant dissimilarity in the connectivity existed among different modules. **(B)** Heat map to display the eigengene adjacencies in some representative modules.

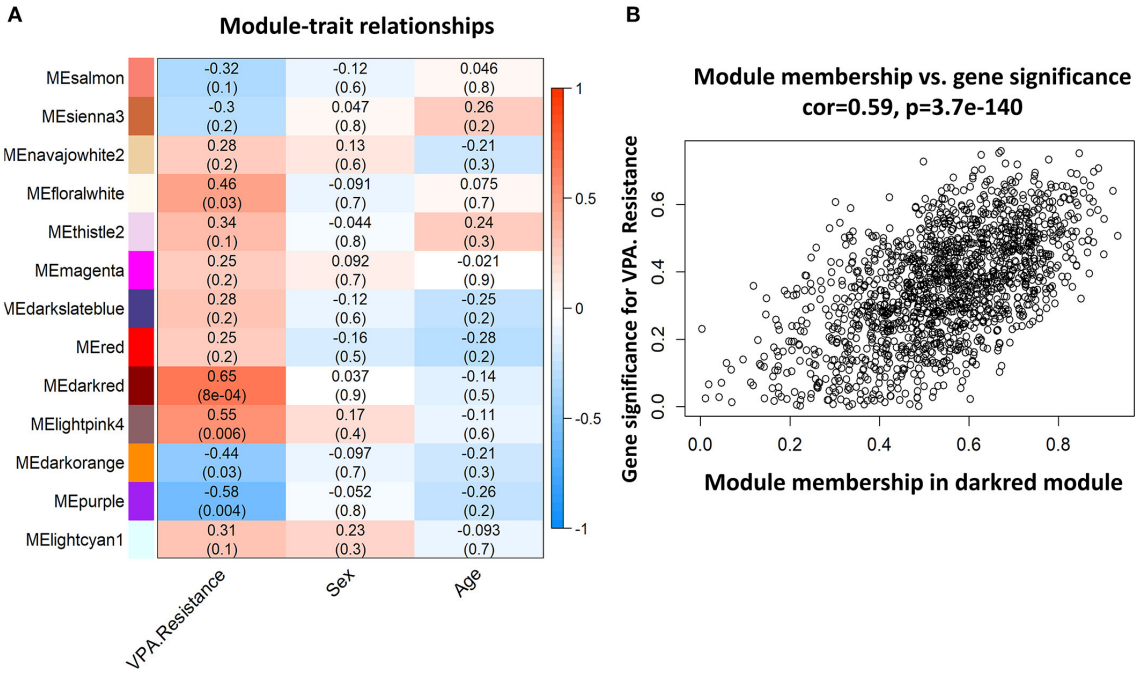

FIGURE 5
Representative heat map of modules-traits relationship and analysis of gene significance and module membership in the darkred module. **(A)** The heat map showed the relationship between different modules and each trait (VPA resistance, sex, or age). The number in each bar denoted the correlation coefficient and *p*-value. The darkred module is most related to VPA resistance. **(B)** Scatter diagram to show the gene significance in VPA resistance and module membership in the darkred module (VPA, valproate).

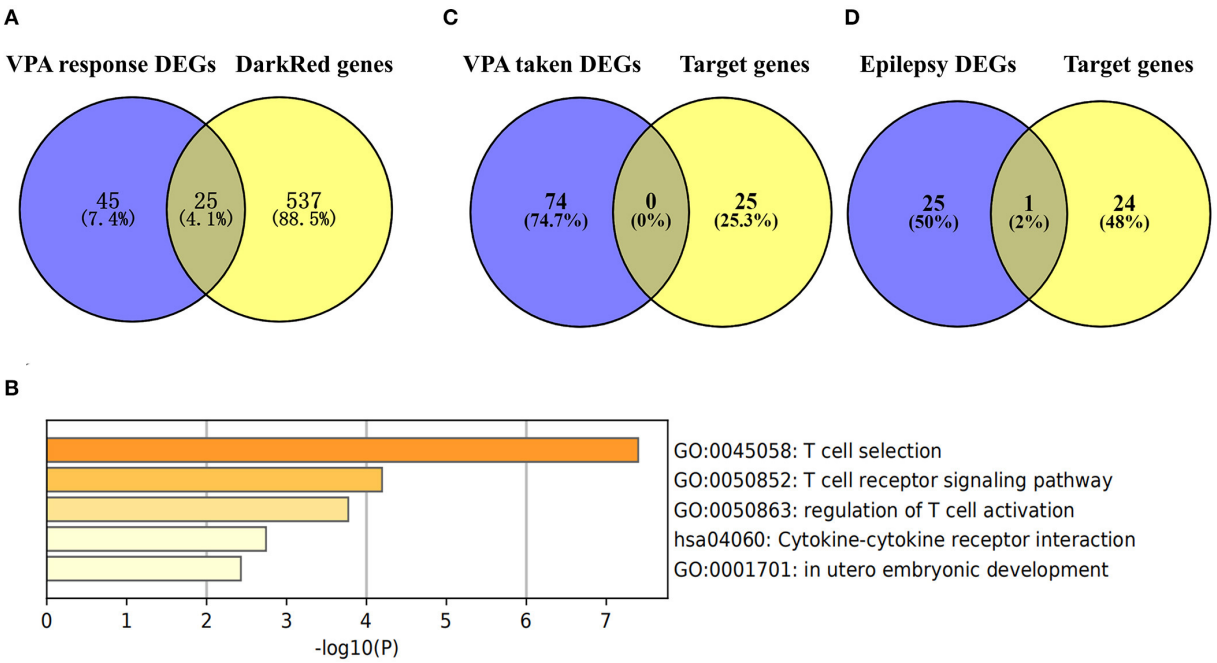

FIGURE 6
Identification of target genes in the key module and bio-function analysis. **(A)** Common genes of DEGs in VPA resistance (the blue circle) and the significant genes in the darkred module (the yellow circle). The DEGs in VPA resistance were obtained using the "Limma" algorithm by |Log2 FC| > 0.5 and *p*-value < 0.05. The darkred module was most related to VPA resistance through WGCNA analysis and the significant module genes were those with *p*-value of gene significance in VPA resistance less than 0.05. By comparing the genes, a total of 25 target genes were obtained. **(B)** The function of the 25 target genes was analyzed by Metascape and top 5 clustered terms were displayed. **(C)** Common genes of target genes and VPA taken DEGs (the blue circle). **(D)** Common genes of target genes and epilepsy DEGs (the blue circle) ["Log10(P)" is the *p*-value in log base 10. DEG, differentially expressed gene; VPA, valproate; WGCNA, weighted gene co-expression network analysis].

were upregulated in VPA-resistant patients except for *RBBP6* and *SNORA28*. Then, we analyzed the function of 25 target genes by Metascape. The enriched top 5 biological processes were T cell receptor recognition, T cell receptor signaling pathway, regulation of T cell activation, cytokine–cytokine receptor interaction, and *in utero* embryonic development (Figure 6B). Further functional analysis using the GeneCards human gene database showed that *CD3D*, *CD3G*, *CXCR3*, *CXCR6*, *GATA3*, *GZMK*, *IL7R*, *LIME1*, *SIRPG*, *THEMIS*, *TRAT1*, and *ZNF683* were directly involved in the T cell development, migration, and activation signaling pathway.

Gene specificity verification

To test whether the 25 target genes associated with VPA resistance were affected by epilepsy or sodium VPA, we compared these 25 genes with the DEGs associated with taking VPA or the DEGs related to epilepsy. The results of the comparisons are presented in Figure 6C. From the Venn diagram, there was no intersection gene between the 25 target genes and DEGs associated with taking VPA. We also intersected these 25 target genes with the 26 DEGs associated with epilepsy and only one gene was common to both groups (Figure 6D).

Discussion

Pharmacoresistance is an important unsolved problem in the field of epilepsy. Searching for hematological markers for epilepsy resistance is helpful to predict the drug response in patients with epilepsy, improve prognosis, and explore the potential mechanisms of drug-resistant epilepsy (20). WGCNA is a widely used bioinformatics analysis method that focuses on the gene modules involved in the common biological pathway and obtains the relationship between modules and traits in interest instead of several DEGs (13). In this article, we used WGCNA to obtain the gene module that most significantly correlated with VPA resistance; furthermore, we found the DEGs in this module closely participated in the T cell selection and activation pathway. Specifically, the DEGs in the significant module are associated with VPA resistance regardless of the presence or absence of seizure or VPA. As there was a close correlation between VPA resistance and epilepsy resistance (8), we proposed that the molecule expression of the T cell activation pathway in peripheral blood could be a good biomarker of epilepsy resistance.

Previous studies have also laid the foundation for T cell activation to be a biomarker of epilepsy resistance. Ouédraogo et al. identified that CD4+ T cells along with pro-inflammatory

cytokines (e.g., interleukin-17A and tumor necrosis factor) expressed by CD4+ T cells were elevated in the peripheral blood of patients with drug-resistant epilepsy compared with that in patients with well-controlled epilepsy (21). T cells were upregulated not only in the peripheral blood of patients with intractable epilepsy but also in brain tissue. Tröscher et al. found that CD3+ as well as CD8+ T cell numbers were significantly elevated in the resected hippocampi of patients with temporal lobe epilepsy (TLE) compared with that in the healthy controls, although the numbers varied significantly among TLE subgroups (22). Animal models of intractable epilepsy also showed that T cells were increased in the epileptic hippocampus (23). Together, our study combined with the results of previous studies showed that the upregulation and activation of T cells in peripheral blood could be a good biomarker for drug-resistant epilepsy.

T cells could also participate in the physiological mechanism of epilepsy resistance. In TLE mice, 60–75% of T cells present in the hippocampus were cytotoxic CD8+ T cells, suggesting a potential role in the damage of hippocampal neurons that was regarded as an important pathophysiological basis for epileptogenesis of TLE (23). A further analysis of TLE showed that the number of T cells in the epileptic hippocampi was significantly correlated with the degree of neuronal loss, but not with seizure frequency or disease duration (22). Importantly, the attack of CD8+ T cells on hippocampal neurons was found to induce hippocampal sclerosis and TLE in limbic encephalitis (24). Pro-inflammatory CD4+ T cells could also cause neuronal damage *in vivo* (25) and directly lead to intractable seizure in an animal model of epilepsy partly through secreting interleukin-17A and granulocyte-macrophage colony-stimulating factor (26). The role of T cells in blood–brain barrier (BBB) injury has also attracted increasing attention (27). Multiple studies in neurological diseases such as Alzheimer's disease and multiple sclerosis suggested that T lymphocytes were closely related to BBB destruction (28, 29). Before entering the brain parenchyma, pro-inflammatory CD17+ T cells were interacted closely with vascular endothelial cells by promoting the downregulation of tight junction protein and adhesion protein, stimulating the expression of pro-inflammatory cytokines, and promoting the transmigration of CD4+ T cells (27, 28). The infiltrated CD8+ T cells also showed to be involved in BBB destruction through a perforin-dependent process (30). Removing T lymphocytes in peripheral blood by Fingomod could reduce BBB injury and P-glycoprotein expression (31). This evidence supported that peripheral blood-derived T cells might play an important role in BBB injury.

This study has some limitations. First, the sample size in our study is limited. Therefore, expanding the sample validation can improve the reliability of the research results. Second, further experimental verification of target gene expression in patients with epilepsy is necessary, and the undifferentiated T cell types need to be further explored in future studies. In addition, as a potential candidate biomarker, the sensitivity and specificity of T cell target gene expression in peripheral blood to predict epilepsy resistance need to be further validated in population data.

In summary, using WGCNA, our study has identified that peripheral blood T lymphocyte activation could be a good biomarker for VPA treatment response. Furthermore, our findings also have guiding significance for further revealing the pathophysiological mechanism of drug-resistant epilepsy.

Data availability statement

The datasets presented in this study can be found in online repositories. The names of the repository/repositories and accession number(s) can be found below: https://www.ncbi.nlm.nih.gov/, GSE143272.

Ethics statement

Ethical review and approval was not required for the study on human participants in accordance with the local legislation and institutional requirements. Written informed consent for participation was not required for this study in accordance with the national legislation and the institutional requirements.

Author contributions

JM participated in bioinformatics analysis and drafting of the manuscript. QC participated in the research design, bioinformatics analysis, and manuscript revision. WW provided help with image production and the manuscript preparation. JZ participated in the research design. XL revised the manuscript. All authors read and approved the final manuscript.

Acknowledgments

We would like to thank Zengsong Zhang for providing help on bioinformatic analysis.

Conflict of interest

The authors declare that the research was conducted in the absence of any commercial or financial relationships that could be construed as a potential conflict of interest.

Publisher's note

All claims expressed in this article are solely those of the authors and do not necessarily represent those

of their affiliated organizations, or those of the publisher, the editors and the reviewers. Any product that may be evaluated in this article, or claim that may be made by its manufacturer, is not guaranteed or endorsed by the publisher.

Supplementary material

The Supplementary Material for this article can be found online at: https://www.frontiersin.org/articles/10.3389/fneur.2022.1019121/full#supplementary-material

References

1. Fisher RS, Acevedo C, Arzimanoglou A, Bogacz A, Cross JH, Elger CE, et al. Ilae official report: a practical clinical definition of epilepsy. *Epilepsia.* (2014) 55:475–82. doi: 10.1111/epi.12550

2. Ngugi AK, Bottomley C, Kleinschmidt I, Sander JW, Newton CR. Estimation of the burden of active and life-time epilepsy: a meta-analytic approach. *Epilepsia.* (2010) 51:883–90. doi: 10.1111/j.1528-1167.2009.02481.x

3. Kwan P, Arzimanoglou A, Berg AT, Brodie MJ, Allen Hauser W, Mathern G, et al. Definition of drug resistant epilepsy: consensus proposal by the ad hoc task force of the ilae commission on therapeutic strategies. *Epilepsia.* (2010) 51:1069–77. doi: 10.1111/j.1528-1167.2009.02397.x

4. Janson MT, Bainbridge JL. Continuing burden of refractory epilepsy. *Ann Pharmacother.* (2021) 55:406–8. doi: 10.1177/1060028020948056

5. Kanner AM. Management of psychiatric and neurological comorbidities in epilepsy. *Nat Rev Neurol.* (2016) 12:106–16. doi: 10.1038/nrneurol.2015.243

6. Tomson T, Battino D, Perucca E. The remarkable story of valproic acid. *Lancet Neurol.* (2016) 15:141. doi: 10.1016/S1474-4422(15)00398-1

7. Misra UK, Kalita J, Patel R. Sodium valproate vs phenytoin in status epilepticus: a pilot study. *Neurology.* (2006) 67:340–2. doi: 10.1212/01.wnl.0000224880.35053.26

8. Gesche J, Khanevski M, Solberg C, Beier CP. Resistance to valproic acid as predictor of treatment resistance in genetic generalized epilepsies. *Epilepsia.* (2017) 58:e64–e9. doi: 10.1111/epi.13702

9. Huang Y, Sadée W. Drug sensitivity and resistance genes in cancer chemotherapy: a chemogenomics approach. *Drug Discov Today.* (2003) 8:356–63. doi: 10.1016/S1359-6446(03)02654-0

10. Farha MA, French S, Brown ED. Systems-level chemical biology to accelerate antibiotic drug discovery. *Acc Chem Res.* (2021) 54:1909–20. doi: 10.1021/acs.accounts.1c00011

11. Zhao C, Gao Y, Guo R, Li H, Yang B. Microarray expression profiles and bioinformatics analysis of mrnas, lncrnas, and circrnas in the secondary temozolomide-resistant glioblastoma. *Invest New Drugs.* (2020) 38:1227–35. doi: 10.1007/s10637-019-00884-3

12. Wang Y, Li Z. Rna-seq analysis of blood of valproic acid-responsive and non-responsive pediatric patients with epilepsy. *Exp Ther Med.* (2019) 18:373–83. doi: 10.3892/etm.2019.7538

13. Langfelder P, Horvath S. Wgcna: an R package for weighted correlation network analysis. *BMC Bioinformatics.* (2008) 9:559. doi: 10.1186/1471-2105-9-559

14. Bian Y, Huang J, Zeng Z, Yao H, Tu J, Wang B, et al. Construction of survival-related co-expression modules and identification of potential prognostic biomarkers of osteosarcoma using wgcna. *Ann Transl Med.* (2022) 10:296. doi: 10.21037/atm-22-399

15. Wang M, Wang L, Pu L, Li K, Feng T, Zheng P, et al. Lncrnas related key pathways and genes in ischemic stroke by weighted gene co-expression network analysis (Wgcna). *Genomics.* (2020) 112:2302–8. doi: 10.1016/j.ygeno.2020.01.001

16. Peng J, Wang P, Fang H, Zheng J, Zhong C, Yang Y, et al. Weighted gene co-expression analysis network-based analysis on the candidate pathways and hub genes in eggplant bacterial wilt-resistance: a plant research study. *Int J Mol Sci.* (2021) 22:13279. doi: 10.3390/ijms222413279

17. Rawat C, Kutum R, Kukal S, Srivastava A, Dahiya UR, Kushwaha S, et al. Downregulation of peripheral Ptgs2/Cox-2 in response to valproate treatment in patients with epilepsy. *Sci Rep.* (2020) 10:2546. doi: 10.1038/s41598-020-59259-x

18. Zhou Y, Zhou B, Pache L, Chang M, Khodabakhshi AH, Tanaseichuk O, et al. Metascape provides a biologist-oriented resource for the analysis of systems-level datasets. *Nat Commun.* (2019) 10:1523. doi: 10.1038/s41467-019-09234-6

19. Safran M, Dalah I, Alexander J, Rosen N, Iny Stein T, Shmoish M, et al. Genecards version 3: the human gene integrator. *Database.* (2010) 2010:baq020. doi: 10.1093/database/baq020

20. Pitkänen A, Ekolle Ndode-Ekane X, Lapinlampi N, Puhakka N. Epilepsy biomarkers - toward etiology and pathology specificity. *Neurobiol Dis.* (2019) 123:42–58. doi: 10.1016/j.nbd.2018.05.007

21. Ouédraogo O, Rébillard RM, Jamann H, Mamane VH, Clénet ML, Daigneault A, et al. Increased frequency of proinflammatory cd4 T cells and pathological levels of serum neurofilament light chain in adult drug-resistant epilepsy. *Epilepsia.* (2021) 62:176–89. doi: 10.1111/epi.16742

22. Tröscher AR, Sakaraki E, Mair KM, Köck U, Racz A, Borger V, et al. T Cell numbers correlate with neuronal loss rather than with seizure activity in medial temporal lobe epilepsy. *Epilepsia.* (2021) 62:1343–53. doi: 10.1111/epi.16914

23. Zattoni M, Mura ML, Deprez F, Schwendener RA, Engelhardt B, Frei K, et al. Brain infiltration of leukocytes contributes to the pathophysiology of temporal lobe epilepsy. *J Neurosci.* (2011) 31:4037–50. doi: 10.1523/JNEUROSCI.6210-10.2011

24. Pitsch J, van Loo KMJ, Gallus M, Dik A, Kamalizade D, Baumgart AK, et al. Cd8(+) T-Lymphocyte-driven limbic encephalitis results in temporal lobe epilepsy. *Ann Neurol.* (2021) 89:666–85. doi: 10.1002/ana.26000

25. Siffrin V, Radbruch H, Glumm R, Niesner R, Paterka M, Herz J, et al. In vivo imaging of partially reversible Th17 cell-induced neuronal dysfunction in the course of encephalomyelitis. *Immunity.* (2010) 33:424–36. doi: 10.1016/j.immuni.2010.08.018

26. Xu D, Robinson AP, Ishii T, Duncan DS, Alden TD, Goings GE, et al. Peripherally derived t regulatory and $\Gamma\delta$ T cells have opposing roles in the pathogenesis of intractable pediatric epilepsy. *J Exp Med.* (2018) 215:1169–86. doi: 10.1084/jem.20171285

27. Kebir H, Kreymborg K, Ifergan I, Dodelet-Devillers A, Cayrol R, Bernard M, et al. Human Th17 lymphocytes promote blood-brain barrier disruption and central nervous system inflammation. *Nat Med.* (2007) 13:1173–5. doi: 10.1038/nm1651

28. Kubick N, Flournoy PCH, Enciu AM, Manda G, Mickael ME. Drugs modulating Cd4+ T cells blood-brain barrier interaction in Alzheimer's disease. *Pharmaceutics.* (2020) 12:880. doi: 10.3390/pharmaceutics12090880

29. Kunkl M, Frascolla S, Amormino C, Volpe E, Tuosto L. T helper cells: the modulators of inflammation in multiple sclerosis. *Cells.* (2020) 9:482. doi: 10.3390/cells9020482

30. Suidan GL, Dickerson JW, Chen Y, McDole JR, Tripathi P, Pirko I, et al. Cd8 T cell-initiated vascular endothelial growth factor expression promotes central nervous system vascular permeability under neuroinflammatory conditions. *J Immunol.* (2010) 184:1031–40. doi: 10.4049/jimmunol.0902773

31. Gao F, Gao Y, Meng F, Yang C, Fu J, Li Y. The sphingosine 1-phosphate analogue Fty720 alleviates seizure-induced overexpression of p-glycoprotein in rat hippocampus. *Basic Clin Pharmacol Toxicol.* (2018) 123:14–20. doi: 10.1111/bcpt.12973

Advantages of publishing in Frontiers

OPEN ACCESS
Articles are free to read for greatest visibility and readership

FAST PUBLICATION
Around 90 days from submission to decision

HIGH QUALITY PEER-REVIEW
Rigorous, collaborative, and constructive peer-review

TRANSPARENT PEER-REVIEW
Editors and reviewers acknowledged by name on published articles

Frontiers
Avenue du Tribunal-Fédéral 34
1005 Lausanne | Switzerland

Visit us: www.frontiersin.org
Contact us: frontiersin.org/about/contact

REPRODUCIBILITY OF RESEARCH
Support open data and methods to enhance research reproducibility

DIGITAL PUBLISHING
Articles designed for optimal readership across devices

FOLLOW US
@frontiersin

IMPACT METRICS
Advanced article metrics track visibility across digital media

EXTENSIVE PROMOTION
Marketing and promotion of impactful research

LOOP RESEARCH NETWORK
Our network increases your article's readership